TECH LIBRARY KAFB, NM
0061718

NASA CONTRACTOR REPORT

NASA CR-2884

NASA CR-

LOAN COPY: RETURN TO
AFWL TECHNICAL LIBRARY
KIRTLAND AFB, N. M.

MODEL PREDICTIONS OF WIND AND TURBULENCE PROFILES ASSOCIATED WITH AN ENSEMBLE OF AIRCRAFT ACCIDENTS

G. G. Williamson, W. S. Lewellen, and M. E. Teske

Prepared by
AERONAUTICAL RESEARCH ASSOCIATES OF PRINCETON, INC.
Princeton, N.J. 08540
for George C. Marshall Space Flight Center

NATIONAL AERONAUTICS AND SPACE ADMINISTRATION • WASHINGTON D. C. • JULY 1977

TECH LIBRARY KAFB, NM

0061718

1. REPORT NO. NASA CR-2884	2. GOVERNMENT ACCESSION NO.	3. RECIPIENT'S CATALOG NO.
4. TITLE AND SUBTITLE Model Predictions of Wind and Turbulence Profiles Associated with an Ensemble of Aircraft Accidents		5. REPORT DATE July 1977
		6. PERFORMING ORGANIZATION CODE
7. AUTHOR(S) G. G. Williamson, W. S. Lewellen, and M. E. Teske		8. PERFORMING ORGANIZATION REPORT # M-225
9. PERFORMING ORGANIZATION NAME AND ADDRESS Aeronautical Research Associates of Princeton, Inc. 50 Washington Road Princeton, New Jersey 08540		10. WORK UNIT NO.
		11. CONTRACT OR GRANT NO. NAS8-32037
12. SPONSORING AGENCY NAME AND ADDRESS National Aeronautics and Space Administration Washington, D. C. 20546		13. TYPE OF REPORT & PERIOD COVERED Contractor (Final Report)
		14. SPONSORING AGENCY CODE

15. SUPPLEMENTARY NOTES

This report was prepared under the technical monitorship of Mr. Dennis W. Camp of the Atmospheric Sciences Division, Space Sciences Laboratory, NASA, Marshall Space Flight Center.

16. ABSTRACT

In a continuation of a research program to determine the feasibility of predicting conditions under which wind/turbulence environments hazardous to aviation operations exist, a number of different accidents have been examined in detail. The Aeronautical Research Associates of Princeton (A. R. A. P.) model of turbulent flow in the atmospheric boundary layer is used to reconstruct the wind and turbulence profiles which may have existed at low altitudes at the time of the accidents. The predictions are consistent with available flight recorder data, but neither the input boundary conditions nor the flight recorder observations are sufficiently precise for these case studies to be interpreted as verification tests of the model predictions. The results do provide a physically consistent set of wind and turbulence profiles which may be used to help understand what meteorological conditions lead to hazardous low-level wind shear and turbulence profiles, as well as providing a set of profiles for use in flight simulation studies which have proved hazardous in the past.

17. KEY WORDS Wind shear Aircraft accidents Thunderstorm gust front Turbulence Numerical model		18. DISTRIBUTION STATEMENT 47	
19. SECURITY CLASSIF. (of this report) Unclassified	20. SECURITY CLASSIF. (of this page) Unclassified	21. NO. OF PAGES 161	22. PRICE $6.75

*For sale by the National Technical Information Service, Springfield, Virginia 22161.

FOREWORD

The research in this document was intended to contribute to determining the feasibility of predicting the conditions under which wind/turbulence environments hazardous to aviation operations exist. Aeronautical Research Associates of Princeton has developed a computer model for solving for the velocity, temperature, and turbulence distributions in the atmospheric boundary layer. The model is based on using invariant modeling for closure of the dynamic equations of the ensemble-averaged, single-point, second-order correlations of the fluctuating velocities and temperature. In this study, the model is used to predict a consistent set of wind and turbulence profiles which may have existed at the time of select accidents. The set of accidents was chosen from the National Transportation Safety Board aircraft accident data bank because wind shear and/or turbulence appeared to be a contributing factor. It is believed that the set of wind shear conditions presented herein should be valuable for future flight simulator studies.

This research was conducted by the Aeronautical Research Associates of Princeton for the National Aeronautics and Space Administration, George C. Marshall Space Flight Center, Huntsville, Alabama, under the technical direction of Mr. Dennis W. Camp and Mrs. Margaret B. Alexander of the Space Sciences Laboratory. The support for this work was provided by Mr. William McGowan of the Aviation Safety Technology Branch, Office of Aeronautics and Space Technology (ROO/OAST), NASA Headquarters.

TABLE OF CONTENTS

	Abstract	i
	Table of Contents	iii
	Nomenclature	iv
	List of Figures	v
1.	SUMMARY AND RECOMMENDATIONS	1
2.	MODEL FORMULATION	3
3.	ACCIDENT ENVIRONMENTS SIMULATED BY THE ONE-DIMENSIONAL MODEL	28
4.	ACCIDENTS INVOLVING THUNDERSTORM GUST FRONTS	94
5.	ACCIDENTS NOT INVESTIGATED IN DETAIL	142
6.	REFERENCES	146

NOMENCLATURE

Symbol

f	coriolis function, $2\,\omega \sin \phi$ $\sim sec^{-1}$
g	gravitational constant ~ 9.81 m/sec^2
IAS	indicated airspeed $\sim$m/sec
K	proportionally constant
l.s.t.	local standard time $\sim$hrs : minutes
mb	millibars of pressure
p	pressure $\sim$millibars
q	turbulence velocity $\sim$m/sec
R	radial position, positive outwards $\sim$m
t	time $\sim$sec
T	temperature $\sim$°C
U	velocity, positive forward $\sim$m/sec
$\sqrt{\overline{u'u'}}$	variance of forward velocity $\sim$m/sec
V	velocity, positive left $\sim$m/sec
$\sqrt{\overline{v'v'}}$	variance of lateral velocity $\sim$m/sec
W	velocity, positive upwards $\sim$m/sec
$\sqrt{\overline{w'w'}}$	variance of vertical velocity $\sim$m/sec
x	horizontal position, positive forwards $\sim$m
y	horizontal position, positive left $\sim$m
z	vertical position, positive upwards $\sim$m
ψ	stream function $\sim$m^2/sec
Λ	macroscale of turbulence $\sim$m
ρ	density $\sim$kg/m^3
θ	virtual potential temperature referenced to 300°C $\sim$°C

Subscripts

g	geostrophic
850	850 millibar altitude

LIST OF ILLUSTRATIONS

Figure

2.2.1 Initial scale and turbulence profiles.

2.3.1 Growth of axisymmetric gust front as illustrated by the $T = -2°C$ contour at $t = 0, 200, 340, 500, 750, 1000$ sec.

2.3.2 Normalized temperature contours as a functions of z and R for an axisymmetric gust front with a 2000 m radius downdraft at $t = 200$ sec. [The numbers represent the percentage of the maximum value indicated across the top. The same number may represent either a ± value. The P represents a positive maximum and M a minimum. The zero contour is outlined.]

2.3.3 As above but $t = 500$ sec. [See figure 2.3.2 for explanation of notation.]

2.3.4 As above but $t = 1000$ sec. [See figure 2.3.2 for explanation of notation.]

2.3.5 Normalized stream function contours as a function of z and R for an axisymmetric gust front with a 2000 m radius downdraft at $t = 200$ sec. [See figure 2.3.2 for explanation of notation.]

2.3.6 As above but $t = 500$ sec. [See figure 2.3.2 for explanation of notation.]

2.3.7 As above but $t = 1000$ sec. [See figure 2.3.2 for explanation of notation.]

2.3.8 Normalized mean radial velocity contours as a function of z and R for an axisymmetric gust front with a 2000 m radius downdraft at $t = 200$ sec. [See figure 2.3.2 for explanation of notation.]

2.3.9 As above but $t = 500$ sec. [See figure 2.3.2 for explanation of notation.]

2.3.10 As above but $t = 1000$ sec. [See figure 2.3.2 for explanation of notation.]

2.3.11 Normalized mean vertical velocity contours as a function of z and R for an axisymmetric gust front with a 2000 m radius downdraft at $t = 200$ sec. [See figure 2.3.2 for explanation of notation.]

2.3.12 As above but $t = 500$ sec. [See figure 2.3.2 for explanation of notation.]

2.3.13 As above but t = 1000 sec. [See figure 2.3.2 for explanation of notation.]

2.3.14 Normalized variance of vertical velocity contours as a function of z and R for an axisymmetric gust front with a 2000 m radius downdraft at t = 200 sec. [See figure 2.3.2 for explanation of notation.]

2.3.15 As above but t = 500 sec. [See figure 2.3.2 for explanation of notation.]

2.3.16 As above but t = 1000 sec. [See figure 2.3.2 for explanation of notation.]

2.3.17 Normalized scale of turbulence contours as a function of z and R for an axisymmetric gust front with a 2000 m radius downdraft at t = 200 sec. [See figure 2.3.2 for explanation of notation.]

2.3.18 As above but t = 500 sec. [See figure 2.3.2 for explanation of notation.]

2.3.19 As above but t = 1000 sec. [See figure 2.3.2 for explanation of notation.]

3.2.1 Aircraft-runway-winds orientation diagram for Boston, December 17, 1973 accident.

3.2.2 Radarscope picture near the time of Boston, December 17, 1973 accident.

3.2.3 Early 850 mb chart for Boston, December 17, 1973 accident.

3.2.4 Late 850 mb chart for Boston, December 17, 1973 accident.

3.2.5 Early surface weather chart for Boston, December 17, 1973 accident.

3.2.6 Late surface weather chart for Boston, December 17, 1973 accident.

3.2.7 Altitude profiles for; a) mean geostrophic velocity component parallel to runway (+ U_g, tailwind), b) mean wind velocity component perpendicular to runway (+ V_g, crosswind from right), c) temperature before and after the Boston December 17, 1973 accident.

3.2.8 Altitude profile of mean wind velocity component parallel to runway (+ U, tailwind) for Boston, December 17, 1973 accident.

3.2.9 Altitude profile of mean wind velocity component perpendicular to runway (+ V, crosswind from right) for Boston, December 17, 1973 accident.

3.2.10 Altitude profile of variance of the total velocity for Boston, December 17, 1973 accident.

3.2.11 Altitude profile of variance of the wind parallel to runway for Boston, December 17, 1973 accident.

3.2.12 Altitude profile of variance of the wind perpendicular to runway for Boston, December 17, 1973 accident.

3.2.13 Altitude profile of variance of the vertical wind for Boston, December 17, 1973 accident.

3.2.14 Altitude profile of scale of turbulence for Boston, December 17, 1973 accident.

3.3.1 Aircraft-runway-winds orientation diagram for La Guardia Airport, January 4, 1971 accident.

3.3.2 Early 850 mb chart for La Guardia Airport, January 4, 1971 accident.

3.3.3 Late 850 mb chart for La Guardia Airport, January 4, 1971 accident.

3.3.4 Early surface weather chart for La Guardia, January 4, 1971 accident.

3.3.5 Late surface weather chart for La Guardia, January 4, 1971 accident.

3.3.6 Altitude profiles for; a) mean geostrophic velocity component parallel to runway (+ U_g, tailwind), b) mean wind velocity component perpendicular to runway (+V_g, crosswind from right), c) temperature before and after the La Guardia Airport, January 4, 1971 accident

3.3.7 Altitude profile of mean wind velocity component parallel to runway for the La Guardia Airport, January 4, 1971 accident (+ U, tailwind).

3.3.8 Altitude profile of mean wind velocity component perpendicular to runway for the La Guardia Airport, January 4, 1971 accident

3.3.9 Altitude profile of variance of the total velocity variance for La Guardia, January 4, 1971 accident.

3.3.10 Altitude profile of variance of the wind parallel to runway for La Guardia Airport, January 4, 1971 accident.

3.3.11 Altitude profile of variance of the wind perpendicular to runway for La Guardia Airport, January 4, 1971 accident.

3.3.12 Altitude profile of variance of the vertical wind for La Guardia Airport, January 4, 1971 accident.

3.3.13 Altitude profile of scale of turbulence for La Guardia Airport, January 4, 1971 accident.

3.4.1 Aircraft-runway-winds orientation diagram for Wichita, Kansas, March 3, 1973 accident.

3.4.2 Early 850 mb chart for Wichita, Kansas, March 3, 1973 accident.

3.4.3 Late 850 mb chart for Wichita, Kansas, March 3, 1973 accident.

3.4.4 Early surface weather chart for Wichita, Kansas, March 3, 1973 accident.

3.4.5 Late surface weather chart for Wichita, Kansas, March 3, 1973 accident.

3.4.6 Altitude profiles for; a) mean geostrophic velocity component parallel to runway (+ U_g, tailwind), b) mean wind velocity component perpendicular to runway (+ V_g, cross-wind from right), c) temperature before and after the Wichita, Kansas, March 3, 1973 accident.

3.4.7 Altitude profile of mean wind velocity component parallel to runway for the Wichita, Kansas, March 3, 1973 accident.

3.4.8 Altitude profile of mean wind velocity component perpendicular to runway for the Wichita, Kansas, March 3, 1973 accident.

3.4.9 Altitude profile of variance of the total velocity variance for Wichita, Kansas, March 3, 1973 accident.

3.4.10 Altitude profile of variance of the wind parallel to runway for Wichita, Kansas, March 3, 1973 accident.

3.4.11 Altitude profile of variance of the wind perpendicular to runway for Wichita, Kansas, March 3, 1973 accident.

3.4.12 Altitude profile of variance of the vertical wind for Wichita, Kansas, March 3, 1973 accident.

3.4.13 Altitude profile of scale of turbulence for Wichita Kansas, March 3, 1973 accident.

3.5.1 Aircraft-runway-winds orientation diagram for JFK Airport, December 12, 1972 accident.

3.5.2 Early 850 mb chart for JFK Airport, December 12, 1972 accident.

3.5.3 Late 850 mb chart for JFK Airport, December 12, 1972 accident.

3.5.4 Early surface weather chart for JFK Airport, December 12, 1972 accident.

3.5.5 Late surface weather chart for JFK Airport, December 12, 1972 accident.

3.5.6 Altitude profiles for; a) mean geostrophic velocity component parallel to runway (+ U_g, tailwind), b) mean wind velocity component perpendicular to runway (+ V_g, crosswind from right), c) temperature before and after the JFK Airport, December 12, 1972 accident.

3.5.7 Altitude profile of mean velocity component parallel to runway (+ U, tailwind) for the JFK Airport, December 12, 1972 accident.

3.5.8 Altitude profile of mean wind velocity component perpendicular to runway (+V, crosswind from right) for the JFK airport, December 12, 1972 accident.

3.5.9 Altitude profile of variance of the total velocity variance for JFK Airport, December 12, 1972 accident.

3.5.10 Altitude profile of variance of the wind parallel to runway for JFK Airport, December 12, 1972 accident.

3.5.11 Altitude profile of variance of the wind perpendicular to runway for JFK Airport, December 12, 1972 accident.

3.5.12 Altitude profile of variance of the vertical wind for JFK Airport, December 12, 1972 accident.

3.5.13 Altitude profile of scale of turbulence for JFK Airport, December 12, 1972 accident.

3.6.1 Aircraft-runway-winds orientation diagram for Johnstown, Pa., January 6, 1974 accident.

3.6.2 Early 850 mb chart for Johnstown, Pa., January 6, 1974 accident.

3.6.3 Late 850 mb chart for Johnstown, Pa., January 6, 1974 accident.

3.6.4 Early surface weather chart for Johnstown, Pa., January 6, 1974 accident.

3.6.5 Late surface weather chart for Johnstown, Pa., January 6, 1974 accident.

3.6.6 Altitude profiles for; a) mean geostrophic velocity component parallel to runway (+ U_g, tailwind), b) mean wind velocity component perpendicular to runway (+ V_g, crosswind from right), c) temperature before and after the Johnstown, Pa., January 6, 1974 accident.

3.6.7 Altitude profile of mean wind velocity component parallel to runway (+ U, tailwind) for the Johnstown, Pa., January 6, 1974 accident.

3.6.8 Altitude profile of mean wind velocity component perpendicular to runway (+ V, crosswind from right) for the Johnstown, Pa., January 6, 1974 accident.

4.2.1 Radarscope picture near the time of the Denver, Colorado August 7, 1975 accident.

4.2.2 Normalized temperature contours as a function of z and R for an axisymmetric gust front with a 500 m radius downdraft at t = 200 sec. [See figure 2.3.2 for explanation of notation.]

4.2.3 Normalized stream function contours as a function of z and R for an axisymmetric gust front with a 500 m radius downdraft at t = 200 sec. [See figure 2.3.2 for explanation of notation.]

4.2.4 Normalized mean radial velocity contours as a function of z and R for an axisymmetric gust front with a 500 m radius downdraft at t = 200 sec. [See figure 2.3.2 for explantion of notation.]

4.2.5 Normalized mean vertical velocity contours as a function of z and R for an axisymmetric gust front with a 500 m radius downdraft at t = 200 sec. [See figure 2.3.2 for explanation of notation.]

4.2.6 Normalized variance of vertical velocity contours as a function of z and R for an axisymmetric gust front with a 500 m radius downdraft at t = 200 sec. [See figure 2.3.2 for explanation of notation.]

4.2.7 Normalized scale of turbulence contours as a function of z and R for an axisymmetric gust front with a 500 m radius downdraft at t = 200 sec. [See figure 2.3.2 for explanation of notation.]

4.2.8 Approximate aircraft trajectory relative to storm cell and initial point of impact for Denver, Colorado, August 7, 1975 accident.

4.2.9 Velocity component of mean wind parallel to runway as a function of horizontal distance from the initial impact point (+ U, tailwind) for the Denver, Colorado, August 7, 1975 accident.

4.2.10 Vertical velocity component of mean wind as function of horizontal distance from the initial impact point (+ W, up) for the Denver, Colorado, August 7, 1975 accident.

4.2.11 Variance of the total velocity as a function of horizontal distance from the initial impact point for the Denver, Colorado, August 7, 1975 accident.

4.2.12 Variance of the wind parallel to runway as a function of horizontal distance from the initial impact point for the Denver, Colorado August 7, 1975, accident.

4.2.13 Variance of the wind perpendicular to runway as a function of horizontal distance from the initial impact point for Denver, Colorado, August 7, 1975 accident.

4.2.14 Variance of the vertical wind as a function of horizontal distance from the initial impact point for Denver, Colorado, August 7, 1975 accident.

4.2.15 Turbulence scale as a function of horizontal distance from the initial impact point for Denver, Colorado, August 7, 1975 accident.

4.3.1 Radarscope picture near the time of Chattanooga, Tenn., November 27, 1973 accident.

4.3.2 Approximate aircraft trajectory relative to storm cell and initial point of impact for Chattanooga, Tenn., November 27, 1973 accident.

4.3.3 Altitude profile of mean wind velocity component parallel to runway (+ U, tailwind) for Chattanooga, Tenn., November 27, 1973 accident.

4.3.4 Altitude profile of mean wind vertical velocity component (+ W, up) for Chattanooga, Tenn., November 27, 1973 accident.

4.3.5 Altitude profile of variance of the total velocity for the Chattanooga, Tenn., November 27, 1973 accident.

4.3.6 Altitude profile of variance of the wind parallel to runway for the Chattanooga, Tenn., November 27, 1973 accident.

4.3.7 Altitude profile of variance of the wind perpendicular to runway for the Chattanooga, Tenn., November 27, 1973 accident.

4.3.8 Altitude profile of variance of the vertical wind for Chattanooga, Tenn., November 27, 1973 accident.

4.3.9 Altitude profile of scale of turbulence for Chattanooga, Tenn., November 27, 1973 accident.

4.4.1 Radarscope picture near the time of the St. Louis, Mo., July 23, 1973 accident.

4.4.2 Normalized temperature contours as a function of z and R for a two-dimensional gust front with a 2000 m radius downdraft at $t = 1000$ sec. [See figure 2.3.2 for explanation of notation.]

4.4.3 Normalized stream function contours as a function of z and R for a two-dimensional gust front with a 2000 m radius downdraft at $t = 1000$ sec. [See figure 2.3.2 for explanation of notation.]

4.4.4 Normalized mean radial velocity contours as a function of z and R for a two-dimensional gust front with a 2000 m radius downdraft at $t = 1000$ sec. [See figure 2.3.2 for explanation of notation.]

4.4.5 Normalized mean vertical velocity contours as a function of z and R for a two-dimensional gust front with a 2000 m radius downdraft at $t = 1000$ sec. [See figure 2.3.2 for explanation of notation.]

4.4.6 Normalized variance of vertical velocity contours as a function of z and R for a two-dimensional gust front with a 2000 m radius downdraft at $t = 1000$ sec. [See figure 2.3.2 for explanation of notation.]

4.4.7 Normalized scale of turbulence contours as a function of z and R for a two-dimensional gust front with a 2000 m radius downdraft at $t = 1000$ sec. [See figure 2.3.2 for explanation of notation.]

4.4.8 Aircraft-runway gust front orientation diagram for the St. Louis, Mo., July 23, 1973 accident.

4.4.9 Projection of aircraft trajectory on the plane of the gust front for the St. Louis, Mo., July 23, 1973 accident.

4.4.10 Altitude profile of horizontal mean wind velocity component along aircraft trajectory for the St. Louis Mo., July 23, 1973 accident, (+ V , crosswind from right).

4.4.11 Altitude profile of vertical mean wind velocity component along aircraft trajectory for the St. Louis Mo., July 23, 1973 accident, (+ W , updraft).

4.4.12 Altitude profile of variance of total velocity along aircraft trajectory for the St. Louis, Mo., July 23, 1973 accident.

4.4.13 Altitude profile of variance of the wind parallel to aircraft trajectory for the St. Louis, Mo., July 23, 1973 accident.

4.4.14 Altitude profile of variance of the wind perpendicular to aircraft trajectory for the St. Louis, Mo., July 23, 1973 accident.

4.4.15 Altitude profile of variance of the vertical wind along aircraft trajectory for the St. Louis, July 23, 1973 accident.

4.4.16 Altitude profile of scale of turbulence along aircraft trajectory for the St. Louis, Mo., July 23, 1973 accident.

5.1.1 Aircraft-runway winds orientation diagram for Raleigh-Durham, N.C., April 2, 1970 accident.

5.2.1 Airport-topography-wind orientation drawing for the two St. Thomas, V.I. accidents.

1. SUMMARY AND RECOMMENDATIONS

Aircraft encounter of severe wind shear or turbulence at low altitudes is a major safety hazard. Flight experience and past theoretical studies indicate that these conditions are most likely to occur in the vicinity of thunderstorms, fronts, thermal winds or topographical irregularities.

In this study, A.R.A.P. estimates the severity of wind shear and turbulence present at the time of certain aircraft accidents when the weather or topographical conditions possibly fell into one of the above mentioned categories. Selection of the ensemble of aircraft accidents was discussed in Ref. 1. The results of the present A.R.A.P. study provide a sample catalogue of weather conditions which have proved hazardous for aircraft operations. The model results predict detailed profiles of wind magnitude, direction, and ensemble-averaged turbulent fluctuations for the lowest 500 m altitude in each case. These model profiles are made available, herein, for further flight simulation studies.

The unique tool A.R.A.P. has used in accomplishing this task is a sophisticated computer model for solving the velocity, temperature, and turbulence distributions in the atmospheric boundary layer. This model is based on using invariant modeling for closure of the dynamic equations of the ensemble-averaged, single-point, second-order correlations of the fluctuating velocities and temperature. This approach to turbulent modeling has been under development at A.R.A.P. for several years (Refs. 2-9).

The boundary conditions needed for each case are obtained using National Weather Service (NWS) data and airport surface weather observations.

In a previous study (Ref. 1) A.R.A.P. has estimated the severity of wind shear and turbulence as a function of the meteorologically significant parameters; surface roughness, surface heating, geostrophic accelerations, atmospheric stability and thermal winds. The emphasis in this study is shifted from parametric variations to several specific examples of weather conditions conducive to hazardous flight.

Model results of the development of a typical thunderstorm gust front are presented in Section 4. The model appears to give a good representation of the physical dynamics associated with a local downdraft. Simulated trajectories flown through these model results demonstrate the types of problems that pilots could have encountered in four specific accidents. Future study should investigate the sensitivity of the wind magnitude, fluctuations, and gradients as a function of the input boundary conditions. Preliminary results indicate the most important variables to be the

temperature decrement and the altitude from which the downdraft originates. Surface roughness and velocity of the storm cell may also be expected to have a strong influence on the winds close to the surface. By varying these boundary conditions it should be possible to determine what input conditions lead to the sharpest gradients across the gust front and the strongest downdrafts close to the surface.

A reasonable representation of accident scenarios involving either cold or warm fronts is presented in Section 3, using the one-dimensional version of A.R.A.P.'s boundary layer model. We believe that a better representation of windshear associated with front passage could be obtained using our two-dimensional version of the model. However, this must await a future study.

Three of the accidents A.R.A.P. has studied, as well as some accidents previously studied by others (Ref. 10) appear to involve the mountain lee wave. Technical constraints on the numerical model have prevented A.R.A.P. from fully utilizing the model to study this type of micrometeorology in the current contract. However, work currently funded by the Naval Air Systems Command will give us the capability in the near future of including terrain features in our boundary conditions for the two-dimensional model. One of the important parameters governing the behavior of the mountain lee wave is the Froude number based on the mean wind component perpendicular to the mountain ridge, the static stability of the atmospheric boundary layer, and the height of the mountain ridge. When this Froude number is large the boundary layer flow will separate at or near the top of the ridge, leaving a separated wake for some distance downwind. In contrast to this, when the Froude number is less than approximately one, the flow can remain attached to the lee slope to form a strong down-slope wind, which subsequently separates in an intense "hydraulic jump" type phenomenon. We believe our A.R.A.P. model should be used to better understand this phenomenon and determine those conditions which are most likely to prove hazardous to aircraft operations.

2. MODEL FORMULATION

2.1 BACKGROUND

As part of the previous study done by A.R.A.P., National Transportation Safety Board (NTSB) aircraft accident data were reviewed to obtain representative cases where wind shear or turbulence caused, or was a factor, in the accident. Cases were selected representing weather conditions which are most likely to produce high values of wind shear (thunderstorms, fronts, thermal winds, and lee waves).

The purpose of this study is to develop a flowfield model for each of the accidents which is consistent with measurements made near the time of the accident. These models can then be used to evaluate the role wind shear and turbulence played in the accident through piloted simulation studies. The flowfield models developed in the present study have the advantage of being more consistent models than those presently used in simulation studies, i.e., they satisfy mass, momentum and energy conservation relations for the turbulent fluctuations as well as for the mean flow variables.

For most of the cases investigated, the flowfield in the vicinity of the accident is a function of synoptic scale variations and is modeled using input data from the 850 mb charts, surface charts and radiosonde measurements. Exceptions are the gust front (thunderstorm) cases where the dominant meteorological phenomenon is of smaller scale. For gust fronts, model technique is, therefore, different and will be discussed near the end of this section.

2.2 GENERAL TECHNIQUE USED FOR MODELING AIRPORT MICROMETEOROLOGY

A.R.A.P. has developed a partial differential equation computer model of the velocity, temperature, and turbulence distributions in the atmospheric boundary layer (Ref. 1). The computer model requires the specification of; 1) the initial values of the above distributions, 2) the boundary conditions at the surface and above the boundary layer, and 3) pressure gradient and heating rate forcing functions. These inputs are calculated based on NWS data as described below.

The data used are:

North American Surface Charts before and after accident
North American 850 mb Charts before and after accident
Nearest radiosonde sounding before and after accident
Airport surface weather observations at time of accident

The geostrophic velocity near 1500 m and at the surface are obtained from the gradient of the isobars on the 850 charts, and surface charts respectively.

$$U_g = -\frac{1}{f\rho}\frac{\partial p}{\partial y} \quad ; \quad V_g = \frac{1}{f\rho}\frac{\partial p}{\partial x} \tag{1}$$

The thermal wind parameter $\frac{\partial U_g}{\partial z}$ is obtained from the gradient of the isotherms on the 850 mb chart.

$$\frac{\partial U_g}{\partial z} = -\frac{g}{fT}\frac{\partial T}{\partial y} \quad ; \quad \frac{\partial V_g}{\partial z} = \frac{g}{fT}\frac{\partial T}{\partial x} \tag{2}$$

The geostrophic velocity profile is then

$$U_g(z) = U_{g850} + \left.\frac{\partial U_g}{\partial z}\right|_{850}\left(z - z_{850}\right) \tag{3}$$

If this profile does not match the value of $U_g(z = 0)$ from the surface chart, the gradient $\partial U_g/\partial z$ must not be constant. It should then be altered to accord with other observations, such as the presence of a cold front. The resulting geostrophic velocity profile is used to set the upper boundary condition on velocity and the pressure gradient forcing function. This process is repeated using the charts after the accident. The velocity boundary condition and the pressure gradient are then assumed to vary in a piecewise linear fashion in time.

The initial temperature and velocity profiles and the upper boundary condition on temperature are obtained from the radiosonde measurements.

Since no attempt has been made in this study to model radiative heating, the temperature equation is forced by a heating rate function which accounts for both radiation and advection. The heating rate profile is determined by the difference between the temperature profiles measured before and after the accident. These temperature profiles are also used to set the upper atmospheric stability level and ground temperature.

The remaining inputs required for this model are the initial scale and turbulence profiles. The resulting velocity, turbulence, and scale profiles even after only one hour simulated time are quite insensitive to the initial scale and turbulence profiles chosen. Typical profiles used are shown in figure 2.2.1.

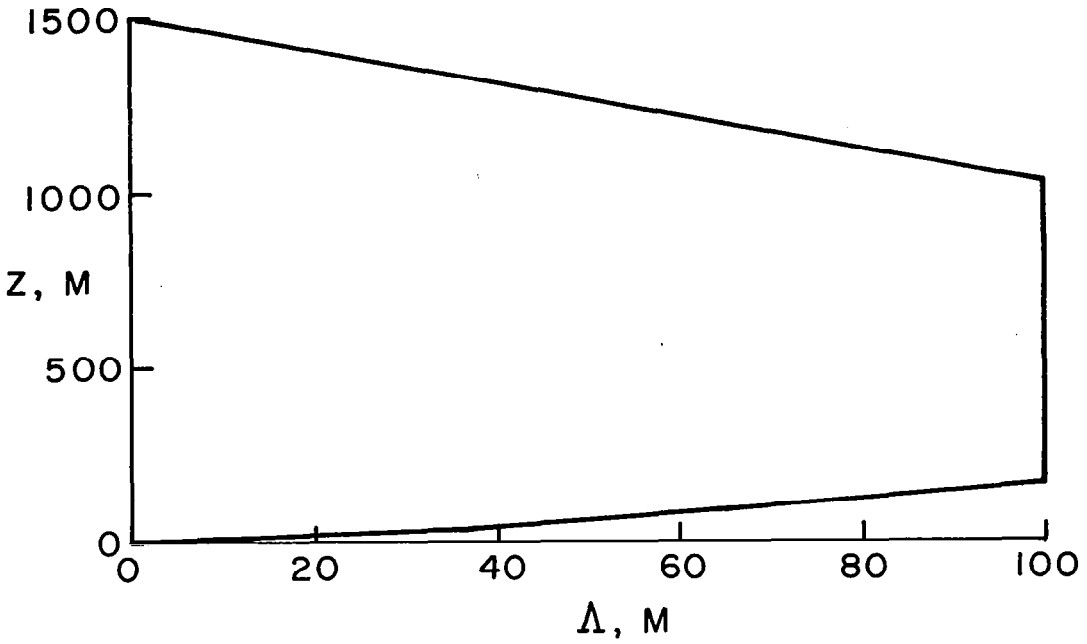

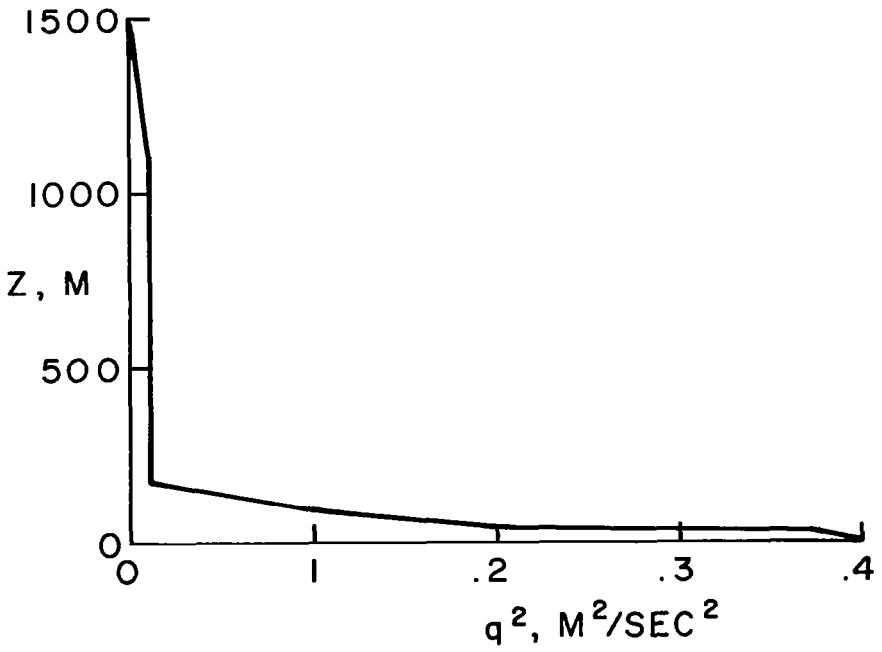

Figure 2.2.1. Initial scale and turbulence profiles.

With these inputs specified, the computer code is run over most of the 12 hour interval covered by the data. The velocity profiles close to the accident time are examined and the set chosen which is in best agreement with surface wind observations and, where available, wind profiles derived from flight recorder data.

It should be clear that neither the input boundary conditions nor flight recorder data of the observed winds are sufficiently precise for these case studies to be interpreted as verification tests of the model predictions. What the model results do provide is a physically consistent set of wind and turbulence profiles which may have existed at the time of the accident.

2.3 Thunderstorm Gust Front Model

As a result of a separate contract with the Nuclear Regulatory Commission for modeling the wind and turbulence field in a tornado, we have developed an axisymmetric version of our program for computing flow in the atmospheric boundary layer. Except for the geometry effects the modeling is identical to that described in Ref. 4 and Ref. 1. No new model constants or coefficients are required. The model incorporates the influence of density variations on both the mean flow and the turbulent fluctuations through the Boussinesq density approximation. Validation of our turbulent closure for a number of different cases of this type flow is given in Ref. 7.

We idealize the cold outflow from the thunderstorm as a cold jet impinging perpendicularly on the ground. The prime variables are the temperature defect of the jet, its diameter and the height at which it is released. Other variables needed to determine the flow are the surface roughness and the larger scale updraft within which the downdraft is imbedded. More specifically the boundary conditions which must be specified are; the surface roughness and temperature of the ground surface, and the stream function, vorticity, temperature, and turbulence at both the top of the domain and the outer radius of the domain.

The temperature defect of the cold downdraft is caused by evaporation of falling rain by relatively dry air at some altitude. For our simulations, herein, we have set this temperature defect at what we believe to be a typical value for a strong downdraft, 10°C. The velocity of the cold jet at the top of the domain has been set at a somewhat arbitrary value of 10 m/sec. Two values of the cold jet diameter, 500 m and 2 km, have been simulated. In each case, the top of the domain was set at 1600 m. The convergence velocity at large radius was set at 2.5 m/sec. The turbulence is taken as isotropic and small at large R and a zero

slope condition is used at large z. Surface roughness is set at 0.1 m.

The flow problem is initialized by taking the boundary values of vorticity and temperature at the top of the domain and extrapolating them linearly to zero value at the surface. The turbulence is initialized as isotropic with a scale equal to the smaller of 0.65 z or 100 m.

Figures 2.3.1 - 2.3.19 present the results of a radial gust front calculation where the spread of the incoming downdraft is 2 km. A good way (short of a motion picture) of following the structure of the developing gust is to observe the movement of a fixed temperature contour, in this case (figure 2.3.1) $T = -2°C$ At $t = 0$ the initial linear profile is shown, but by $t = 200$ sec that structure has developed into the moving front. At $t = 340$ sec the front has torn away from the downdraft region. In continuing times the strength of the gust decreases as the effect of the area change becomes more important. Nevertheless, the height of the gust appears to grow slowly so that by $t = 1000$ sec, the $T = -2°$ line reaches nearly 1 km in altitude at a distance of nearly 8 km from the source centerline. The front is still quite strong at this point. Complete contour profiles for T at $t = 200$, 500, and 1000 sec are shown in figures 2.3.2 - 2.3.4. The low temperature in the gust front region is eroded as the run proceeds, even as the front itself enlarges in altitude. The accompanying profiles at the same times as figures 2.3.2 - 2.3.4 for the streamfunction Ψ, radial velocity U, vertical velocity W, vertical energy component $\overline{w'w'}$ and turbulence scale Λ are shown in figures 2.3.5 - 2.3.19.

The streamfunction Ψ, figures 2.3.5 - 2.3.7, begins as a downdraft cell contained by the inflow stagnation flow at large z. Arrowheads have been added to enhance flow visualization. By $t = 500$ sec a distinctive cell structure has developed near the front. This structure persists at $t = 1000$ sec as the front moves across our computational domain toward the right boundary.

The radial velocity U, in figures 2.3.8 - 2.3.10 shows a line of demarcation between flows away from and toward the axis lying between 600 m - 1 km. Its maximum value is about 24 m/sec near the surface. At the two later times this line has dropped closer to the surface (about 300 m) with mass continuity then permitting the maximum velocity to remain nearly constant. Arrows indicate the flow direction. The vertical velocity W in figures 2.3.11 - 2.3.13 shows the very strong downdraft near the centerline. Although we are forcing an inflow of 10 m/sec, the simulation determines a downward jet of over 18 m/sec throughout most of the run. Secondary up- and down-drafts near the gust front develop in the later stages of the run.

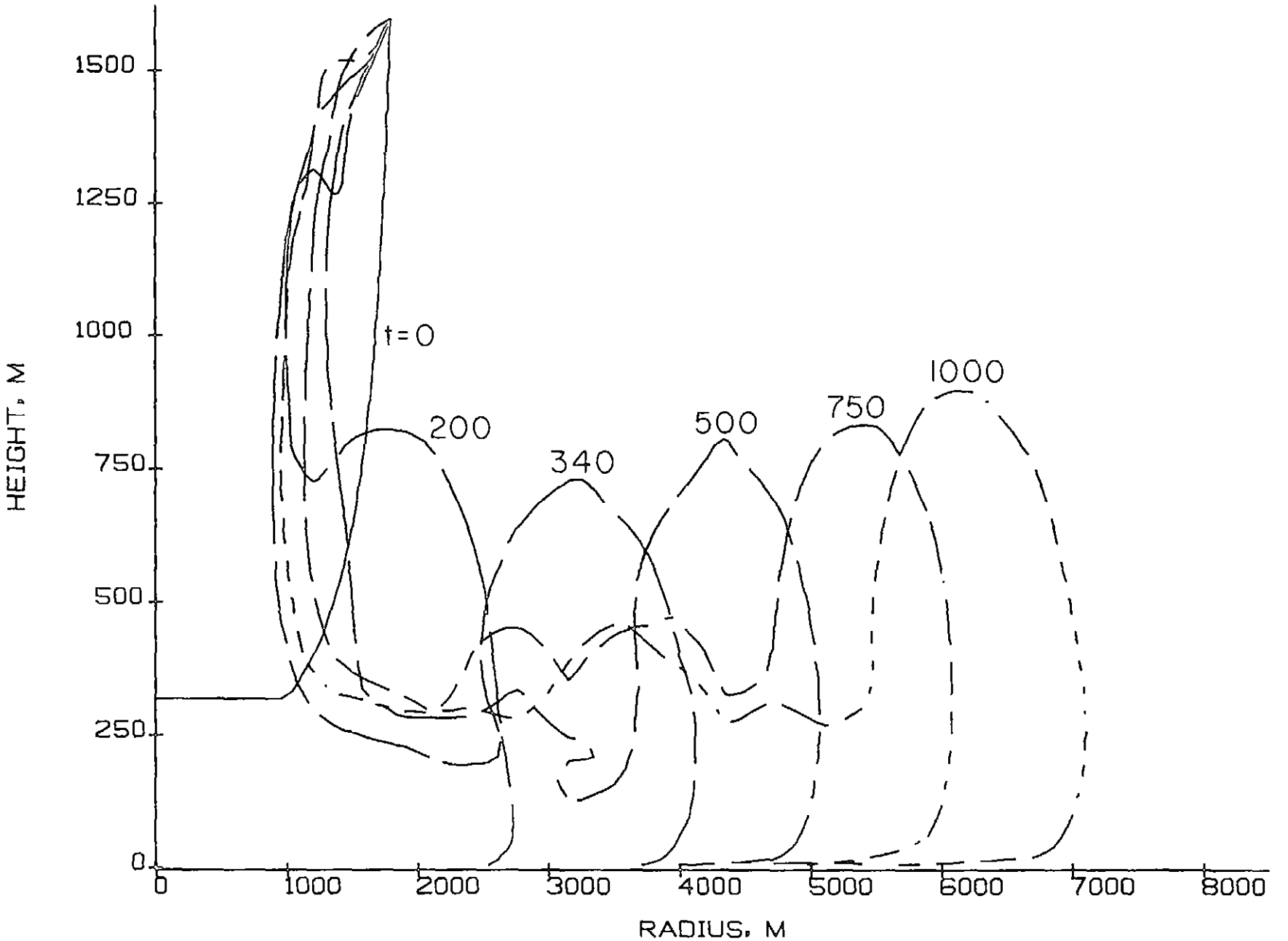

Figure 3.3.1. Growth of axisymmetric gust front as illustrated by the T=-2°C contour at t = 0, 200, 340, 500, 750, 1000 sec.

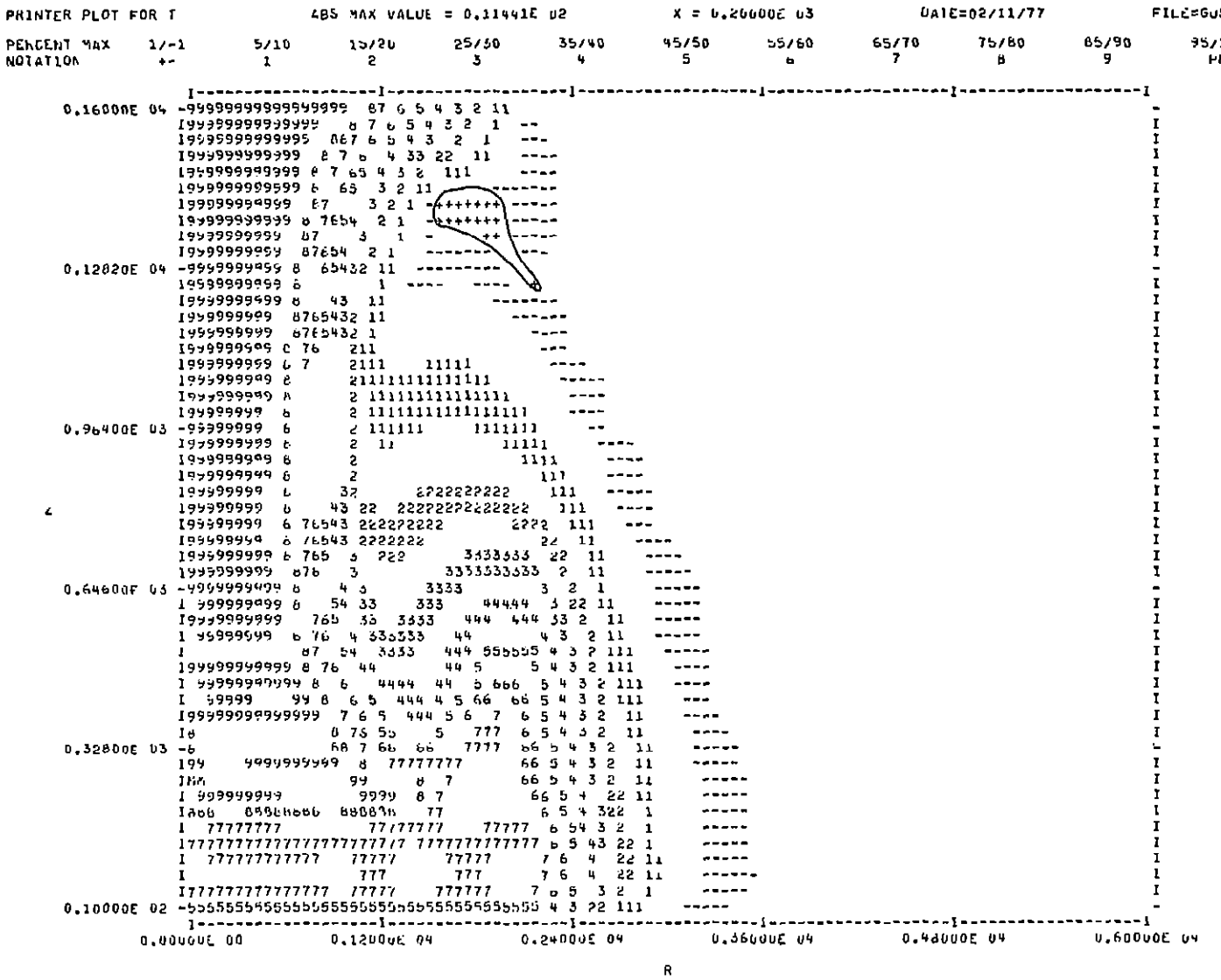

Figure 2.3.2. Normalized temperature contours as a function of z and R for an axisymmetric gust front with a 2000 m radius downdraft at t = 200 sec. [The numbers represent the percentage of the maximum value indicated across the top. The same number may represent either a ± value. The P represents a positive maximum and M as minimum. The zero contour is outlined.]

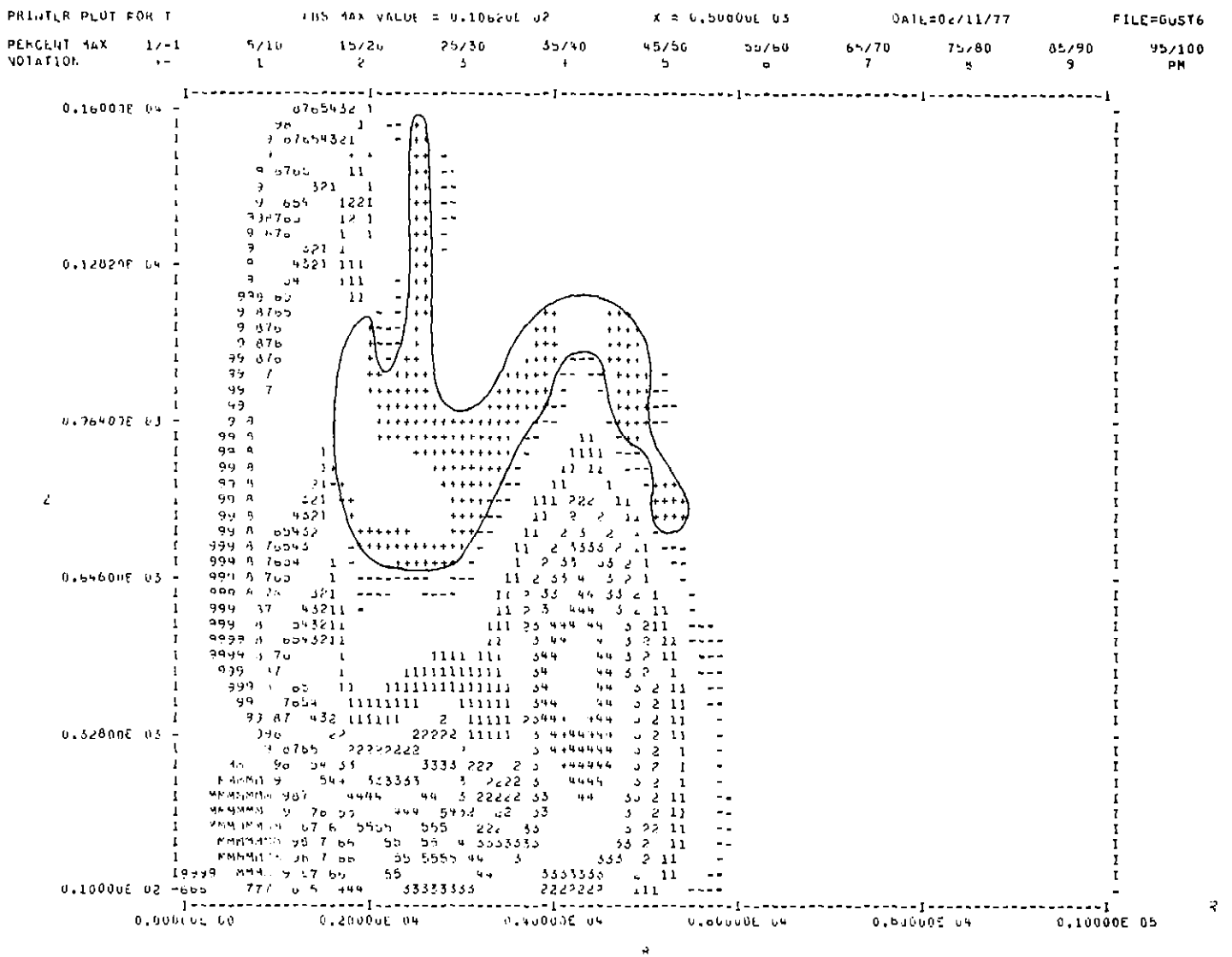

Figure 2.3.3. As above but t = 500 sec. [See figure 2.3.2 for explanation of notation.]

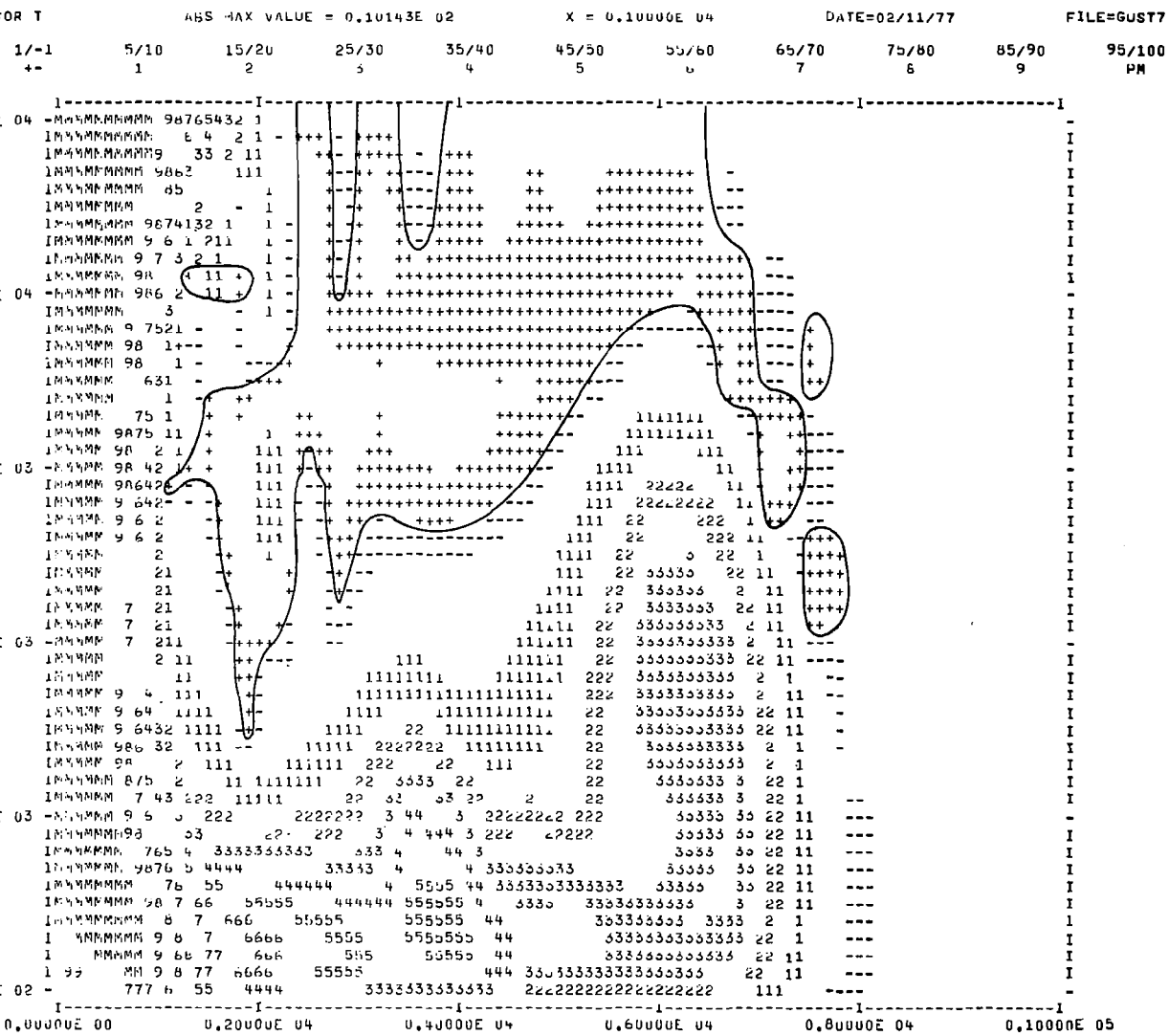

Figure 2.3.4. As above but t = 1000 sec. [See figure 2.3.2 for explanation of notation.]

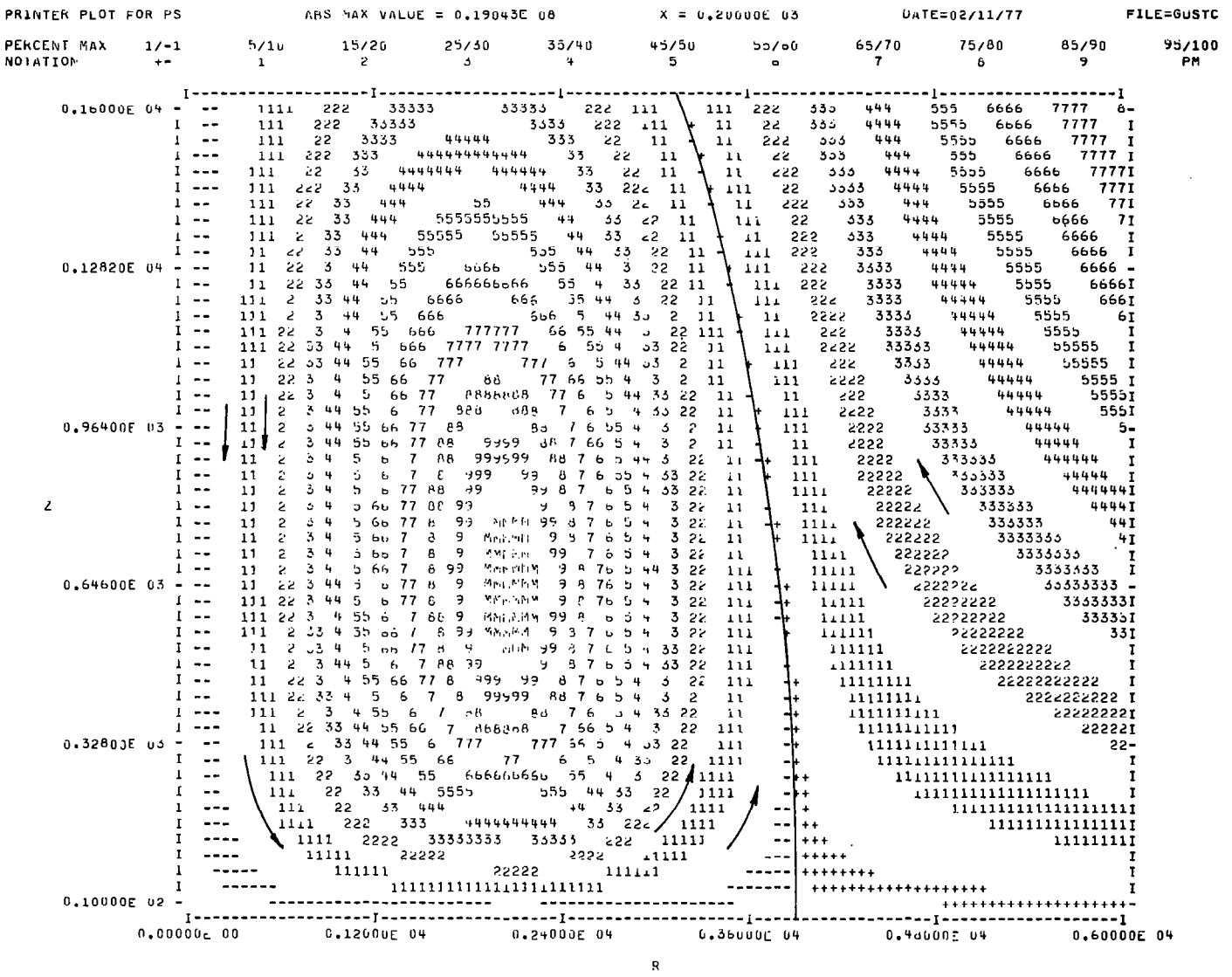

Figure 2.3.5. Normalized stream function contours as a function of z and R for an axisymmetric gust front with a 2000 m radius downdraft at t = 200 sec. [See figure 2.3.2 for explanation of notation.]

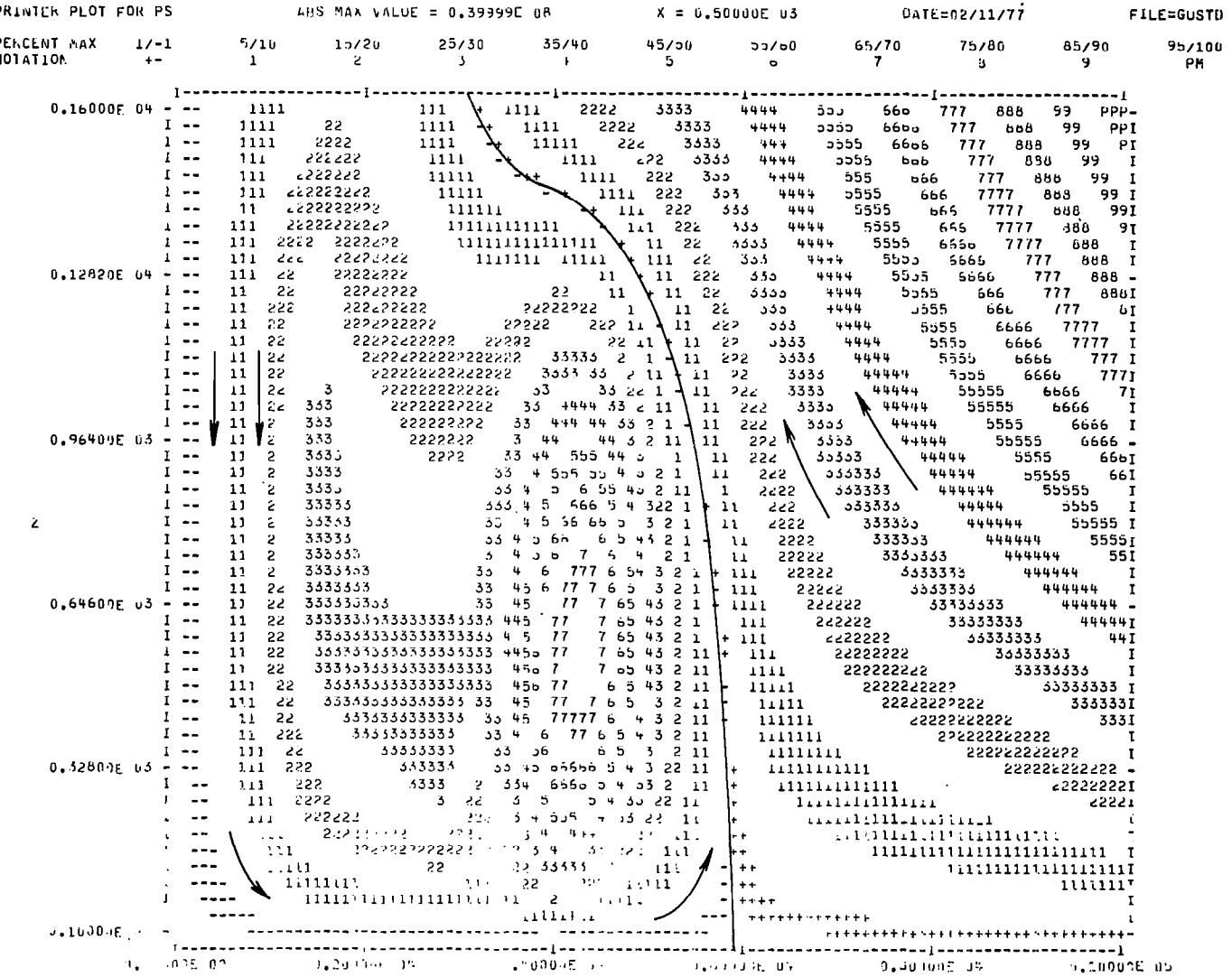

Figure 2.3.6. As above but t = 500 sec. [See figure 2.3.2 for explanation of notation.]

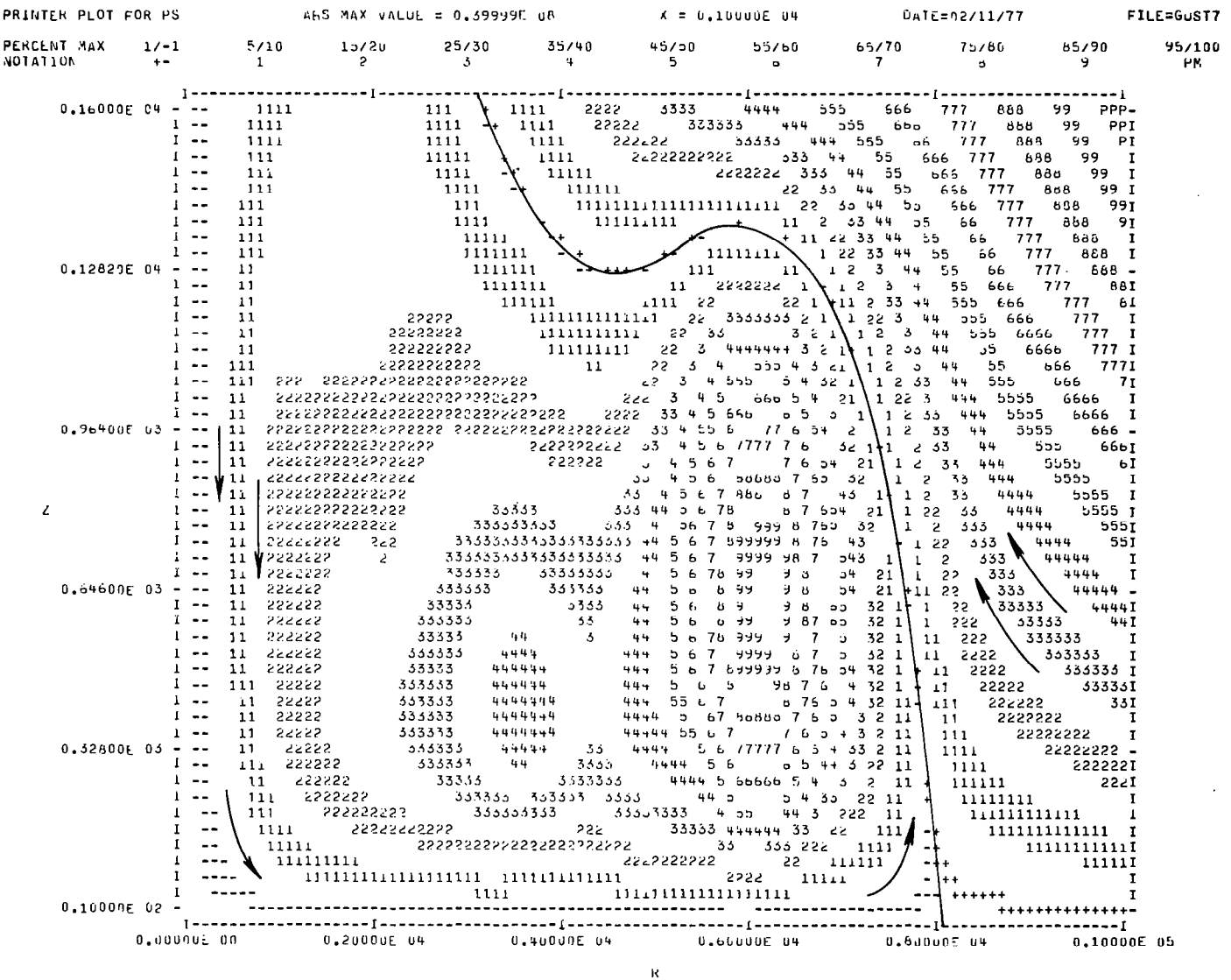

Figure 2.3.7. As above but t = 1000 sec. [See figure 2.3.2 for explanation of notation.]

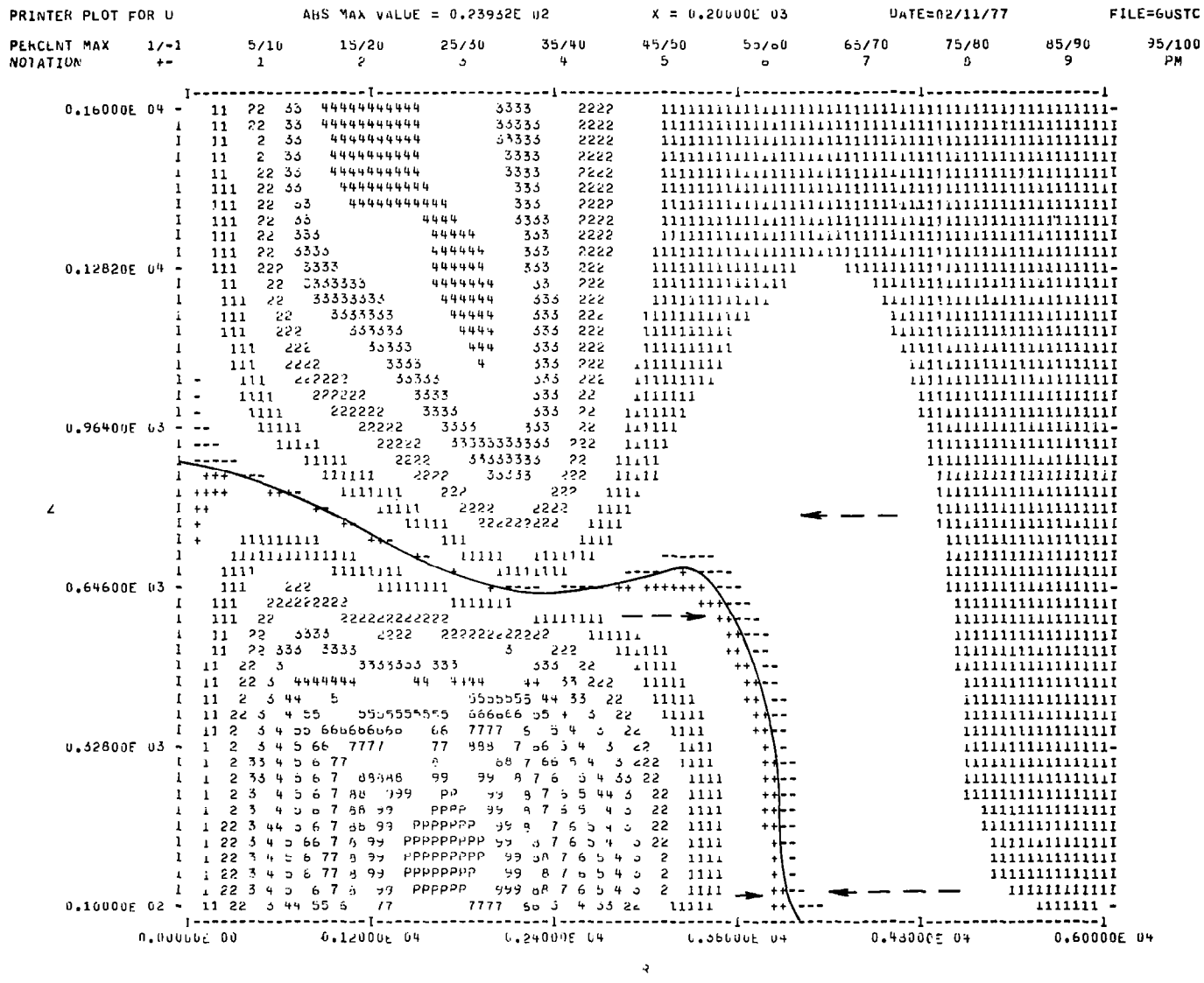

Figure 2.3.8. Normalized mean radial velocity contours as a function of z and R for an axisymmetric gust front with a 2000 m radius downdraft at t = 200 sec. [See figure 2.3.2 for explanation of notation.]

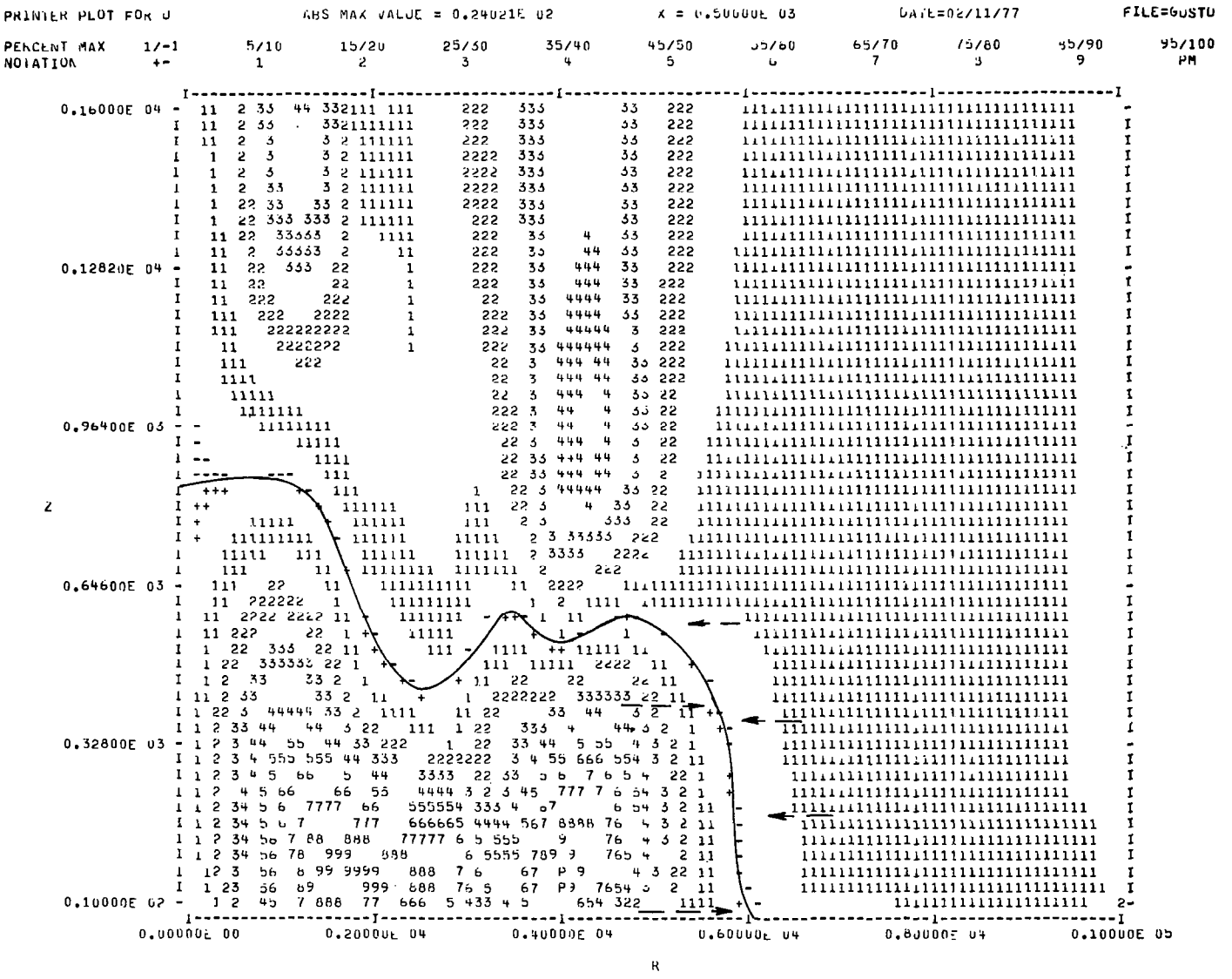

Figure 2.3.9. As above but t = 500 sec. [See figure 2.3.2 for explanation of notation.]

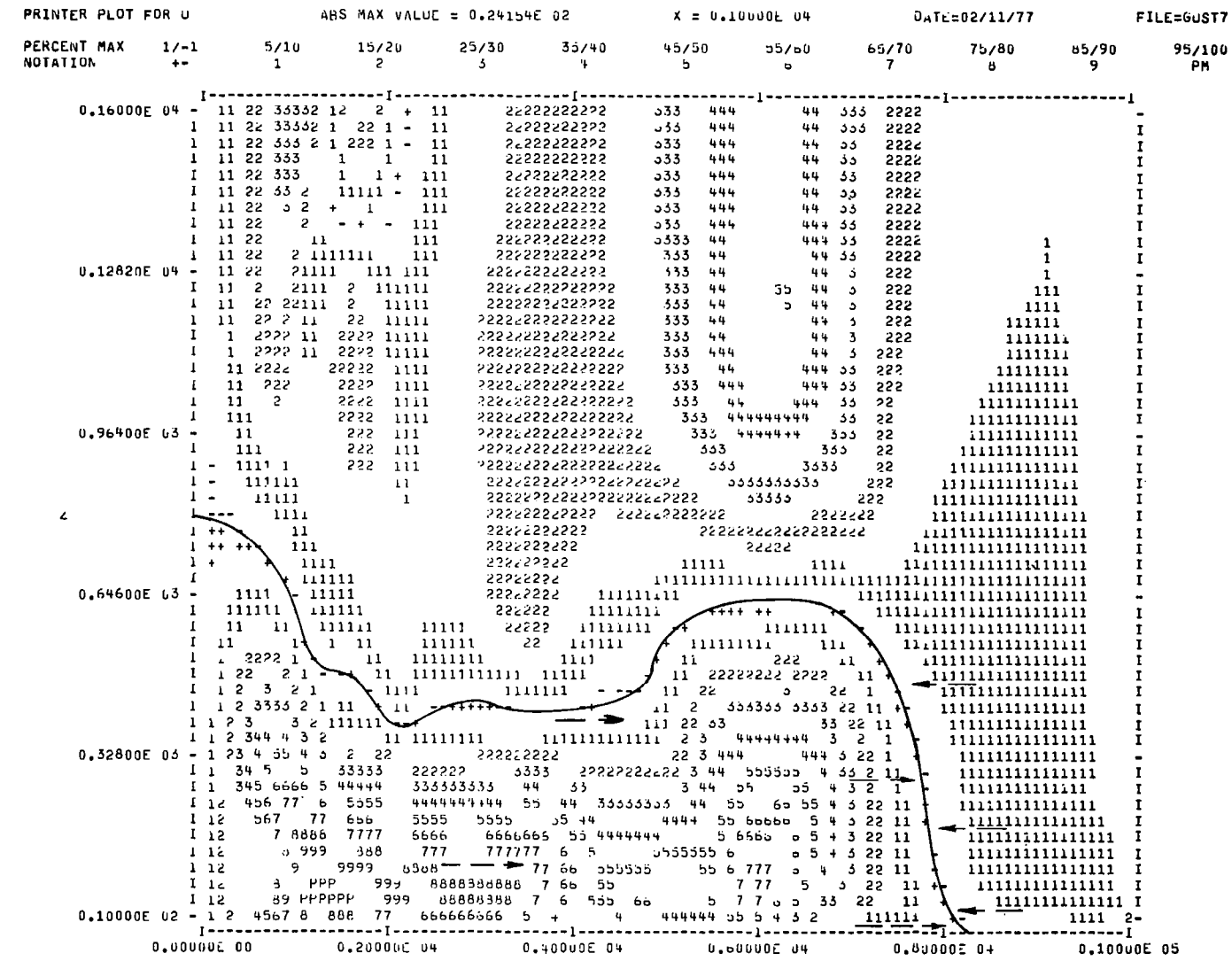

Figure 2.3.10. As above but t = 1000 sec. [See figure 2.3.2 for explanation of notation.]

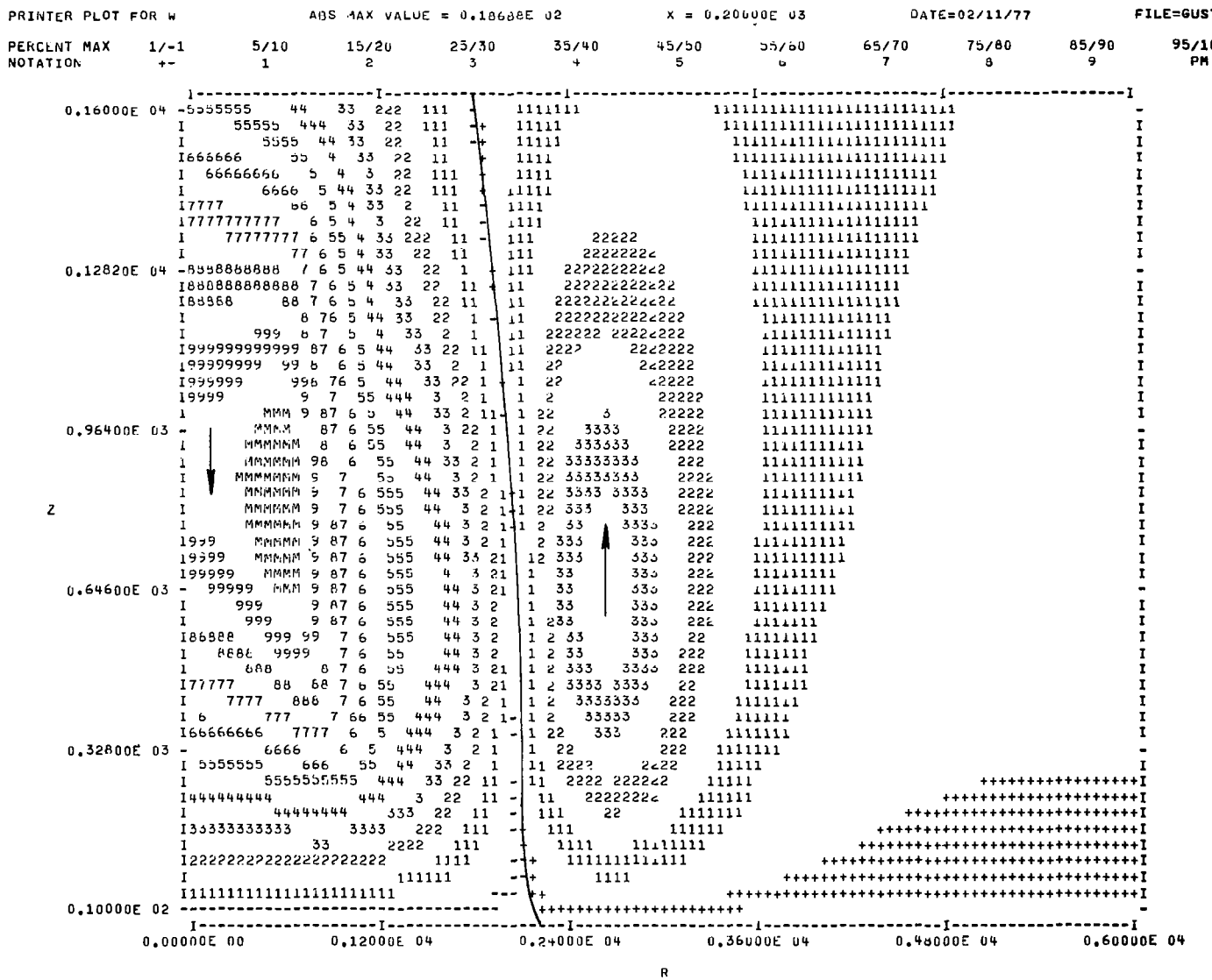

Figure 2.3.11. Normalized mean vertical velocity contours as a function of z and R for an axisymmetric gust front with a 2000 m radius downdraft at t = 200 sec. [See figure 2.3.2 for explanation of notation.]

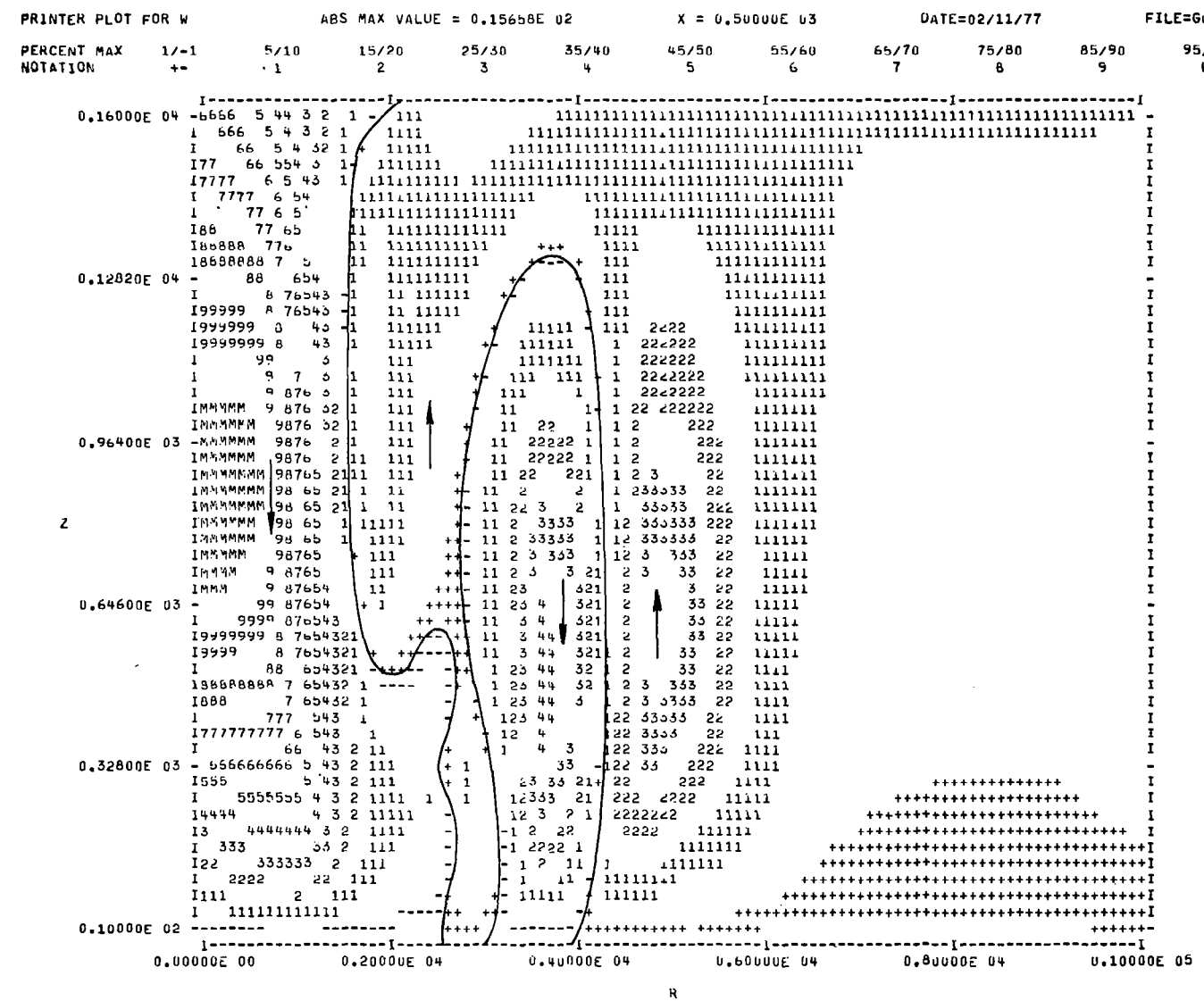

Figure 2.3.12. As above but t = 500 sec. [See figure 2.3.2 for explanation of notation.]

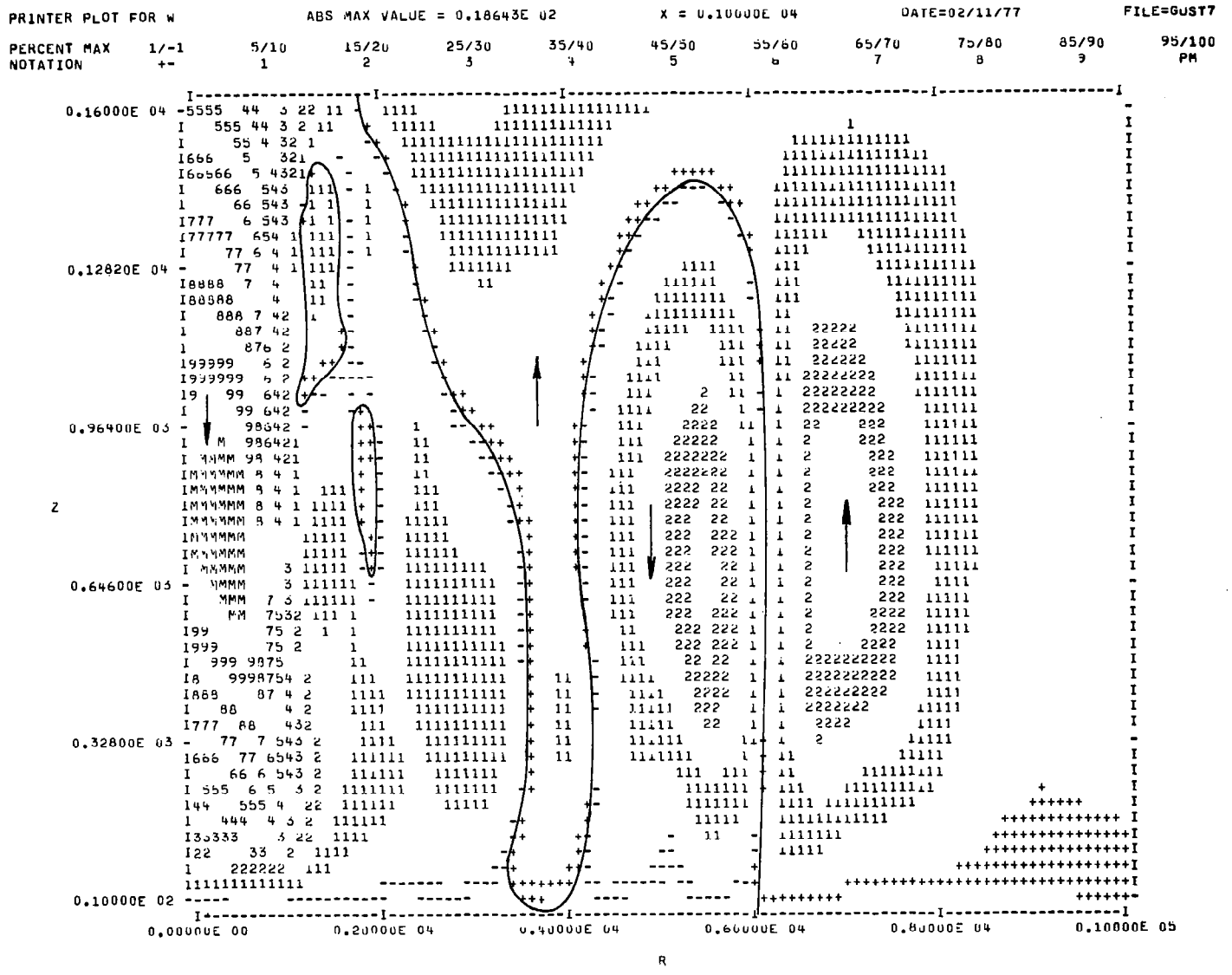

Figure 2.3.13. As above but t = 1000 sec. [See figure 2.3.2 for explanation of notation.]

We show the vertical energy component w'w' in figures 2.3.14 - 2.3.16. At $t = 200$ sec the largest values occur in the region of greatest production - near the centerline at the surface. Subsequent profiles at 500 and 1000 sec show the development near the axis, and the decay of generated turbulence in the gust front region.

A straight trade-off between potential energy and kinetic energy suggests that the maximum winds in the gust front will vary roughly as the square root of the product of the temperature defect and the characteristic height of the region of depressed temperature. In fact this rough scaling agrees quite well for both the maximum velocity of the downdraft and the maximum velocity of the radial outflow. The maximum mean velocity occurs at some altitude before the jet starts to stagnate as it approaches the surface. Thus, the height associated with W is less than that for U.

Typical cross-sectional contours of the scale length Λ are shown in figures 2.3.17 - 2.3.19 for these same times.

Three different computations of this type have been made to date. These are inadequate to clarify the sensitivity of the simulations to the boundary conditions but are useful to demonstrate the type of environment the pilot could have encountered at the time of the accidents studied in Section 4.

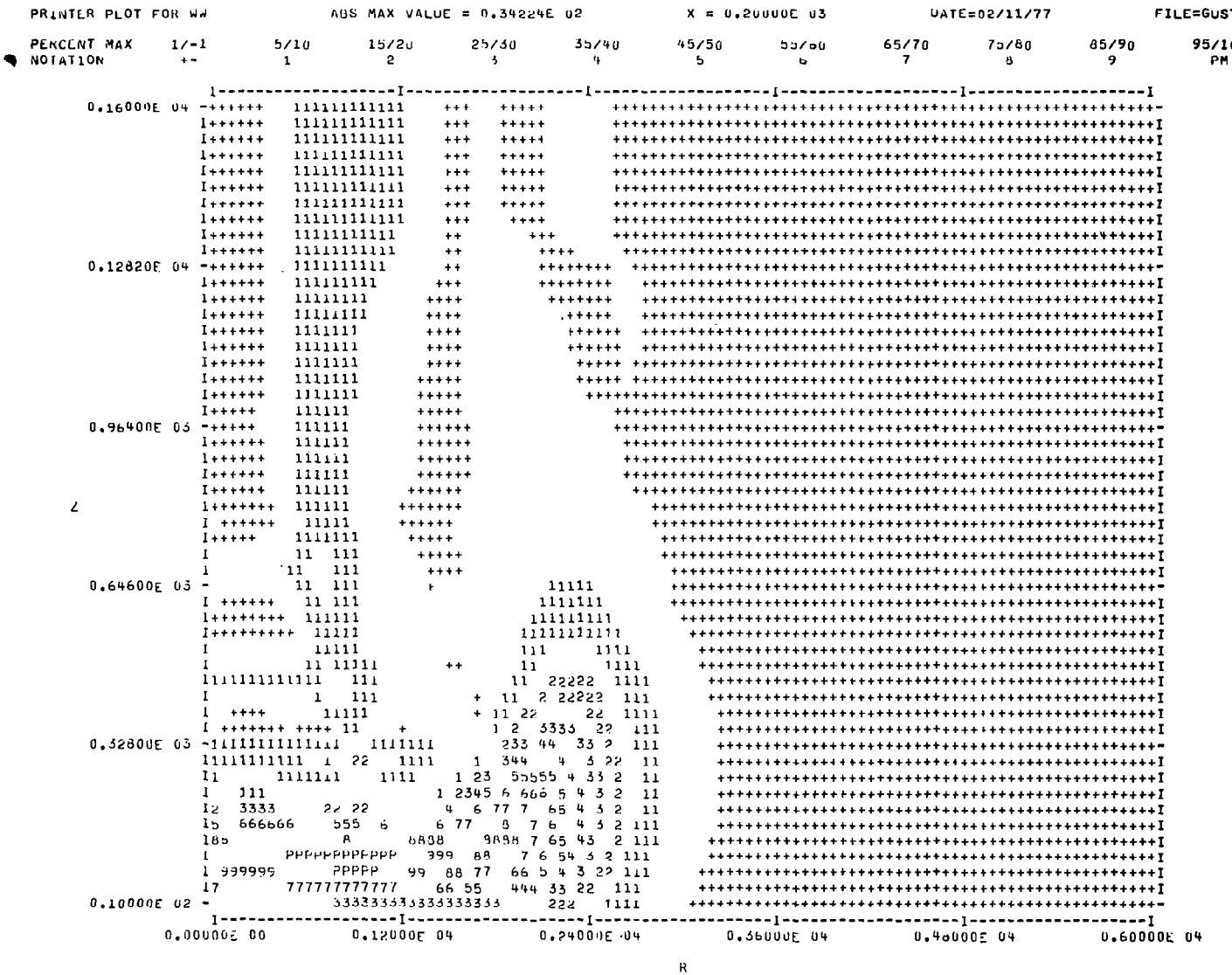

Figure 2.3.14. Normalized variance of vertical velocity contours as a function of z and R for an axisymmetric gust front with a 2000 m radius downdraft at t = 200 sec. [See figure 2.3.2 for explanation of notation.]

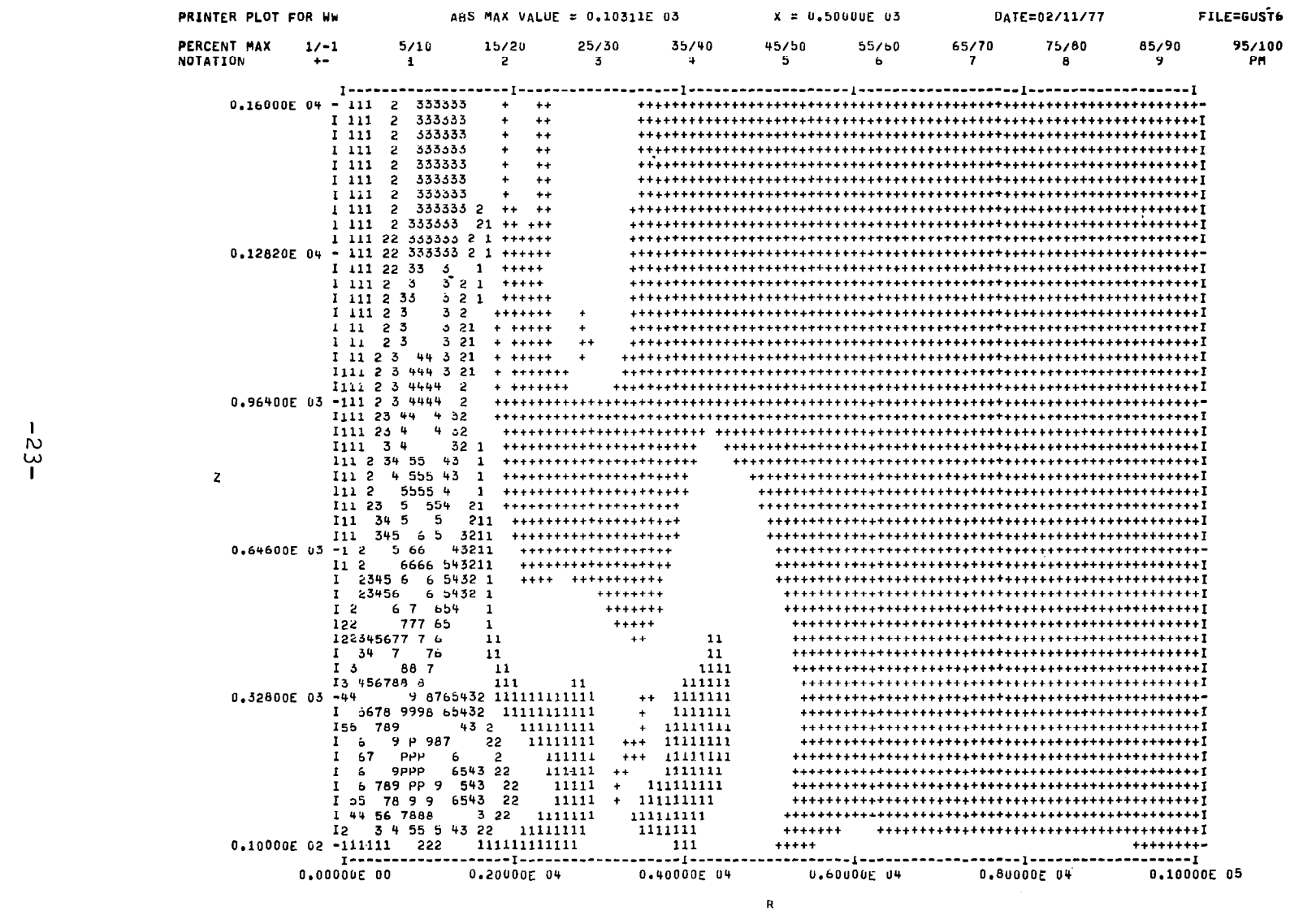

Figure 2.3.15. As above but t = 500 sec. [See figure 2.3.2 for explanation of notation.]

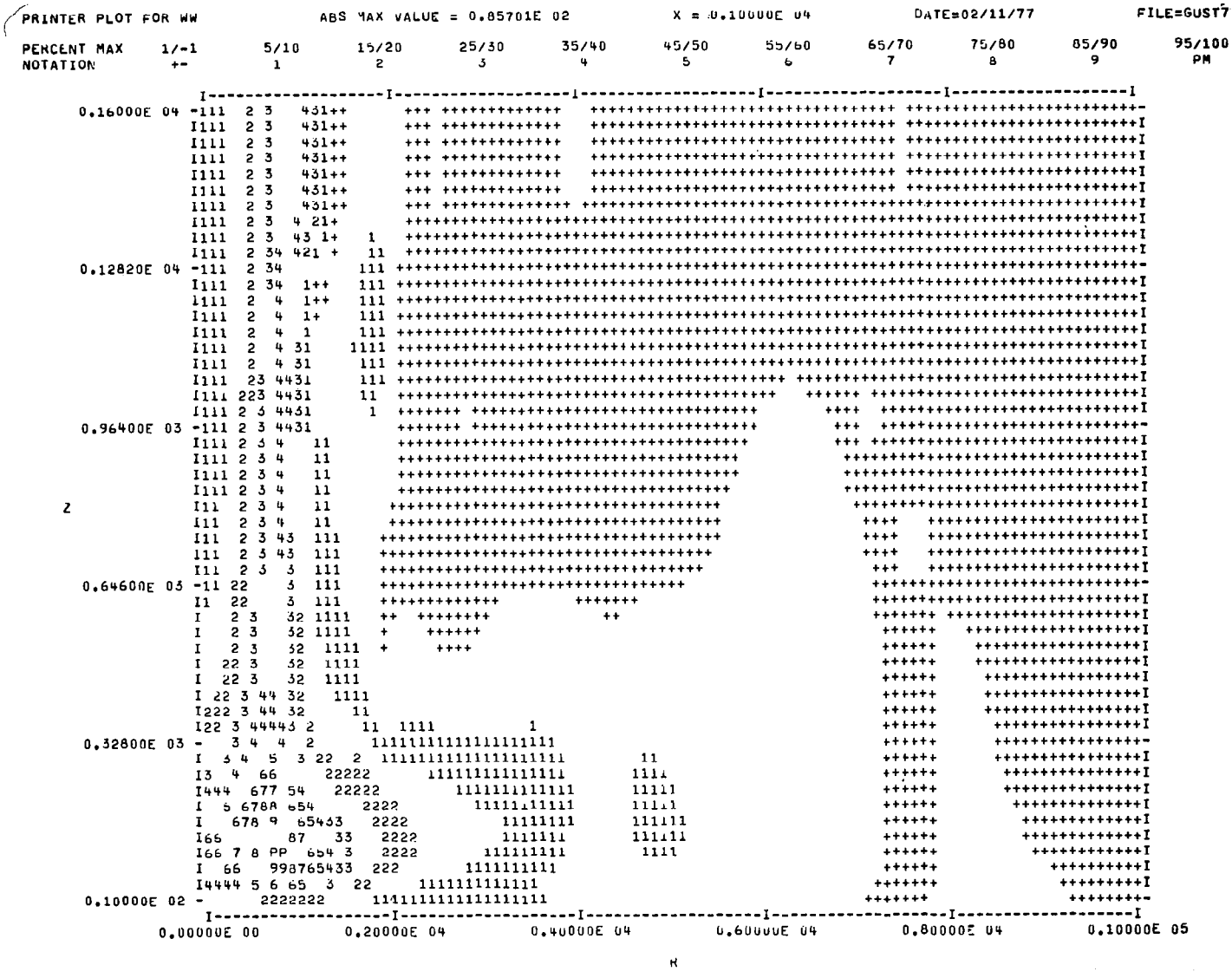

Figure 2.3.16. As above but t = 1000 sec. [See figure 2.3.2 for explanation of notation.]

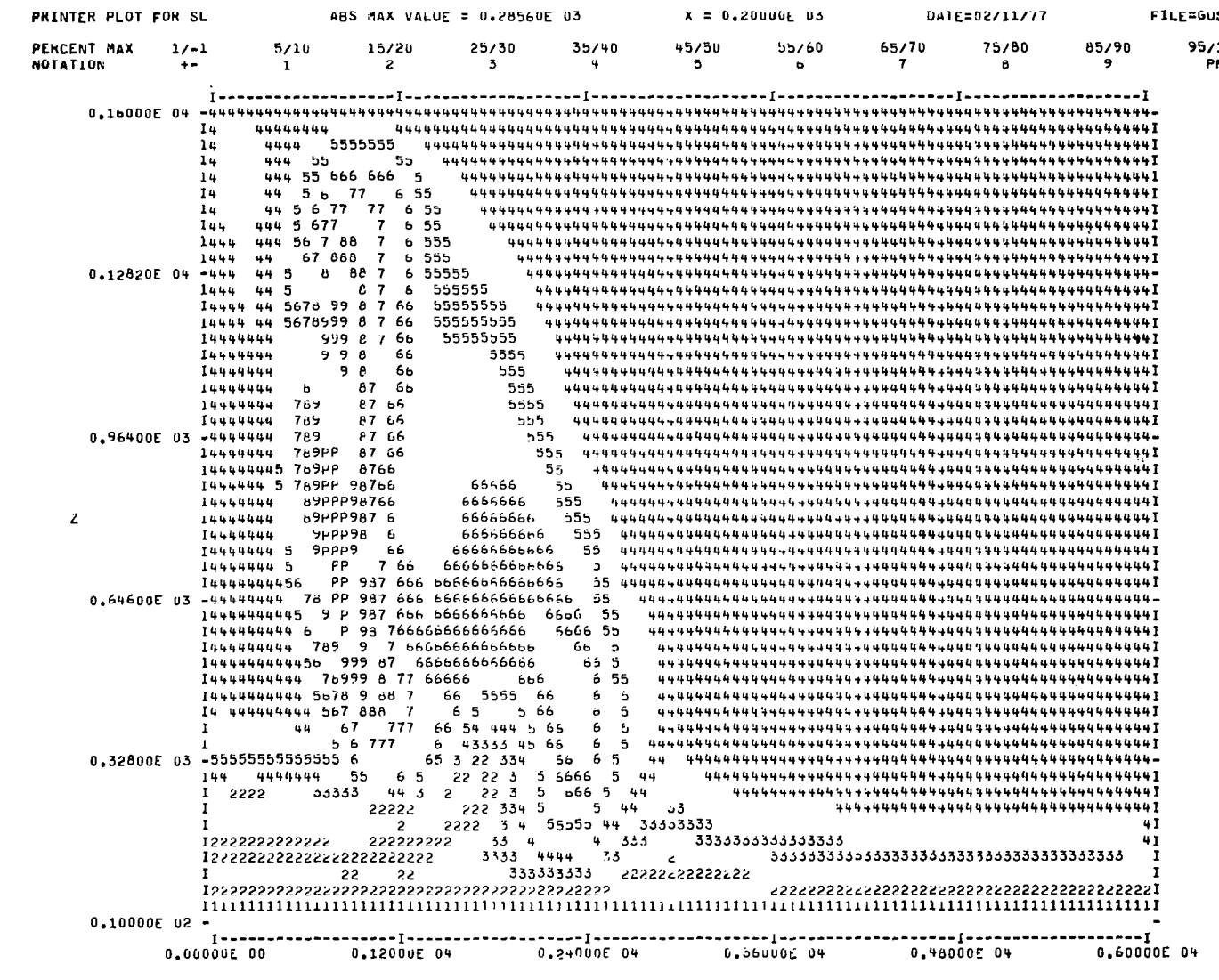

Figure 2.3.17. Normalized scale of turbulence contours as a function of z and R for an axisymmetric gust front with a 2000 m radius downdraft at t = 200 sec. [See figure 2.3.2 for explanation of notation.]

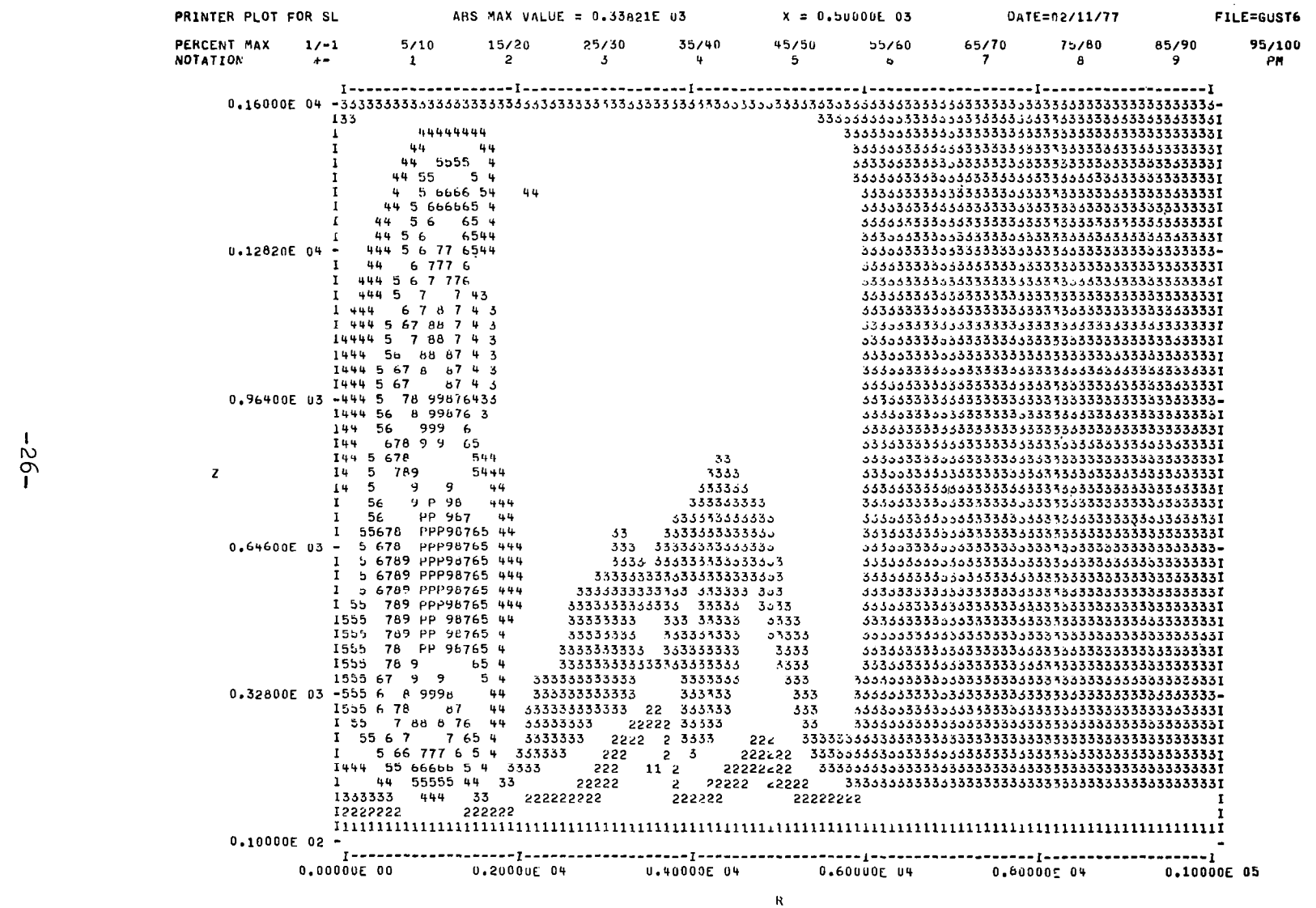

Figure 2.3.18. As above but t = 500 sec. [See figure 2.3.2 for explanation of notation.]

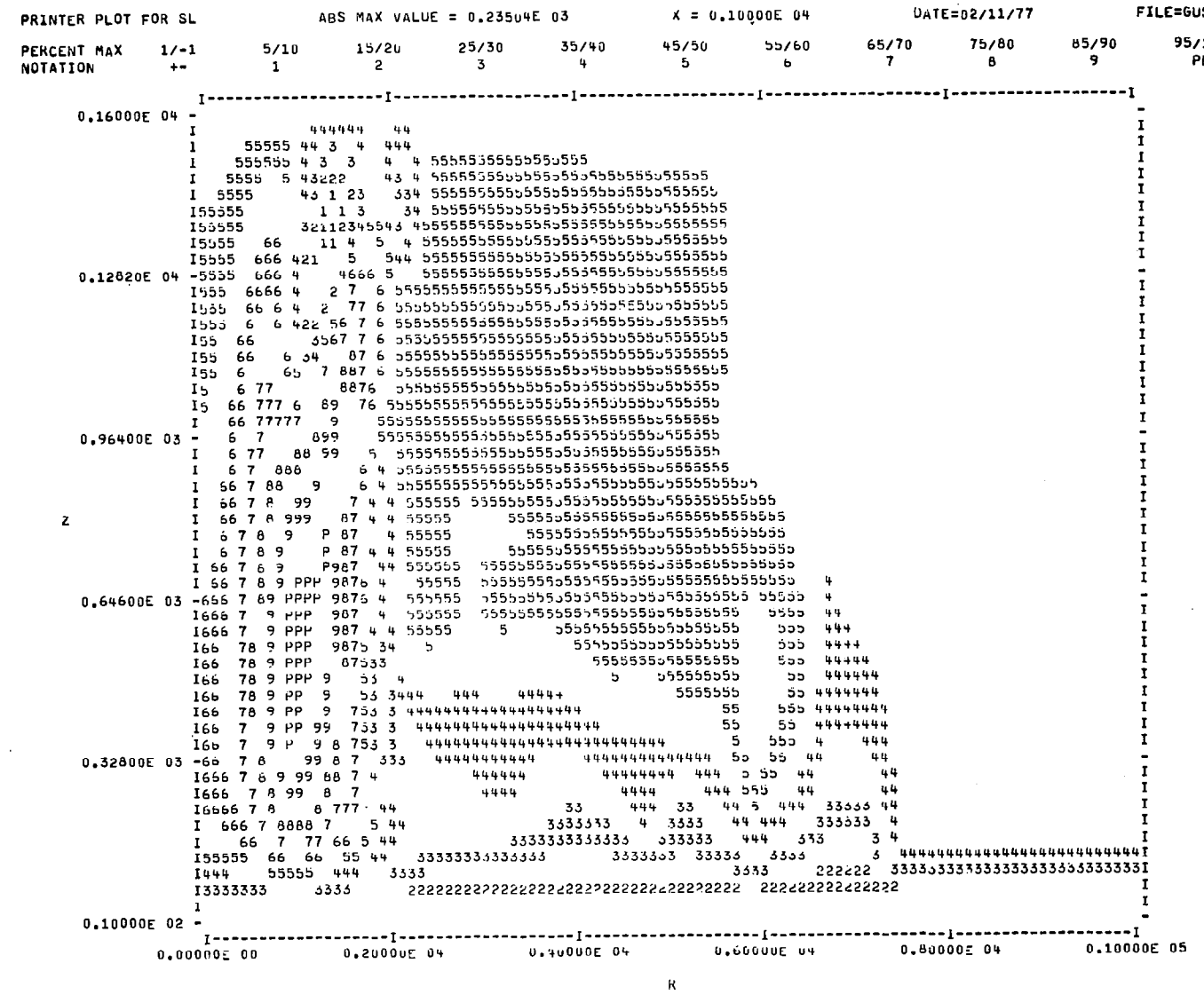

Figure 2.3.19. As above but t = 1000 sec. [See figure 2.3.2 for explanation of notation.]

3. ACCIDENT ENVIRONMENTS SIMULATED BY THE ONE-DIMENSIONAL MODEL

3.1 INTRODUCTION

In this section we present both the input boundary conditions and the model results for five accidents which have been modeled using the approach outlined in Section 2.2. These include both cases where well defined fronts appear to be passing at the time of the accident and where less well developed fronts, but still significant horizontal temperature gradients, are present. Any special peculiarities of the input conditions are noted for each case.

3.2 BOSTON, DECEMBER 1973

At 1543 l.s.t. on December 17, 1973 an Iberian Airlines DC-10 crashed while landing on Runway 33L at Logan Airport, Boston, Massachusetts. The aircraft was making an Instrument Landing System (ILS) autopilot coupled approach in rain and fog. The captain disengaged the autopilot three seconds after passing the middle marker (altitude = 60 m) at which point the aircraft was on glideslope. Nine seconds later the aircraft had pitched up and thrust was increased in order to arrest the rapid state of descent which had developed. Several seconds after this, the aircraft struck the approach light piers and then an embankment short of the runway (figure 3.2.1, Ref. 12).

The significant meteorological conditions in this case were rain and fog at the airport. A precipitation area 400 km in diameter encompassing the airport was observed on the Chatham weather radar. Only weak precipitation echoes showed over the accident site (figure 3.2.2). Surface weather charts showed a front in the general vicinity of the accident (figures 3.2.3-3.2.6). In addition, there existed a temperature differential between the land and the ocean. Either or both of these phenomena may have contributed to the geostrophic velocity differences existing between the surface and 850 mb altitude at 1300 l.s.t. and at 1600 l.s.t. The time variation of the geostrophic velocity distribution used was a linear interpolation between the profiles shown in figure 3.2.7 down to 200 m. Below this altitude the geostrophic velocity profile was altered to account for a horizontal temperature gradient assumed to start one hour before the accident (1443 l.s.t.) and remain until 1900 l.s.t. The magnitude and shape of the change in geostrophic velocity assumed is seen in the profile for U_g at 1900 l.s.t. The resulting velocity profiles at the time of the accident along with estimates obtained from flight recorder data and simulation studies are shown in figures 3.2.8 and 3.2.9.

The agreement in wind shear (.13 sec^{-1}) and surface velocity is good. However, the results obtained from the A.R.A.P. weather model extend the shear over a larger altitude interval, thus resulting in a 5 m/sec greater change in forward velocity. Agreement could be further improved by increasing the surface roughness

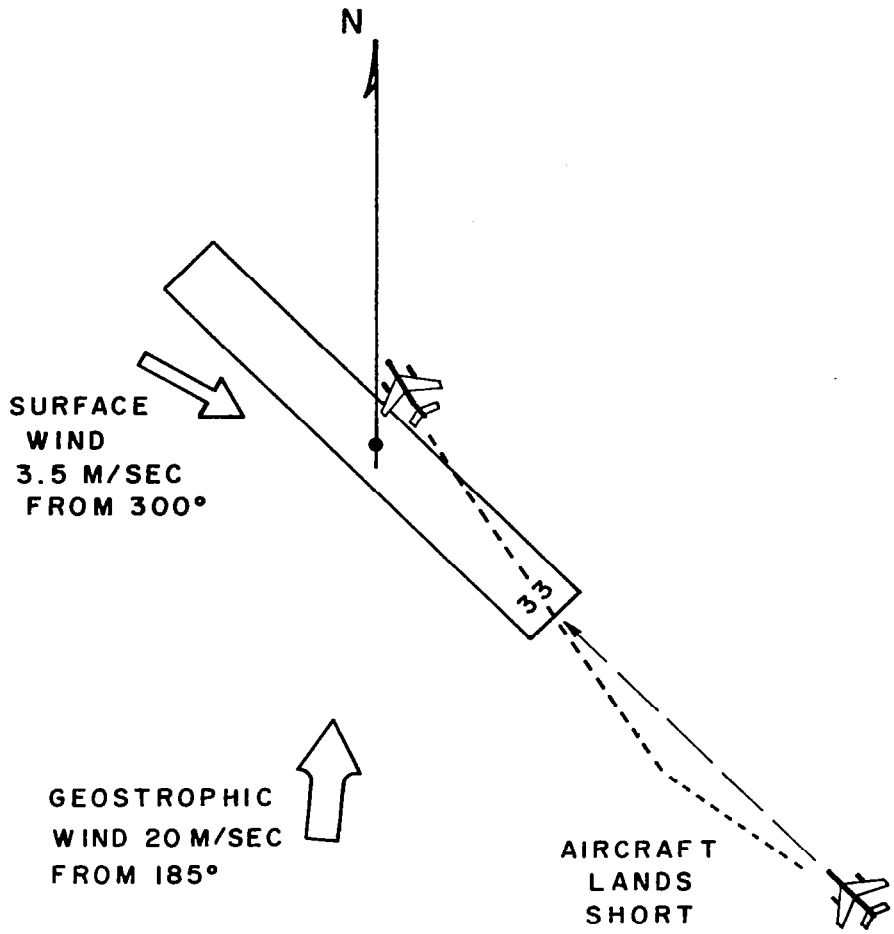

Figure 3.2.1. Aircraft-runway-winds orientation diagram for Boston, December 17, 1973 accident.

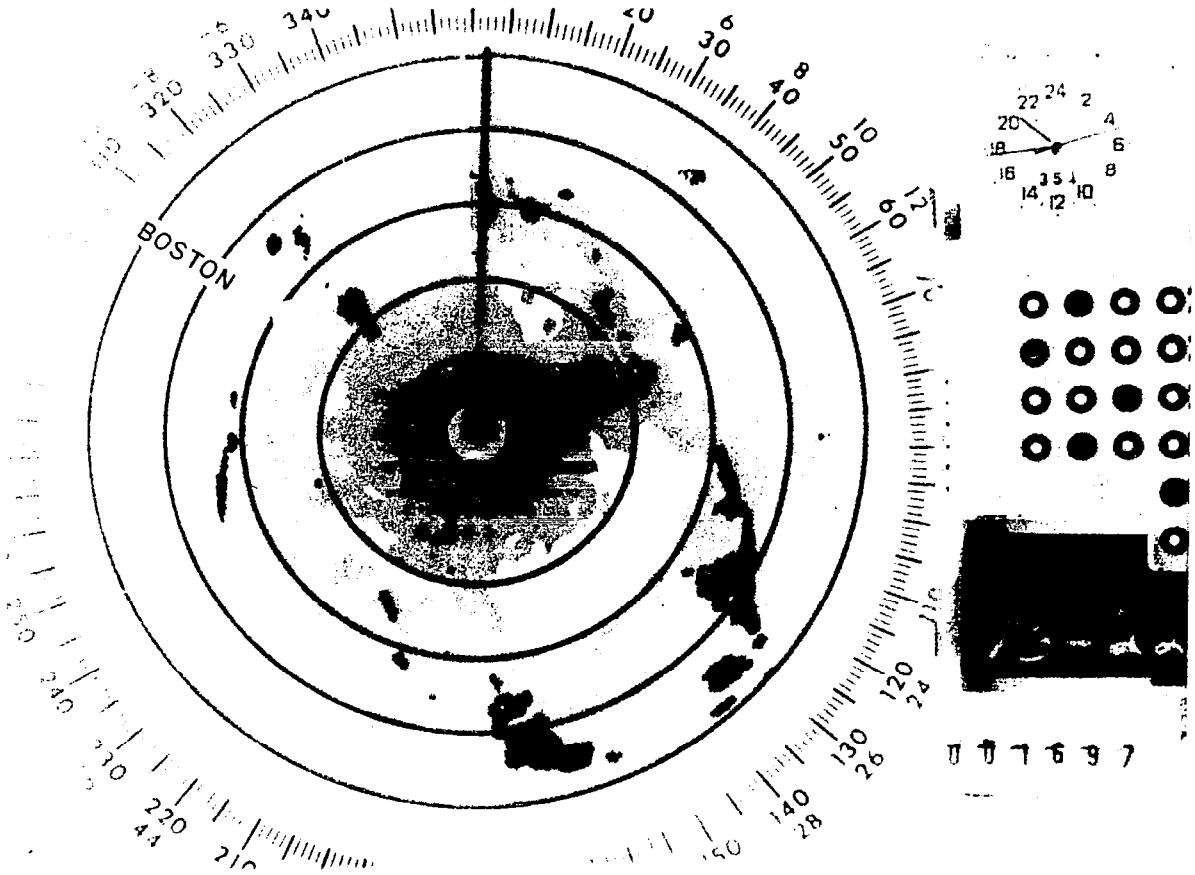

Figure 3.2.2. Radarscope picture near the time of Boston, December 17, 1973 accident.

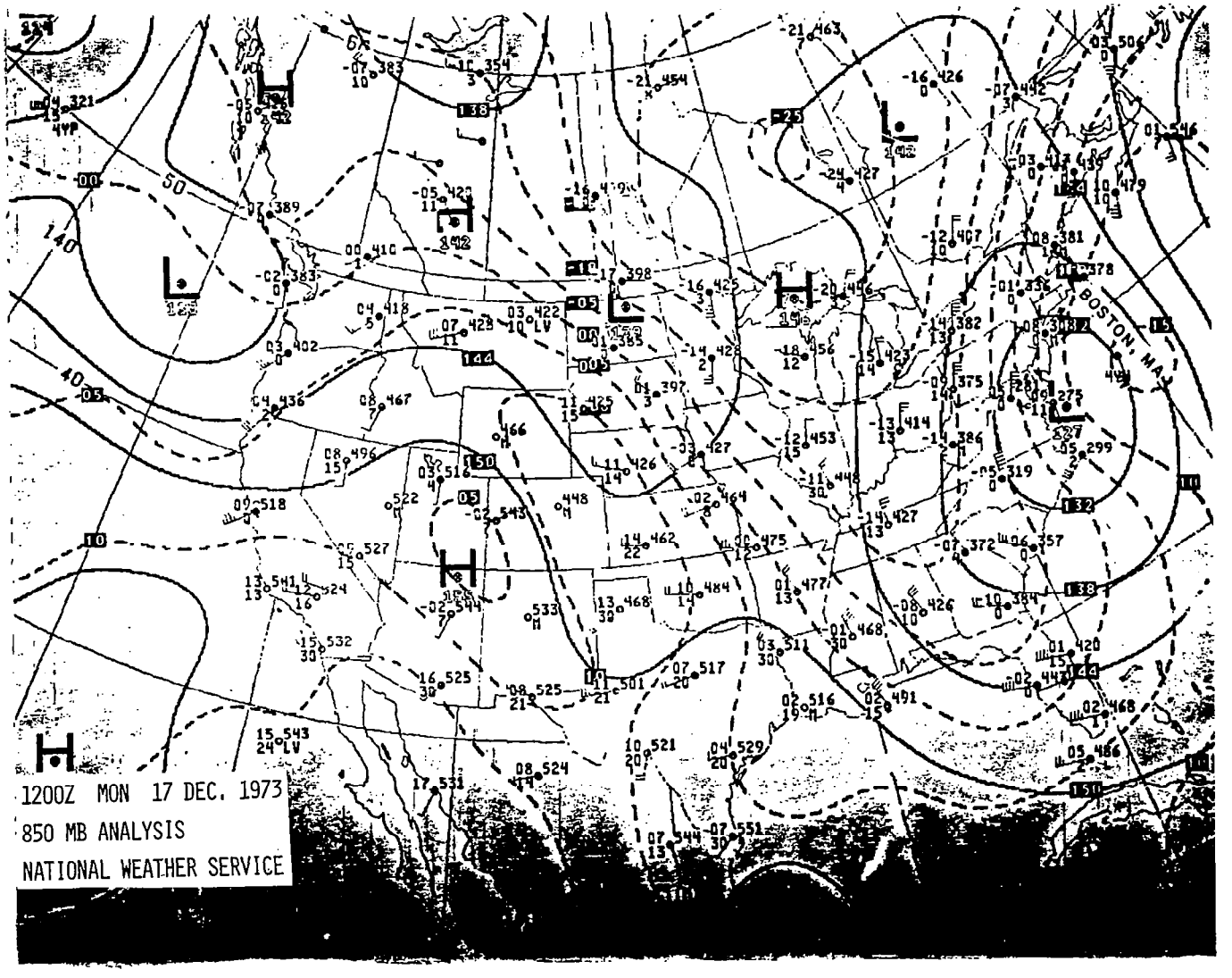

Figure 3.2.3. Early 850 mb chart for Boston, December 17, 1973 accident.

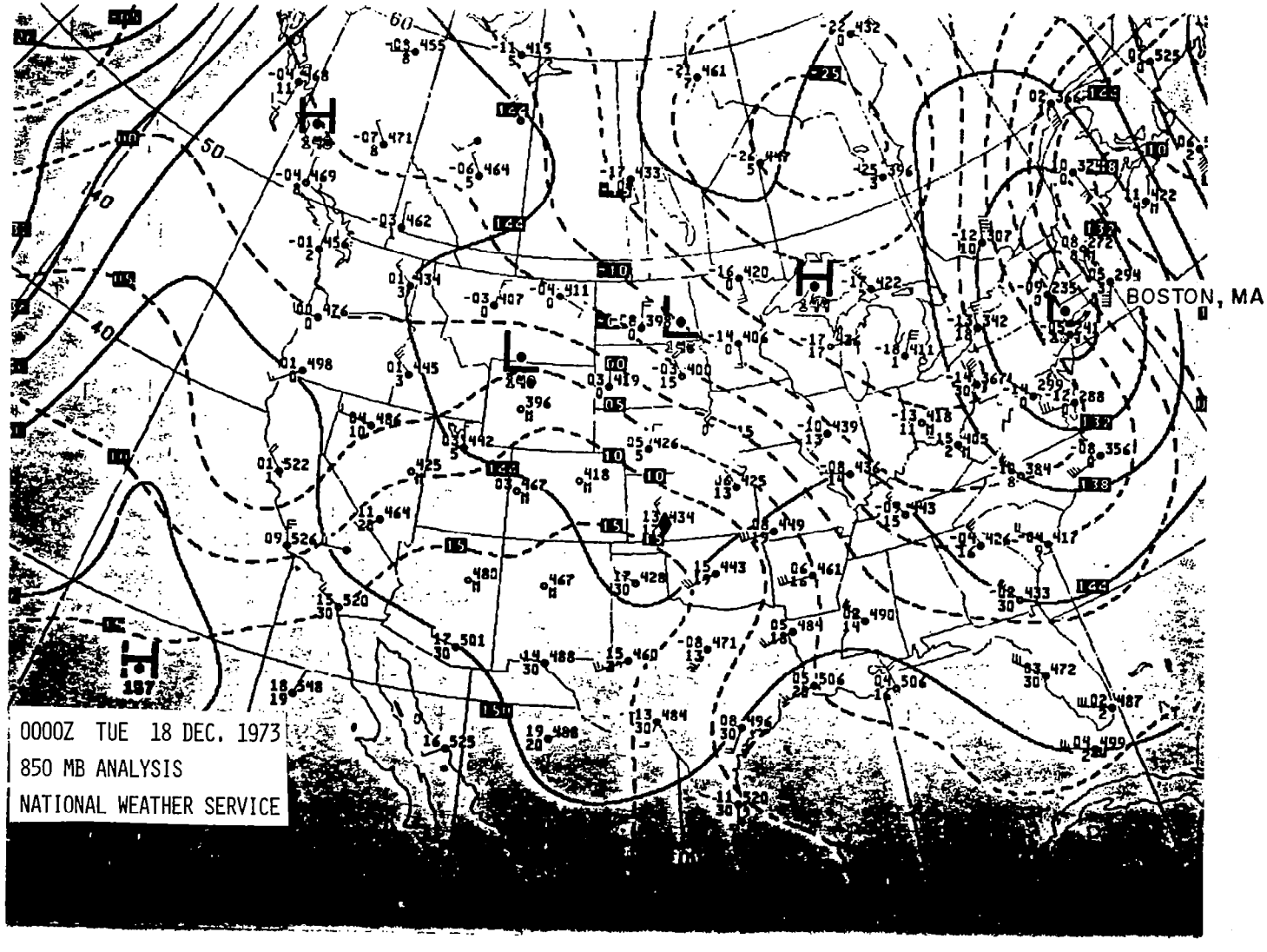

Figure 3.2.4. Late 850 mb chart for Boston, December 17, 1973 accident.

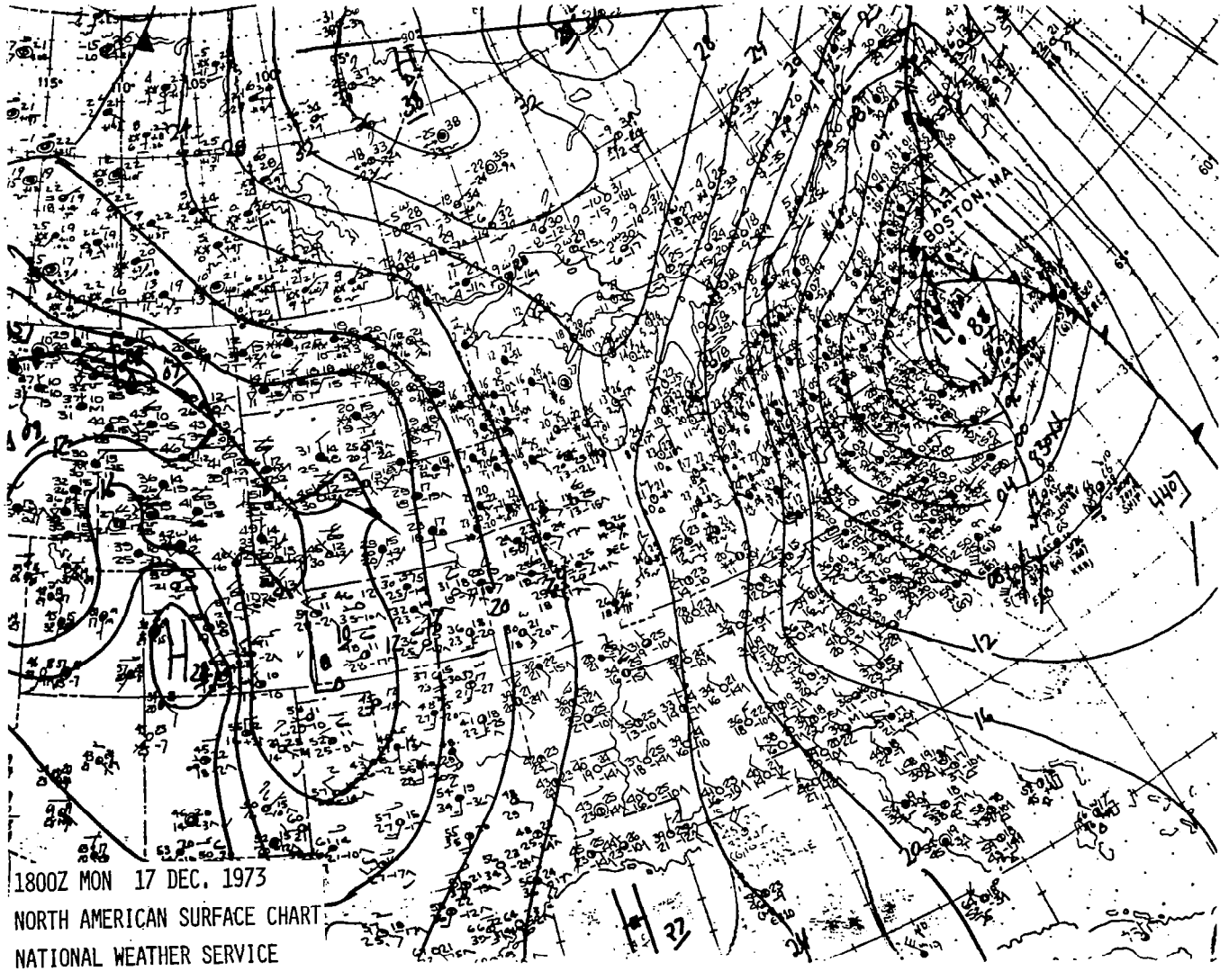

Figure 3.2.5. Early surface weather chart for Boston, December 17, 1973 accident.

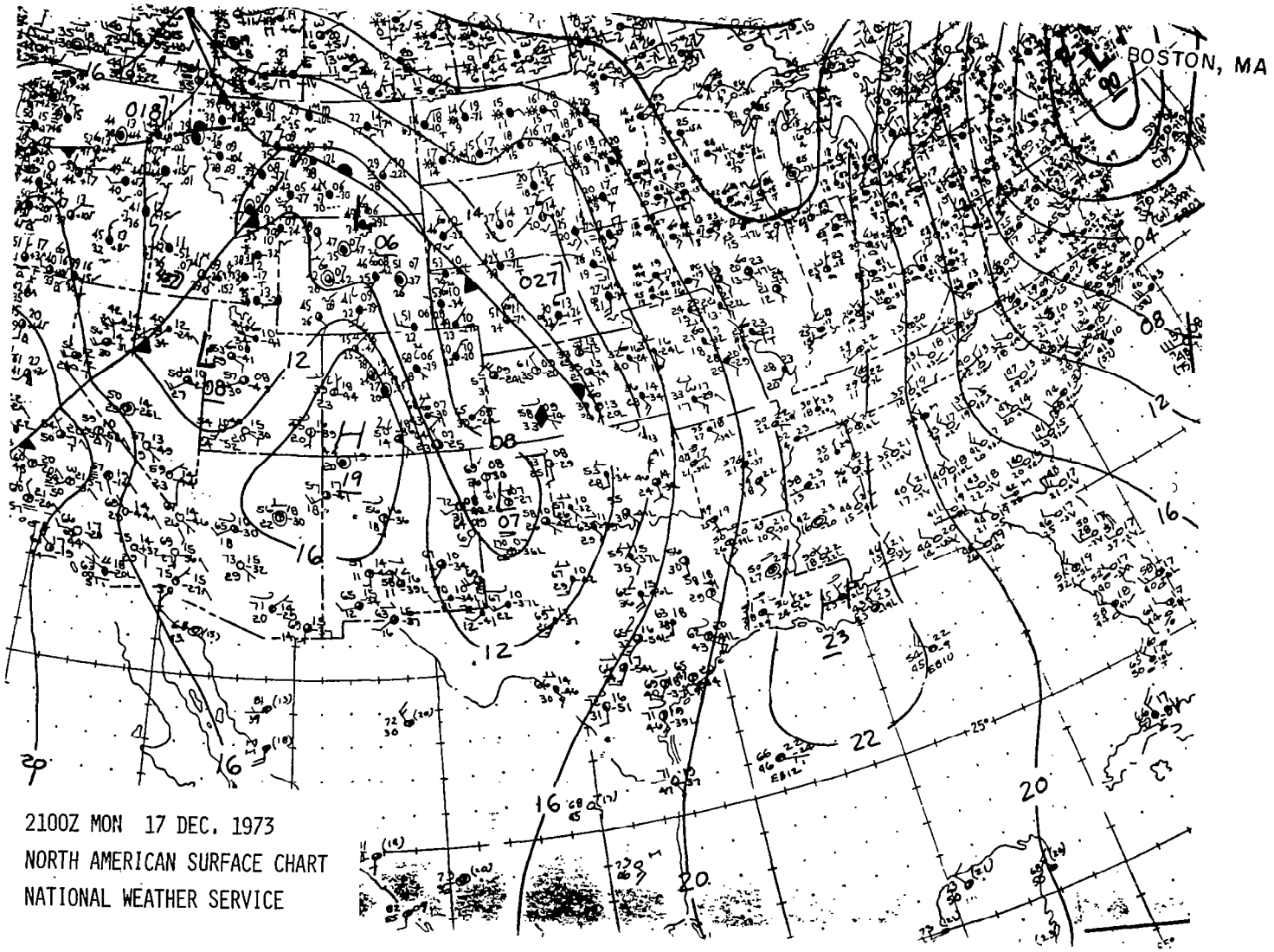

Figure 3.2.6. Late surface weather chart for Boston, December 17, 1973 accident.

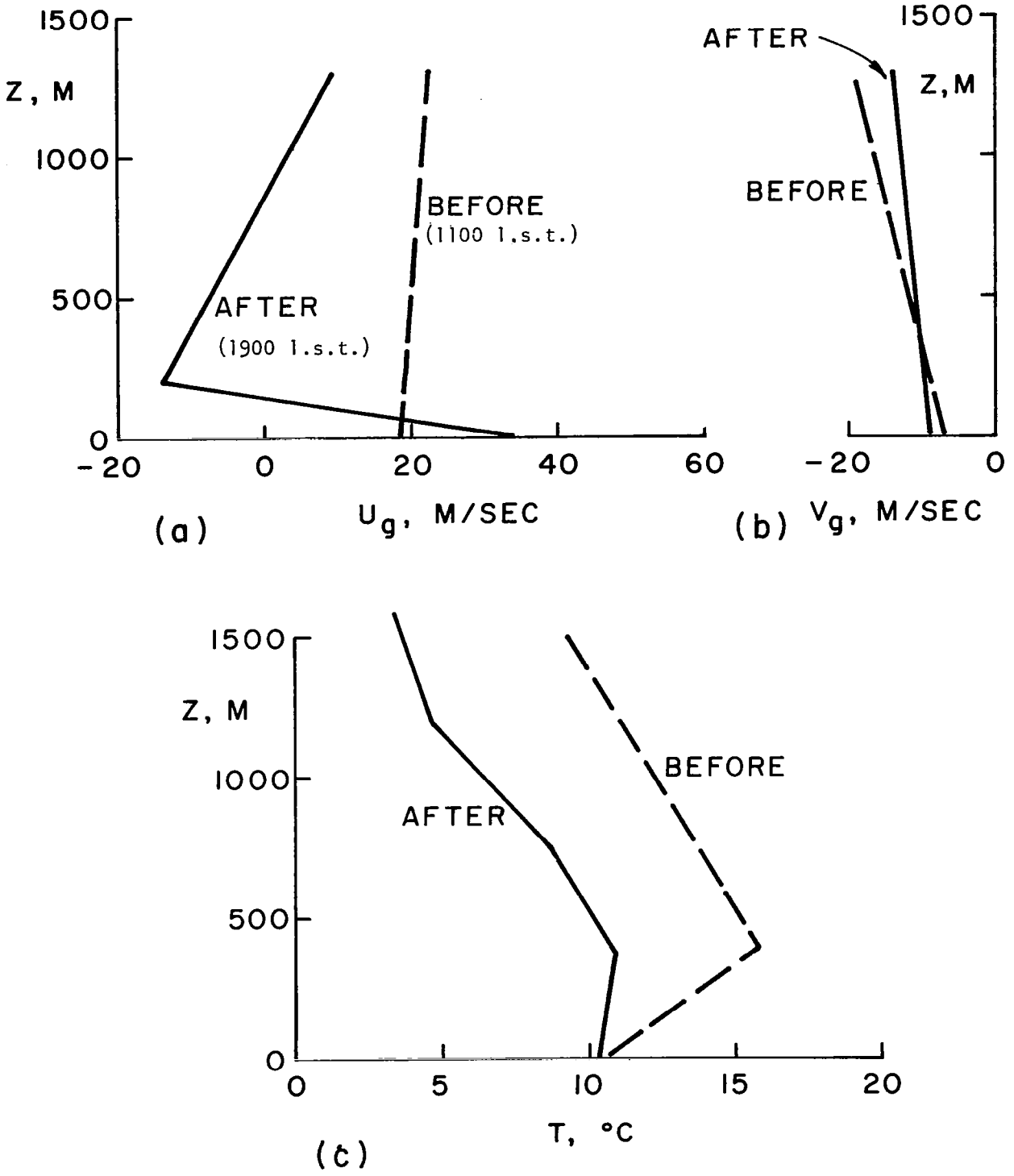

Figure 3.2.7. Altitude profiles for; a) mean geostrophic velocity component parallel to runway (+ U_g, tailwind), b) mean wind velocity component perpendicular to runway (+ V_g, crosswind from right), c) temperature before and after the Boston December 17, 1973 accident.

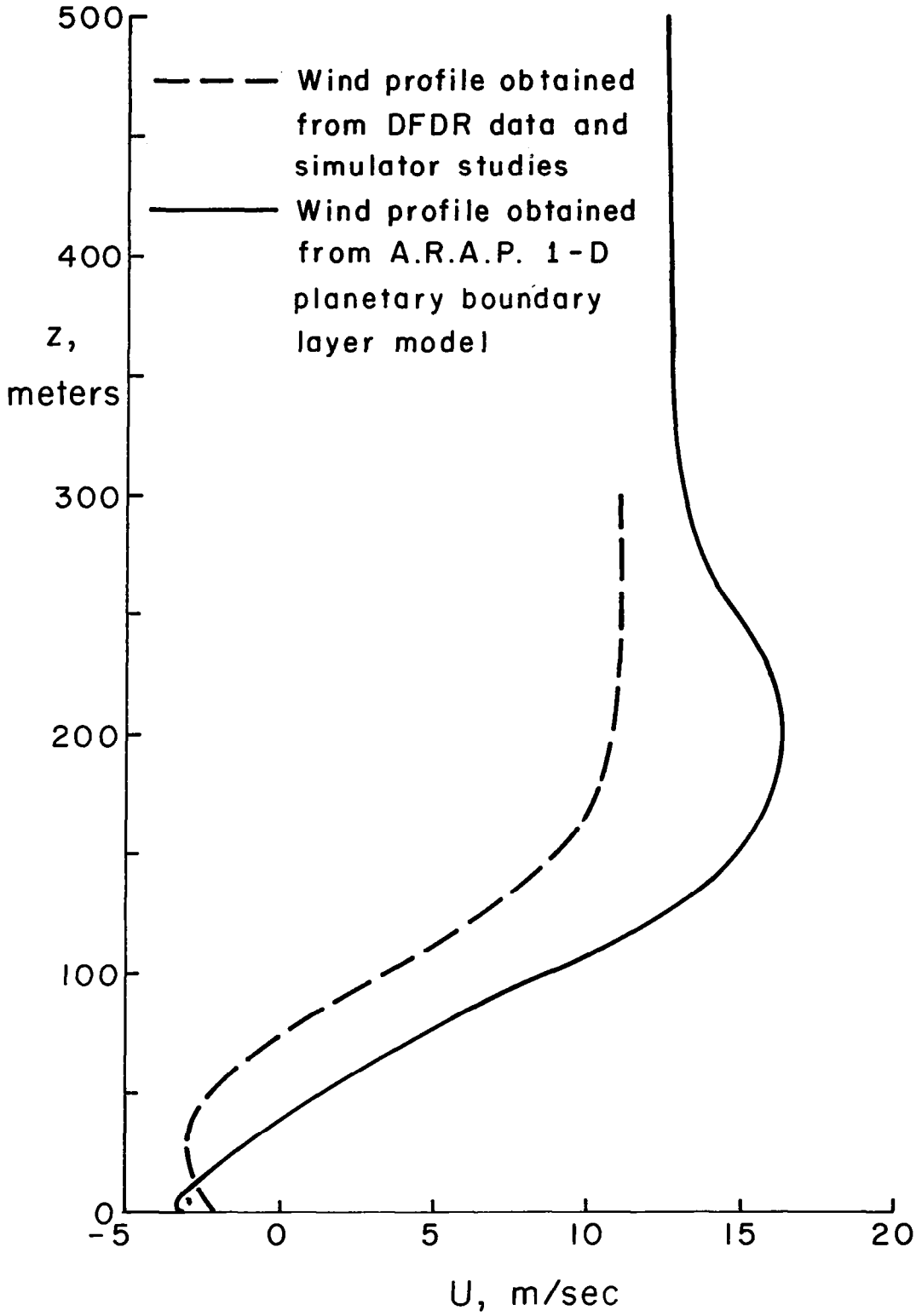

Figure 3.2.8. Altitude profile of mean wind velocity component parallel to runway (+ U, tailwind) for Boston, December 17, 1973 accident.

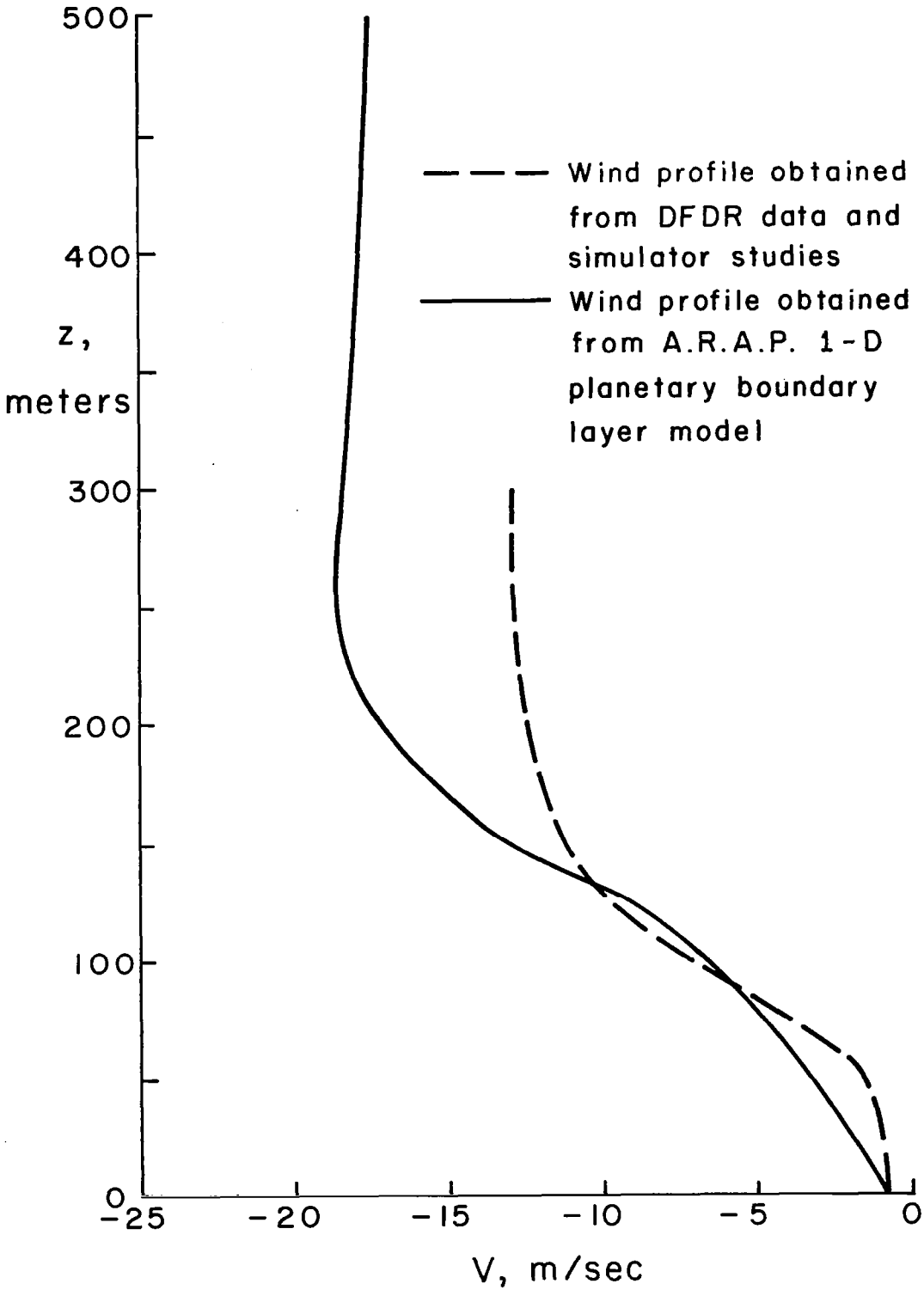

Figure 3.2.9. Altitude profile of mean wind velocity component perpendicular to runway (+ V, crosswind from right) for Boston, December 17, 1973 accident.

dimension from .01 to .1 m. However, the present run is certainly representative and does present even more of a challenge for pilots and autopilots to experience via flight simulation studies. The crosswind shear and turbulence characteristics (figures 3.2.9 - 3.2.14) should not complicate the approach and landing tasks.

3.3 LA GUARDIA, JANUARY 1971

At 1832 l.s.t. on January 4, 1971 an FAA DC-3 crashed attempting to land on Runway 4 at La Guardia Airport, New York. The aircraft was making an ILS approach and landed 600 m short of the runway threshold (figure 3.3.1). Several other pilots reported that they had encountered wind shear on approach strong enough to require significant changes in power setting (Ref. 13).

At the time of the accident radiosonde measurements made at JFK airport show a strong tailwind above 1000 m (30 m/sec from 220° - 240°). Surface weather observations indicate a headwind (6 m/sec from 60°) thus, a reasonable shear may be expected on approach to Runway 4. Consistent with this, the surface weather charts (figures 3.3.2 - 3.3.5) indicate a slowly moving warm front just east of La Guardia.

As a result of our investigation of free shear layers it appears appropriate to model a warm or cold front as an essentially discontinuous change in the geostrophic velocity (variation in U_g over a 10 m altitude layer). This permits turbulent mixing to determine a natural shear layer thickness consistent with the given velocity and temperature change.

For the purpose of this study it is assumed that the velocity change parallel to the front increased linearly over a one hour period, just prior to the accident. The height of the frontal shear layer is set at 200 m in order to best agree with the altitudes at which pilot reports of wind shear were given (between 360 m and 120 m). The geostrophic wind and temperature profiles are shown in figure 3.3.6.

Using these inputs and boundary conditions plus a roughness scale of 0.1 m the model yields the profiles for mean velocity, velocity variance and turbulence scale profiles given in figures 3.3.7-3.3.13.

As shown in figure 3.3.7 a 22 m/sec decrease in tailwind occurred between 350 m and 100 m. This is not only a large decrease in velocity but a reasonably large wind shear (.09 sec^{-1}). If power is not added during the descent phase the aircraft will drop below the glideslope and land short of the runway. This is particularly true if the visual cuing is degraded by rain, fog and darkness. The crosswind shear, in this case, is a factor of 3 lower (figure 3.3.8) and the maximum velocity variance is only 1.4 m/sec. The observed surface wind was 6 m/sec from 60° and that computed from our model at an altitude of 10 m, is 3.6 m/sec from 74°.

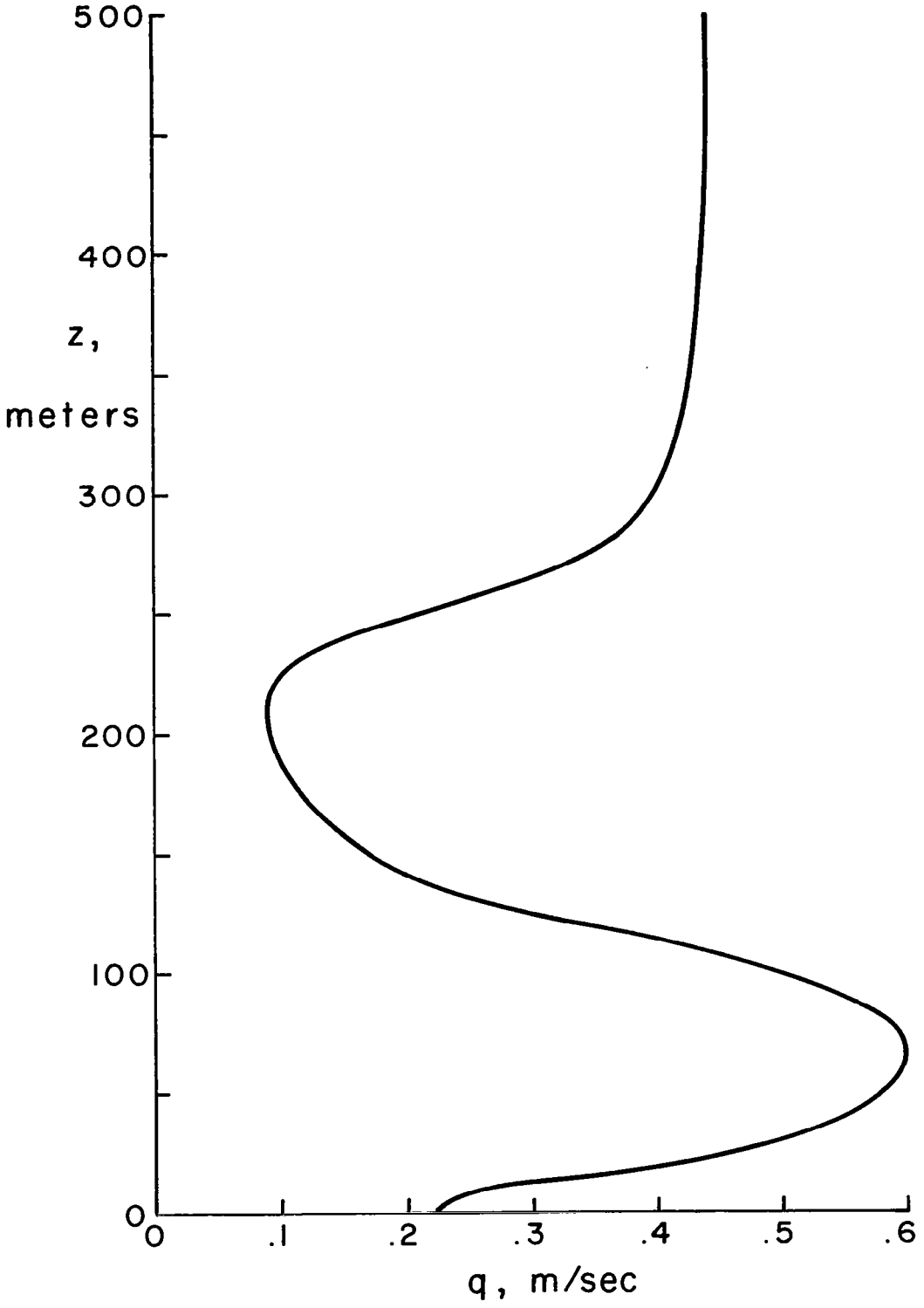

Figure 3.2.10. Altitude profile of variance of the total velocity for Boston, December 17, 1973 accident.

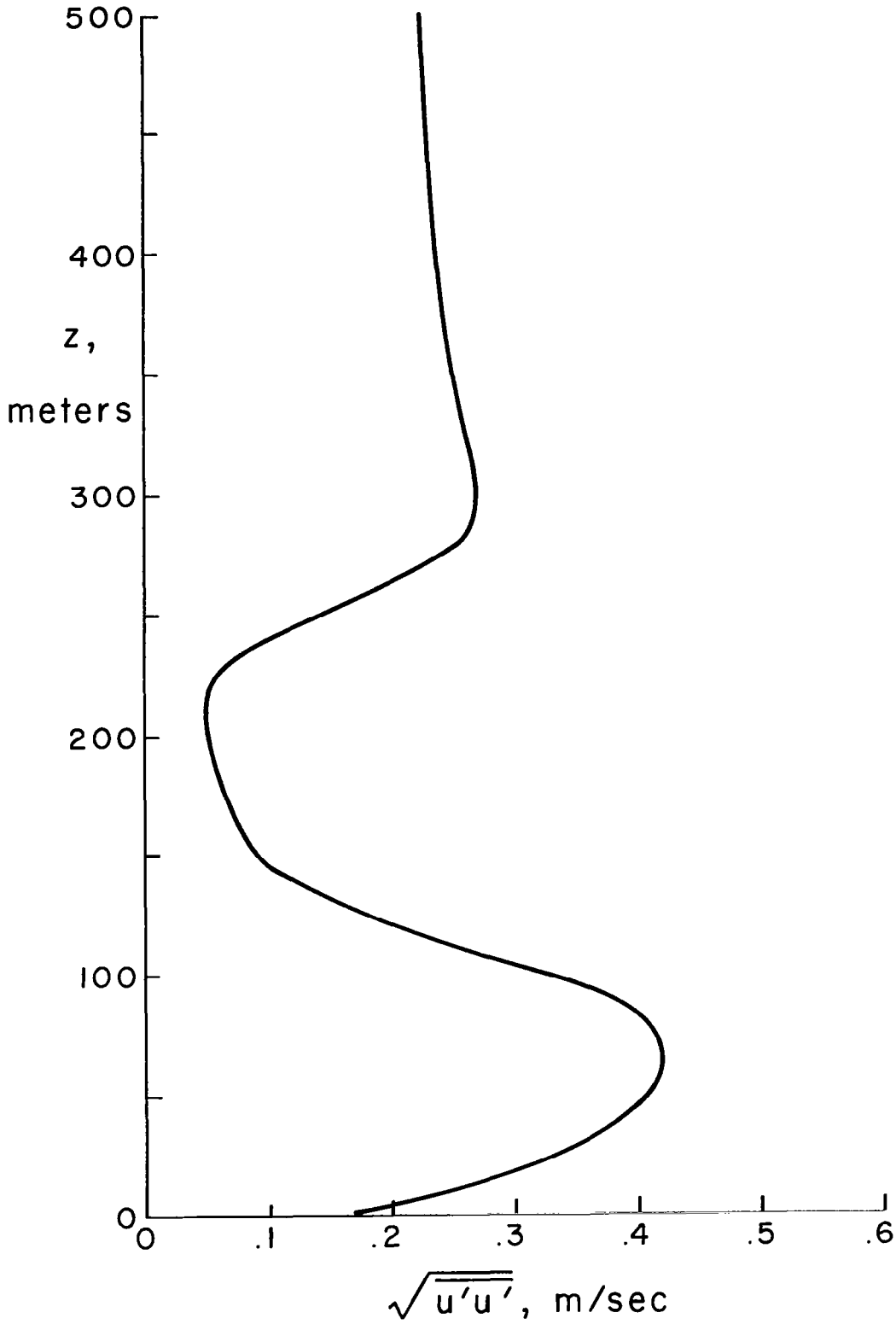

Figure 3.2.11. Altitude profile of variance of the wind parallel to runway for Boston, December 17, 1973 accident.

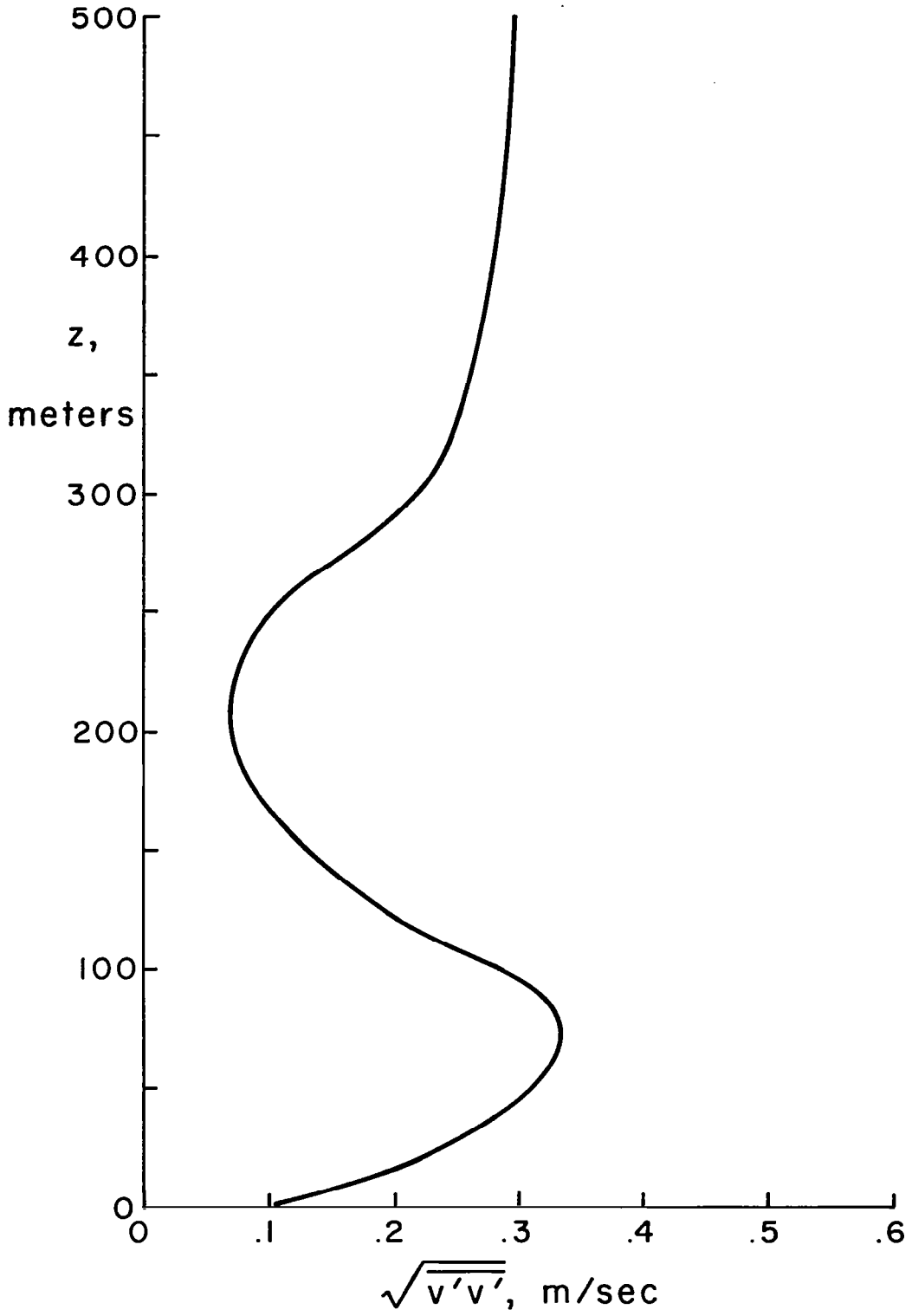

Figure 3.2.12. Altitude profile of variance of the wind perpendicular to runway for Boston, December 17, 1973 accident.

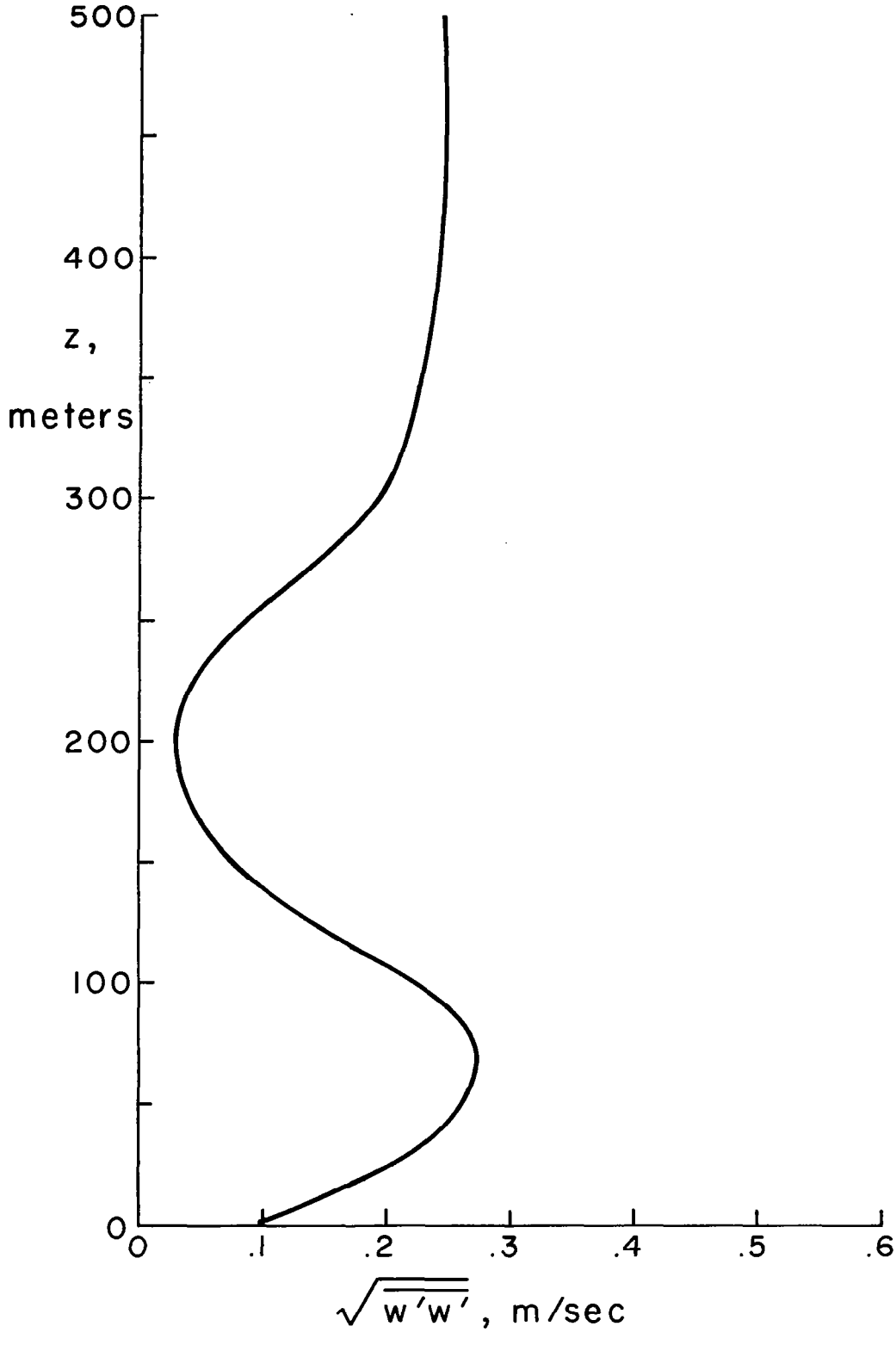

Figure 3.2.13. Altitude profile of variance of the vertical wind for Boston, December 17, 1973 accident.

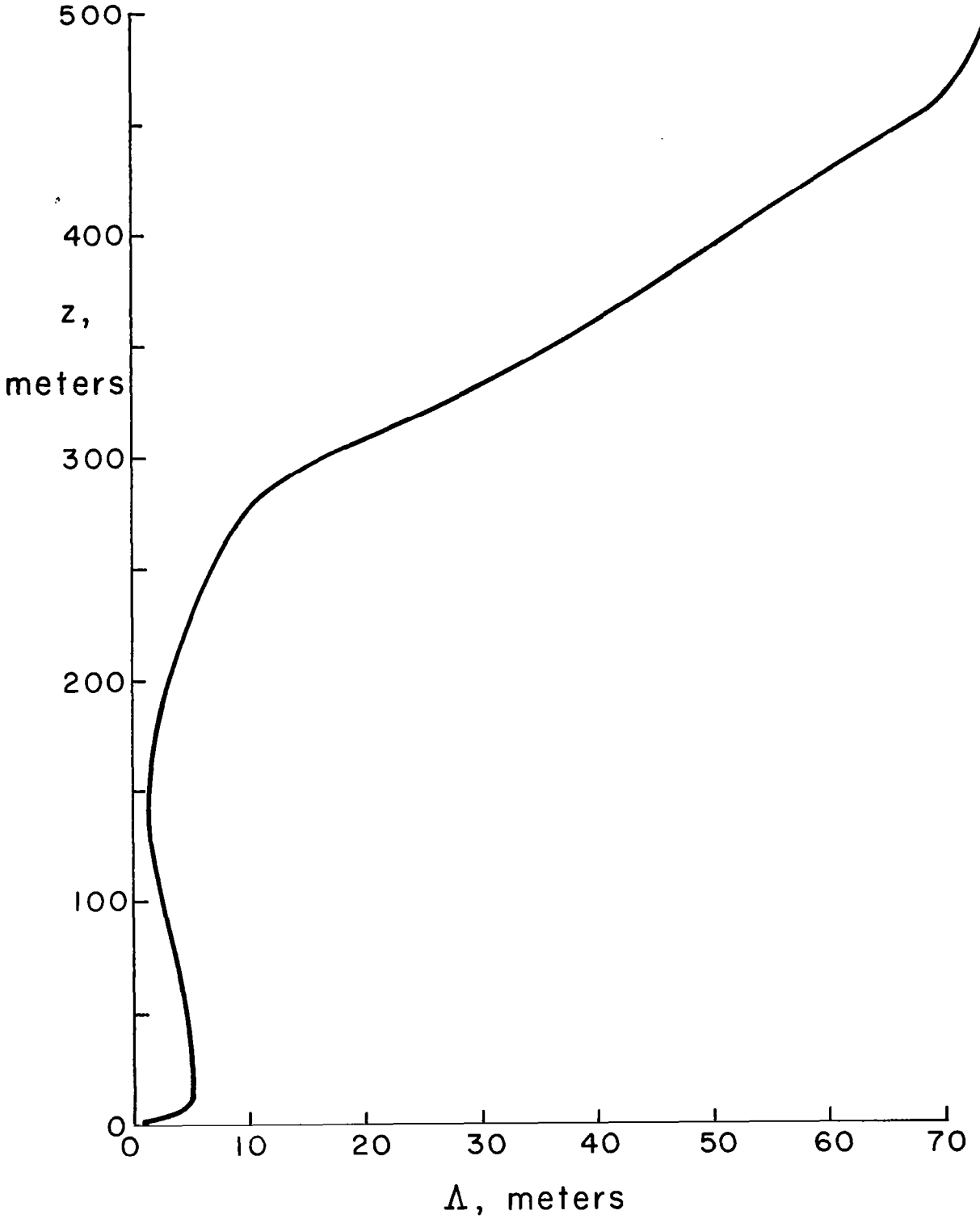

Figure 3.2.14. Altitude profile of scale of turbulence for Boston, December 17, 1973 accident.

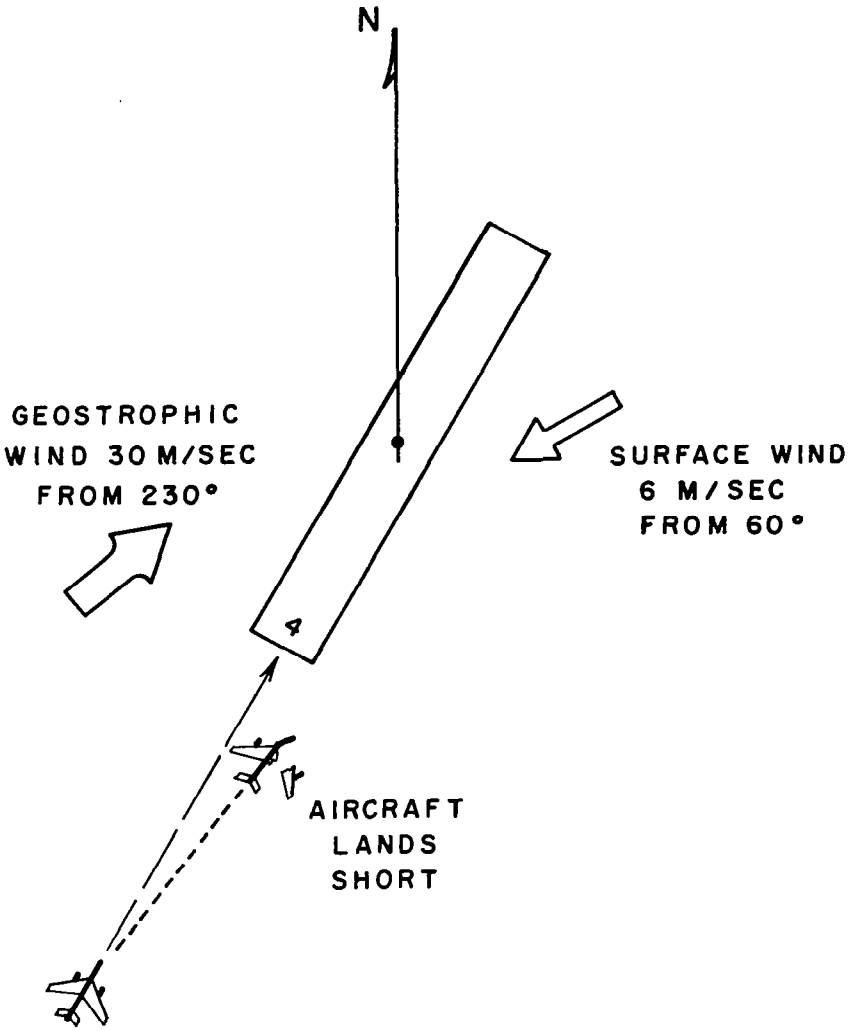

Figure 3.3.1. Aircraft-runway-winds orientation diagram for La Guardia Airport, January 4, 1971 accident.

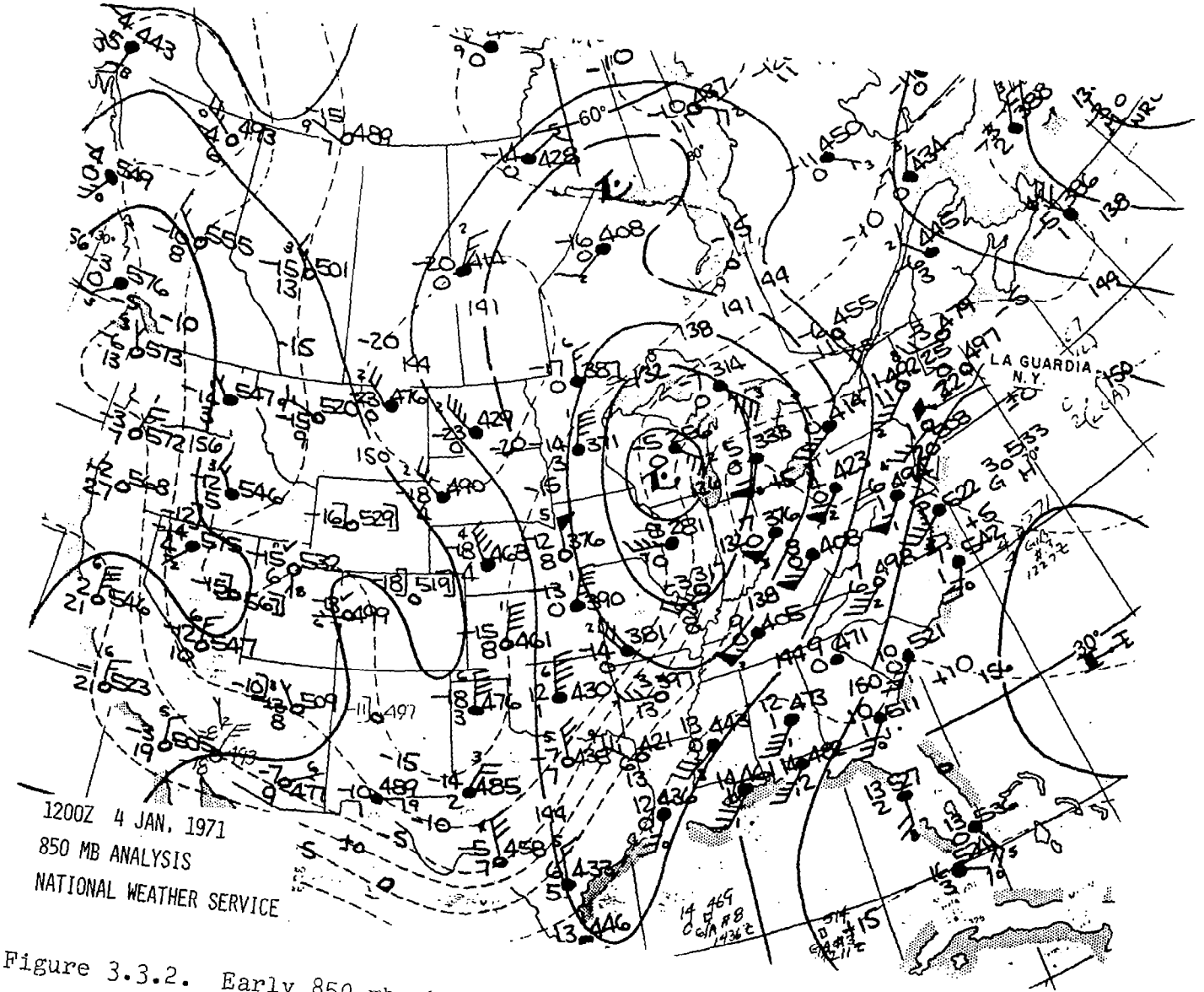

Figure 3.3.2. Early 850 mb chart for La Guardia Airport, January 4, 1971 accident.

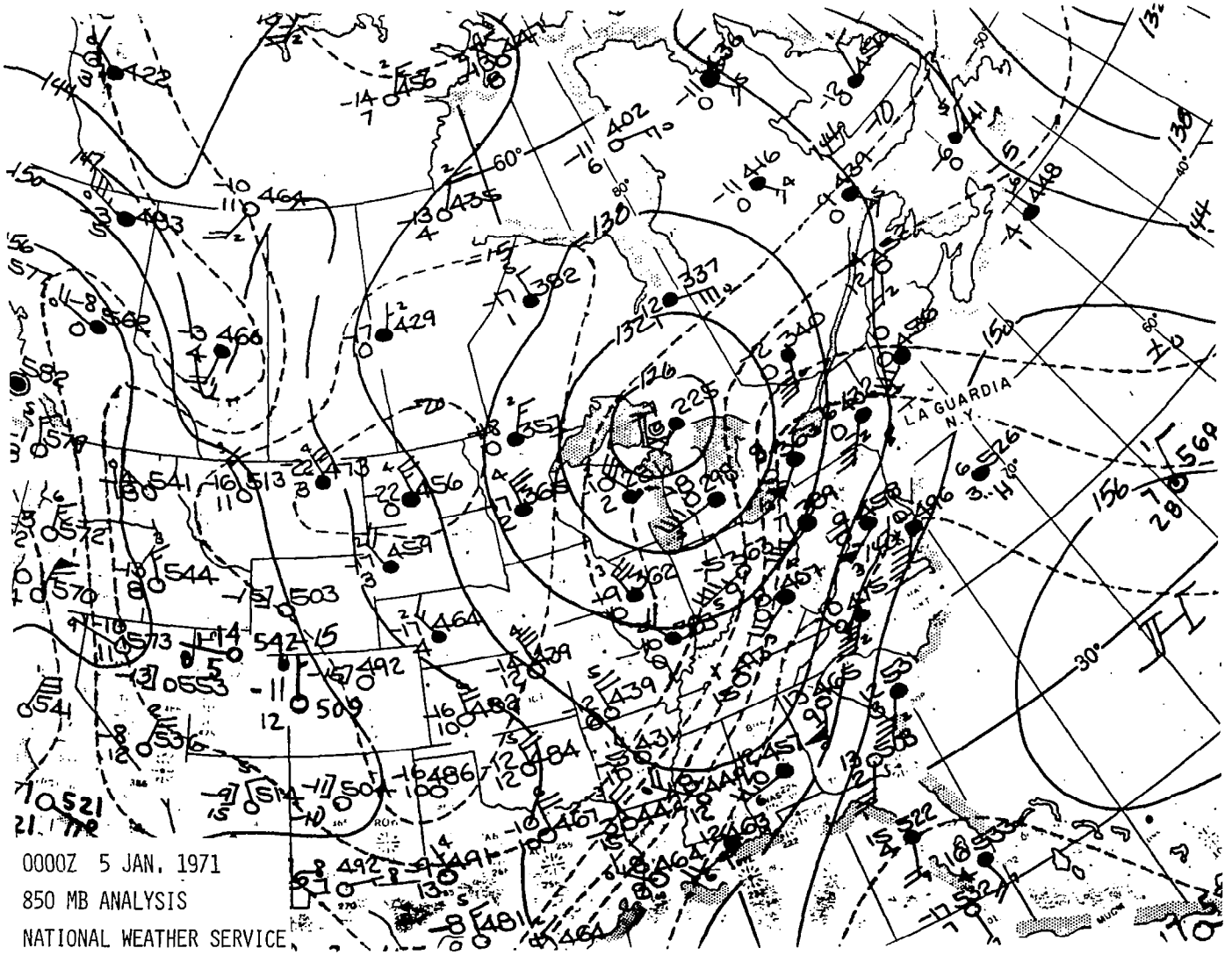

Figure 3.3.3. Late 850 mb chart for La Guardia Airport, January 4, 1971 accident.

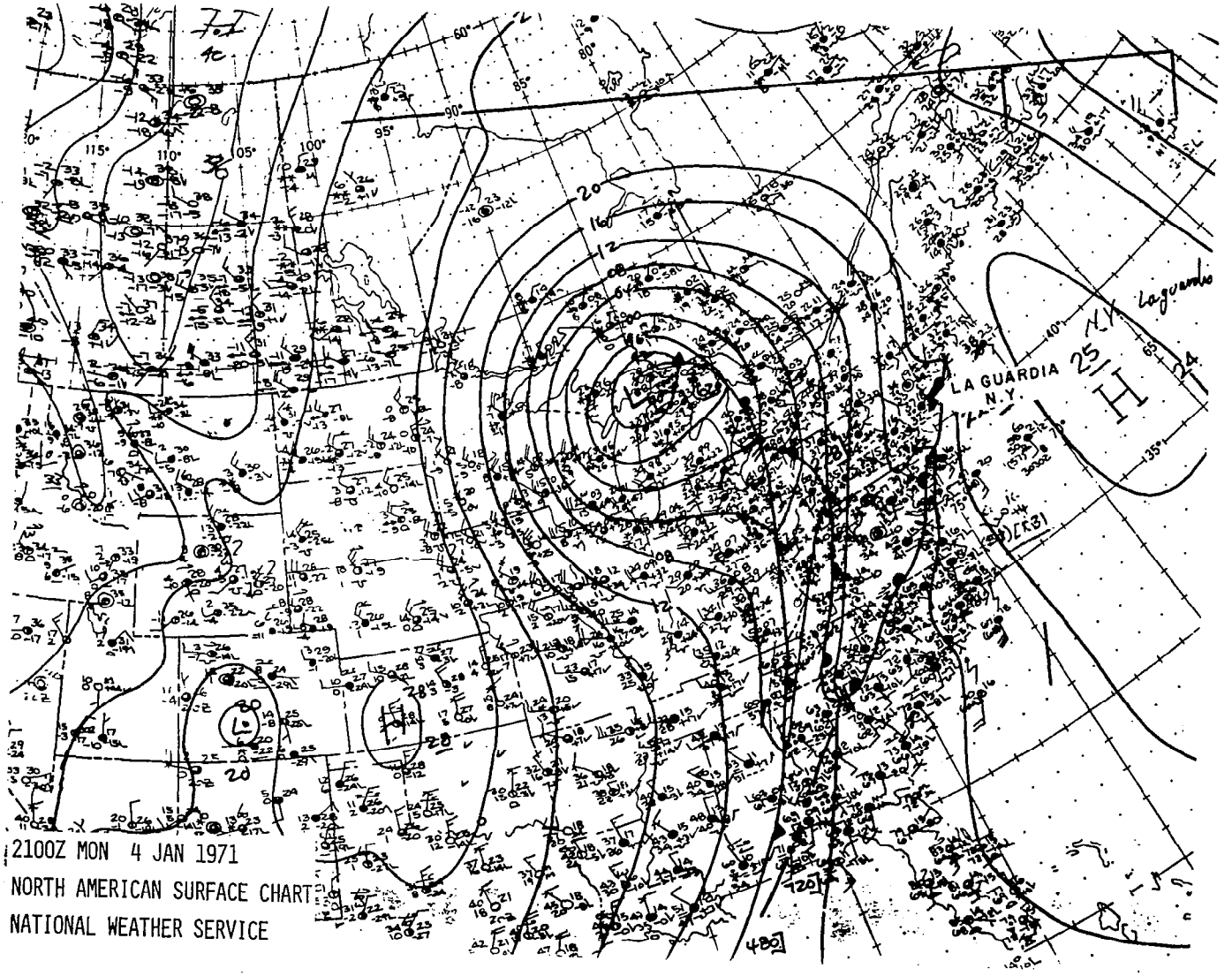

Figure 3.3.4. Early surface weather chart for La Guardia, January 4, 1971 accident.

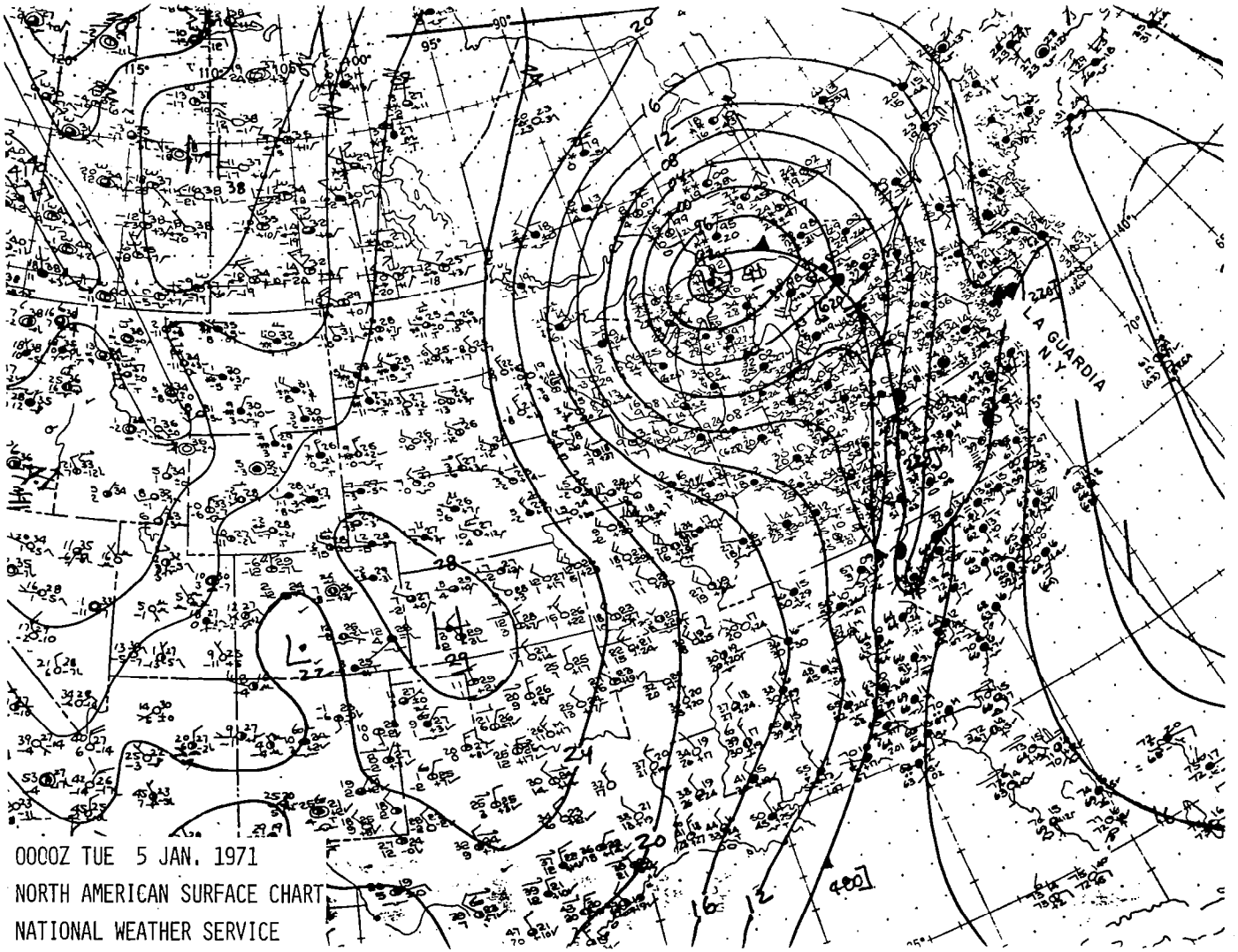

Figure 3.3.5. Late surface weather chart for La Guardia, January 4, 1971 accident.

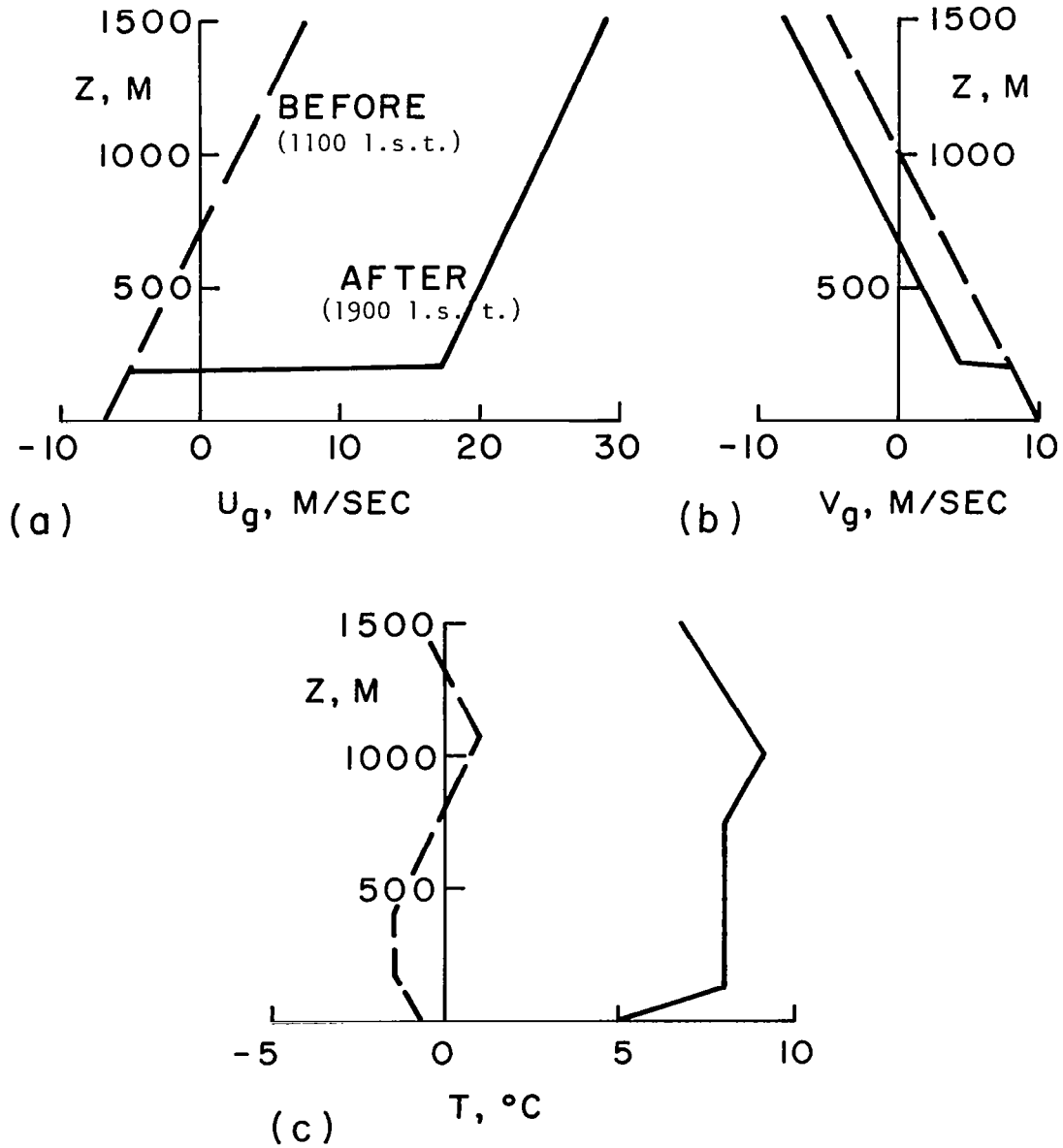

Figure 3.3.6. Altitude profiles for; a) mean geostrophic velocity component parallel to runway (+ U_g, tailwind), b) mean wind velocity component perpendicular to runway (+ V_g, crosswind from right), c) temperature before and after the La Guardia Airport, January 4, 1971 accident.

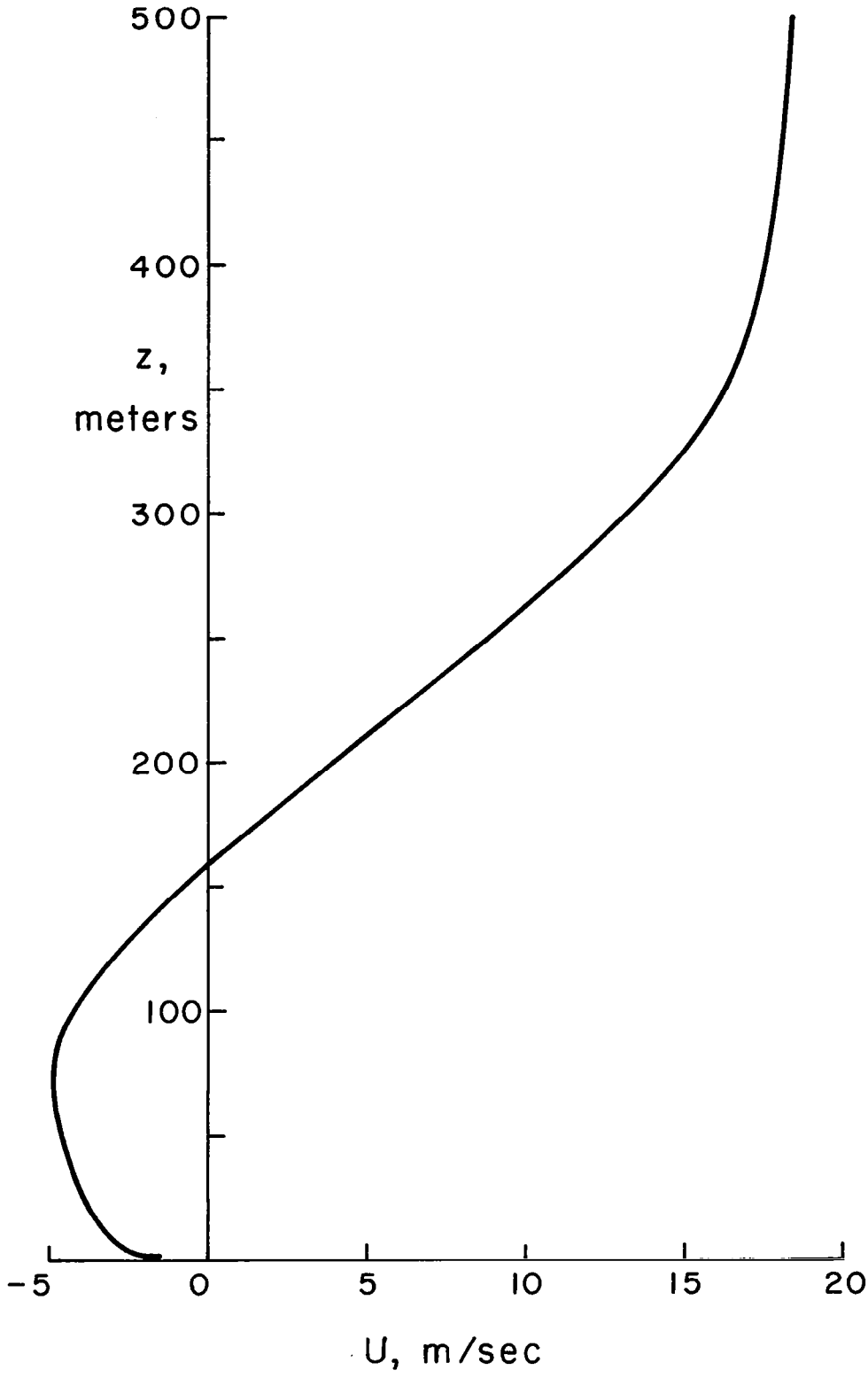

Figure 3.3.7. Altitude profile of mean wind velocity component parallel to runway for the La Guardia Airport, January 4, 1971 accident (+ U, tailwind).

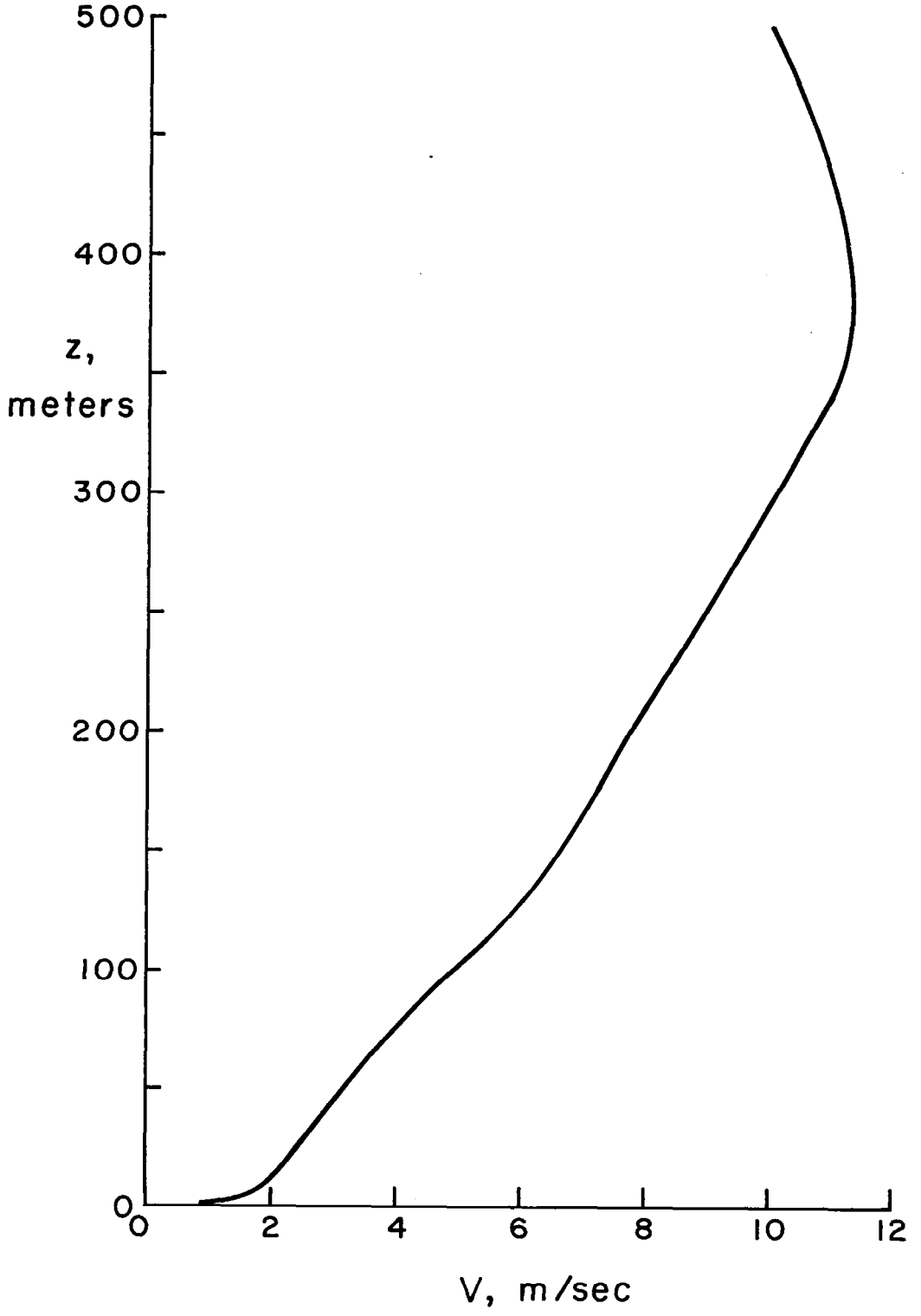

Figure 3.3.8. Altitude profile of mean wind velocity component perpendicular to runway for the La Guardia Airport, January 4, 1971 accident.

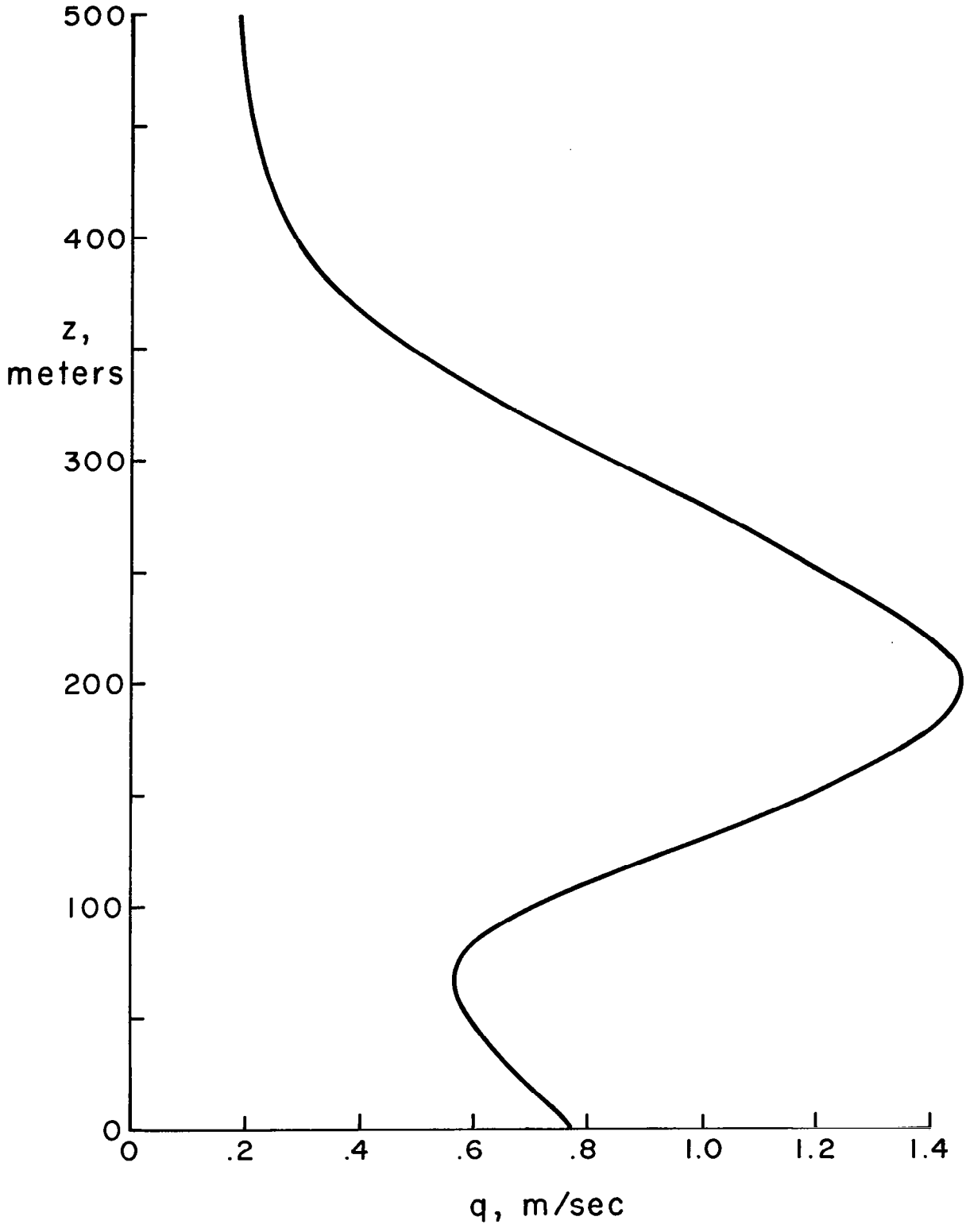

Figure 3.3.9. Altitude profile of variance of the total velocity variance for La Guardia, January 4, 1971 accident.

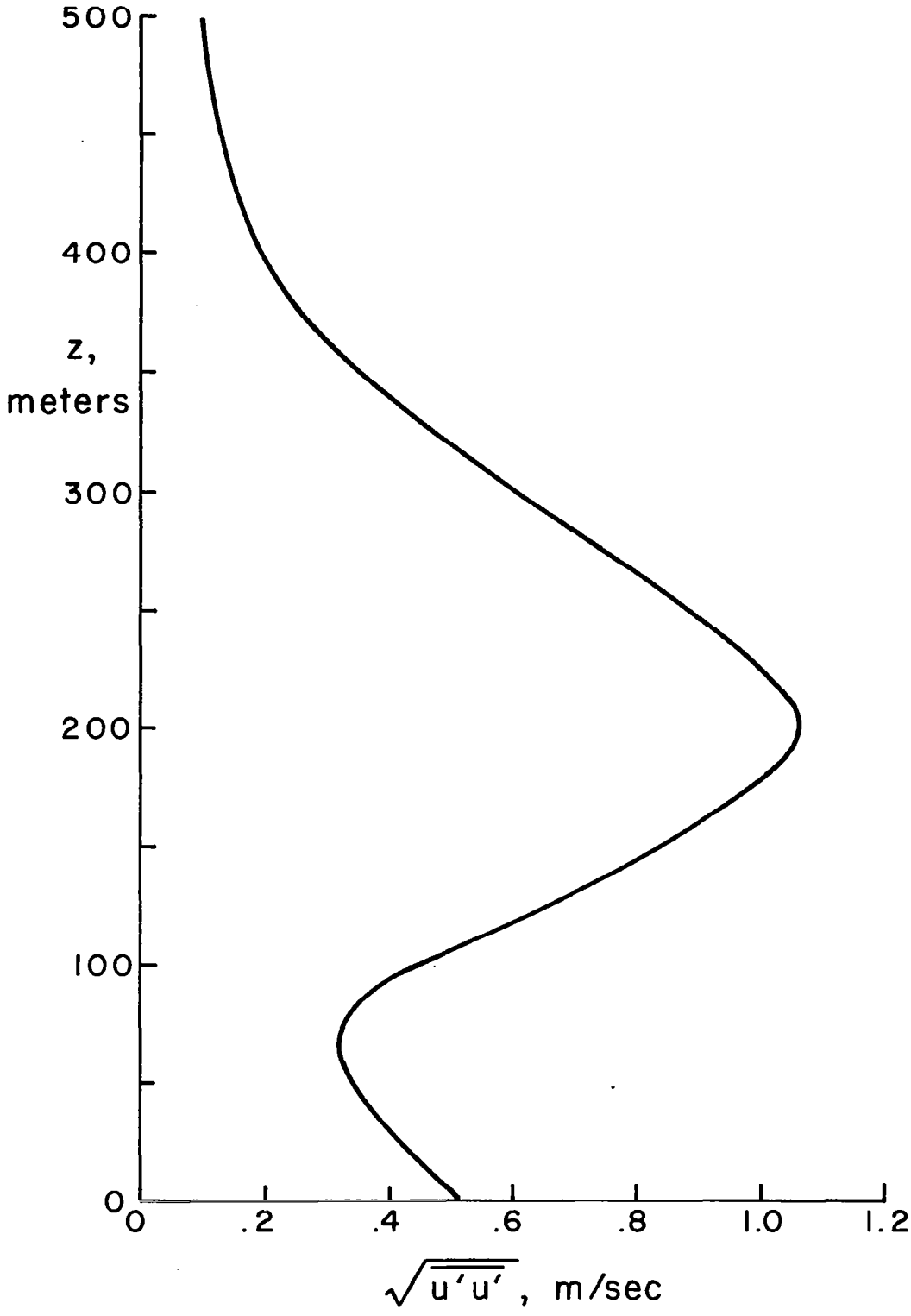

Figure 3.3.10. Altitude profile of variance of the wind parallel to runway for La Guardia Airport, January 4, 1971 accident.

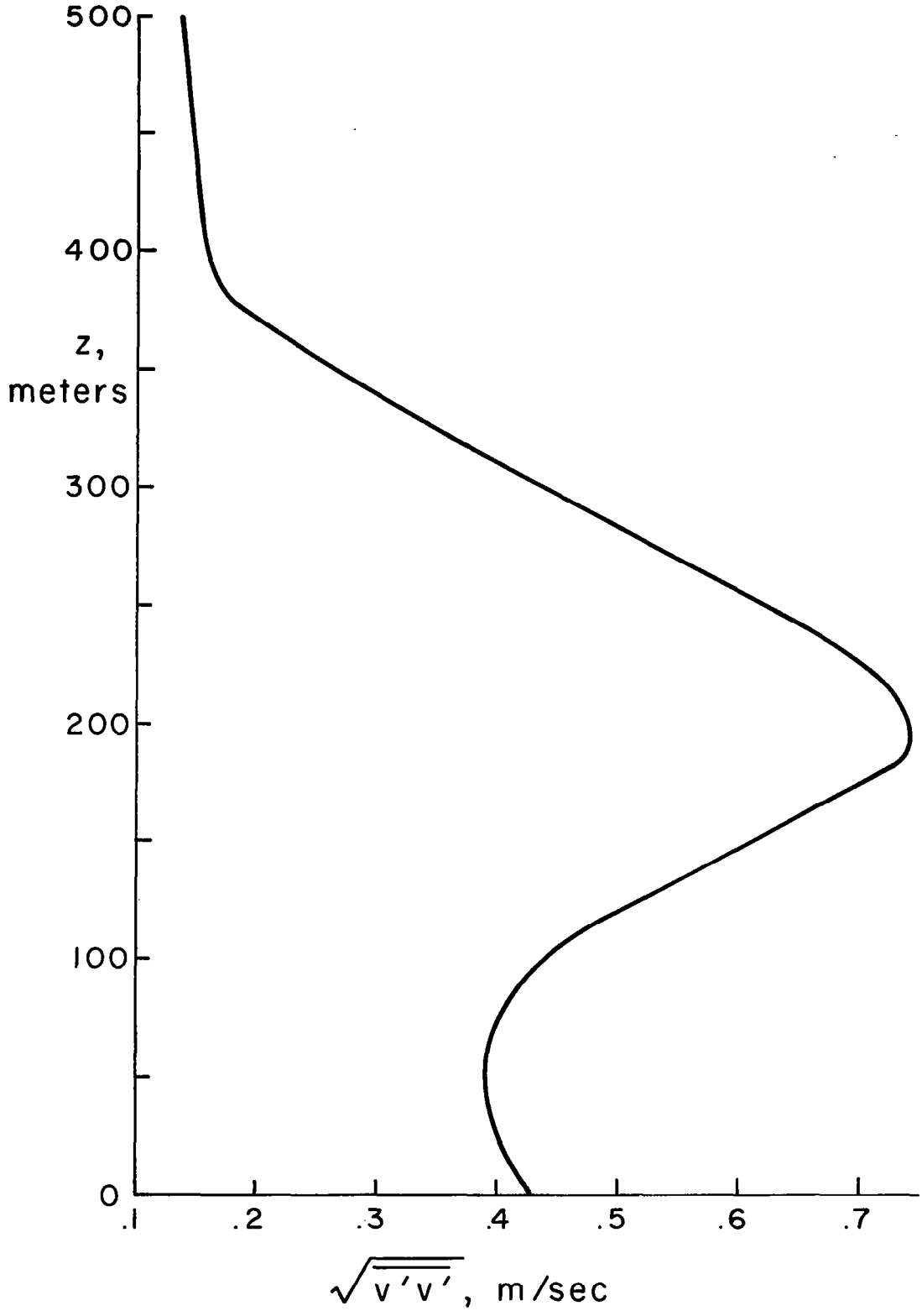

Figure 3.3.11. Altitude profile of variance of the wind perpendicular to runway for La Guardia Airport, January 4, 1971 accident.

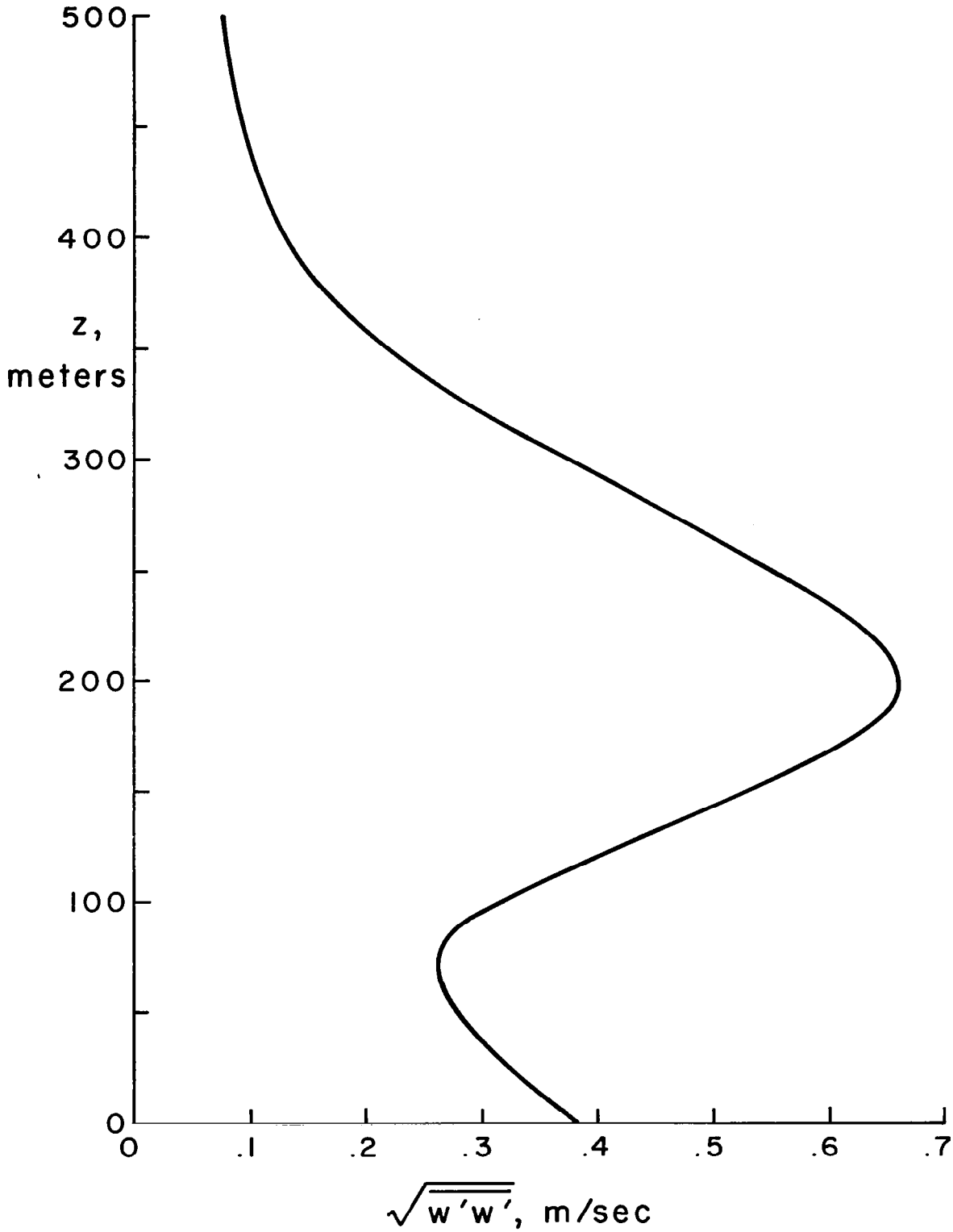

Figure 3.3.12. Altitude profile of variance of the vertical wind for La Guardia Airport, January 4, 1971 accident.

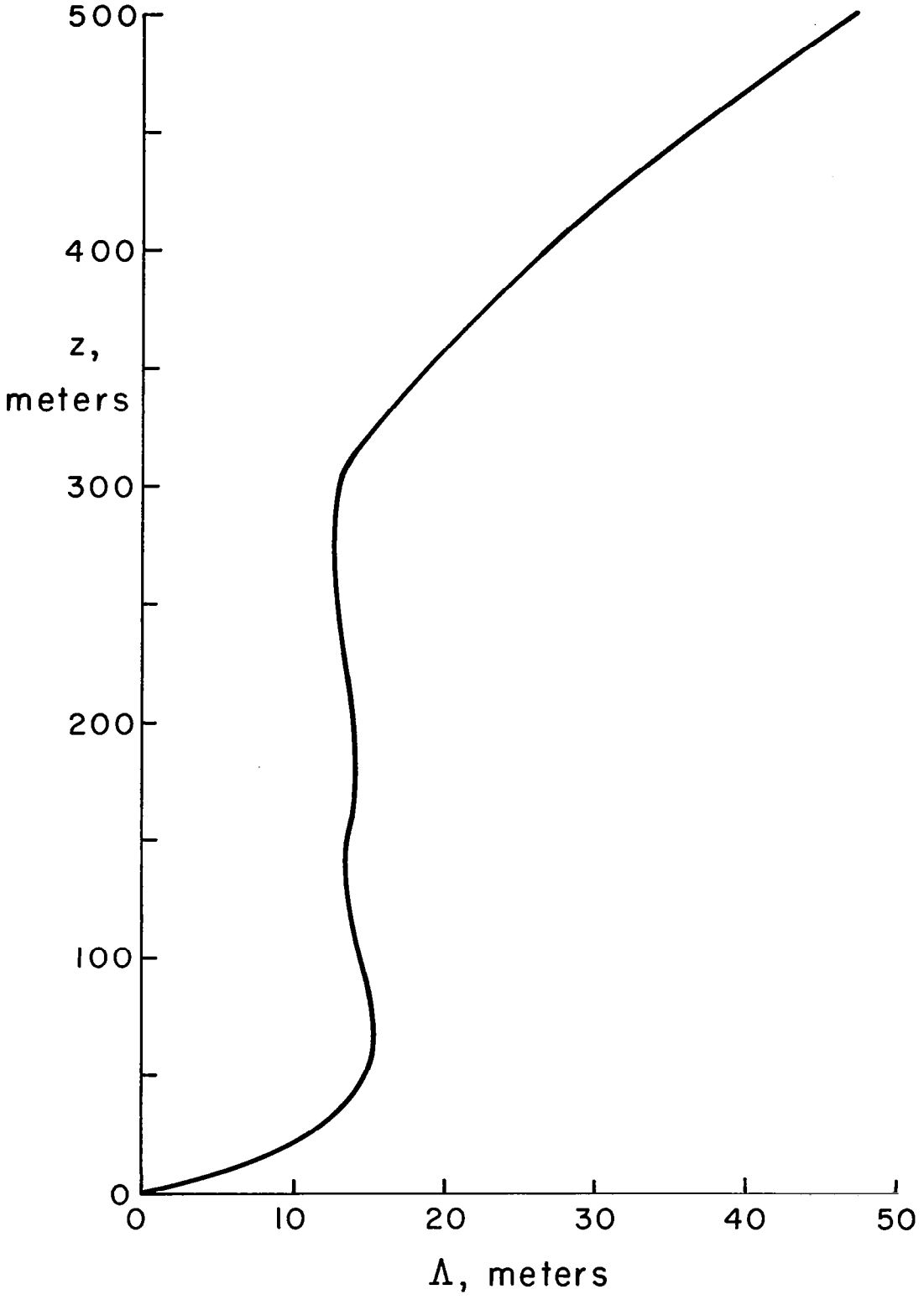

Figure 3.3.13. Altitude profile of scale of turbulence for La Guardia Airport, January 4, 1971 accident.

This case illustrates the large change in airspeed which can occur when a large vertical gradient in temperature exists. Pilots reported that the windshear stopped around an altitude of 100 m. This would normally give time to execute a missed approach if necessary. However, at an earlier time in the passage of the front the maximum windshear can occur at lower altitudes.

3.4 WICHITA, MARCH 1973

At 1250 l.s.t. on March 3, 1973 a TWA 727 landed and ran off the side of Runway 19R at the Wichita, Kansas Airport. The Controller observed that aircraft to touchdown about 600 m past the landing threshold. The captain indicated that the initial deceleration was normal but subsequent braking action was not satisfactory due to water on the runway. He, therefore, intentionally departed from the runway rather than go off the end of it (figure 3.4.1, Ref. 14).

Rain showers and thunderstorms were observed in the vicinity both during and prior to the accident. These were associated with a cold front moving in a southeasterly direction across the airport at the time of the accident. (Figures 3.4.2 - 3.4.5.) The flight recorder malfunctioned during landing and no wind profiles were estimated from the data.

The cause of the accident was a combination of landing well past the threshold and poor braking action on the wet runway. It is possible that windshear due to the cold front affected the accuracy of the landing. A weather scenario including the passage of a cold front is, therefore, modeled in this analysis as described below. The front is modeled in the same manner as in Section 3.3.

Geostrophic wind profiles in figure 3.4.6 are shown before the front arrived and at the time when the leading edge of the front is $\sim$ 100 km past the airport.

The velocity, turbulence and macroscale profiles characterizing the weather at the time of the accident are shown in figures 3.4.7 - 3.4.13. The surface wind observations provide the only realistic check on the wind profiles generated in this study, since there are no wind profile estimates from flight test data. At the time of the accident, surface weather observations reported the surface wind as 3 - 6 m/sec from 90° - 110°. Our study results in a surface wind of 5.7 m/sec from 100°. The main result pertinent to the accident is the decreasing headwind below an altitude of 400 m (figure 3.4.7) which could contribute to overshooting the touchdown point if no corrections were made. Figures 3.4.8 through 3.4.13 indicate that crosswind and turbulence should not have been a problem.

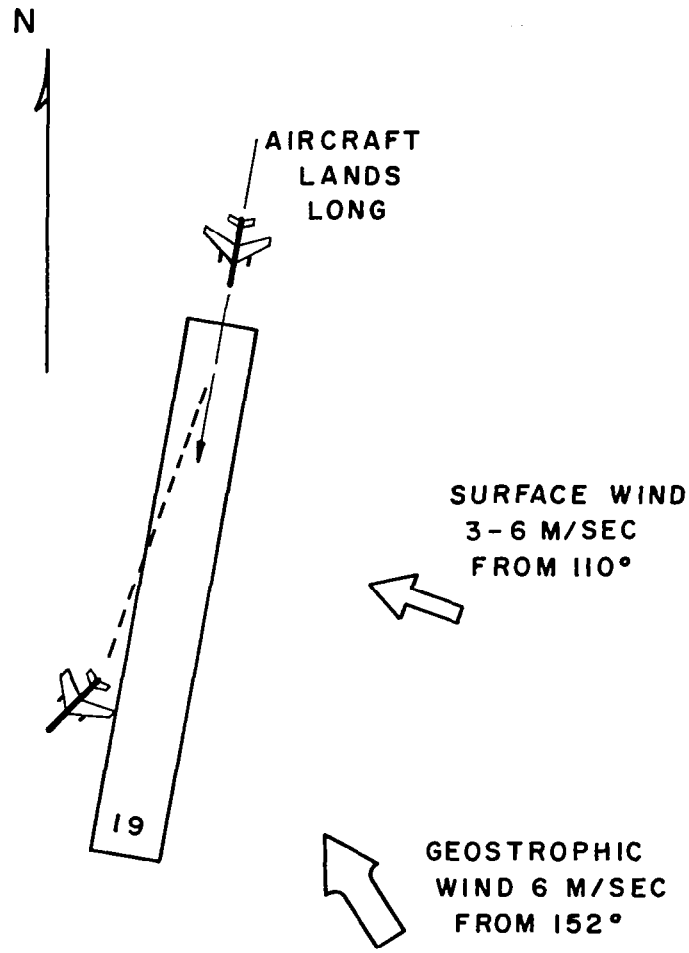

Figure 3.4.1. Aircraft-runway-winds orientation diagram for Wichita, Kansas, March 3, 1973 accident.

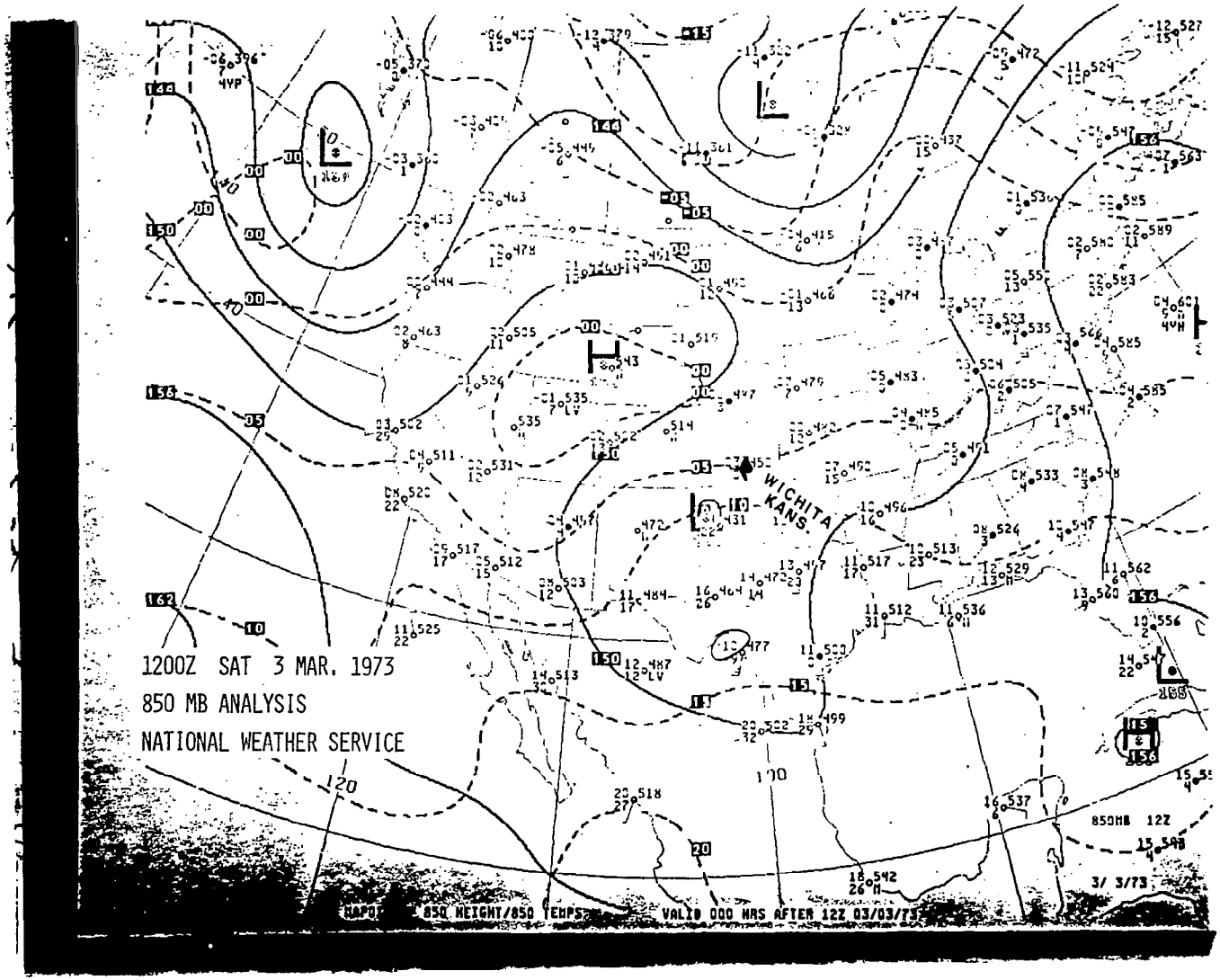

Figure 3.4.2. Early 850 mb chart for Wichita, Kansas, March 3, 1973 accident.

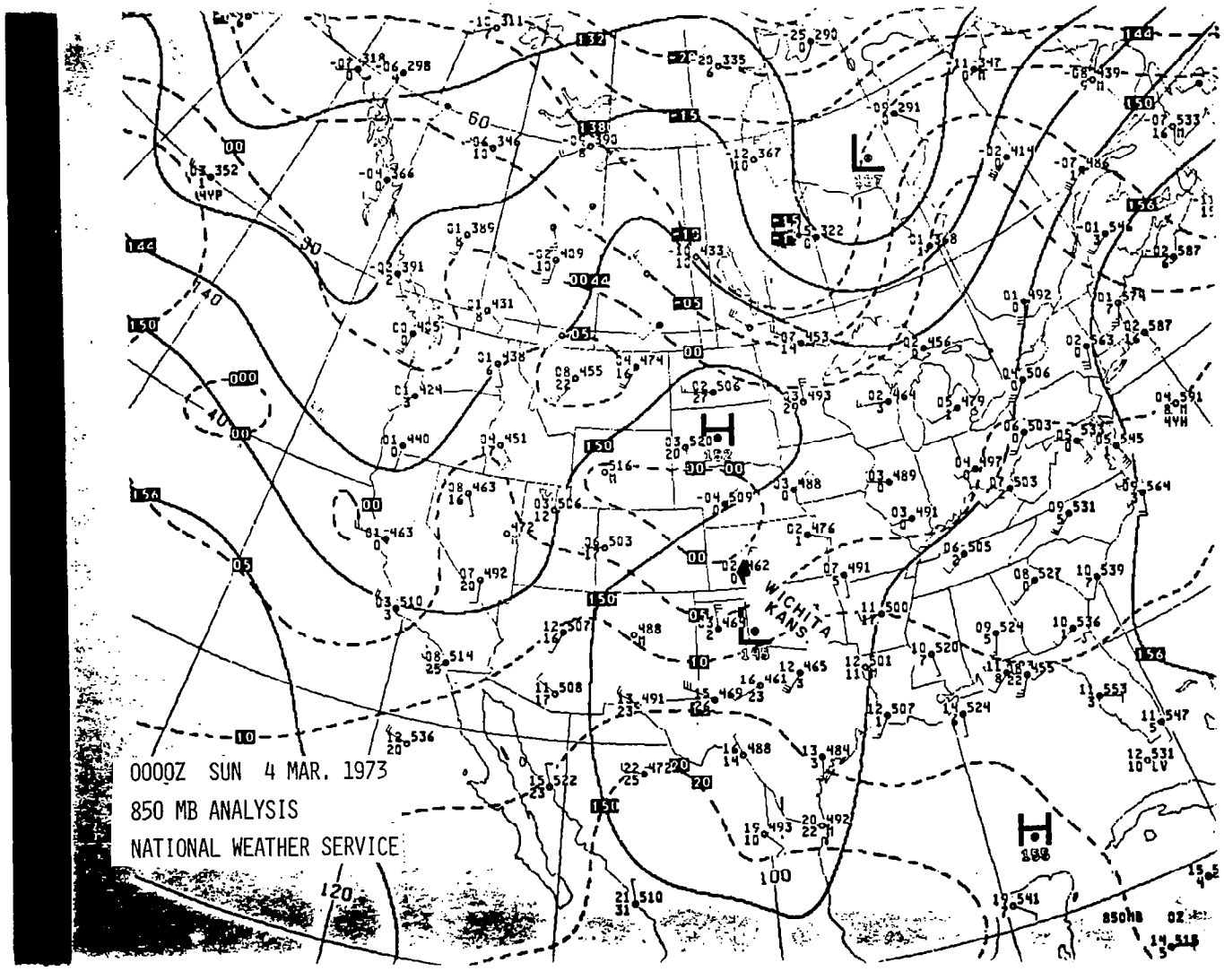

Figure 3.4.3. Late 850 mb chart for Wichita, Kansas, March 3, 1973 accident.

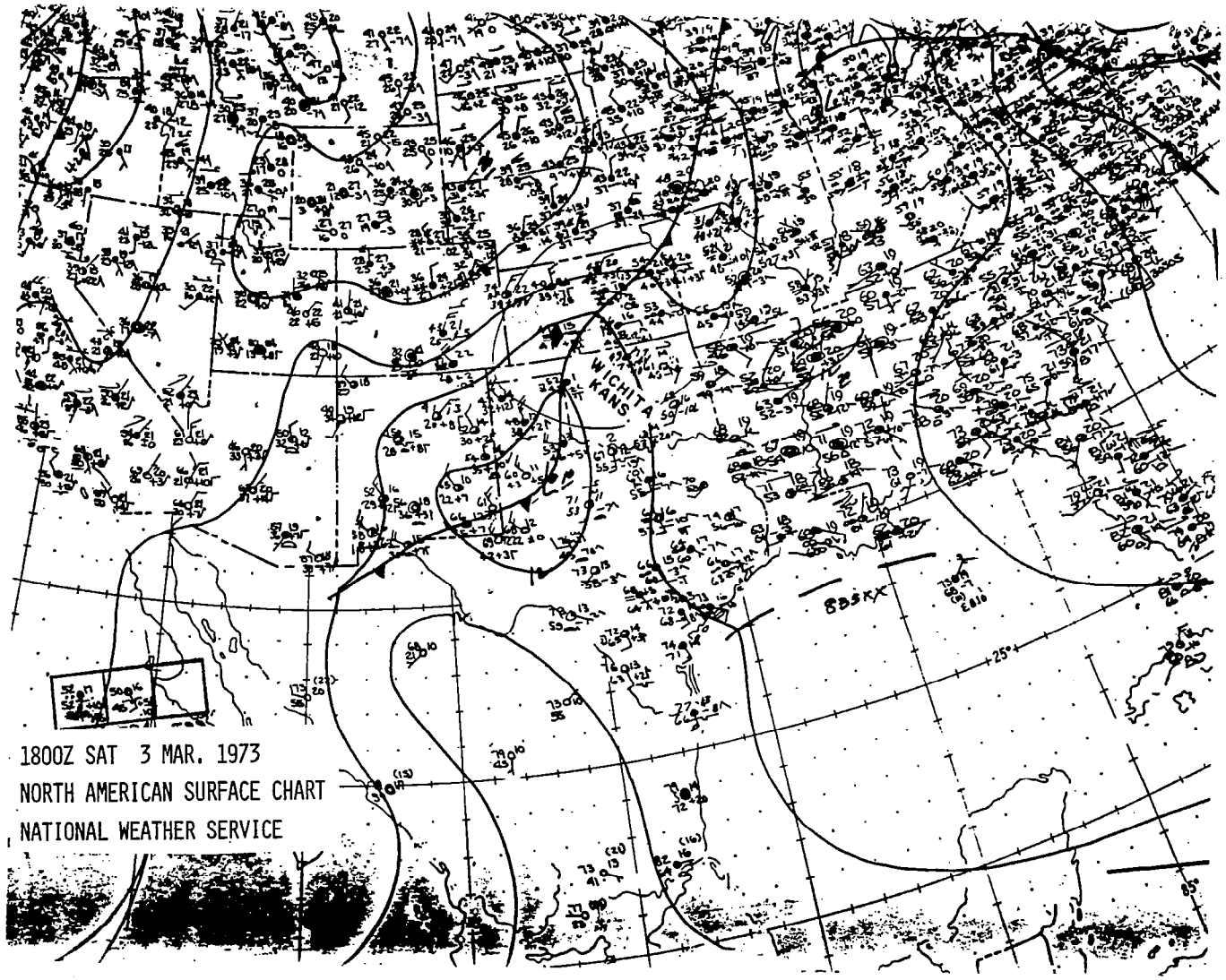

Figure 3.4.4. Early surface weather chart for Wichita, Kansas, March 3, 1973 accident.

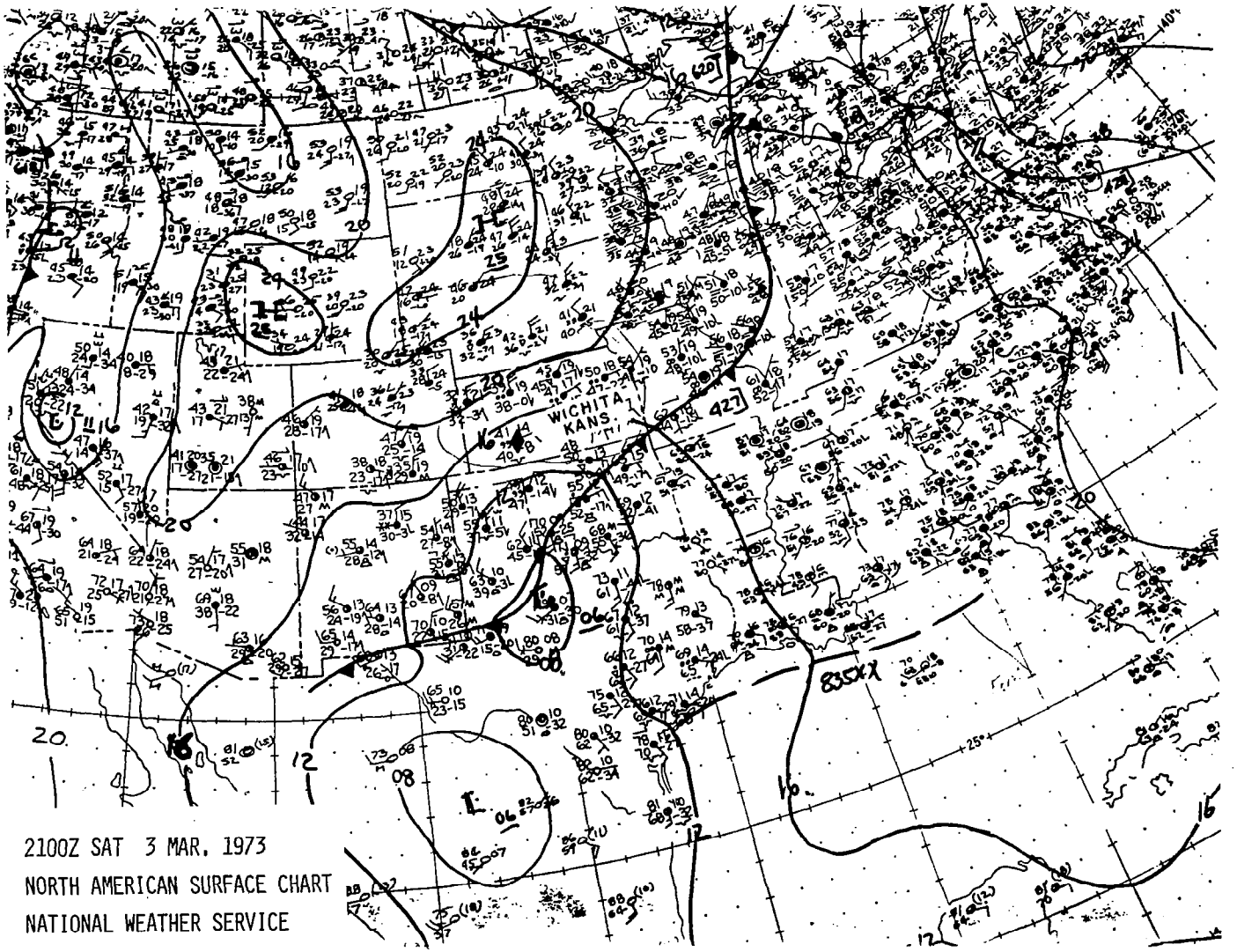

Figure 3.4.5. Late surface weather chart for Wichita, Kansas, March 3, 1973 accident.

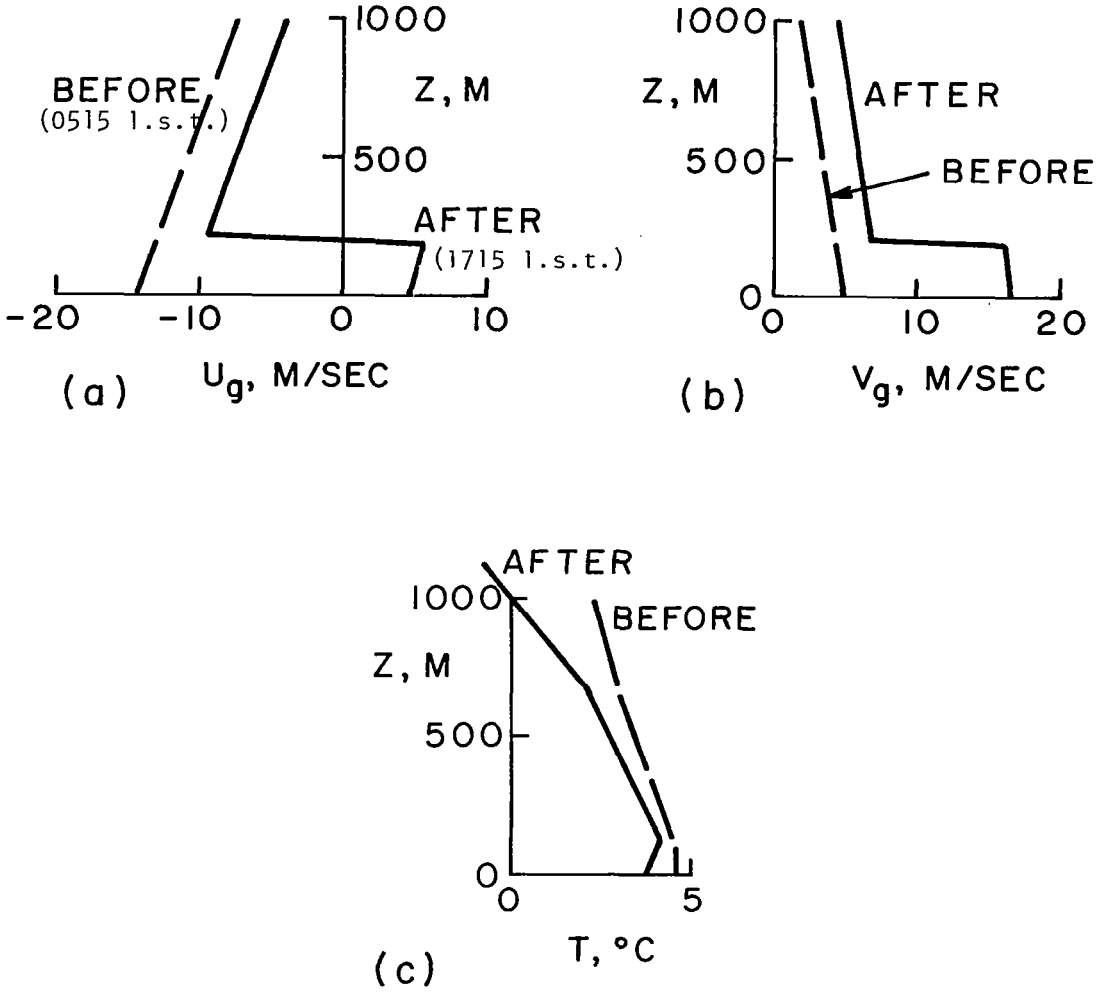

Figure 3.4.6. Altitude profiles for; a) mean geostrophic velocity component parallel to runway (+ U_g, tailwind), b) mean wind velocity component perpendicular to runway (+ V_g, crosswind from right), c) temperature before and after the Wichita, Kansas, March 3, 1973 accident.

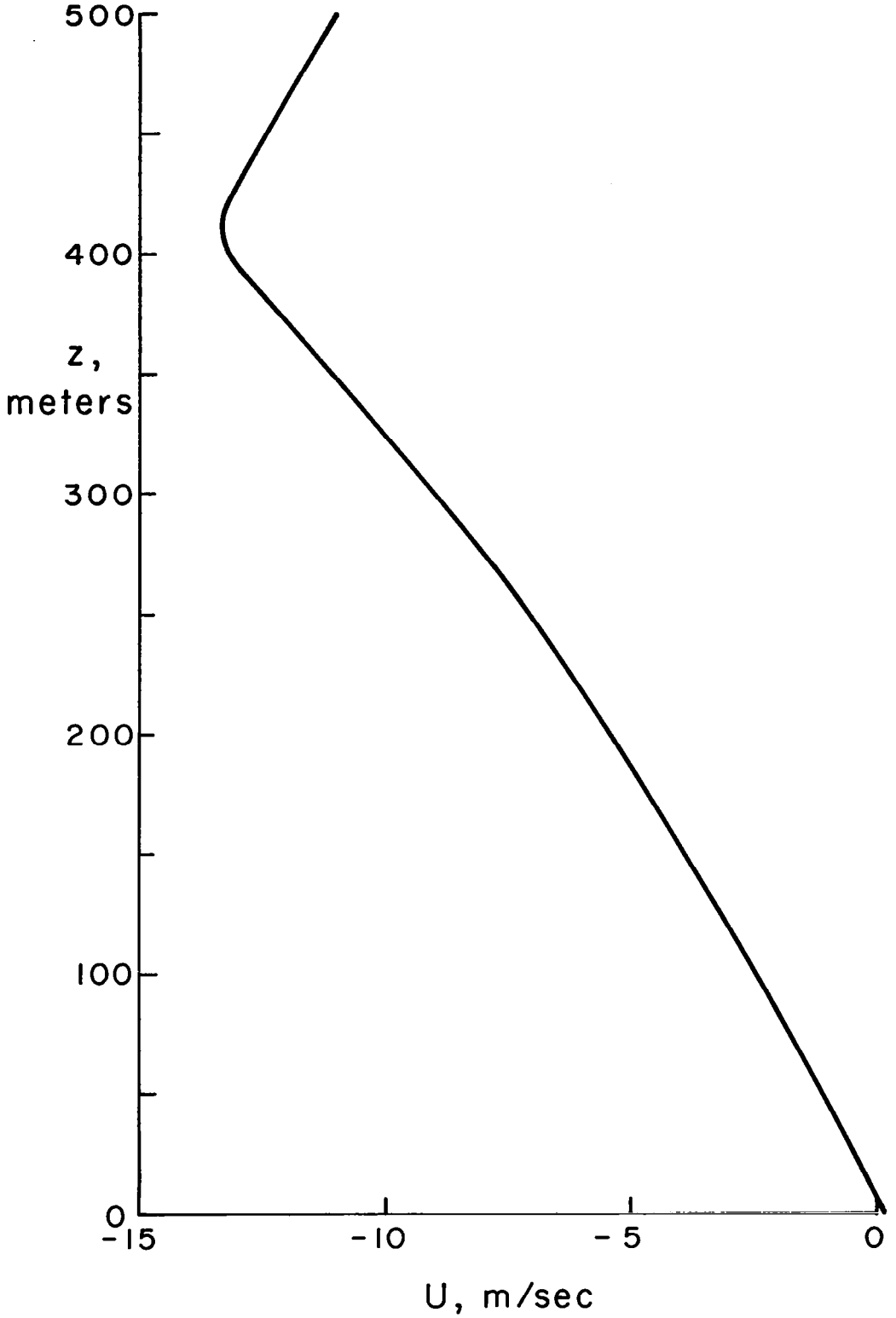

Figure 3.4.7. Altitude profile of mean wind velocity component parallel to runway for the Wichita, Kansas, March 3, 1973 accident.

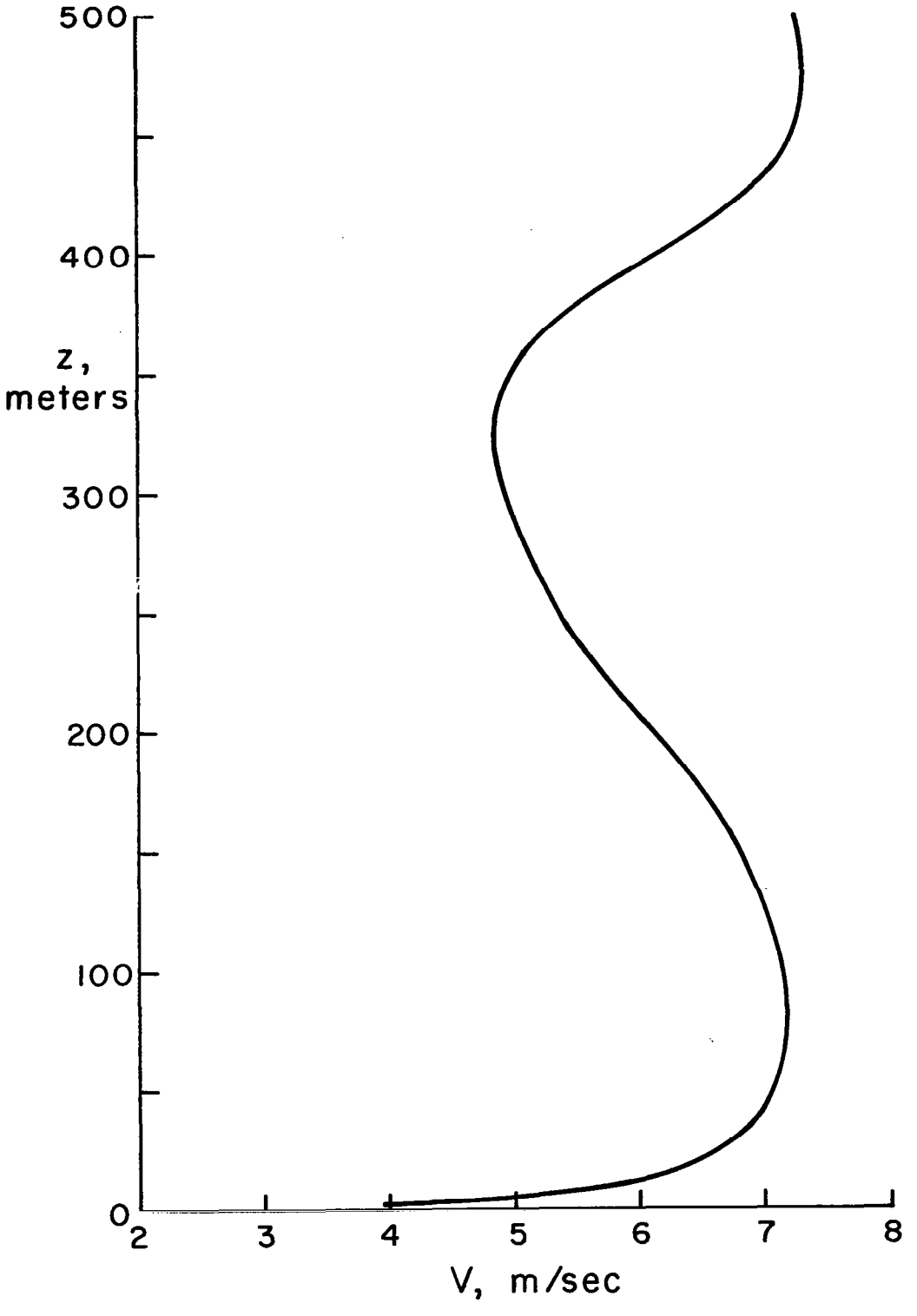

Figure 3.4.8. Altitude profile of mean wind velocity component perpendicular to runway for the Wichita, Kansas, March 3, 1973 accident.

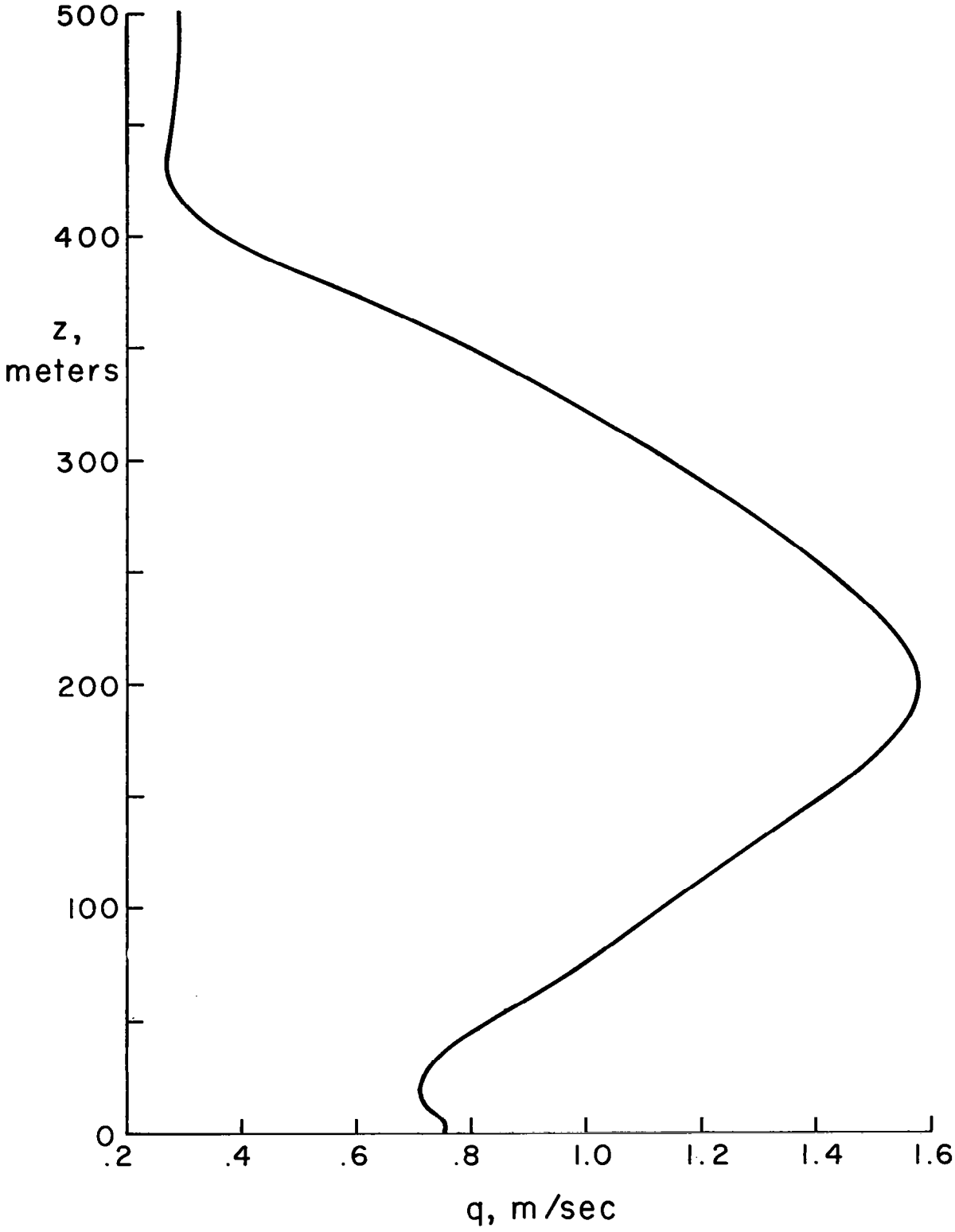

Figure 3.4.9. Altitude profile of variance of the total velocity variance for Wichita, Kansas, March 3, 1973 accident.

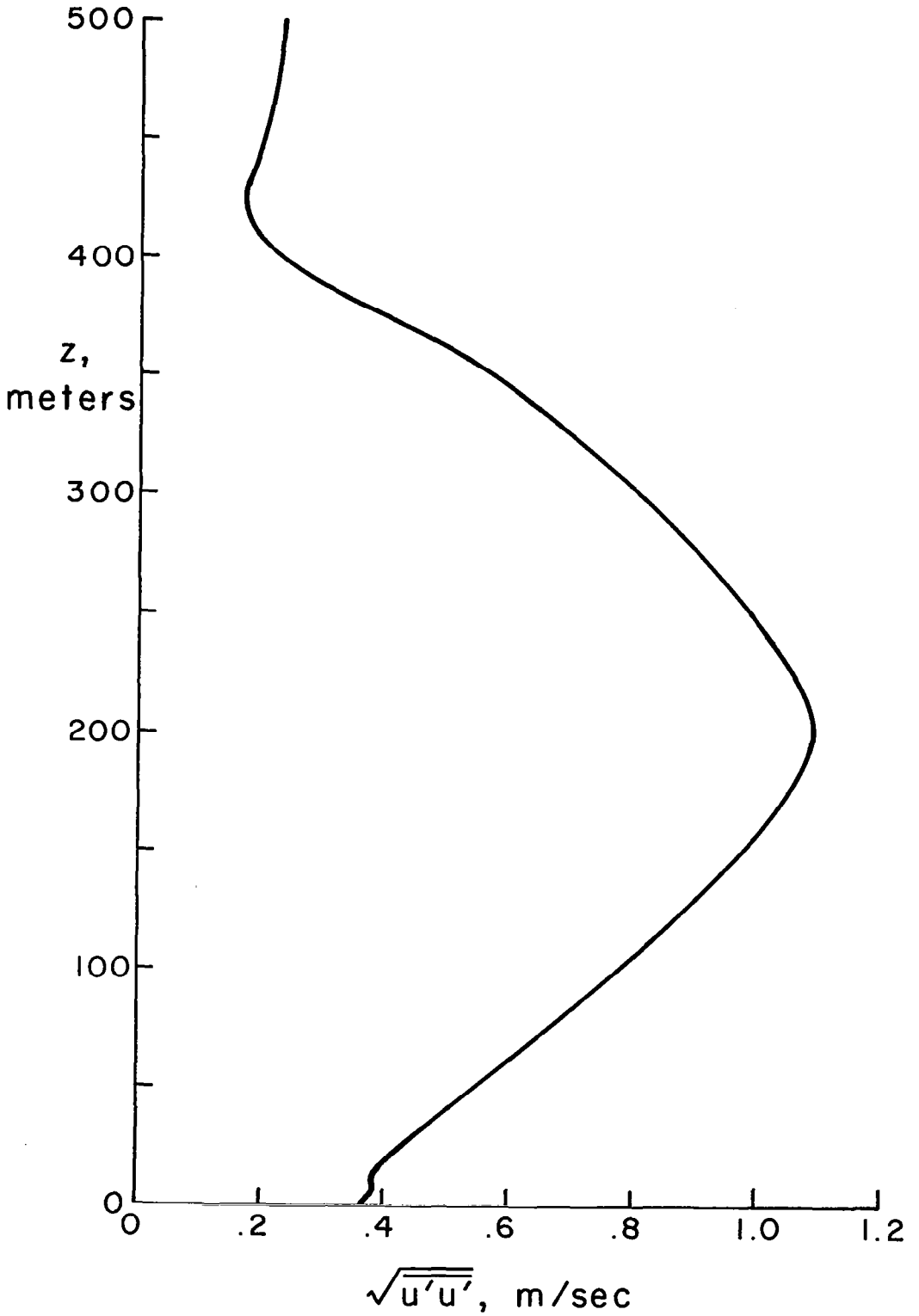

Figure 3.4.10. Altitude profile of variance of the wind parallel to runway for Wichita, Kansas, March 3, 1973 accident.

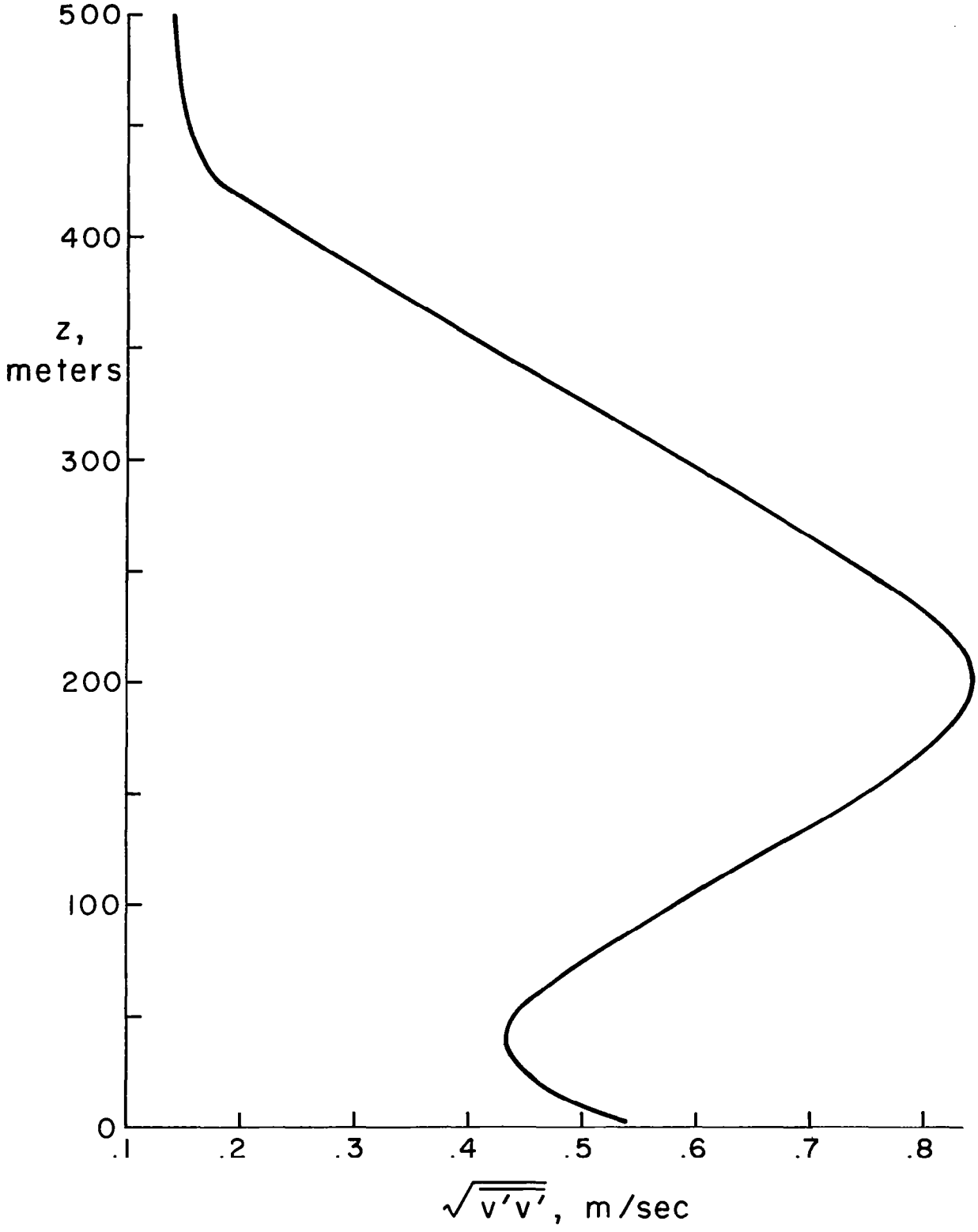

Figure 3.4.11. Altitude profile of variance of the wind perpendicular to runway for Wichita, Kansas, March 3, 1973 accident.

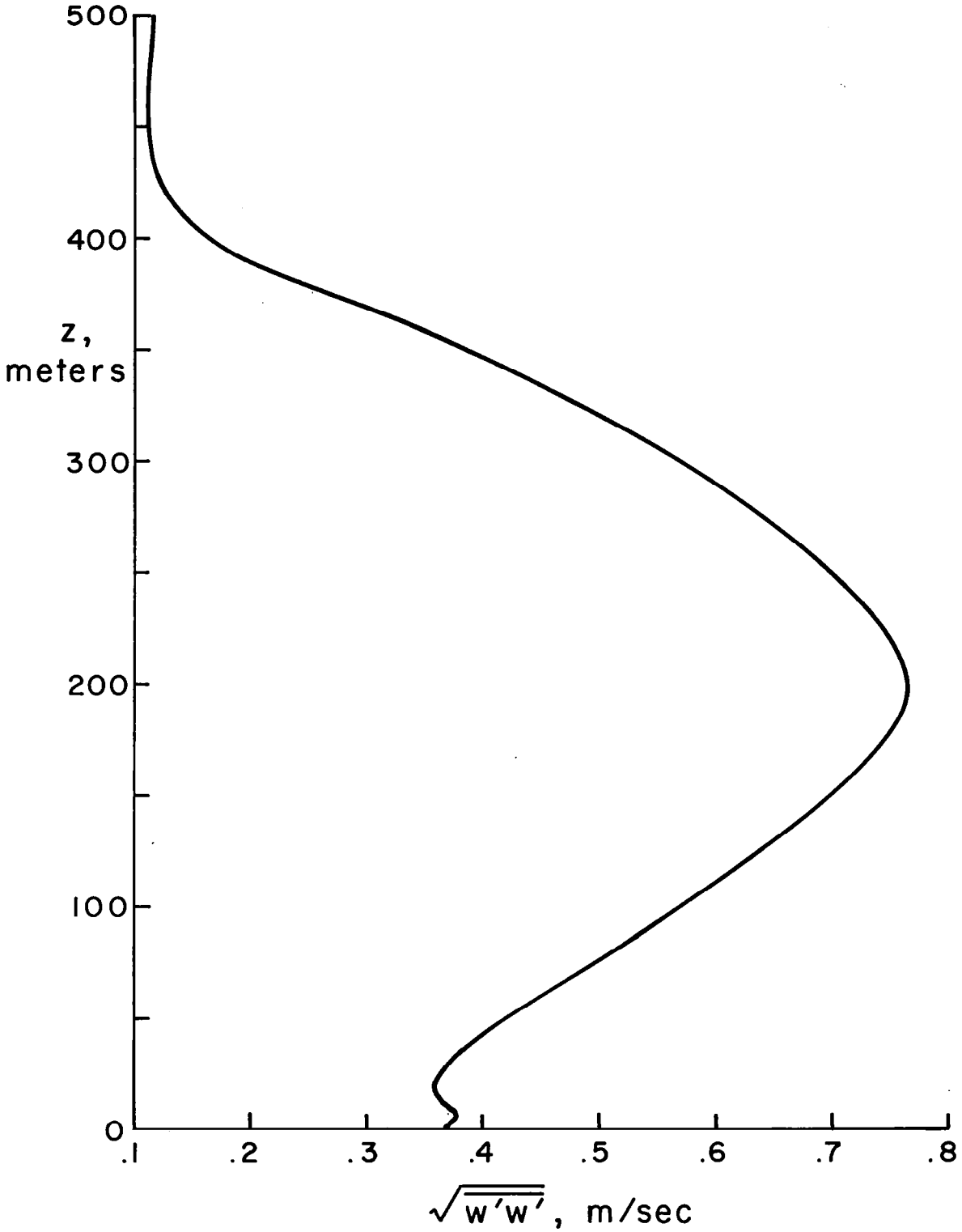

Figure 3.4.12. Altitude profile of variance of the vertical wind for Wichita, Kansas, March 3, 1973 accident.

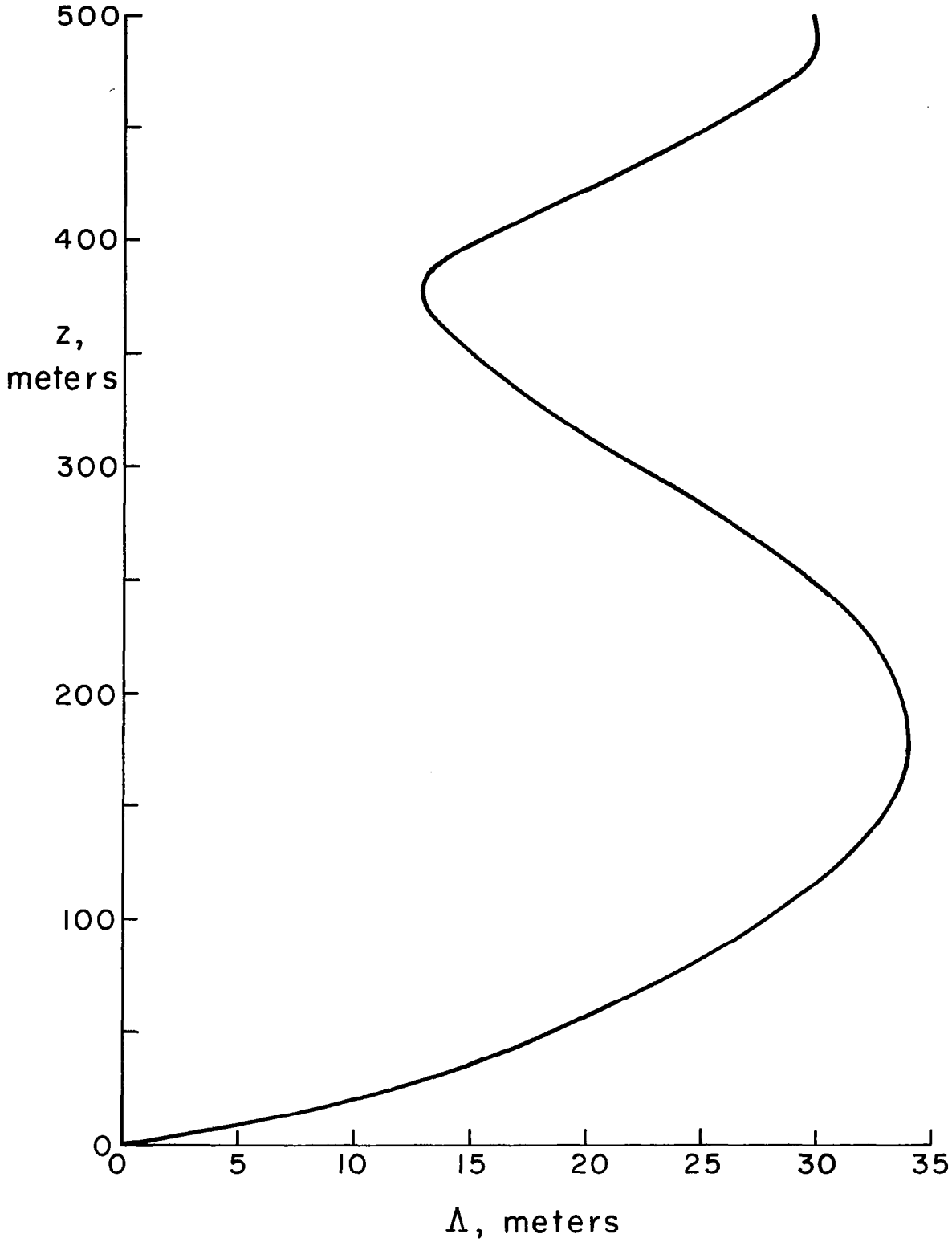

Figure 3.4.13. Altitude profile of scale of turbulence for Wichita, Kansas, March 3, 1973 accident.

3.5 JFK NEW YORK, DECEMBER 1972

At 2302 l.s.t. on December 12, 1972 a TWA 707 crashed while attempting to land on Runway 4R at JFK International Airport, New York. The automatic pilot and approach coupler were engaged down to an altitude of 90 m. After uncoupling, the aircraft deviated below glideslope, struck the approach lighting system, and then crashed onto the runway (figure 3.5.1, Ref. 15).

NWS radar in New York City showed no precipitation echoes over the accident site. The local weather included light drizzle, fog, absolutely unstable air below 40 m and stable air up through 1500 m. The surface wind was 2 m/sec from 40° and the upper geostrophic wind profiles obtained from the weather charts (figures 3.5.2 - 3.5.5) and temperature profiles from the radiosonde data are shown in figure 3.5.6.

The flight data was recorded normally but was not used to estimate wind profiles. The resulting velocity profile (figure 3.5.7) indicates that the strong tailwind aloft increases to a 10 m/sec headwind down at 140 m. From here on down the headwind drops off to 2 m/sec at ground level which could present problems if timely corrections were not applied. The wind estimate at the 10 m altitude is 2.7 m/sec from 40° as compared with an observed value of 2 m/sec from 40°. The estimated crosswind and turbulence distributions are not large enough to be hazardous for flight operation (figures 3.5.8 - 3.5.13).

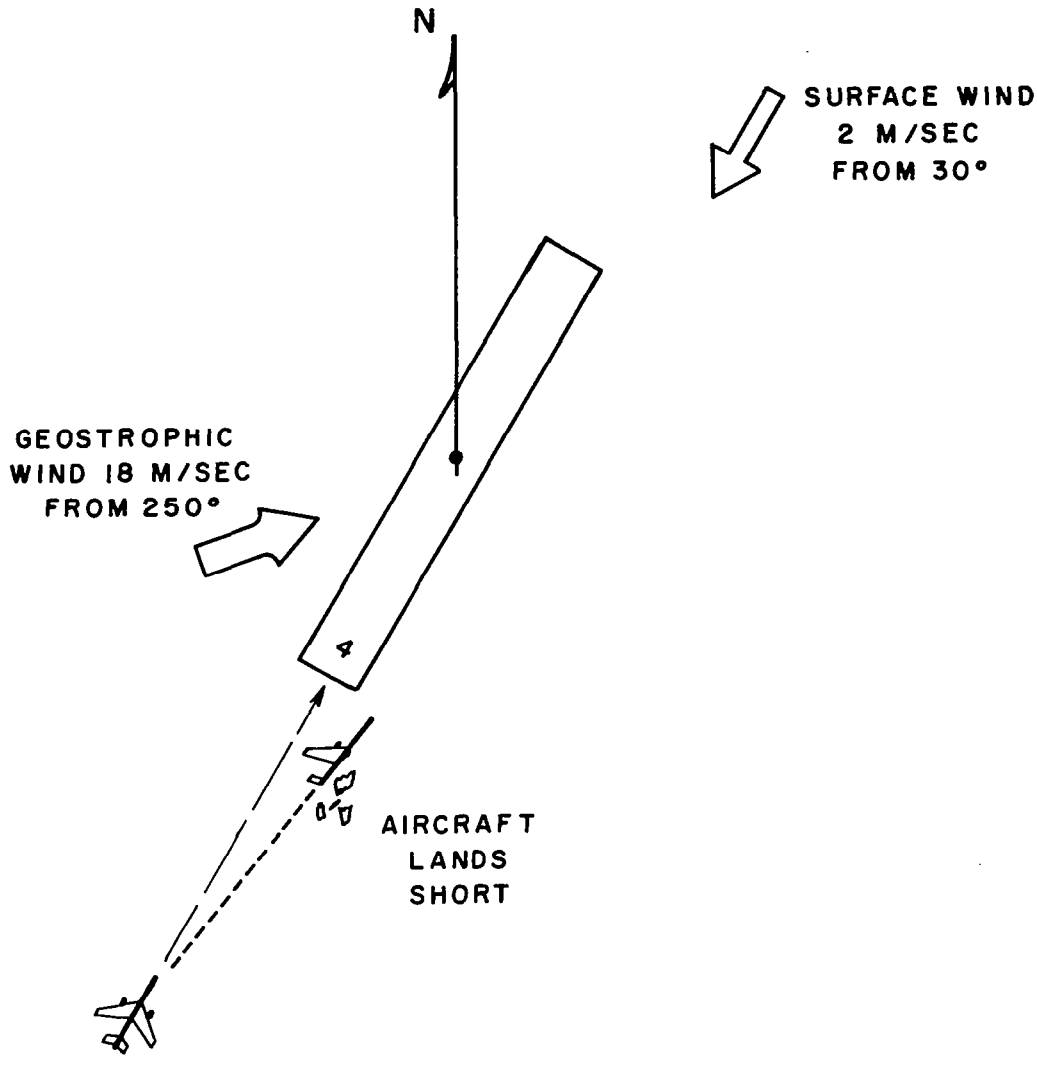

Figure 3.5.1. Aircraft-runway-winds orientation diagram for JFK Airport, December 12, 1972 accident.

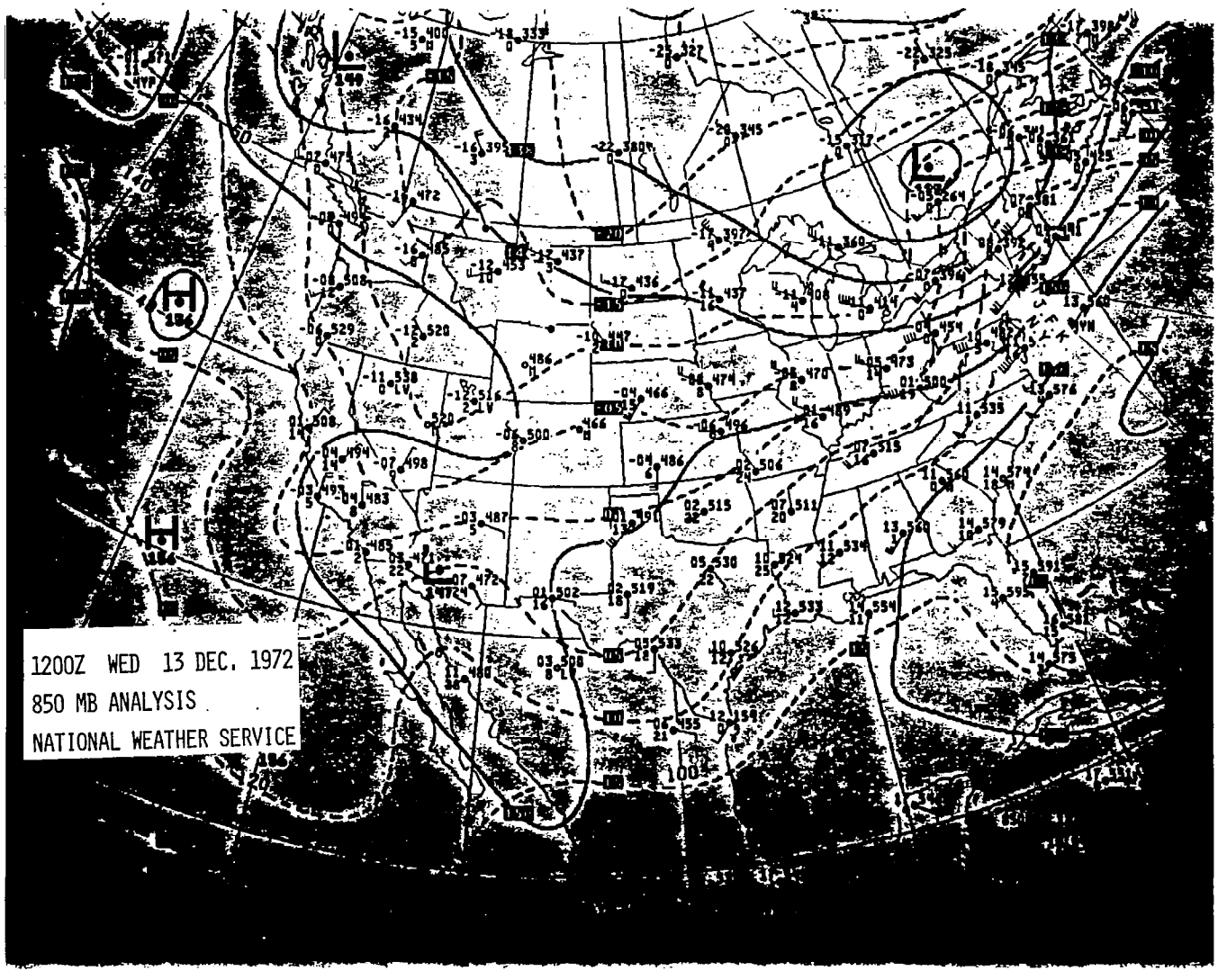

Figure 3.5.2. Early 850 mb chart for JFK Airport, December 12, 1972 accident.

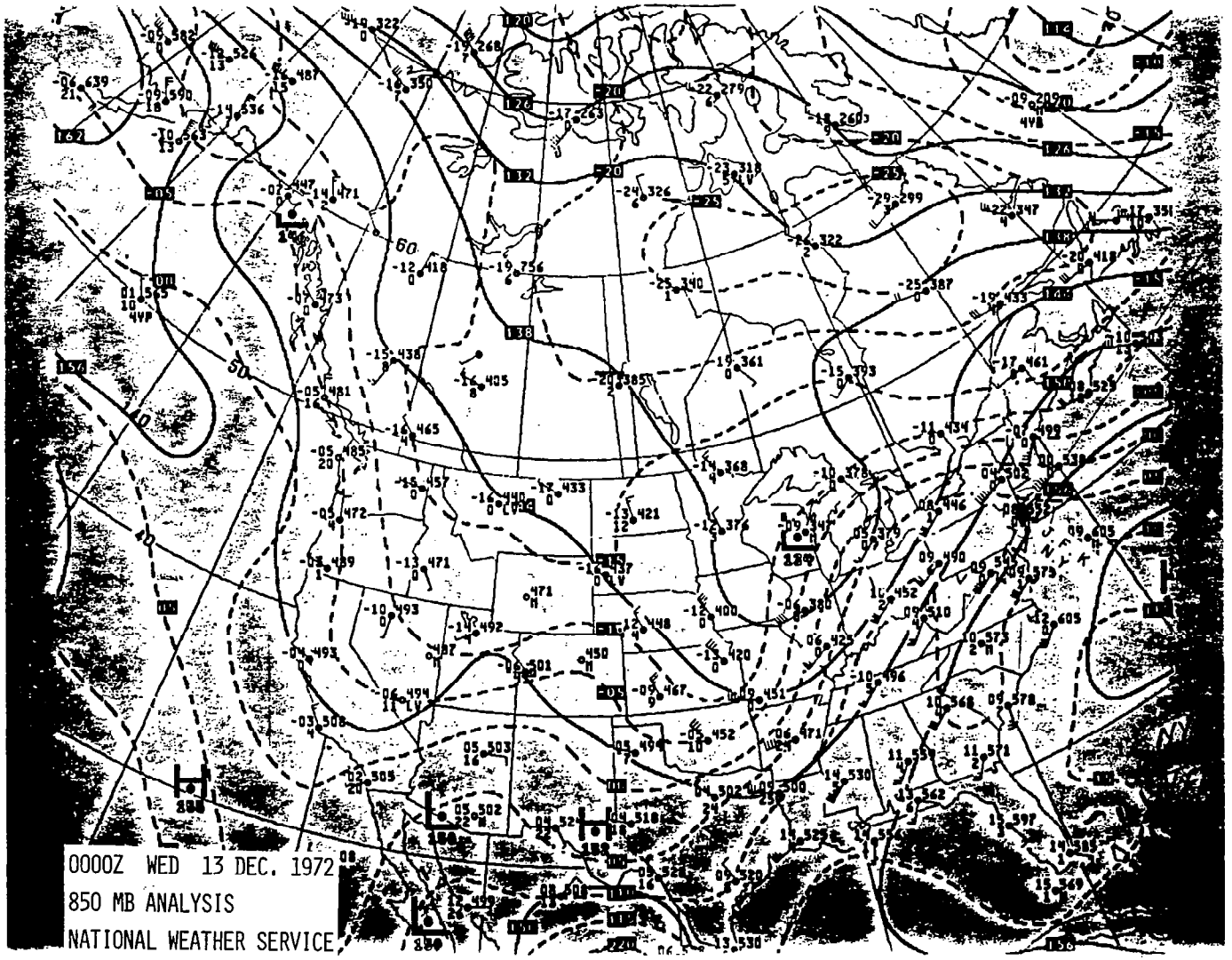

Figure 3.5.3. Late 850 mb chart for JFK Airport, December 12, 1972 accident.

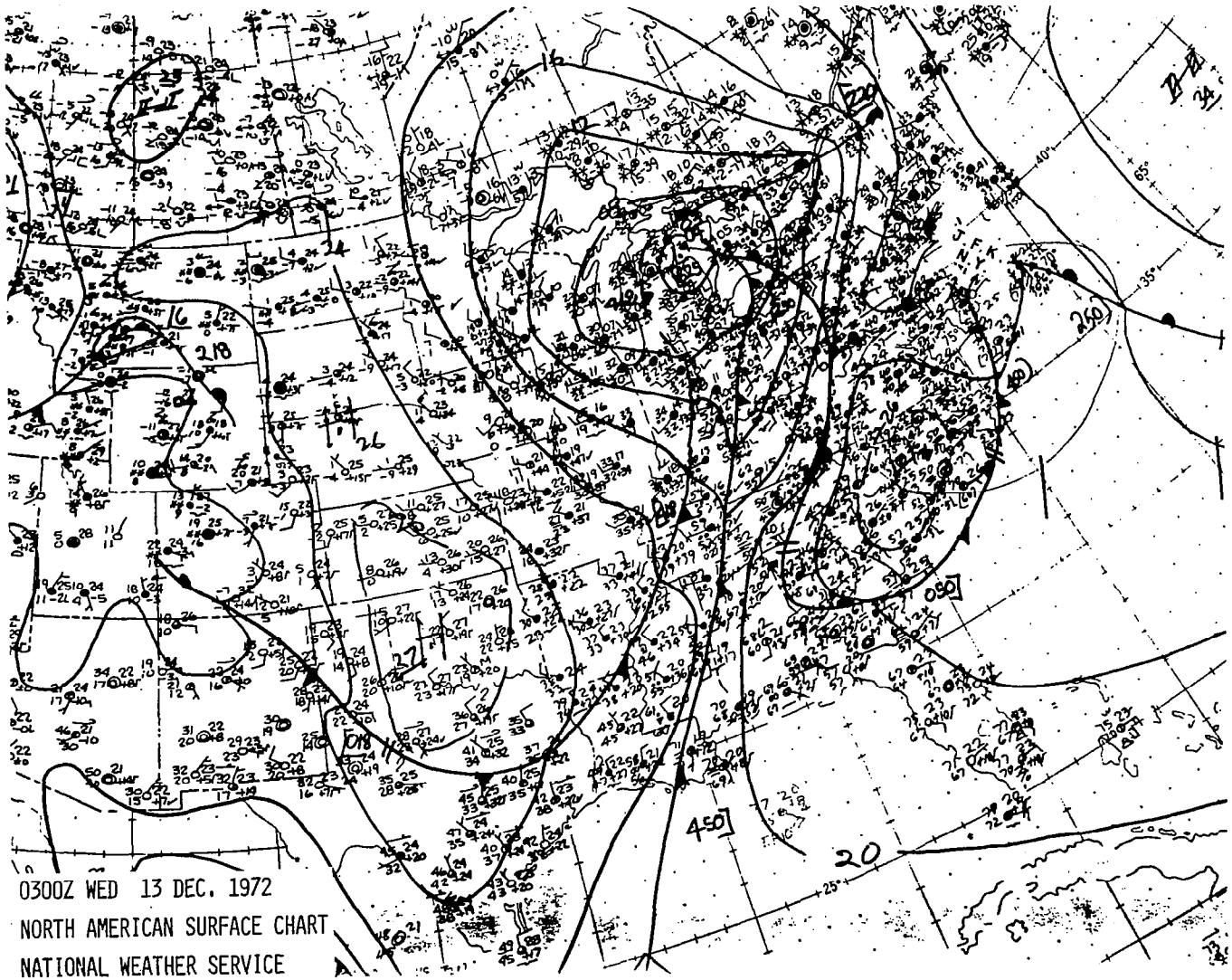

Figure 3.5.4. Early surface weather chart for JFK airport, December 12, 1972 accident.

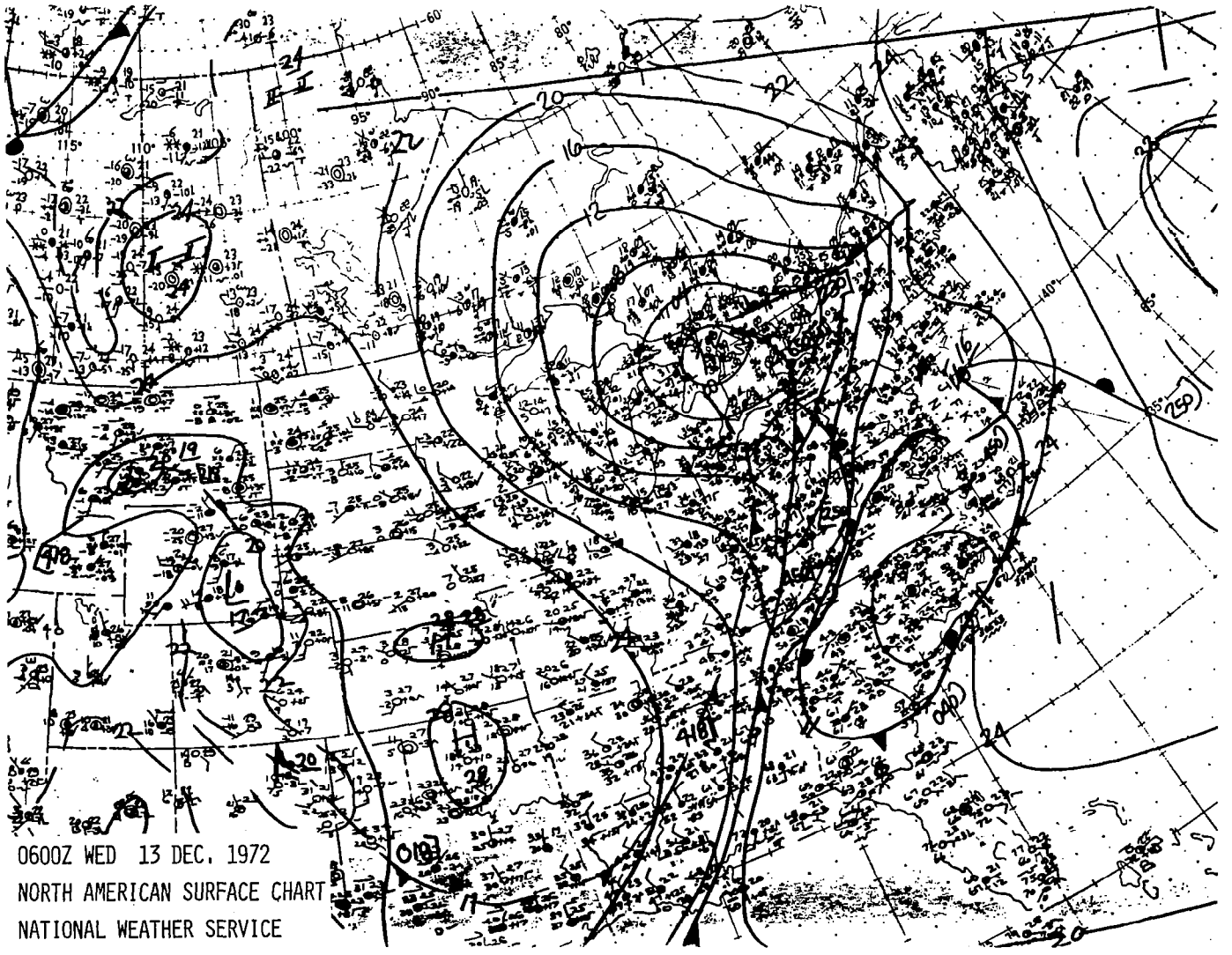

Figure 3.5.5. Late surface weather chart for JFK Airport, December 12, 1972 accident.

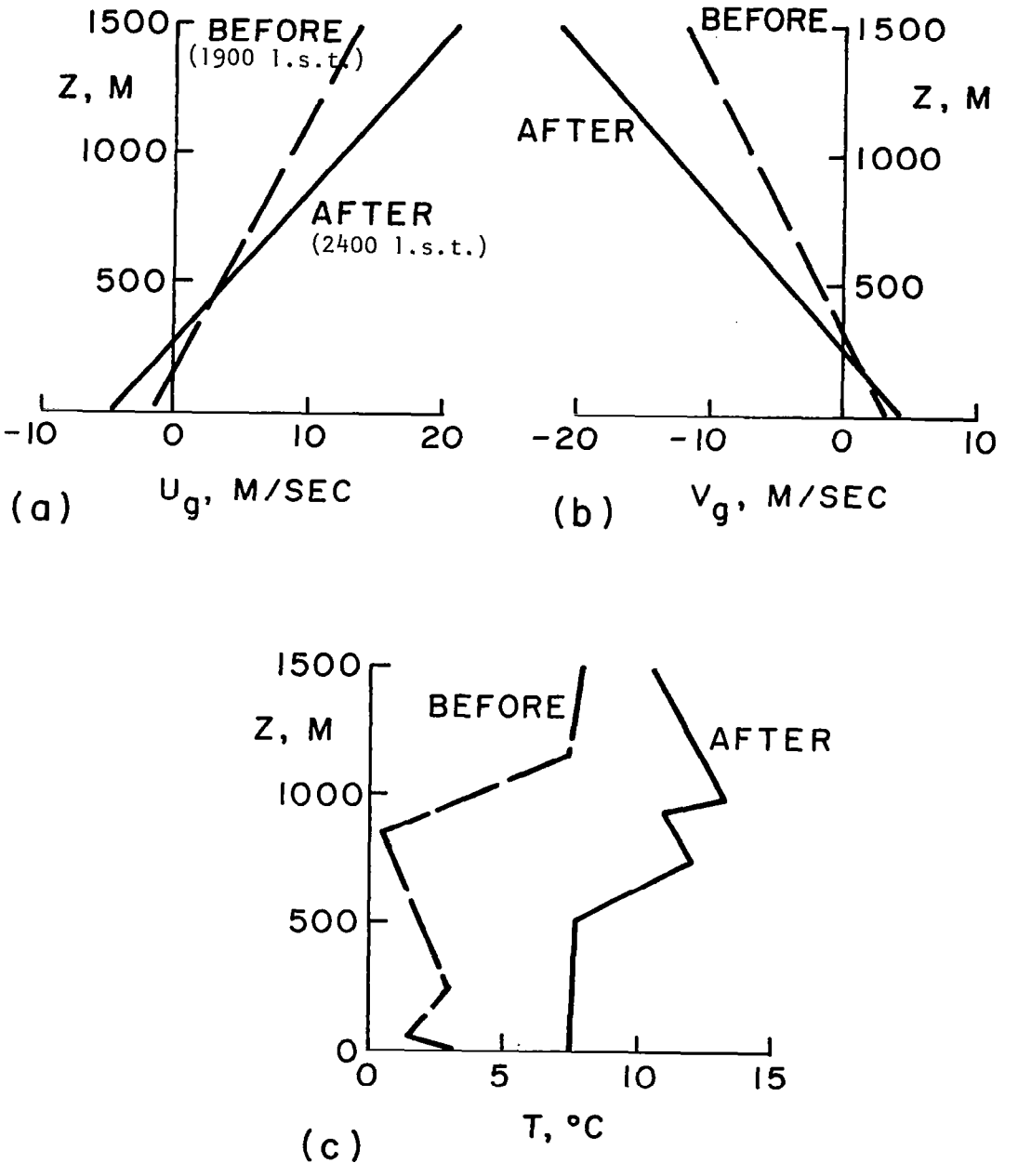

Figure 3.5.6. Altitude profiles for; a) mean geostrophic velocity component parallel to runway (+ U_g, tailwind), b) mean wind velocity component perpendicular to runway (+ V_g, crosswind from right), c) temperature before and after the JFK Airport, December 12, 1972 accident.

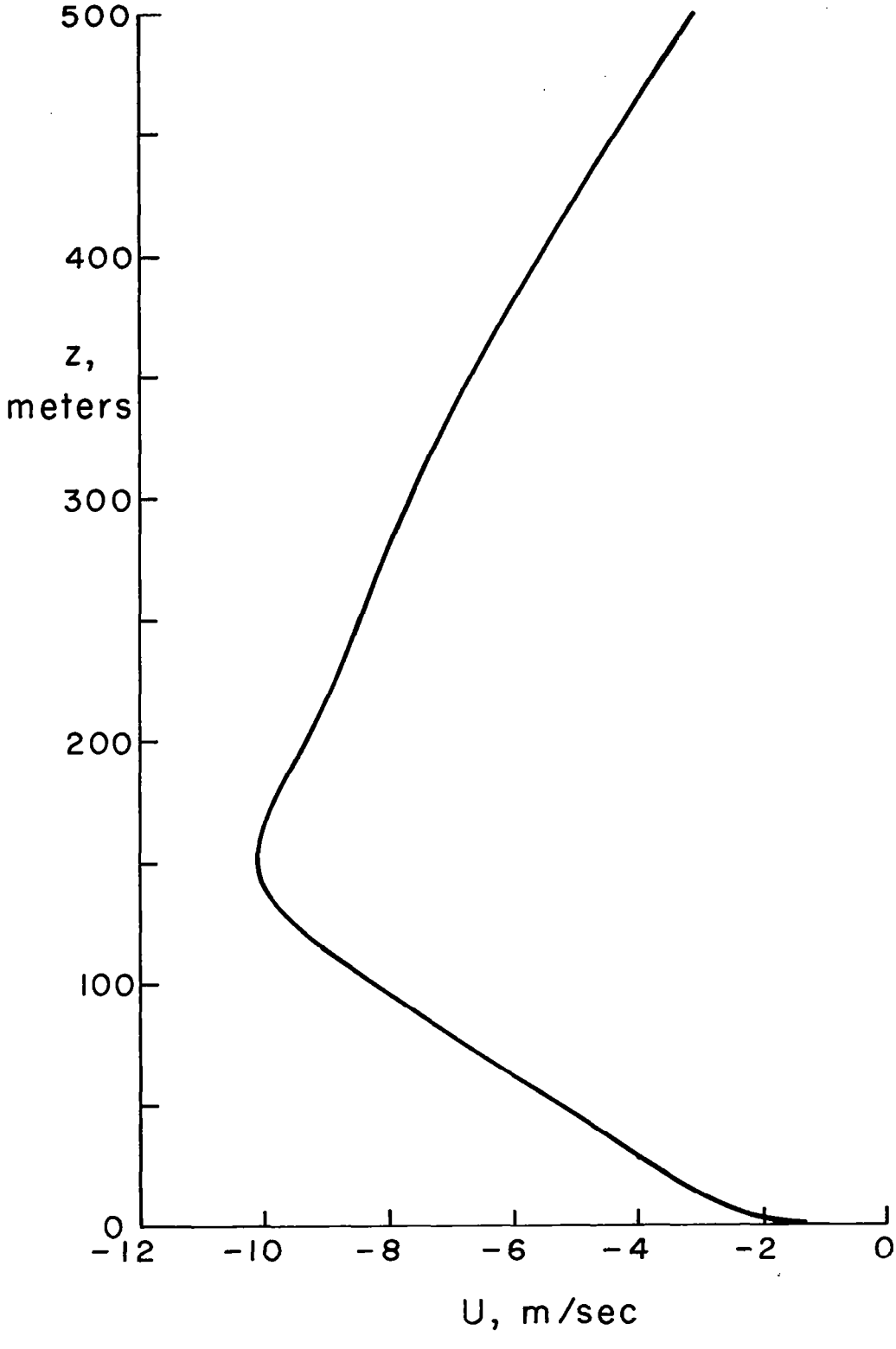

Figure 3.5.7. Altitude profile of mean velocity component parallel to runway (+ U, tailwind) for the JFK Airport, December 12, 1972 accident.

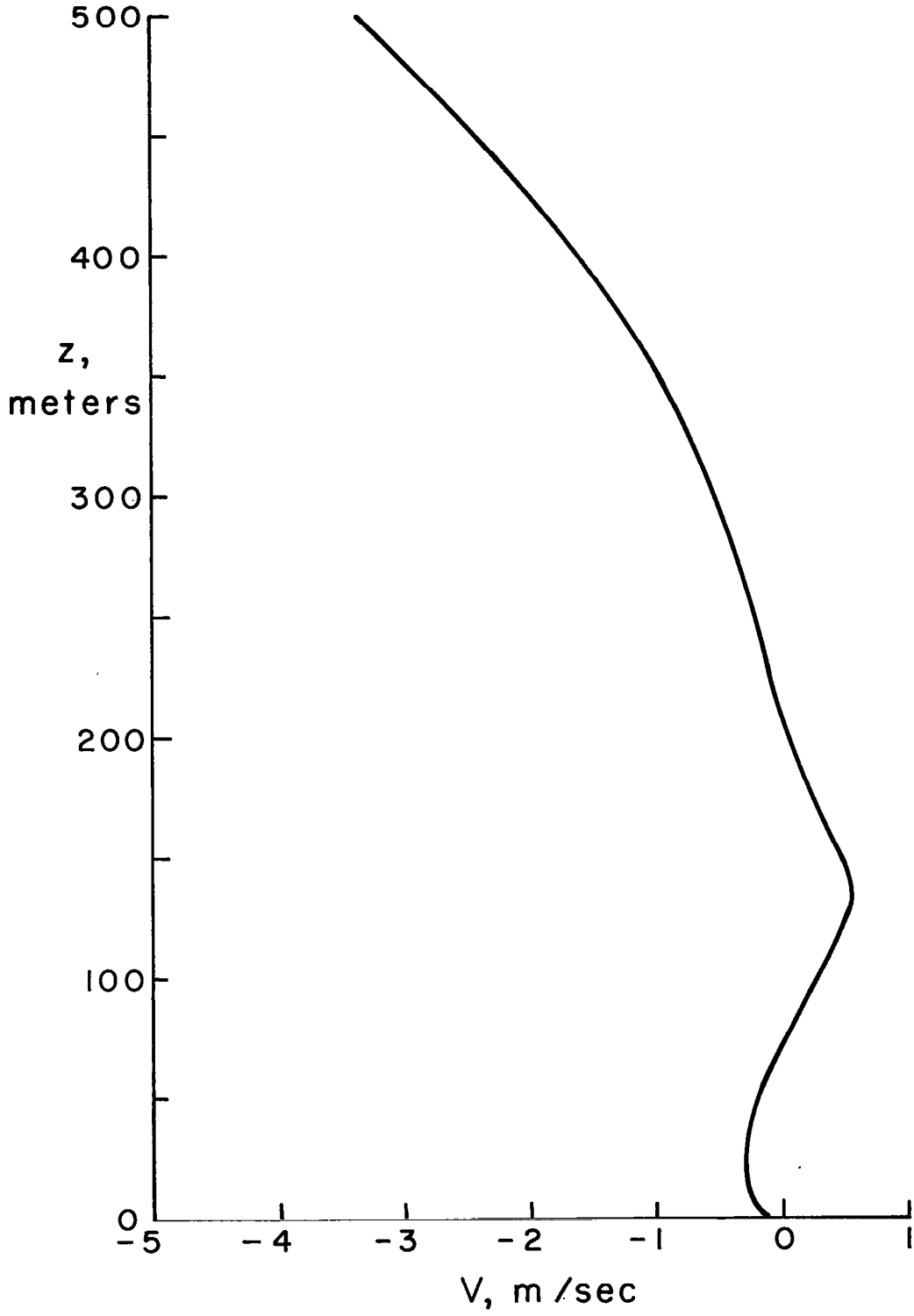

Figure 3.5.8. Altitude profile of mean wind velocity component perpendicular to runway (+ V, crosswind from right) for the JFK airport, December 12, 1972 accident.

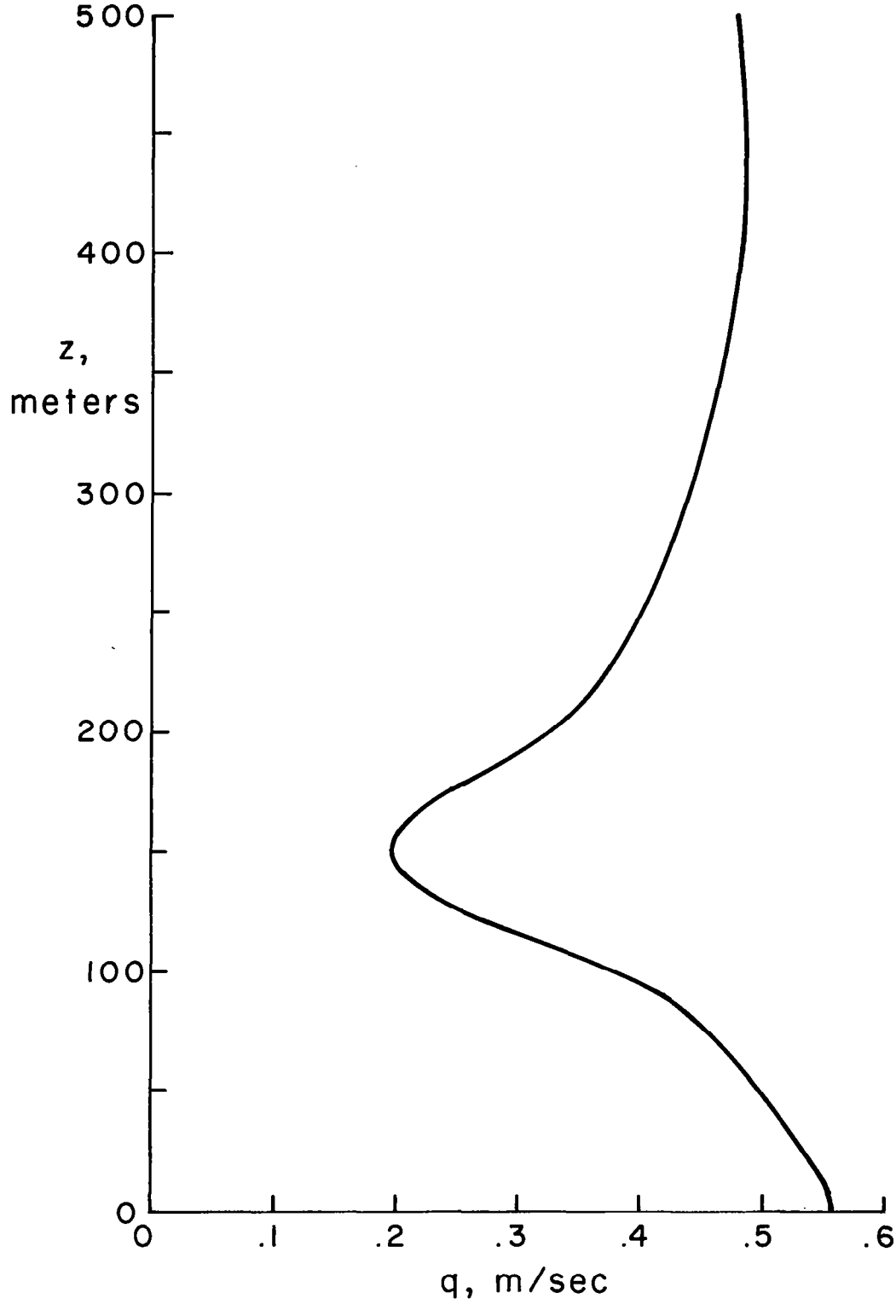

Figure 3.5.9. Altitude profile of variance of the total velocity variance for JFK Airport, December 12, 1972 accident.

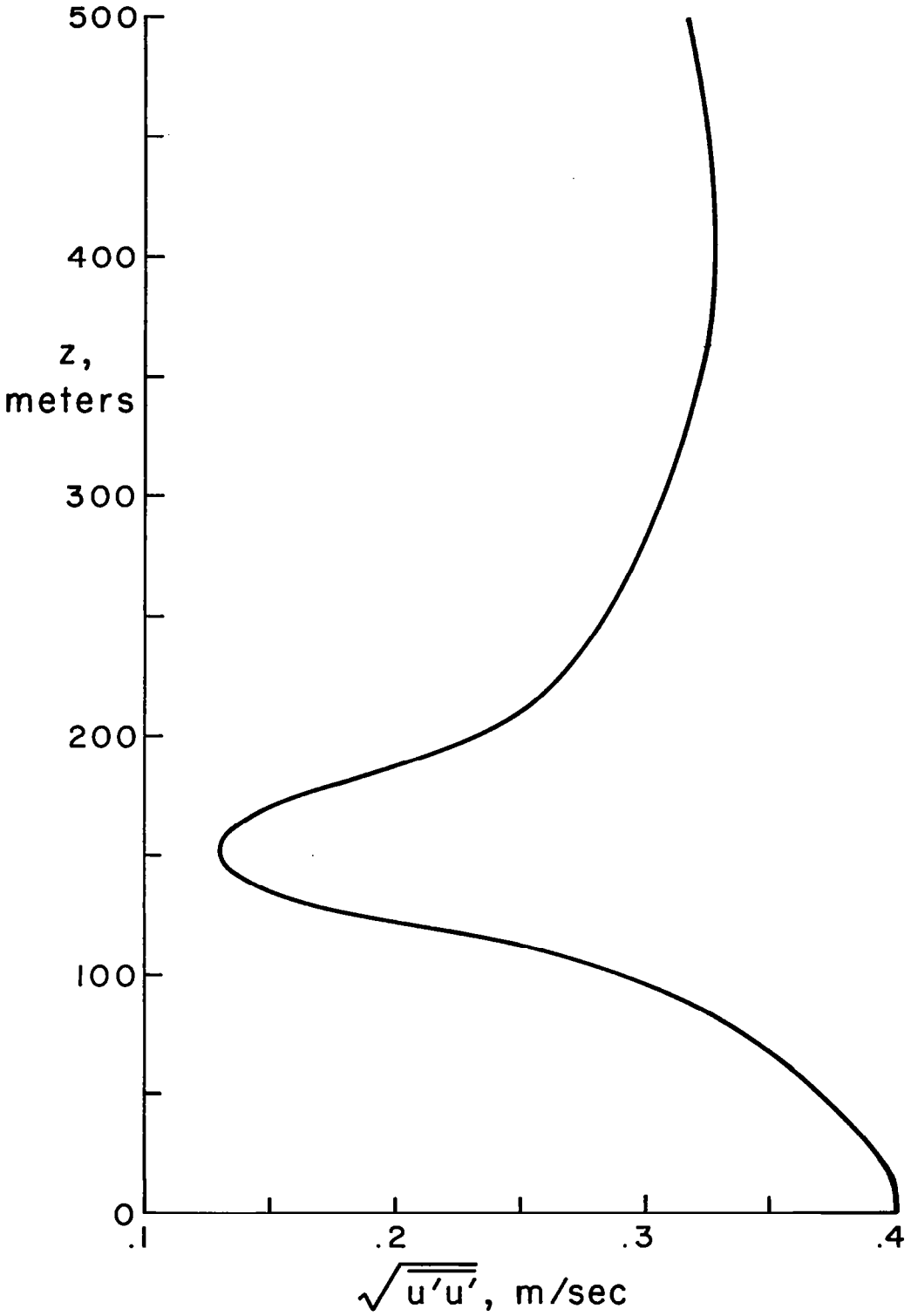

Figure 3.5.10. Altitude profile of variance of the wind parallel to runway for JFK Airport, December 12, 1972 accident.

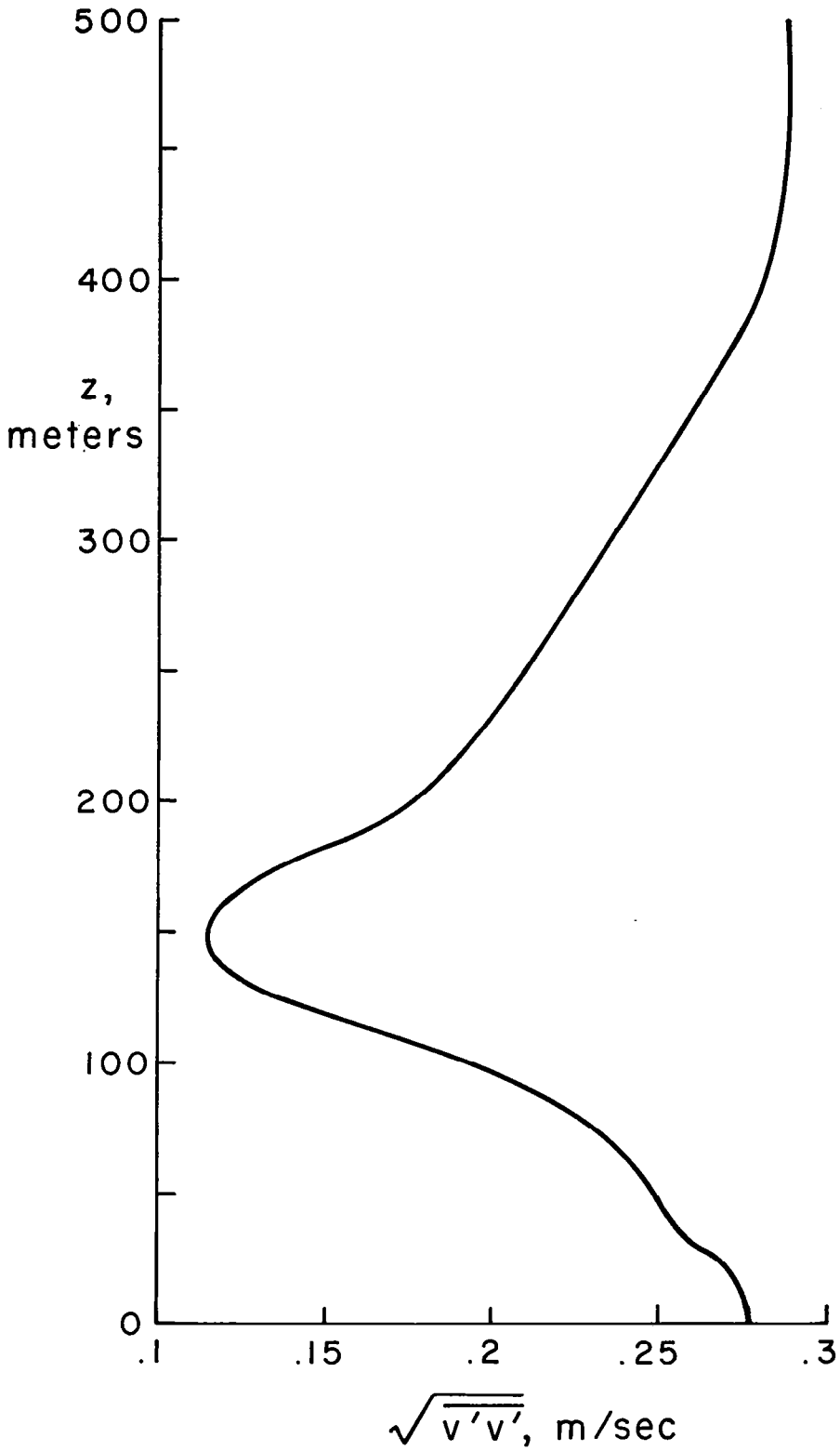

Figure 3.5.11. Altitude profile of variance of the wind perpendicular to runway for JFK Airport, December 12, 1972 accident.

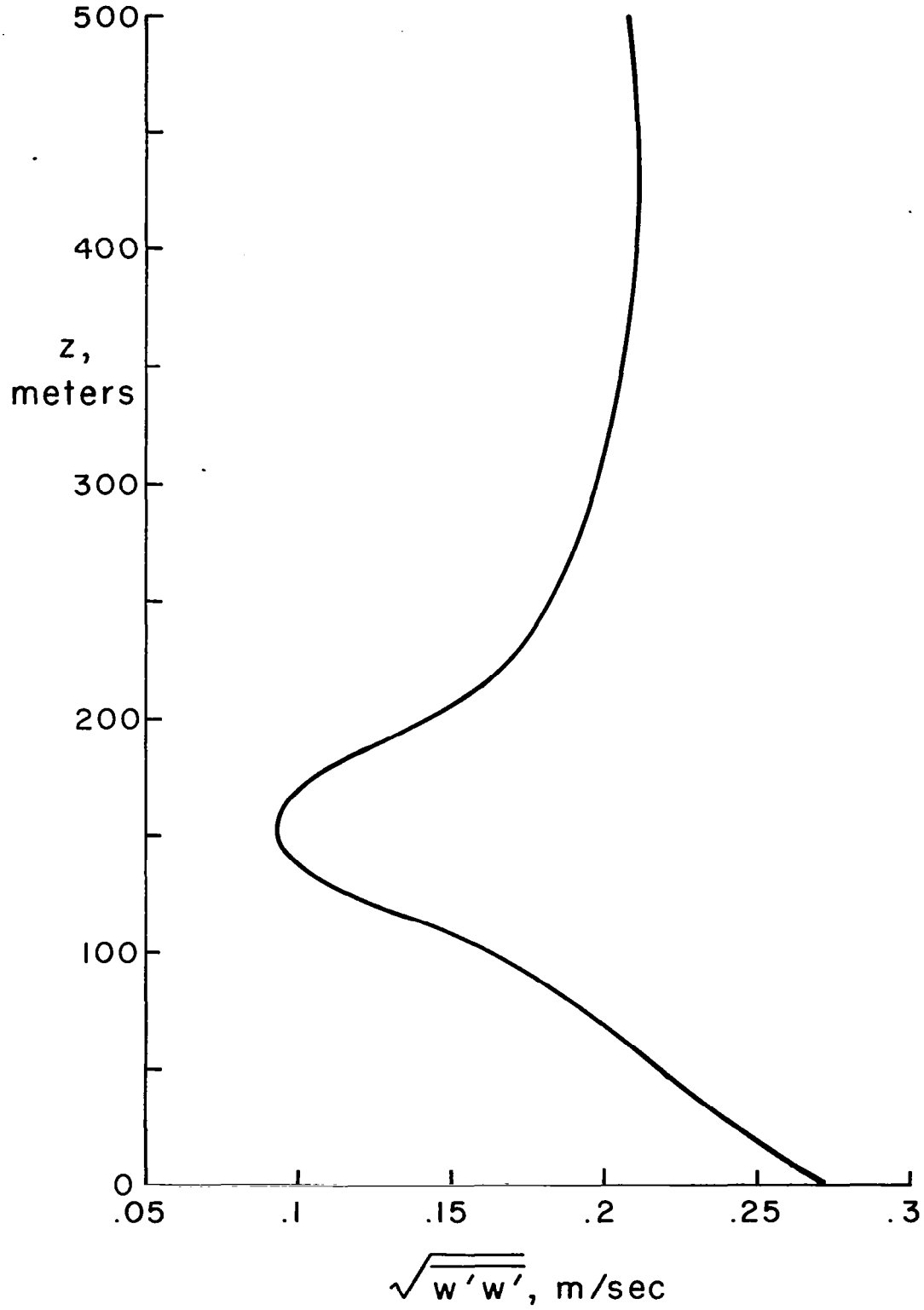

Figure 3.5.12. Altitude profile of variance of the vertical wind for JFK Airport, December 12, 1972 accident.

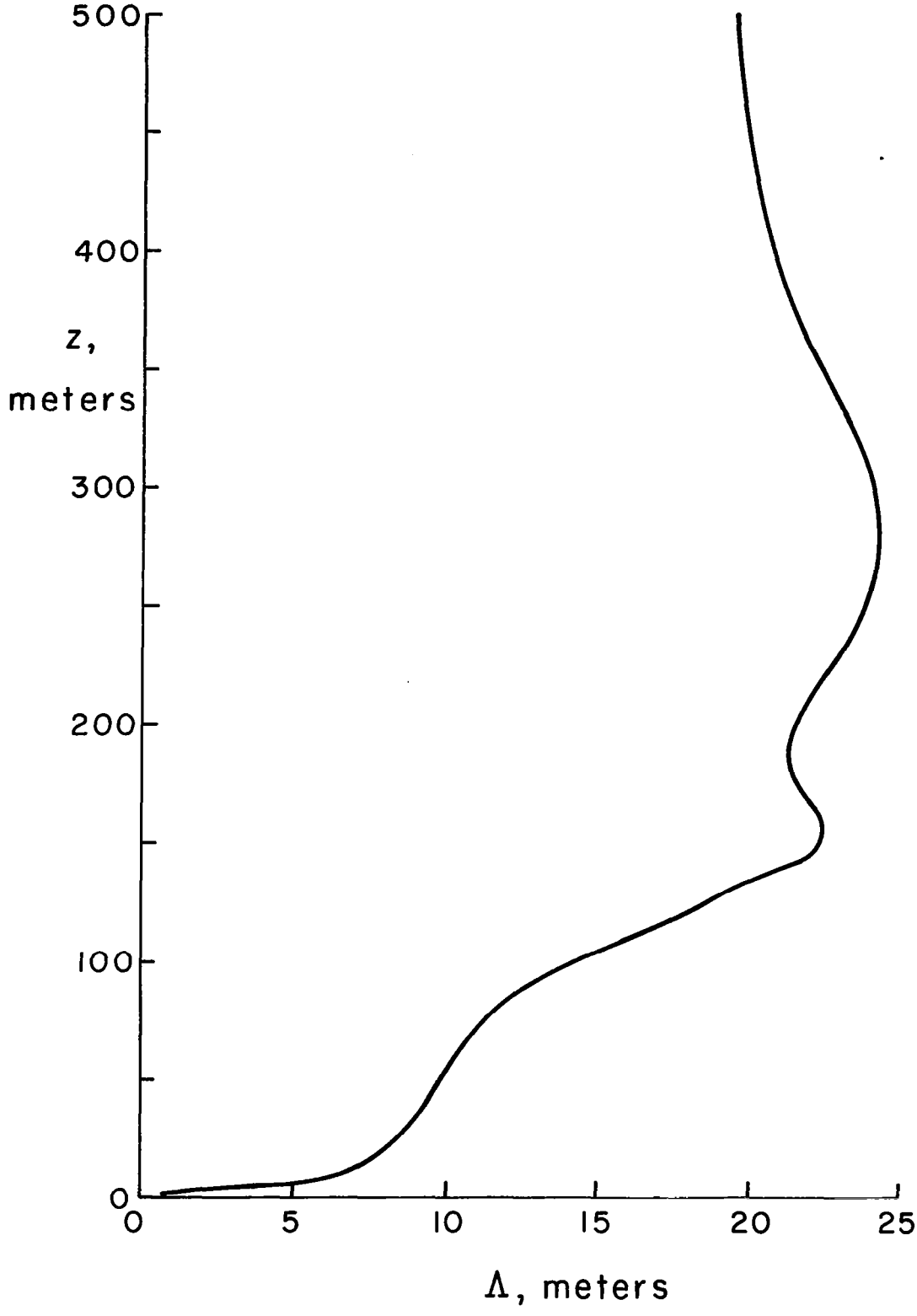

Figure 3.5.13. Altitude profile of scale of turbulence for JFK Airport, December 12, 1972 accident.

3.6 JOHNSTOWN, JANUARY 1974

At 1905 l.s.t. on January 6, 1974 an Air East Beechcraft 99A crashed while attempting to land on Runway 33 at the Johnstown Airport, Pennsylvania (figure 3.6.1). The aircraft was making an ILS approach in light snow and fog conditions when it struck an approach light tower 90 m from the runway threshold and crashed into an embankment 60 m from the threshold.

NWS radar at Pittsburg indicated no precipitation echoes in the Johnstown area at the time of the accident. At this time, the geostrophic wind velocity at the 850 mb altitude was 14 m/sec from 270° and the surface wind was 6 m/sec from 280° (figures 3.6.2 - 3.6.5). Radiosonde data indicated conditionally unstable air below 1300 mean sea level (m.s.l.) (figure 3.6.6). The above conditions would not be expected to produce hazardous wind shear. However, the case was further investigated and profiles characteristic of this weather situation were generated. As expected, the unstable air does not support significant wind shear so the major velocity changes occur above this layer and at ground level (figures 3.6.7 and 3.6.8).

The wind shear does not appear to have been large enough to affect the landing. More likely causes, for the accident are the low approach piloting technique, possible downdraft due to terrain variations, and low visibility due to fog and snow as discussed in the accident investigation (Ref. 16).

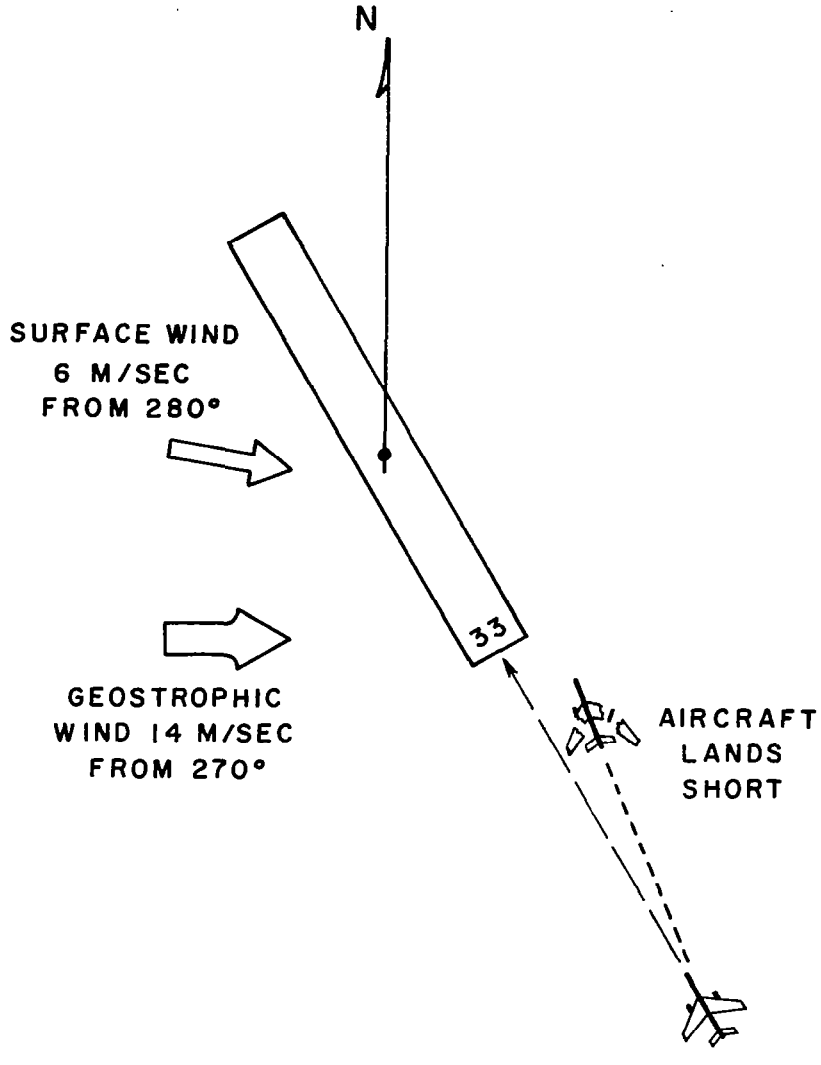

Figure 3.6.1. Aircraft-runway-winds orientation diagram for Johnstown, Pa., January 5, 1974 accident.

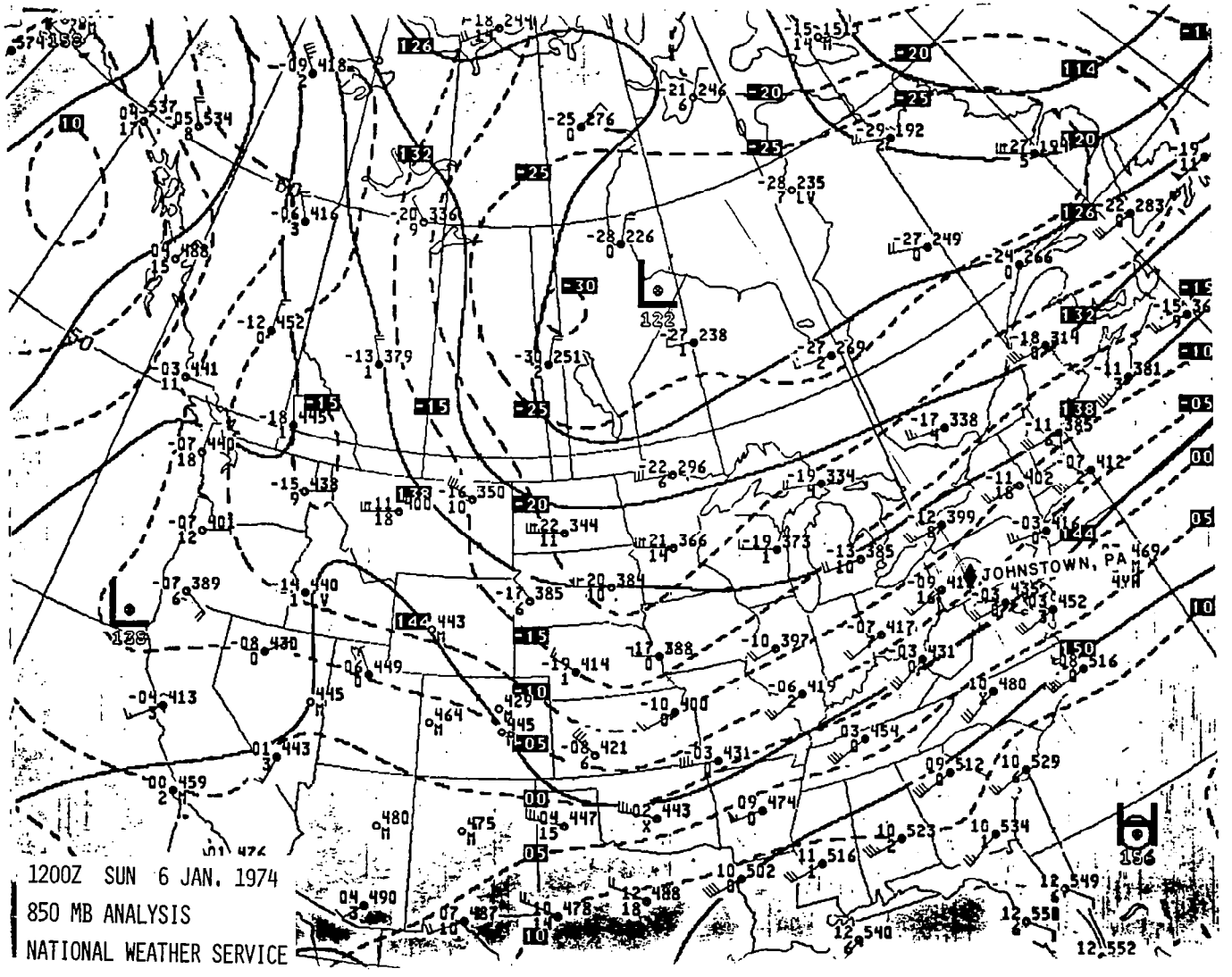

Figure 3.6.2. Early 850 mb chart for Johnstown, Pa., January 6, 1974 accident.

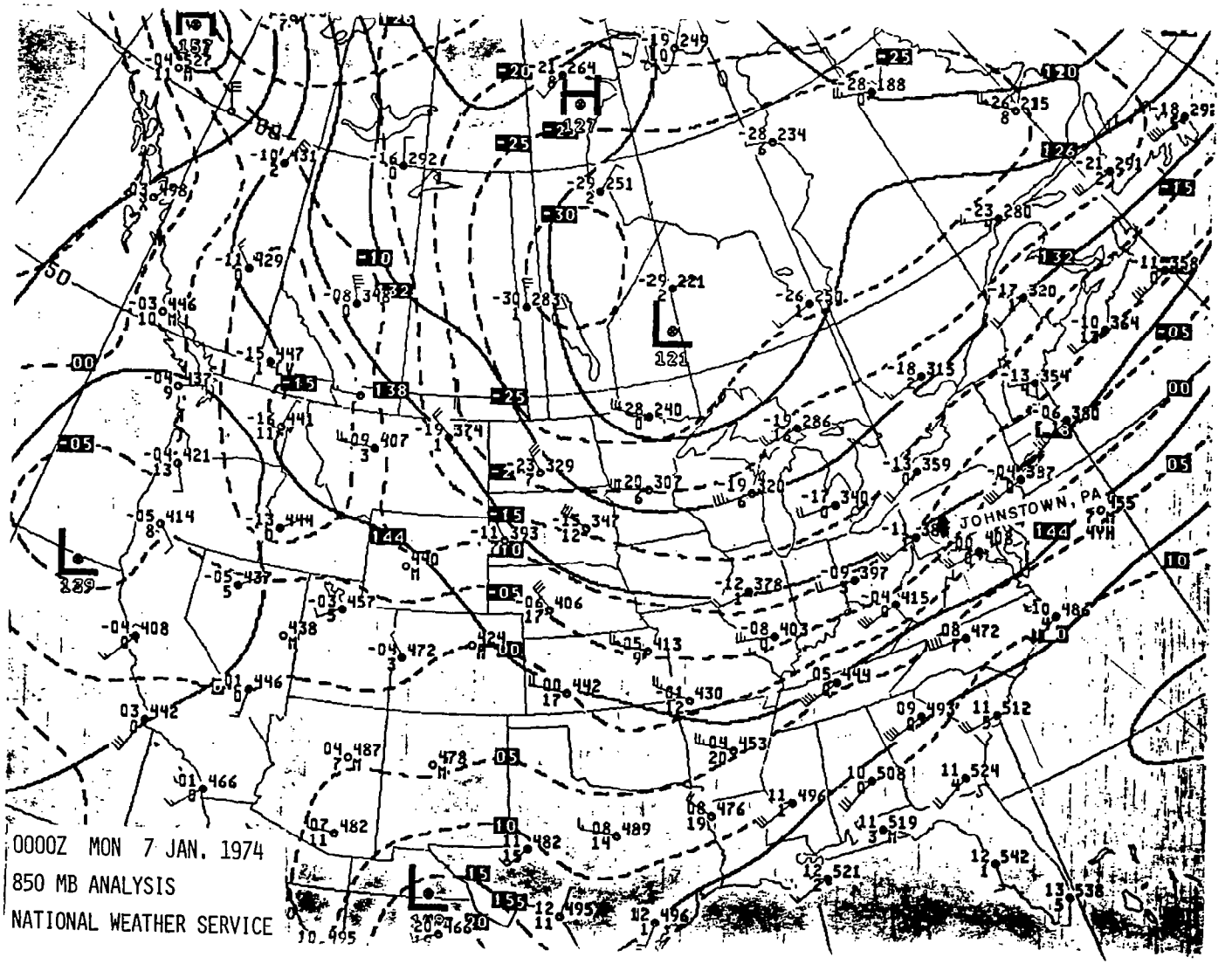

Figure 3.6.3. Late 850 mb chart for Johnstown, Pa., January 6, 1974 accident.

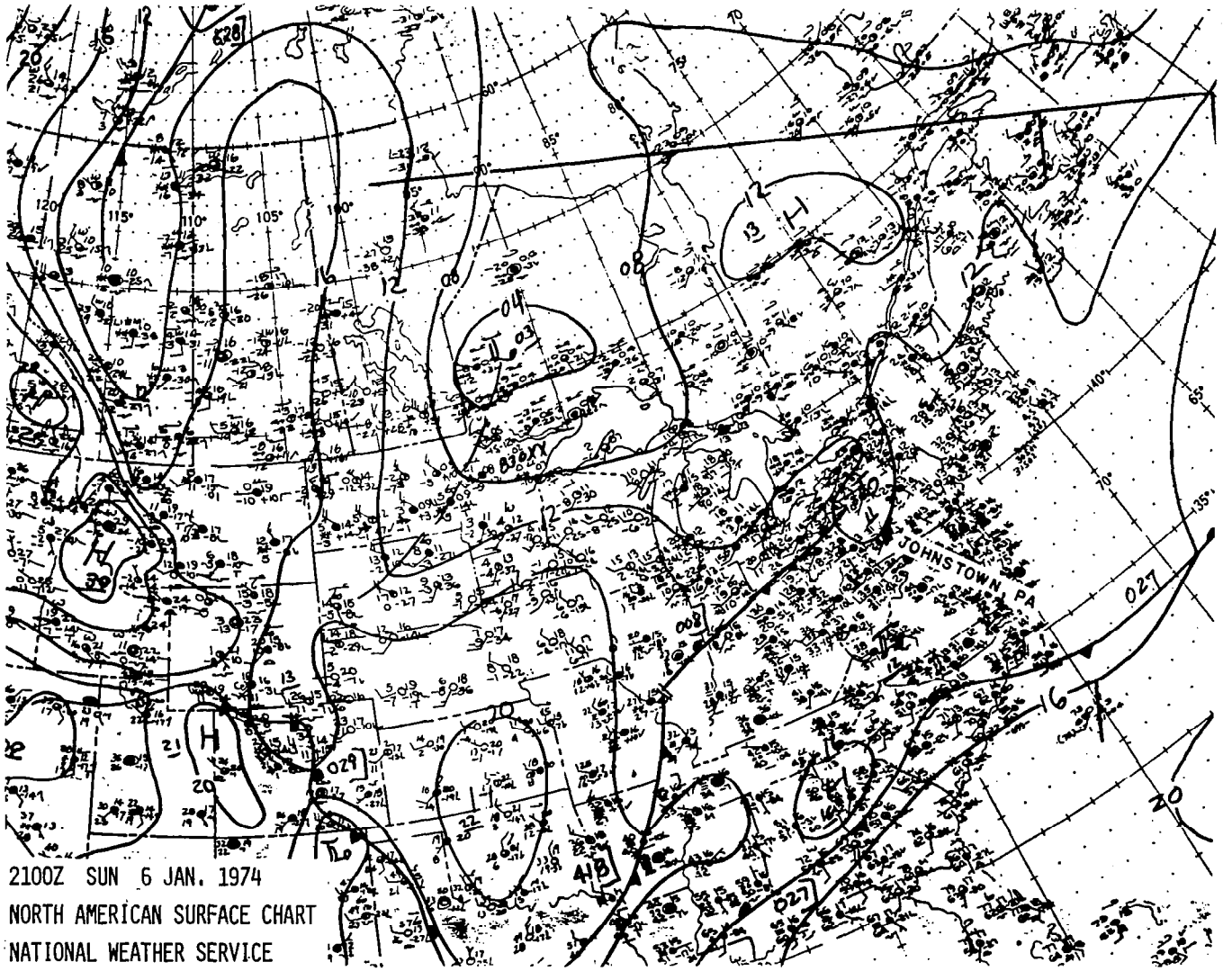

Figure 3.6.4. Early surface weather chart for Johnstown, Pa., January 6, 1974 accident.

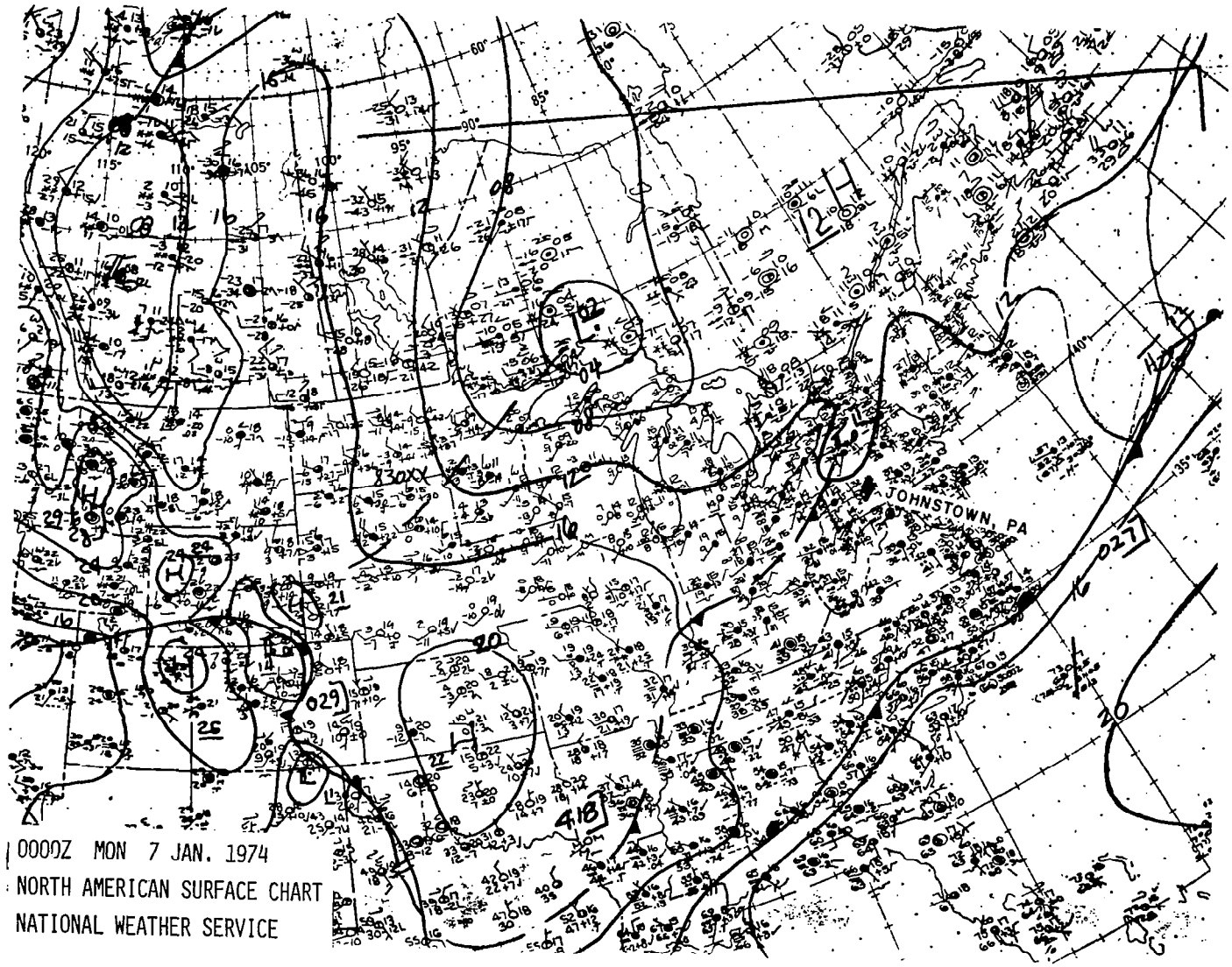

Figure 3.6.5. Late surface weather chart for Johnstown, Pa., January 6, 1974 accident.

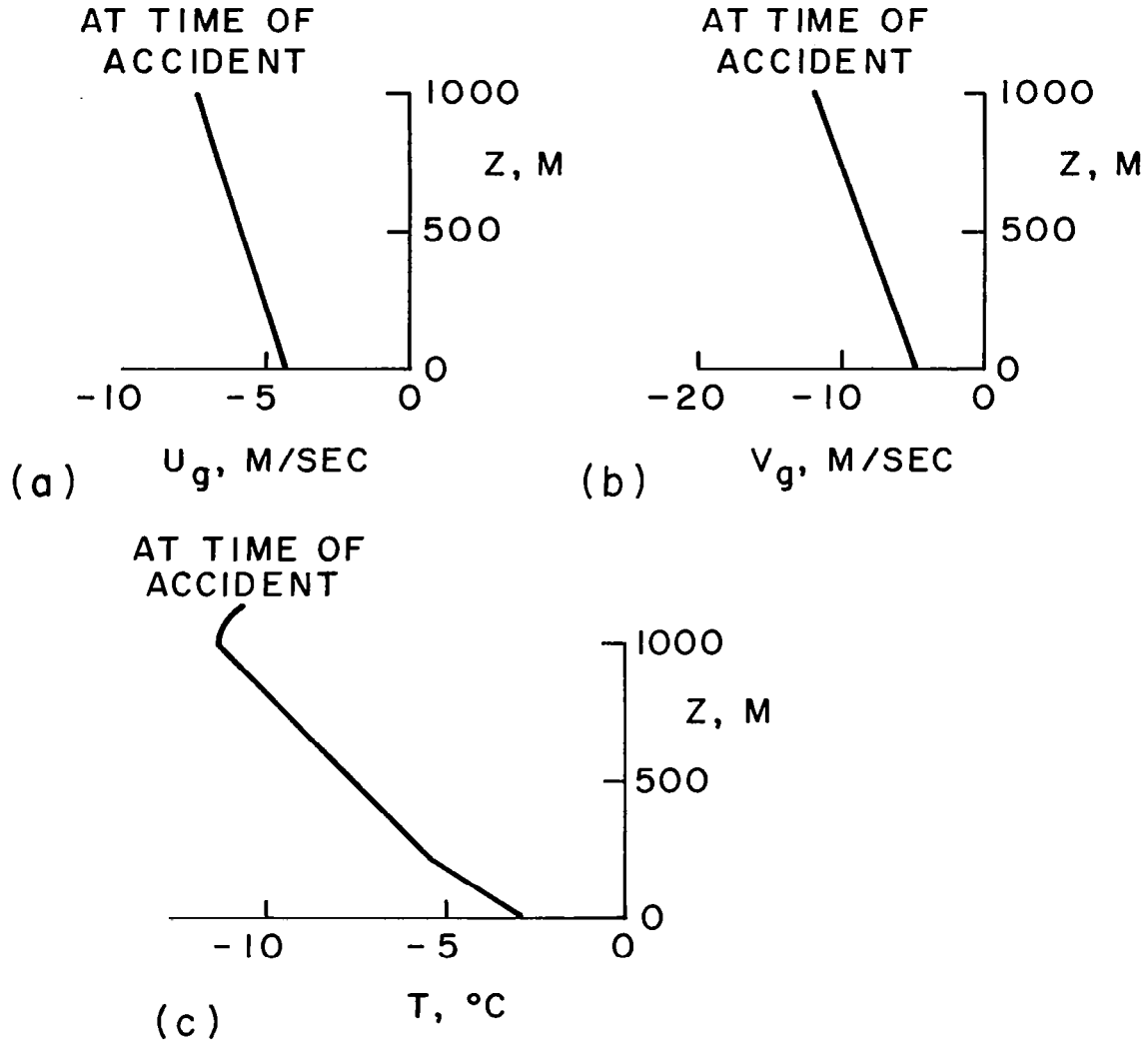

Figure 3.6.6. Altitude profiles for: a) mean geostrophic velocity component parallel to runway (+ U_g, tailwind), b) mean wind velocity component perpendicular to runway (+ V_g, crosswind from right), c) temperature before and after the Johnstown, Pa., January 6, 1974 accident.

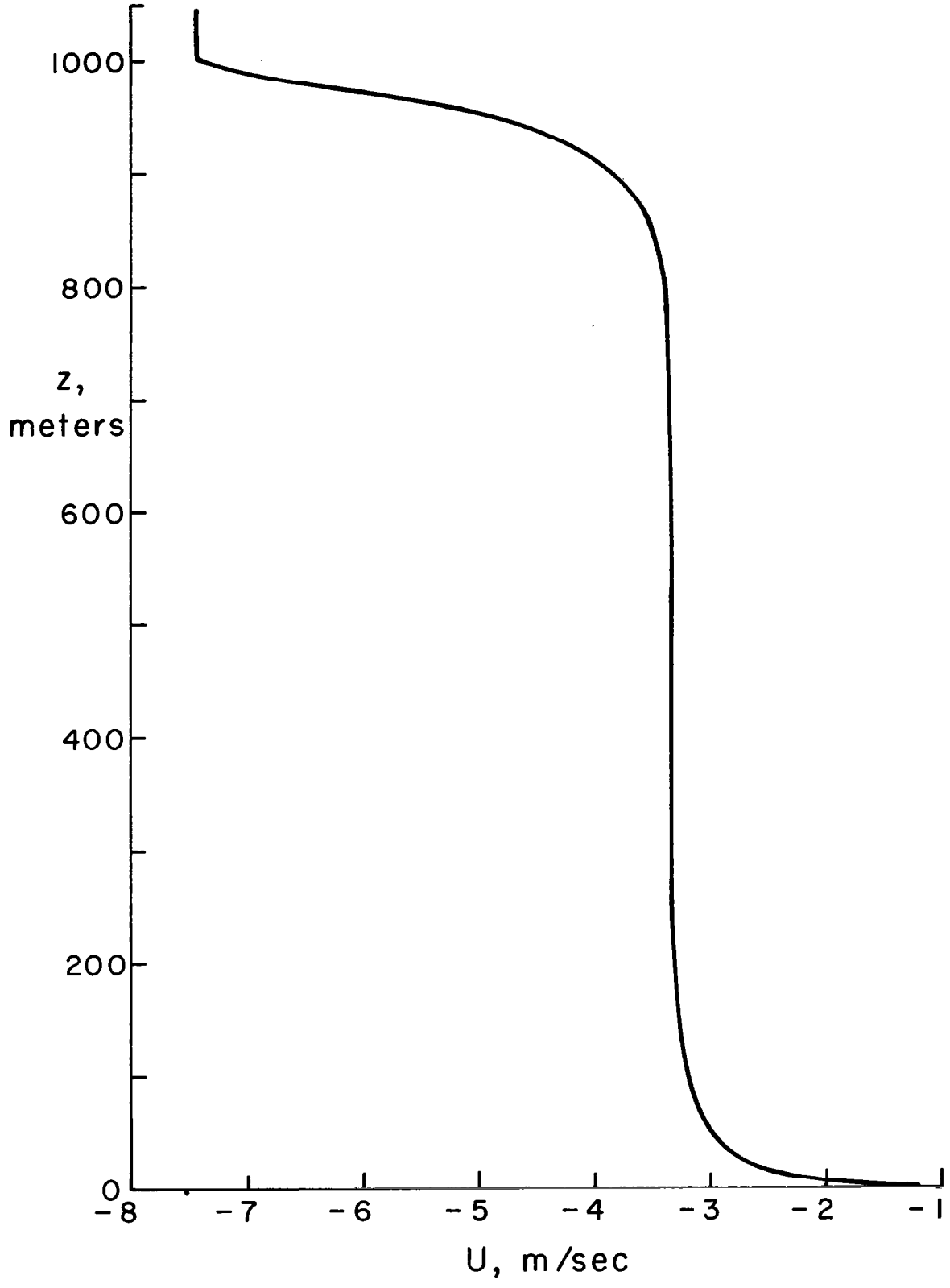

Figure 3.6.7. Altitude profile of mean wind velocity component parallel to runway (+ U, tailwind) for the Johnstown, Pa., January 6, 1974 accident.

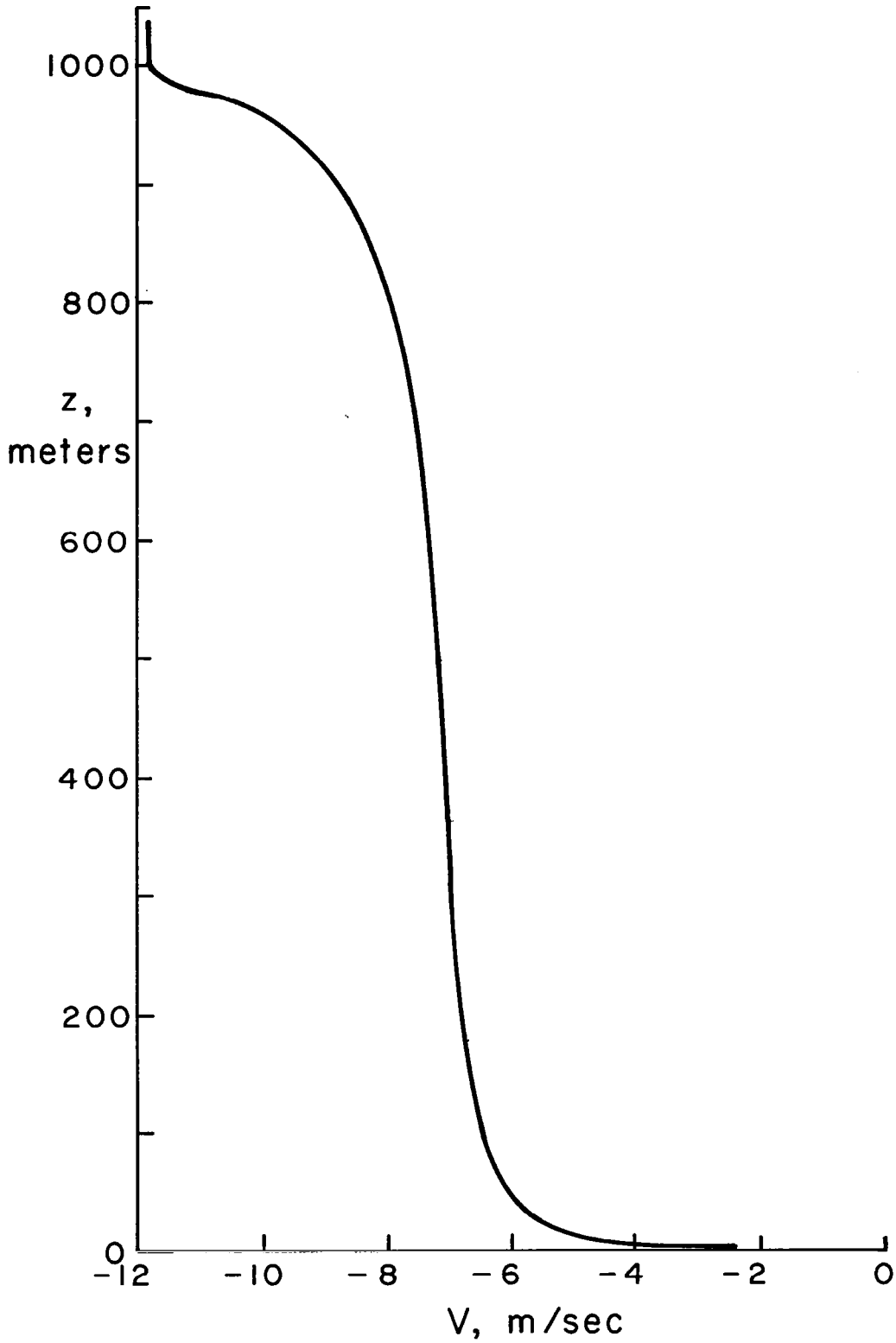

Figure 3.6.8. Altitude profile of mean wind velocity component perpendicular to runway (+ V, crosswind from right) for the Johnstown, Pa., January 6, 1974 accident.

4. ACCIDENTS INVOLVING THUNDERSTORM GUST FRONTS

4.1 INTRODUCTION

The following sections of this report discuss the modeling details peculiar to four accidents and presents the input data and results for each case. A fifth case that fits into this category is the June, 1975 Eastern Airlines crash at JFK, which was considered in an earlier report (Ref. 11).

4.2 DENVER, AUGUST 1975

At 1511 l.s.t. on August 7, 1975 a Continental Airlines 727 crashed on take-off from Runway 352, Stapleton Airport, Denver, Colorado. The pilot of the preceding aircraft observed virga above the runway prior to take-off and reported wind shear at about 70 m altitude (Ref. 17). The NWS radar at Limon, Colorado, noted a precipitation echo near Stapleton airport at the time of the accident (figure 4.2.1). The recorded flight data show a large decrease in indicated airspeed and large variations in normal acceleration. Thus, it appears probable that the aircraft encountered a downdraft and loss of headwind due to the gust front associated with a small thunderstorm cell. A.R.A.P. has modeled such a gust front as described in Section 2.3. The simulation with a 500 m downdraft at the top of the domain appears to be the type of cell which swept across the airport at the time of the accident. The radially expanding gust front has spread to approximately 2.5 km, 200 sec of simulated time after initialization. The flowfield at this time is shown in figures 4.2.2 - 4.2.7 as a function of R and z. The flowfield was, of course, changing as the aircraft passed through it, but for purposes of this simulation it appears adequate to keep the flowfield frozen and let the aircraft fly through it. The additional correlations $\overline{u'u'}$ and $\overline{v'v'}$ are not included in this set, but are included, later in the study, as a function of aircraft range from impact.

The aircraft trajectory through the flowfield (figure 4.2.8) has been estimated based on the description given by the flight crew and accident investigators. The main points are:

1. The vehicle became airborne after approximately 1400 m ground roll.

2. After normal initial ascent the craft lost airspeed and stopped ascending at an altitude of approximately 70 m.

3. The aircraft initially impacted approximately 2500 m from the start of its ground roll.

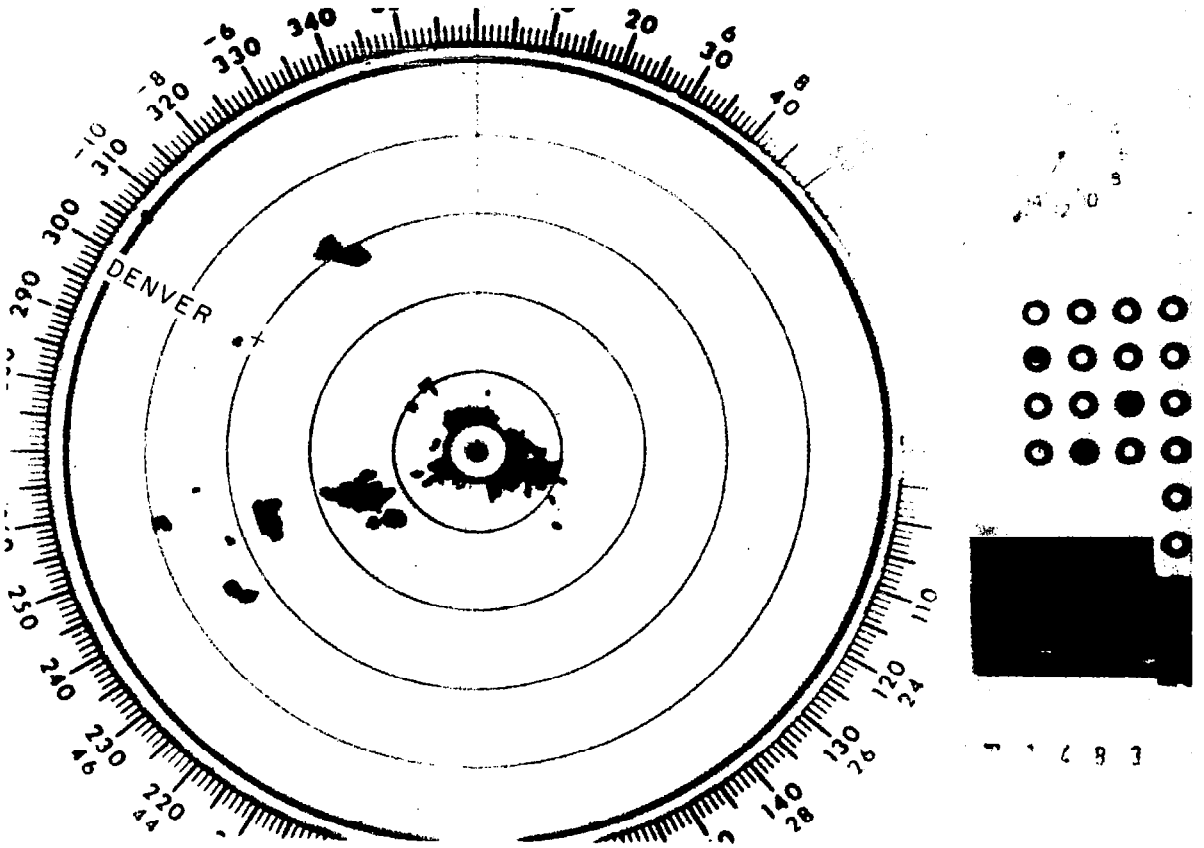

Figure 4.2.1. Radarscope picture near the time of the Denver, Colorado, August 7, 1975 accident.

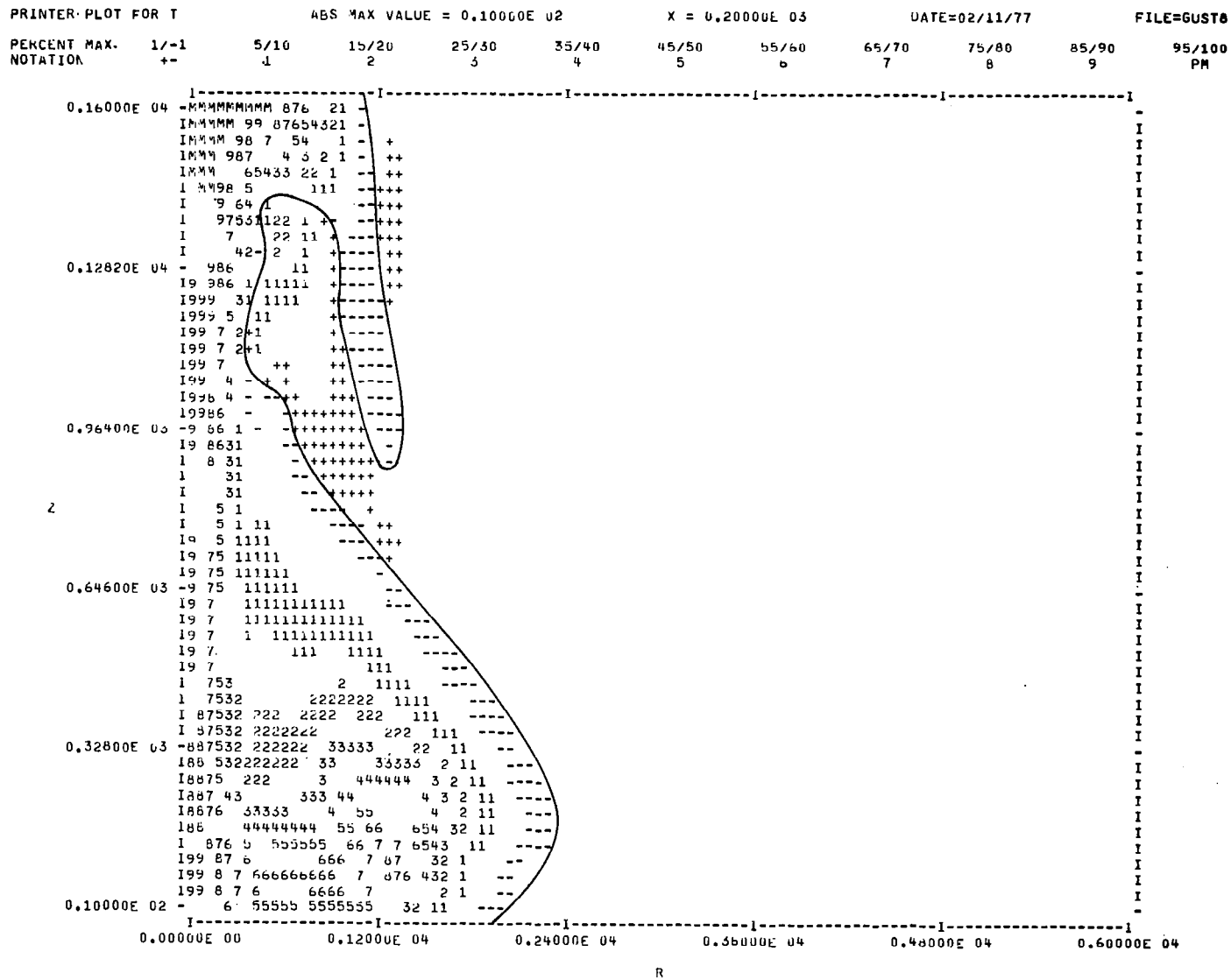

Figure 4.2.2. Normalized temperature contours as a function of z and R for an axisymmetric gust front with a 500 m radius downdraft at t = 200 sec. [See figure 2.3.2 for explanation of notation.]

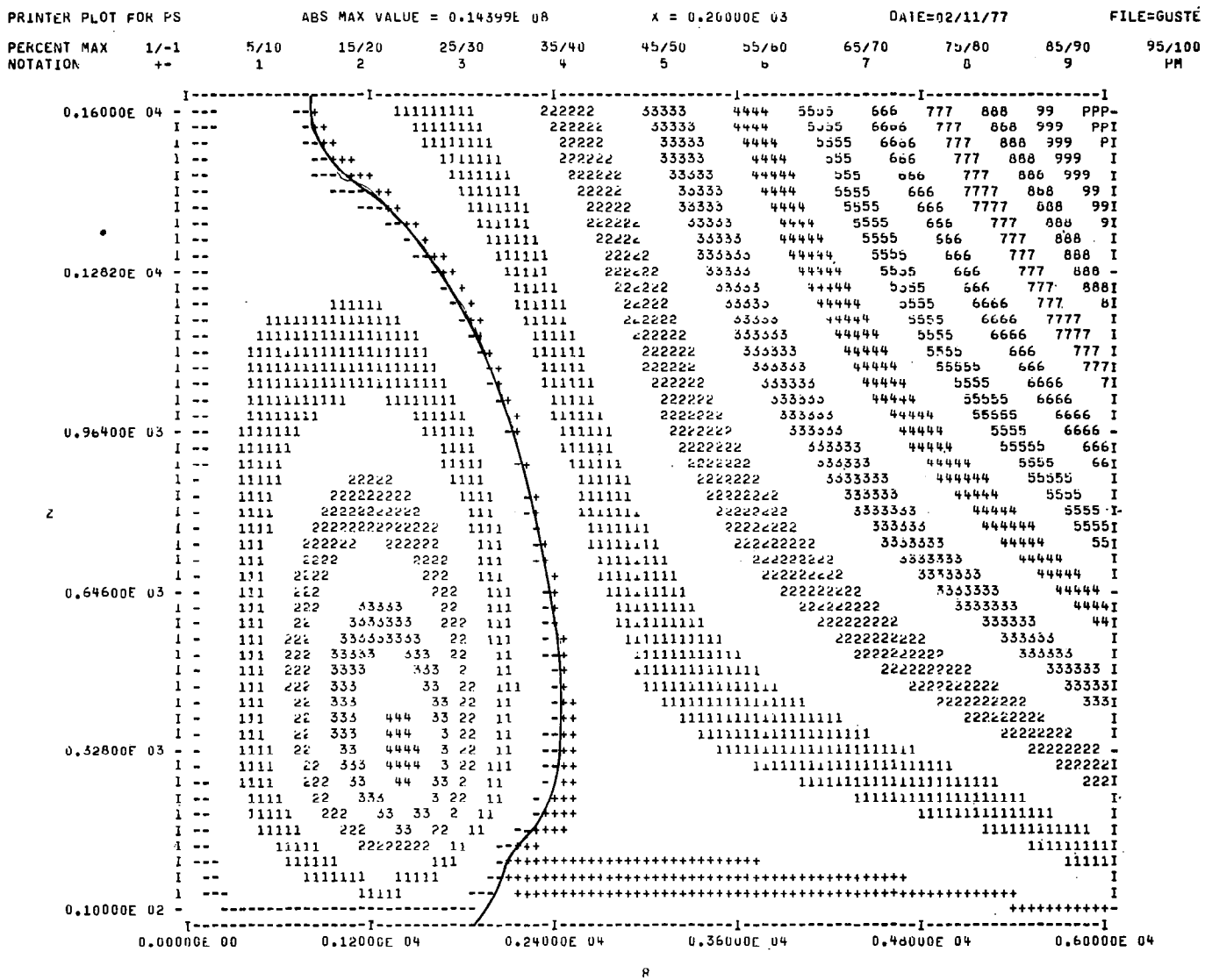

Figure 4.2.3. Normalized stream function contours as a function of z and R for an axisymmetric gust front with a 500 m radius downdraft at t = 200 sec. [See figure 2.3.2 for explanation of notation.]

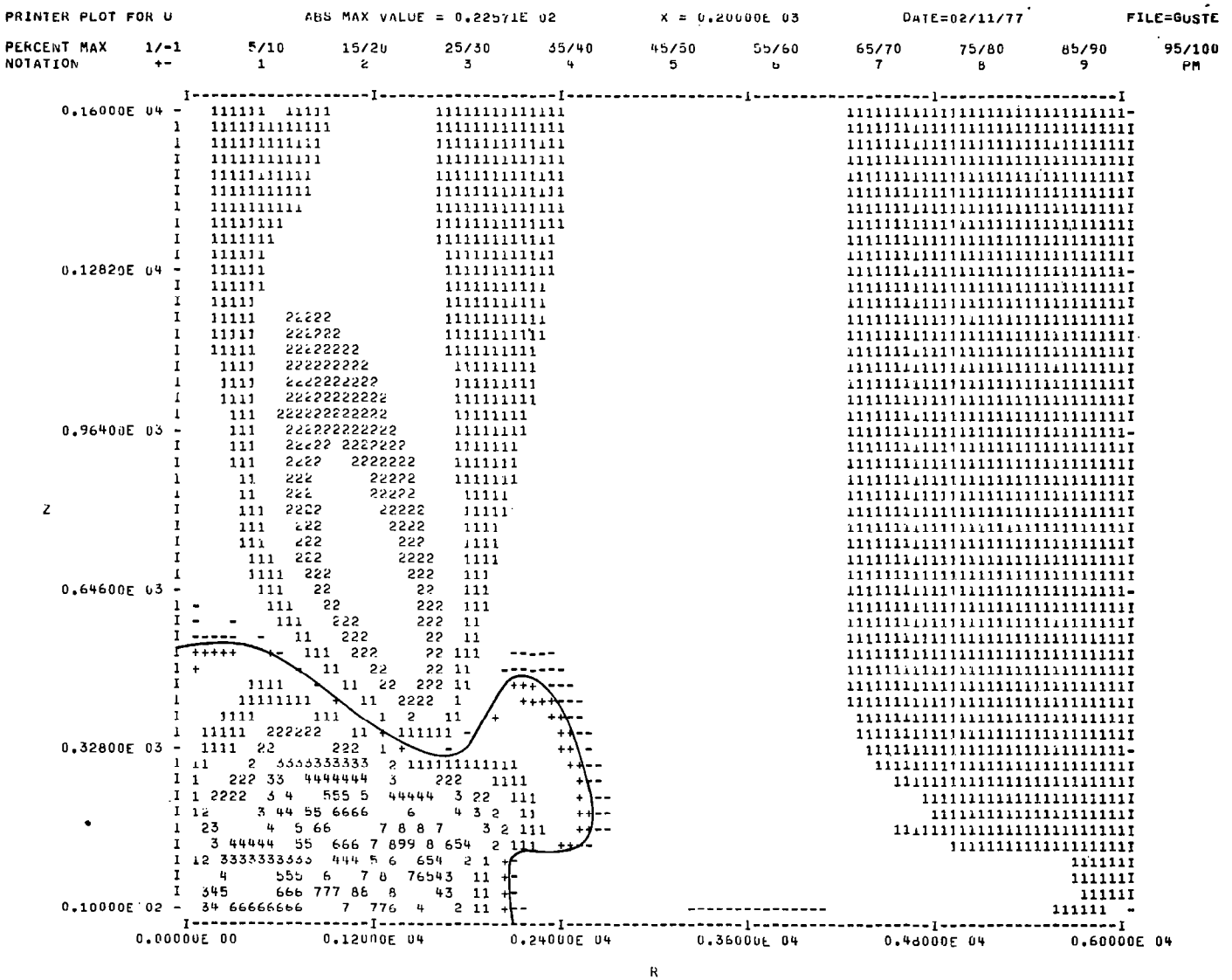

Figure 4.2.4. Normalized mean radial velocity contours as a function of z and R for an axisymmetric gust front with a 500 m radius downdraft at t = 200 sec. [See figure 2.3.2 for explanation of notation.]

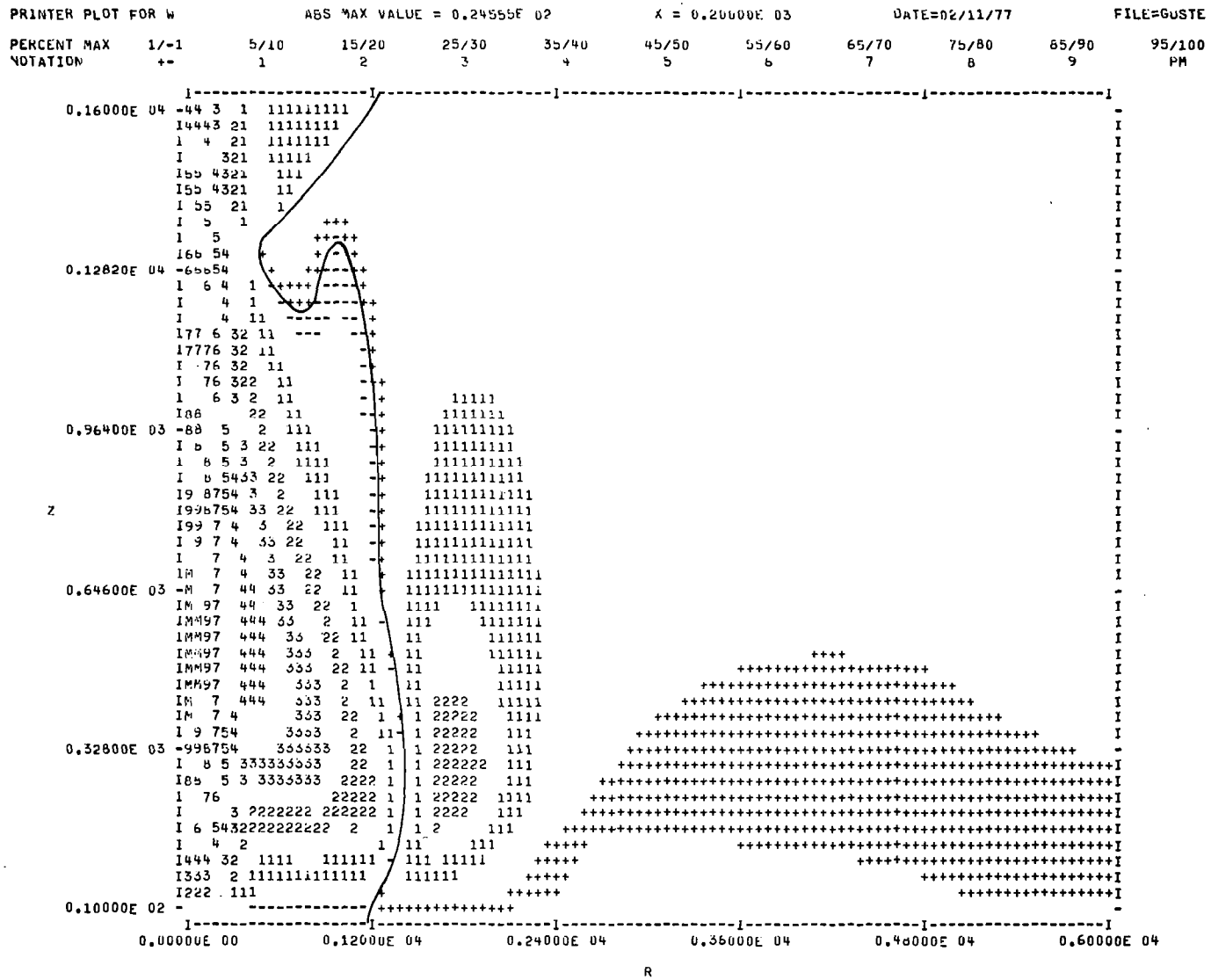

Figure 4.2.5. Normalized mean vertical velocity contours as a function of z and R for an axisymmetric gust front with a 500 m radius downdraft at t = 200 sec. [See figure 2.3.2 for explanation of notation.]

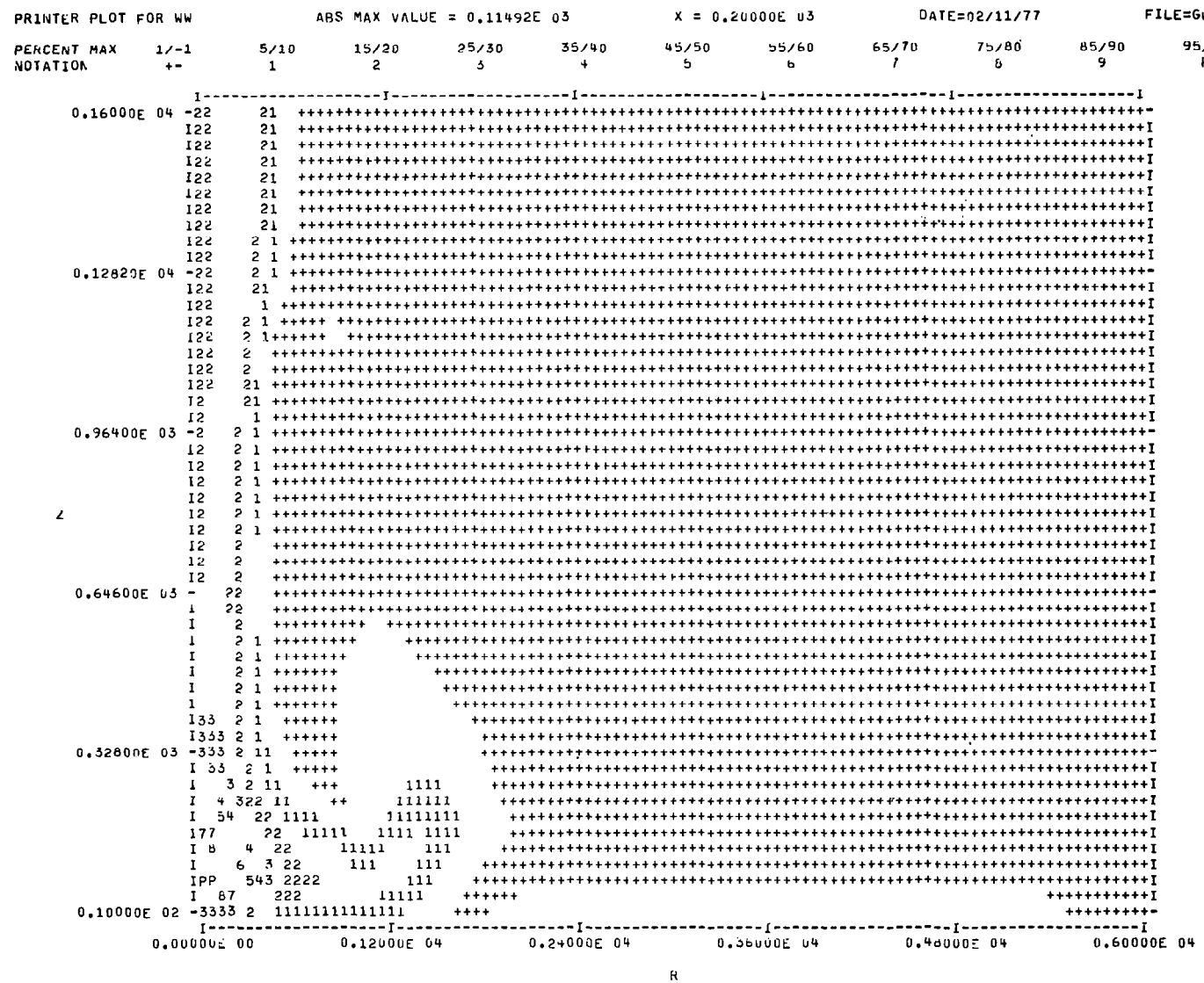

Figure 4.2.6. Normalized variance of vertical velocity contours as a function of z and R for an axisymmetric gust front with a 500 m radius downdraft at t = 200 sec. [See figure 2.3.2 for explanation of notation.]

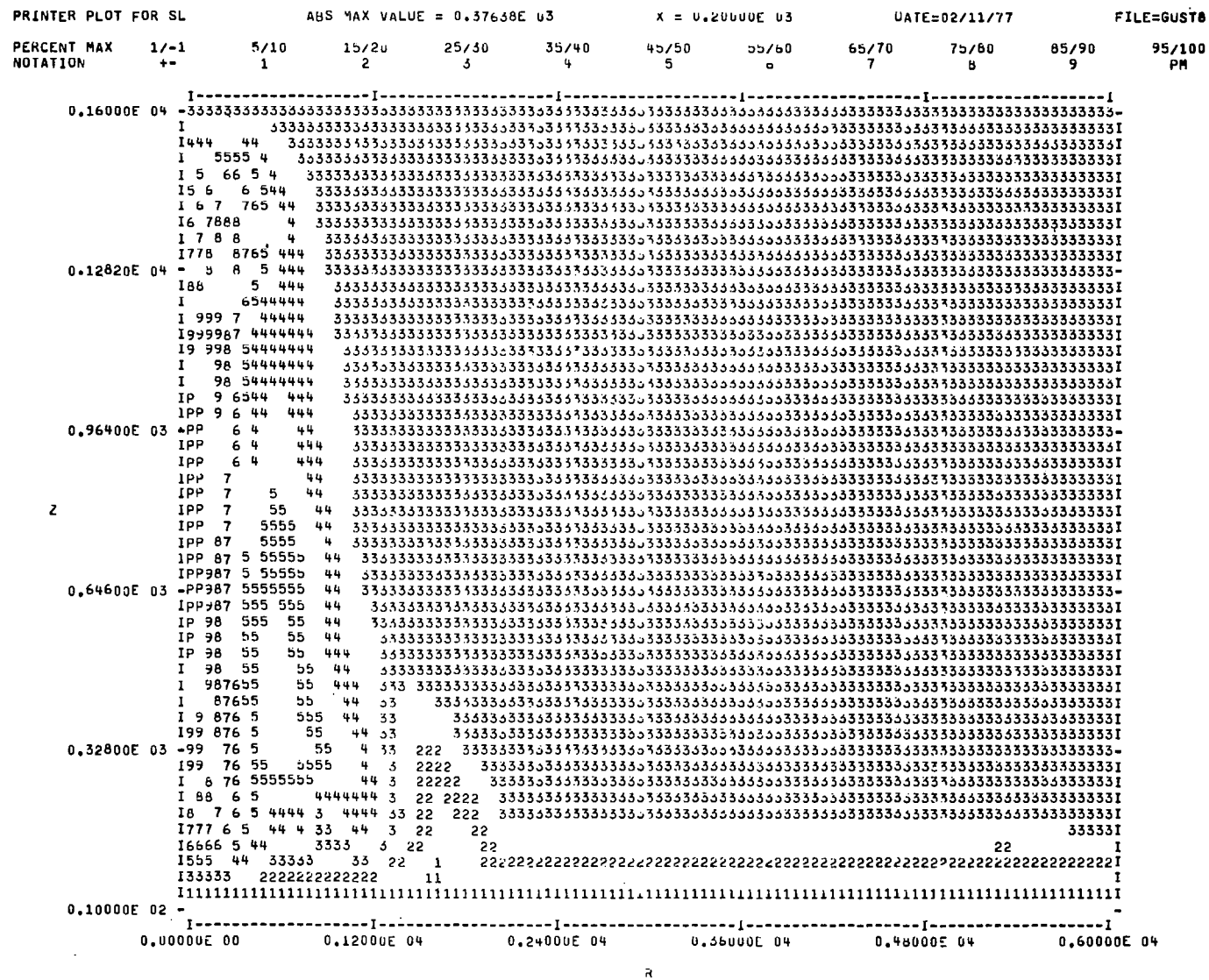

Figure 4.2.7. Normalized scale of turbulence contours as a function of z and R for an axisymmetric gust front with a 500 m radius downdraft at t = 200 sec. [See figure 2.3.2 for explanation of notation.]

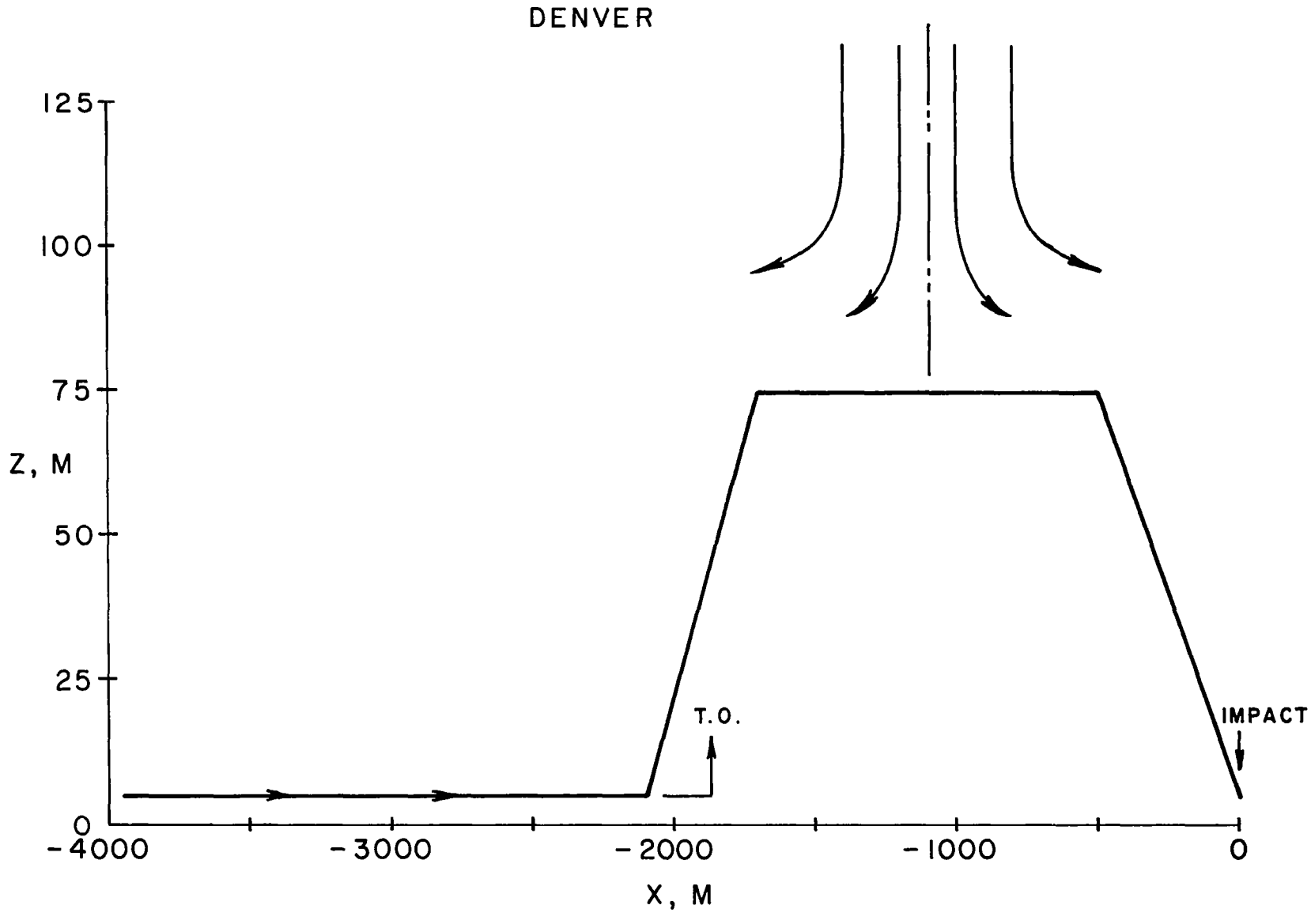

Figure 4.2.8. Approximate aircraft trajectory relative to storm cell and initial point of impact for Denver, Colorado, August 7, 1975 accident.

For modeling purposes, the center of the storm has been located directly over the runway, at a longitudinal position midway between lift off and impact. The resulting velocity, turbulence and scale distributions are shown as a function of range in figures 4.2.9 - 4.2.15. The use of range rather than altitude as the dependent variable is to eliminate the confusing multivalued function. In addition, the altimeter data is suspect and, therefore, the use of range rather than altitude makes for a better comparison with flight recorder data. Figure 4.2.9 indicates a 35 m/sec decrease in the horizontal wind between lift off and impact. In our analysis, the storm is assumed to be stationary, thus, giving equal headwind and tailwind values. If, however, it were moving northward (down the runway) at 7 to 10 m/sec, the headwind would be decreased and the weather model estimate would be in better agreement with the wind estimates based on the recorded flight data. These wind estimates are approximate because the recorded data is not sufficient to uniquely specify wind conditions. Assumptions concerning initial position, actual thrust, take-off performance, and maximum altitude attained, must be made in order to compute these wind profiles. In the Boeing Company's analysis of this accident wind profiles were computed based on six different sets of assumptions. The resulting horizontal wind profiles, as shown in figure 4 of Ref. 17, are somewhat sensitive to these assumptions and the vertical winds are extremely sensitive to them. More confidence should, therefore, be placed on the horizontal than on the vertical wind estimates. A.R.A.P. has chosen to compare wind estimates with the Boeing case IV in which the aircraft is assumed to reach the highest maximum altitides (46 m). The Boeing estimates are presented as a function of time rather than distance. In order to convert these functions from time to distance from impact A.R.A.P. used the following assumptions. First, the pilot will not attempt lift off until the indicated airspeed is at least 68 m/sec. This occurs at 40 sec flight recorder time. Impact is at 60 sec so the distance between lift off and impact (2100 m) must be covered in that time. Ground speed and indicated airspeed are related by

$$U_g = K(IAS) + U_{wind} \qquad (4)$$

A value of U_{wind} = 7 m/sec is used and the K is determined such that $\int_{40}^{60} U_g \cdot dt$ = distance in air = 2100 m. With this relation for ground speed and airspeed, it is possible to relate time and distance working backwards from the location of initial impact.

The Boeing Company's estimates for horizontal and vertical winds assuming a maximum altitude of 46 m are shown in figures 4.2.9 and 4.2.10. The Boeing and A.R.A.P. estimates are consistent if the

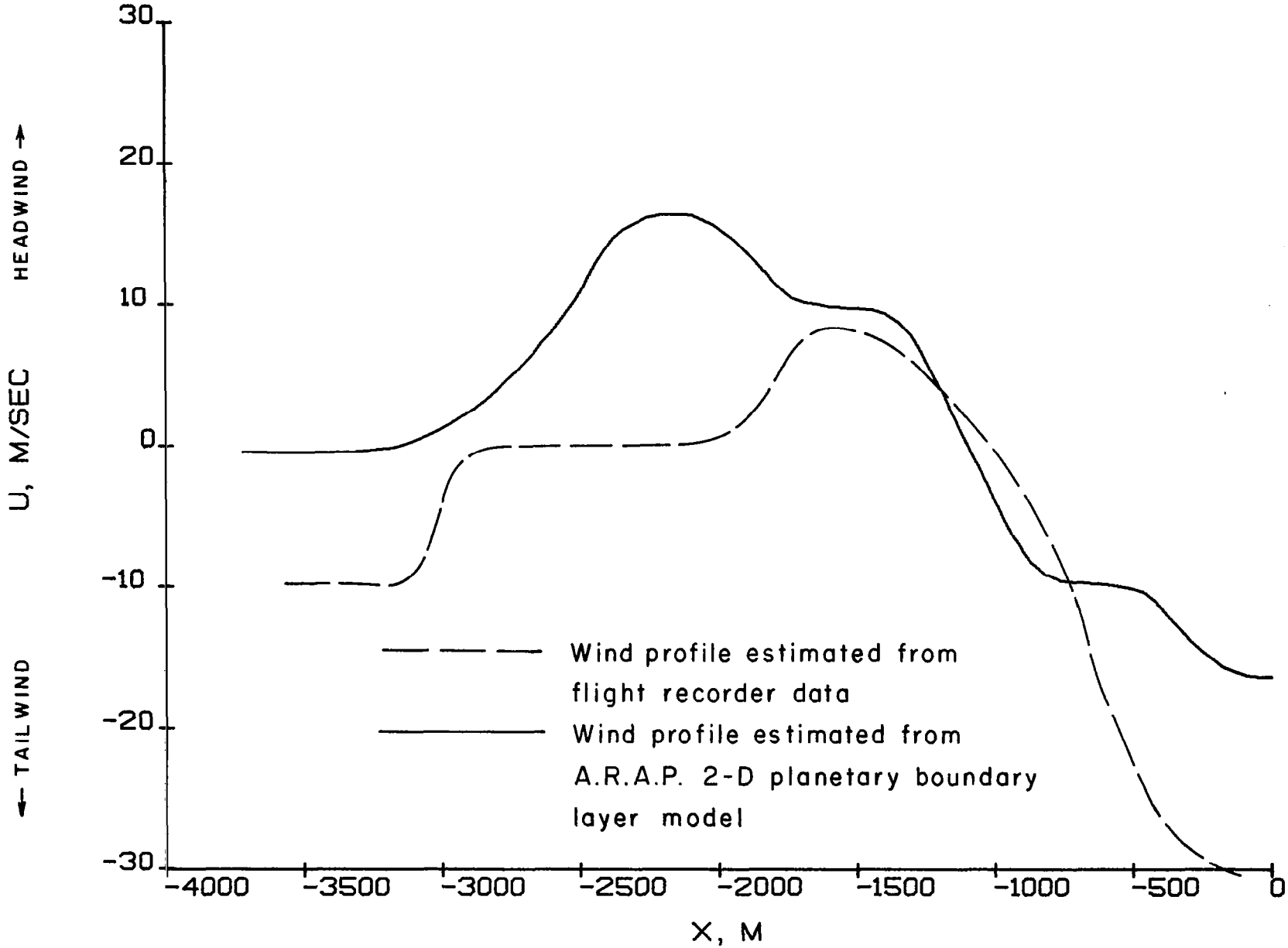

Figure 4.2.9. Velocity component of mean wind parallel to runway as a function of horizontal distance from the initial impact point (+ U, tailwind) for the Denver, Colorado, August 7, 1975 accident.

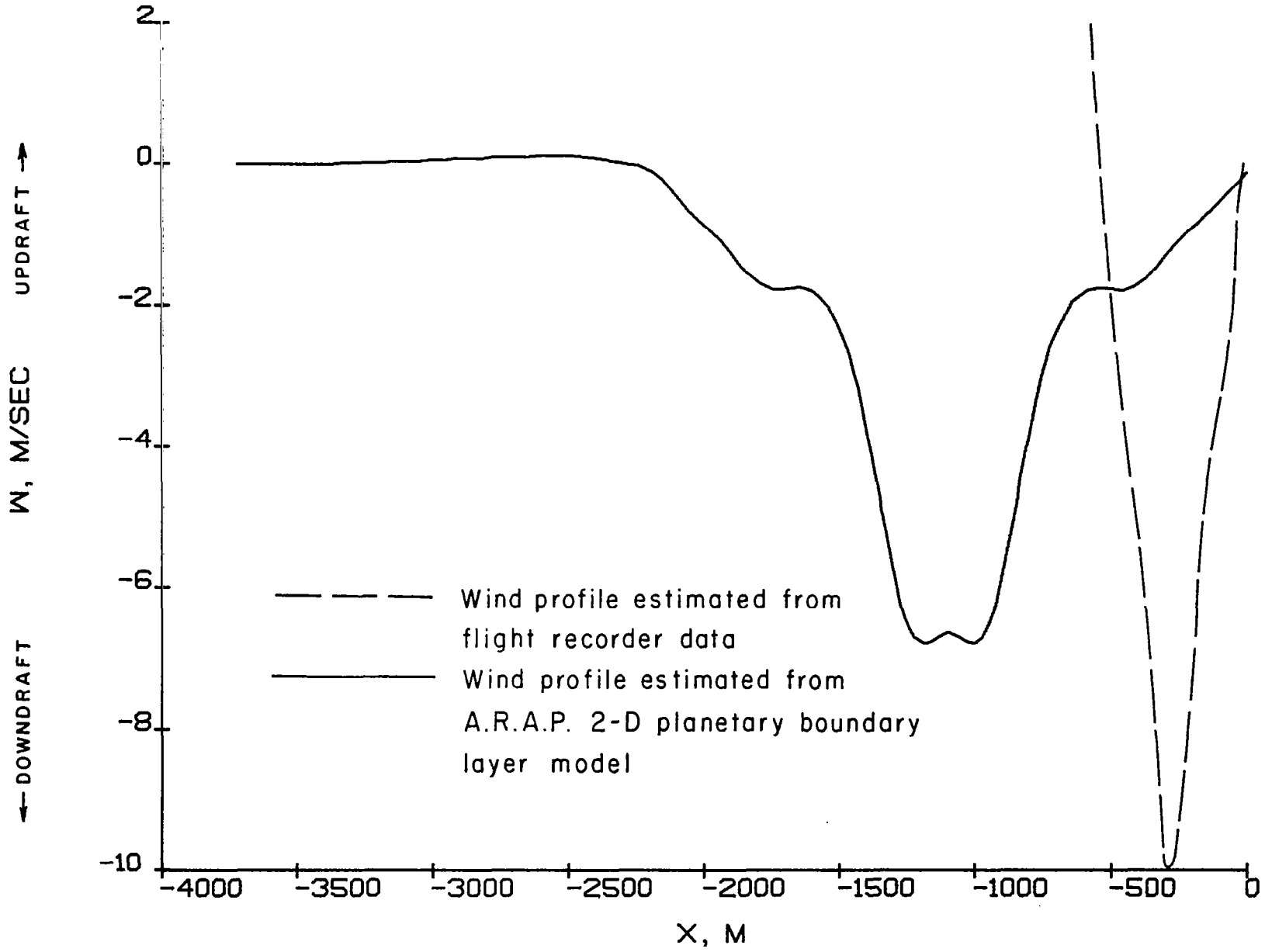

Figure 4.2.10. Vertical velocity component of mean wind as function of horizontal distance from the initial impact point (+ W, up) for the Denver, Colorado, August 7, 1975 accident.

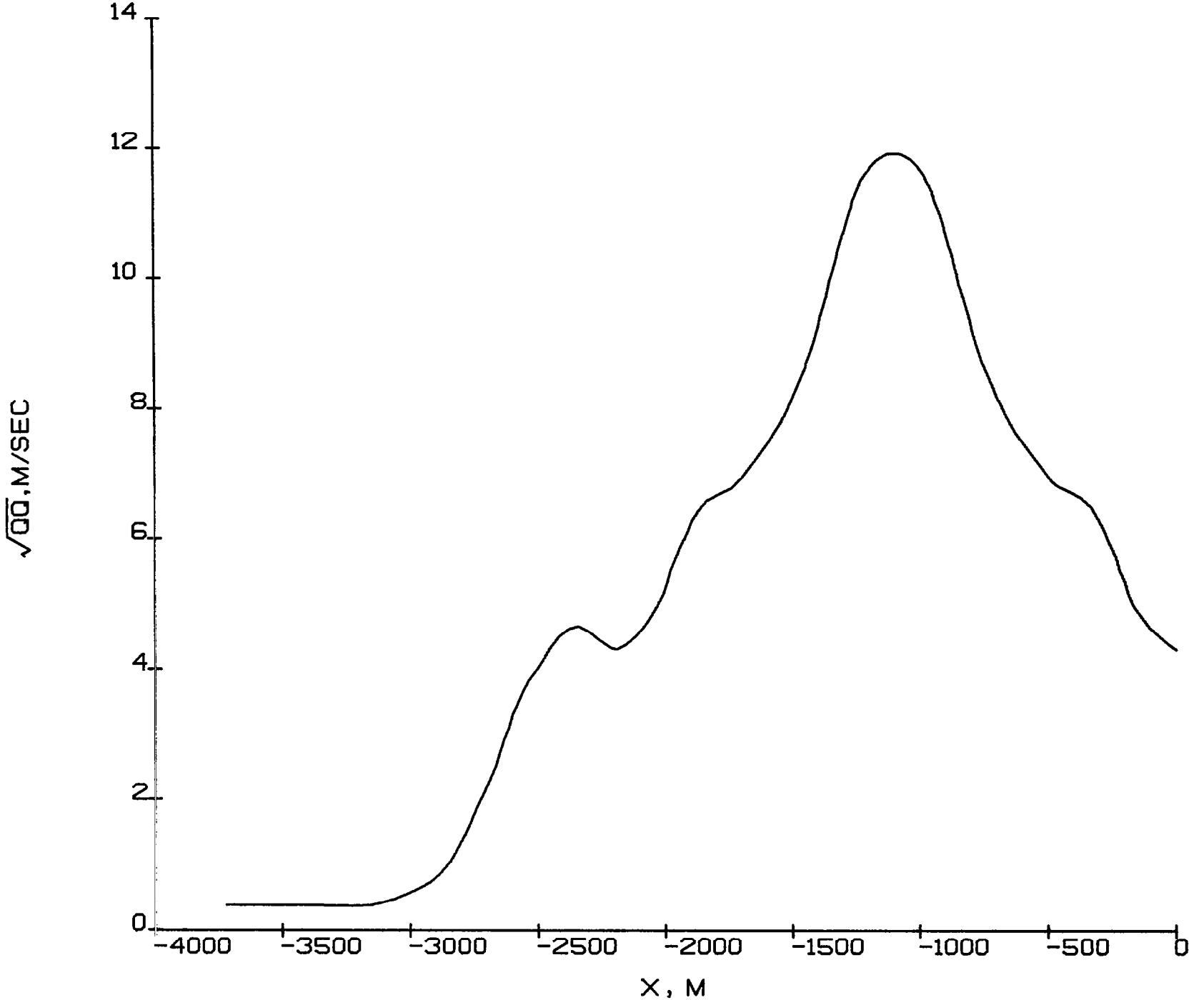

Figure 4.2.11. Variance of the total velocity as a function of horizontal distance from the

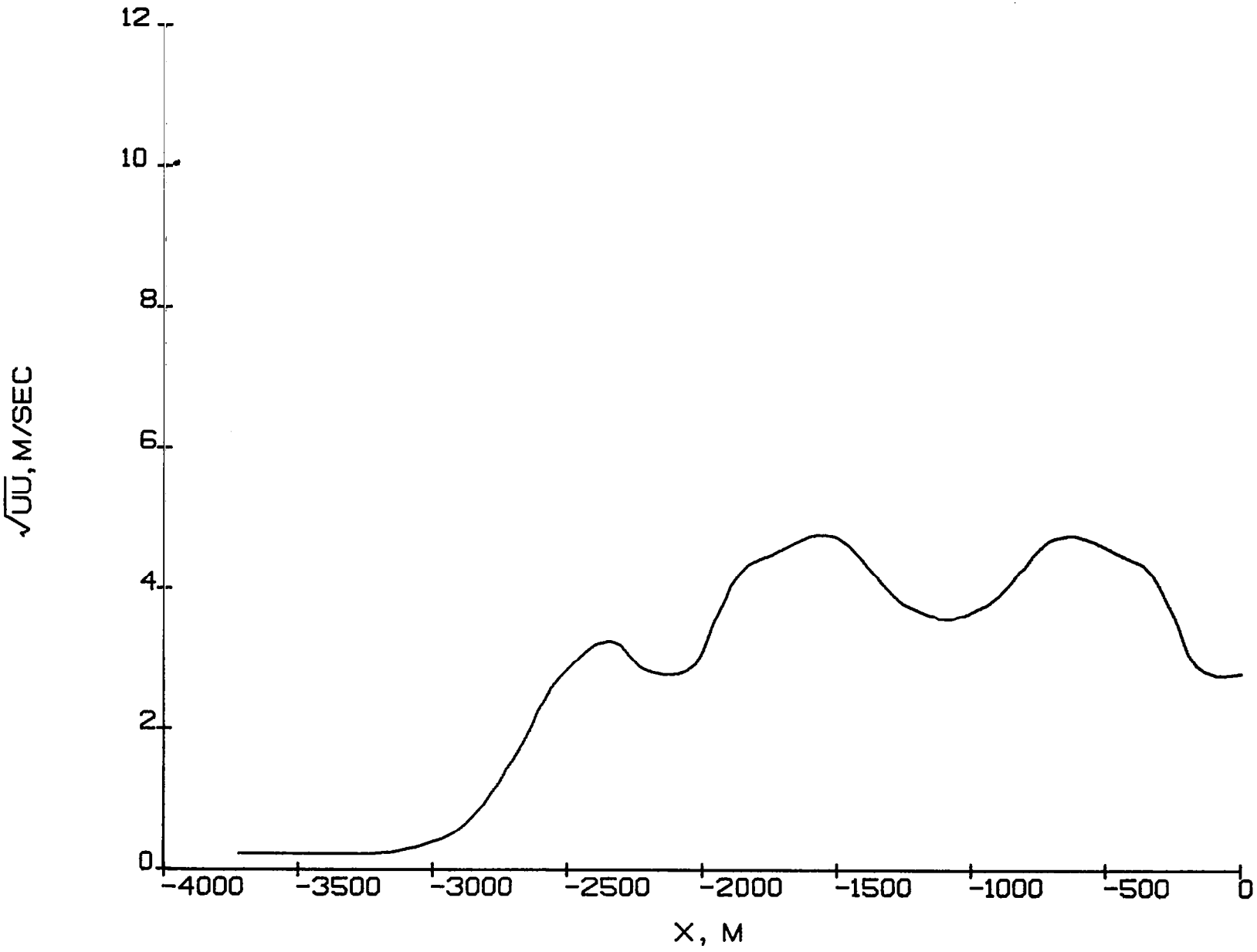

Figure 4.2.12. Variance of the wind parallel to runway as a function of horizontal distance from the initial impact point for the Denver, Colorado, August 7, 1975 accident.

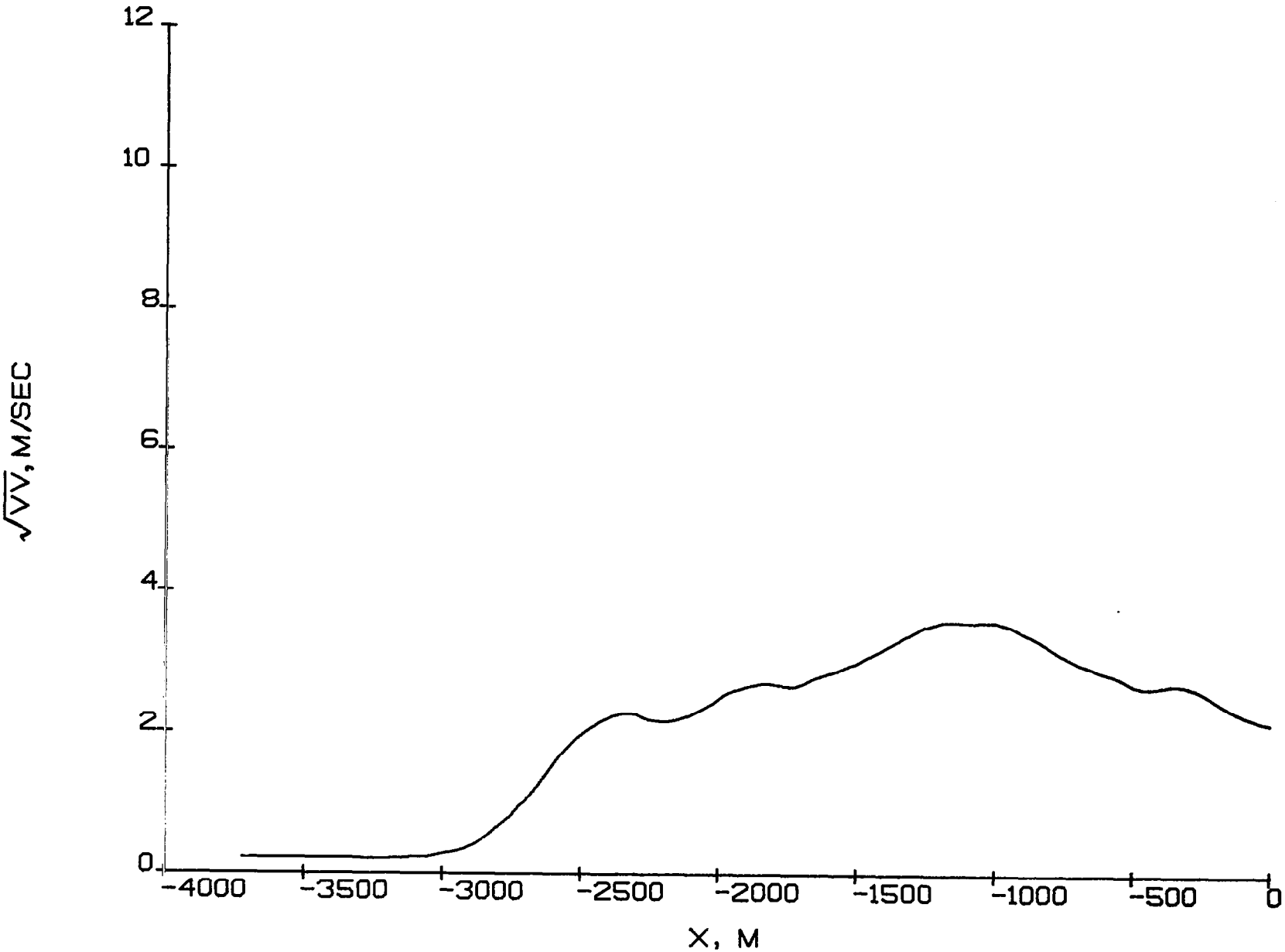

Figure 4.2.13. Variance of the wind perpendicular to runway as a function of horizontal distance from the initial impact point for Denver, Colorado, August 7, 1975 accident.

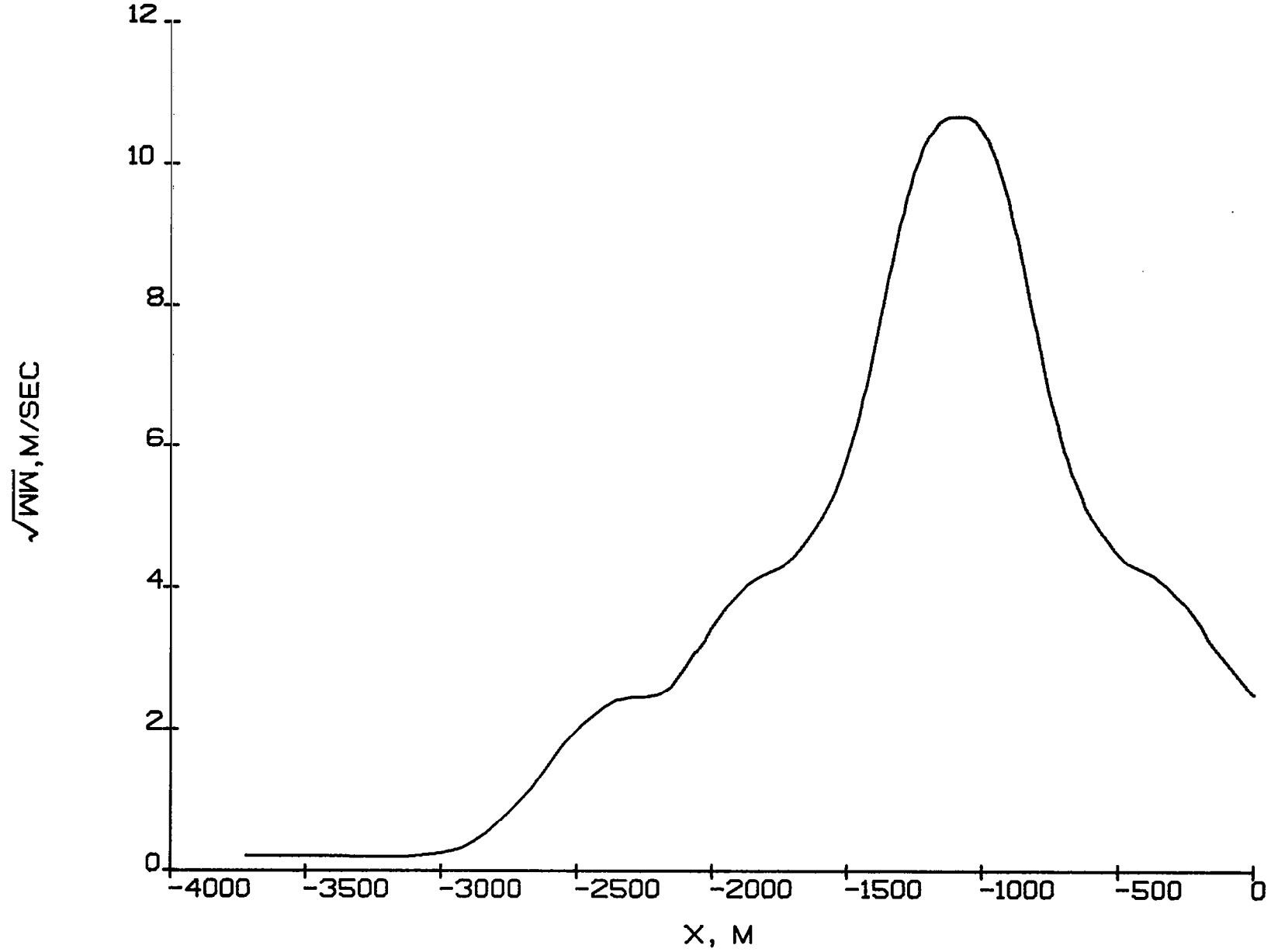

Figure 4.2.14. Variance of the vertical wind as a function of horizontal distance from the initial impact point for Denver, Colorado, August 7, 1975 accident.

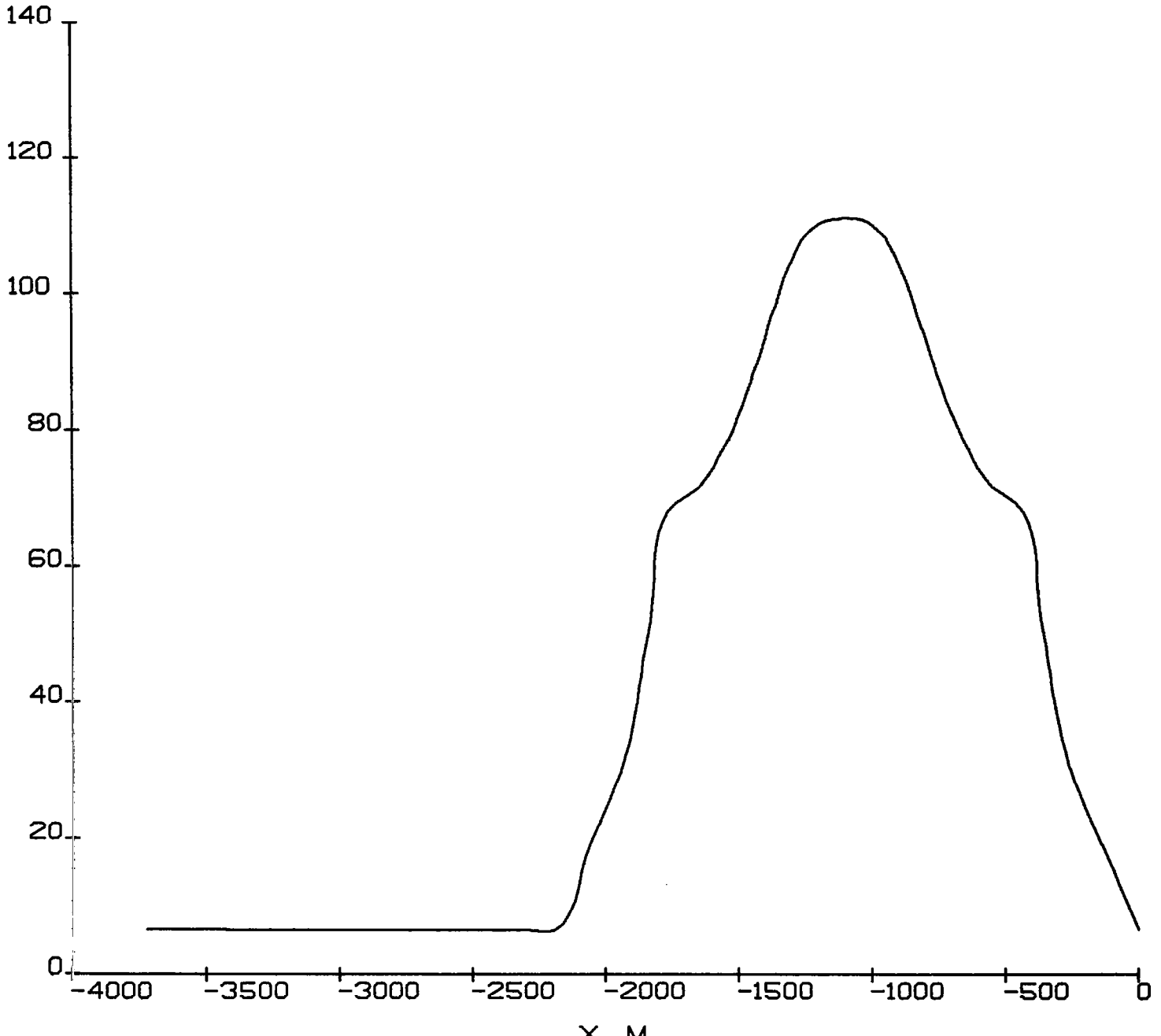

Figure 4.2.15. Turbulence scale as a function of horizontal distance from the initial impact point for Denver, Colorado, August 7, 1975 accident.

storm is assumed to be moving northward at 7 to 10 m/sec, thus shifting A.R.A.P.'s estimates down by this amount. Agreement between the vertical wind estimates is not as good. However, the estimation accuracy for this component based on flight data is not high. When the vertical velocity fluctuations shown in figure 4.2.14 are added to the mean vertical velocity distribution of figure 4.2.10 the model does provide for the possibility of instantaneous downdrafts of a magnitude as high as that deduced from the flight recorder. But these modeled downdrafts occur slightly earlier in the trajectory of the airplane.

The maximum downdraft velocity obtained in this analysis is 6.8 m/sec (figure 4.2.10). No significant steady state updrafts occur. However, the primary component of the turbulence (figure 4.2.14) is the vertical velocity with a maximum rms value of almost 11 m/sec. Significant transient updrafts as well as downdrafts should, therefore, occur.

This case well illustrates the dangers of taking off through a storm cell even when the shear condition has been reported. The meteorological data model developed in A.R.A.P. analysis should be useful for future piloted flight simulation studies.

4.3 CHATTANOOGA, NOVEMBER 1973

At 1851 l.s.t. on November 27, 1973 a Delta DC9 crashed 488 m short of Runway 20 at Chattanooga Municipal Airport, Tennessee. A heavy rain shower was in progress at the time the accident occurred. Flights preceding the accident reported gusty winds on approach, and also observed lightning in the area. The captain of a United flight noted a cigar shaped precipitation pattern lying on the localizer. NWS radar at Nashville showed moderate precipitation echoes in the Chattanooga area (figure 4.3.1). The captain of the Delta flight reported that he made an autopilot coupled approach that appeared normal until five seconds after reaching Decision Height (62 m). At that time, the sight picture flattened out and the crew realized that the aircraft was too low (Ref. 18).

The recorded flight data show that the indicated airspeed begins to increase at 220 m above ground level (AGL) which would possibly account for the aircraft responding to an increasing headwind. From the altimeter time history it can be seen that the sink rate increased by 1.7 meters per second from an altitude of 130 m AGL down to impact.

At the time of the accident, winds aloft at Chattanooga were estimated by the NTSB based on radiosonde data from Nashville, Tennessee and Athens, Georgia. The wind estimates indicate that the aircraft should have experienced an 8.5 m/sec decrease in headwind between 400 m and 100 m AGL. For an autocoupled approach with no autothrottle this would result in an increase in airspeed as observed. These conditions, in combination with pilot error in the last 100 m, could result in an undershot approach. However, the undershoot could also have been caused by the characteristic headwind-downdraft-tailwind sequence of changing winds associated with a small storm cell. Which accident scenario is more likely can best be ascertained by estimating the horizontal and vertical winds using all of the recorded flight data. Since this was not done by the accident investigators, the storm scenario is chosen for this analysis in order to illustrate the piloting problem associated with shooting an approach through a local downdraft.

For modeling purposes A.R.A.P. has chosen the same small axisymmetric gust front as used in the Denver case (figures 4.2.2 - 4.2.7). The landing trajectory is a three degree glideslope approach into the storm followed by an increase to a six degree glideslope due to the downdraft (figure 4.3.2). The vertical placement of this trajectory was chosen such that the initial headwind encounter occurs at 220 m. The complete horizontal wind profile is shown in figure 4.3.3 as a function of altitude. This trajectory and storm cell model results in a loss of 32 m/sec in an altitude of 130 m. This is a wind shear of .25 sec^{-1}, a dangerously high shear to encounter. The corresponding vertical wind velocity profile is shown in figure 4.3.4. The maximum downdraft velocity of

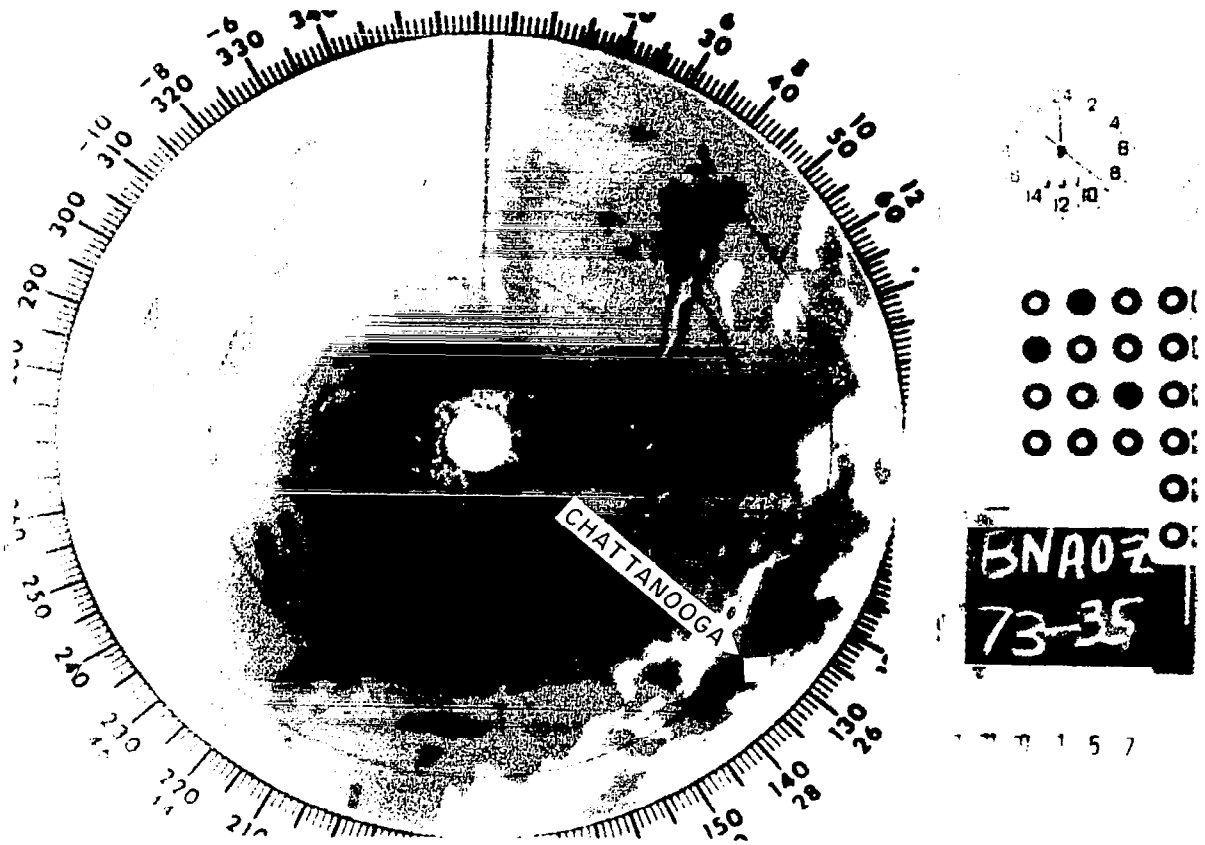

Figure 4.3.1. Radarscope picture near the time of Chattanooga, Tenn., November 27, 1973 accident.

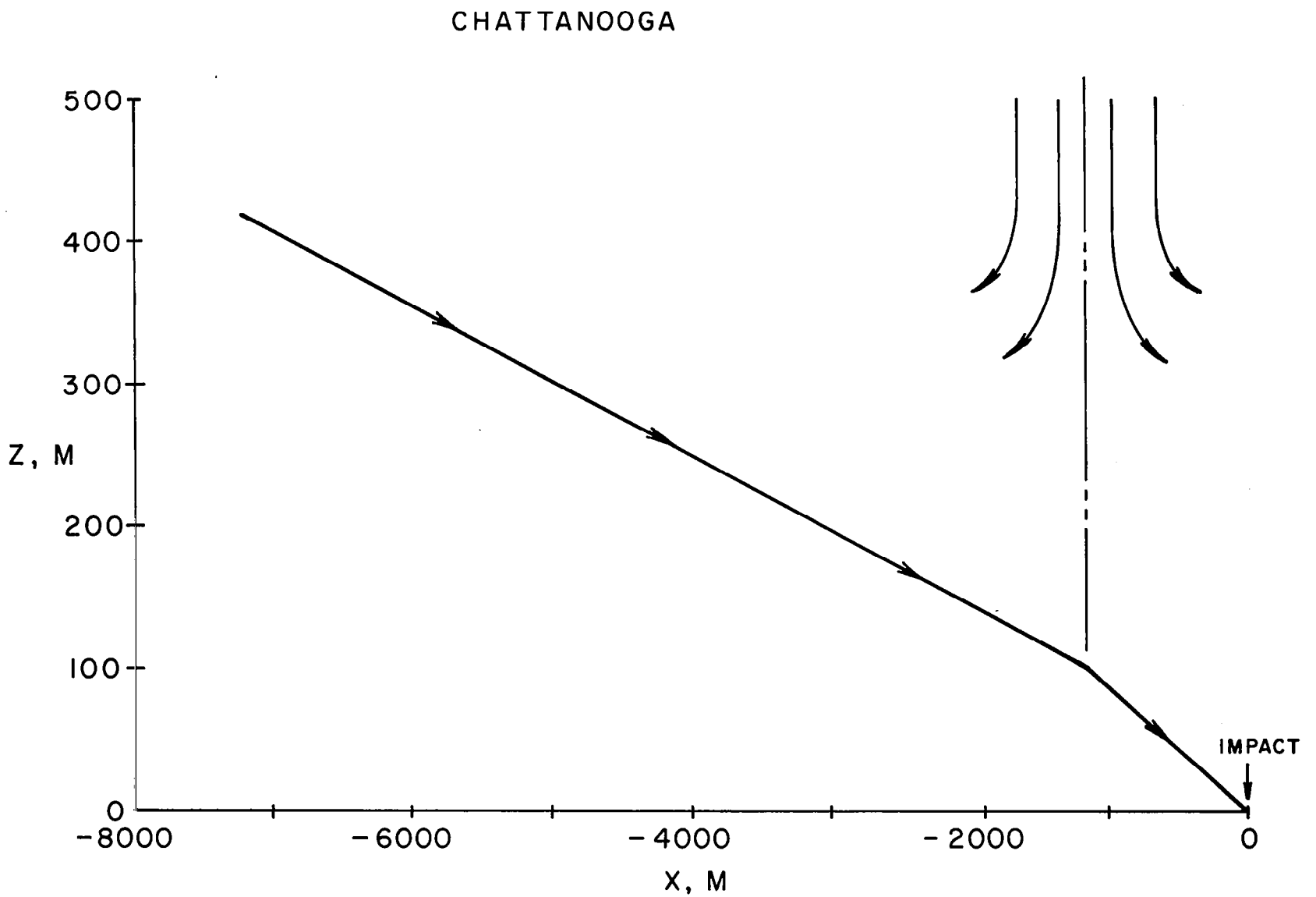

Figure 4.3.2. Approximate aircraft trajectory relative to storm cell and initial point of impact for Chattanooga, Tenn., November 27, 1973 accident.

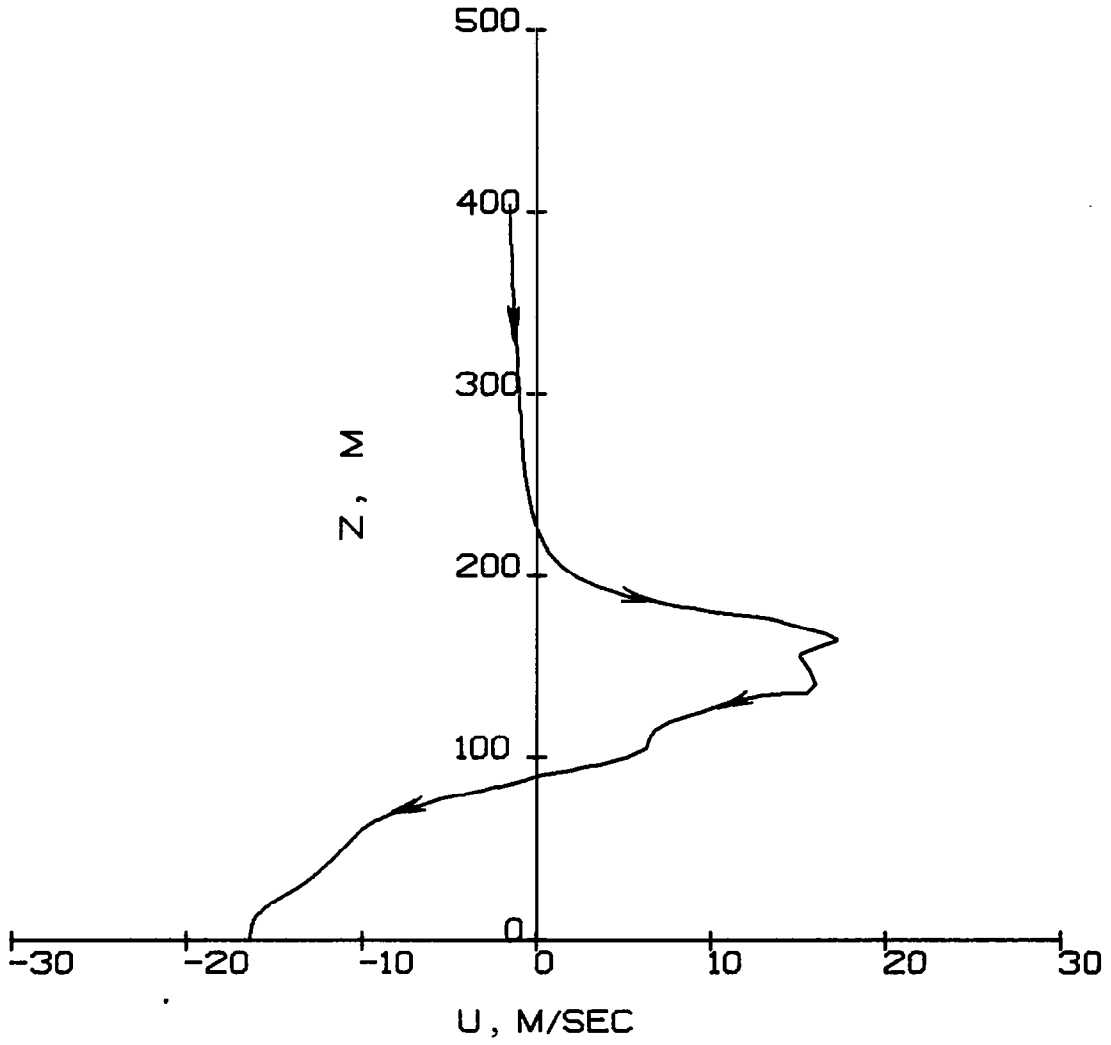

Figure 4.3.3. Altitude profile of mean wind velocity component parallel to runway (+U, tailwind) for Chattanooga, Tenn., November 27, 1973 accident.

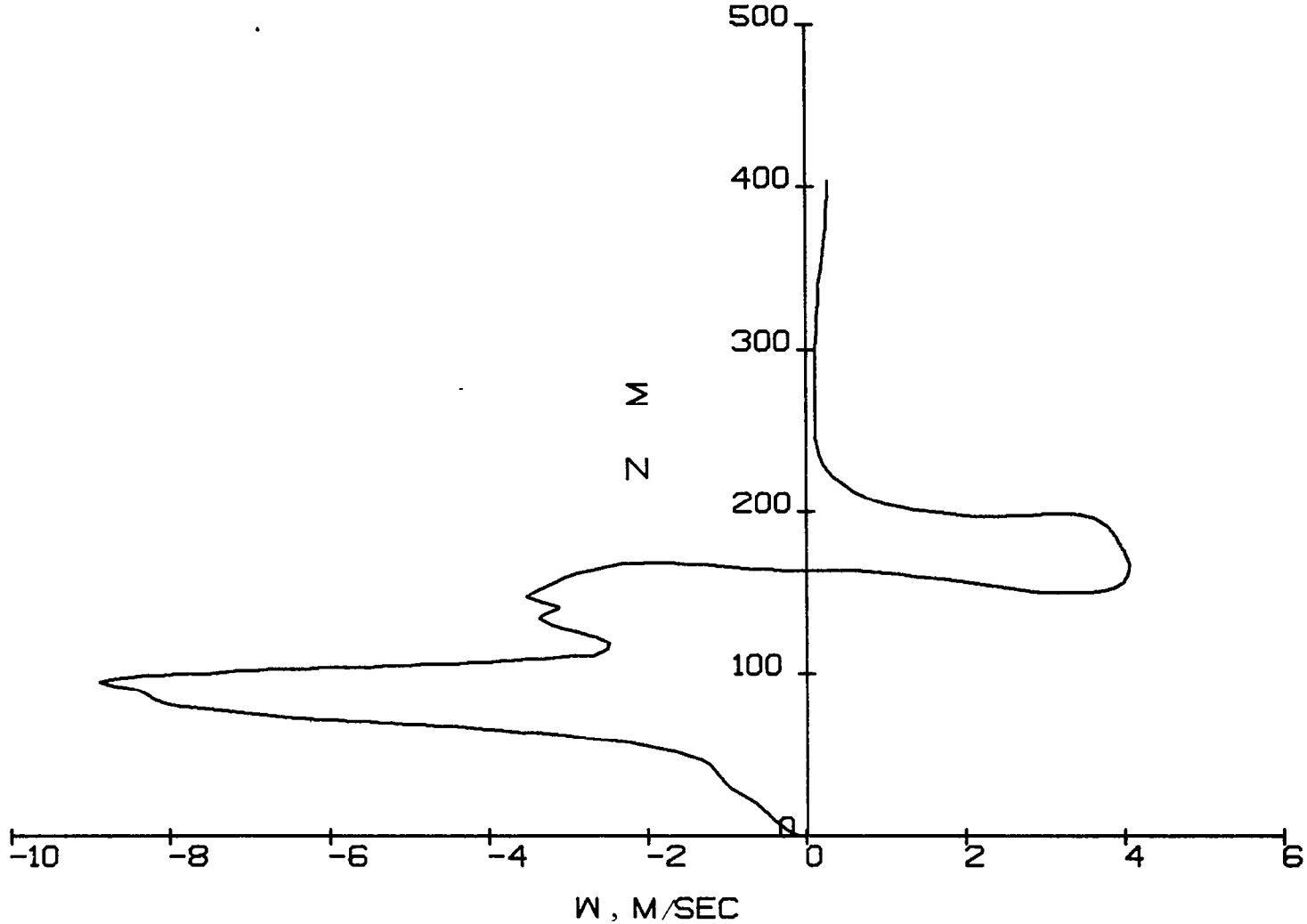

Figure 4.3.4. Altitude profile of mean wind vertical velocity component (+ W, up) for Chattanooga, Tenn., November 27, 1973 accident.

9 m/sec is what would be felt if the aircraft flew right through the center of the storm cell. If the aircraft misses the center by 300 m the maximum downdraft velocity is less than 4 m/sec. Due to the severity of the accident the smaller value is probably more reasonable for this particular case. The most severe storm cell encounter is, however, of greater interest for simulator wind shear studies. The corresponding turbulence and scale profiles for this condition are given in figures 4.3.5 - 4.3.9. It should again be noted, that for simulator studies allowing significant flight path variations, the wind shear data for the axisymmetric storm cell must be stored as tabulated functions of range and altitude plus an analytic function of azimuth angle from storm center.

The primary conclusion to be drawn from analysis of this case is that very large wind shears and turbulence exist in the vicinity of storm cells and, therefore, pilots should avoid flying through them. The results obtained here form a consistent package of meteorological data which can be used in future piloted simulator studies.

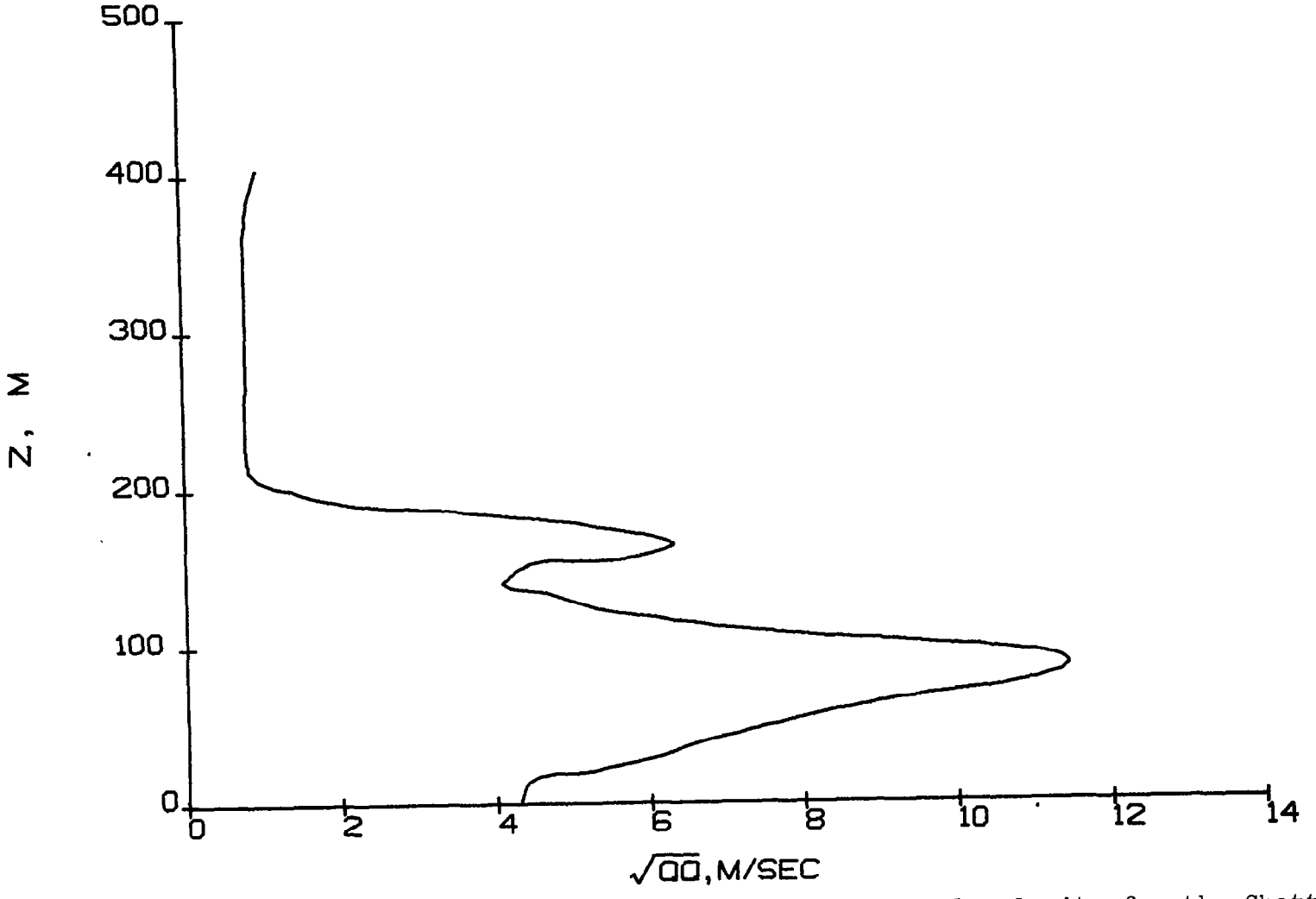

Figure 4.3.5. Altitude profile of variance of the total velocity for the Chattanooga, Tenn., November 27, 1973 accident.

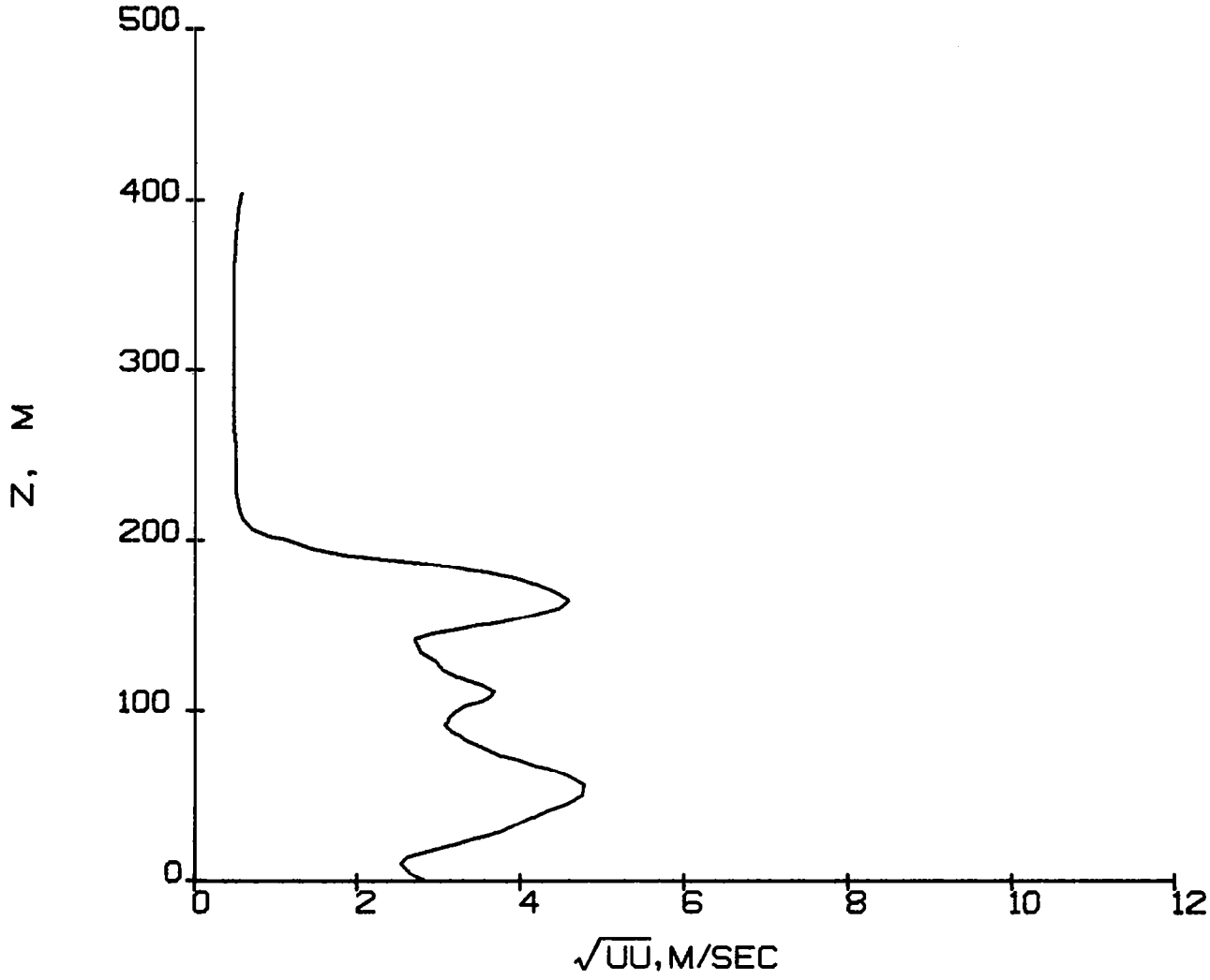

Figure 4.3.6. Altitude profile of variance of the wind parallel to runway for the Chattanooga, Tenn., November 27, 1973 accident.

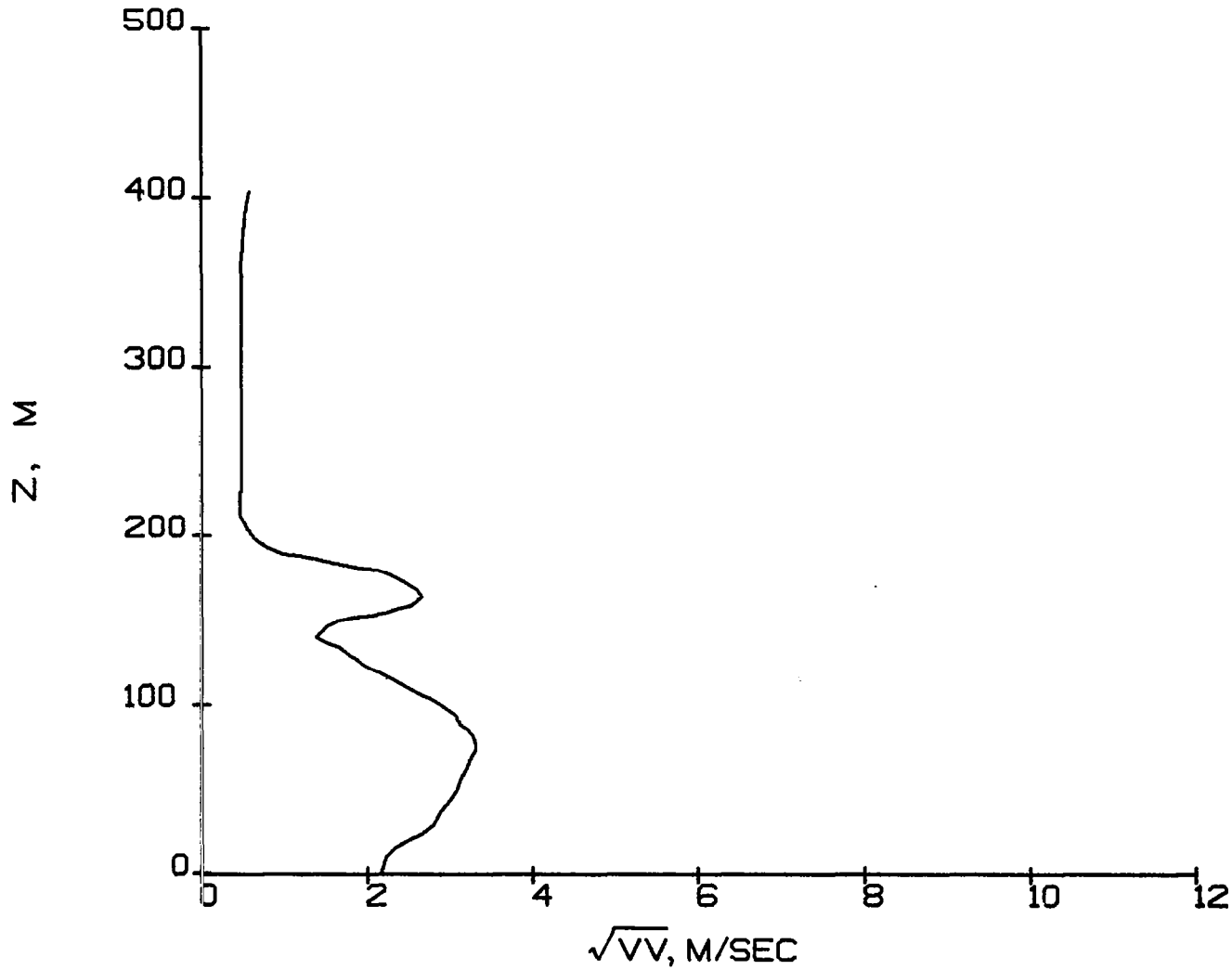

Figure 4.3.7. Altitude profile of variance of the wind perpendicular to runway for the Chattanooga, Tenn., November 27, 1973 accident.

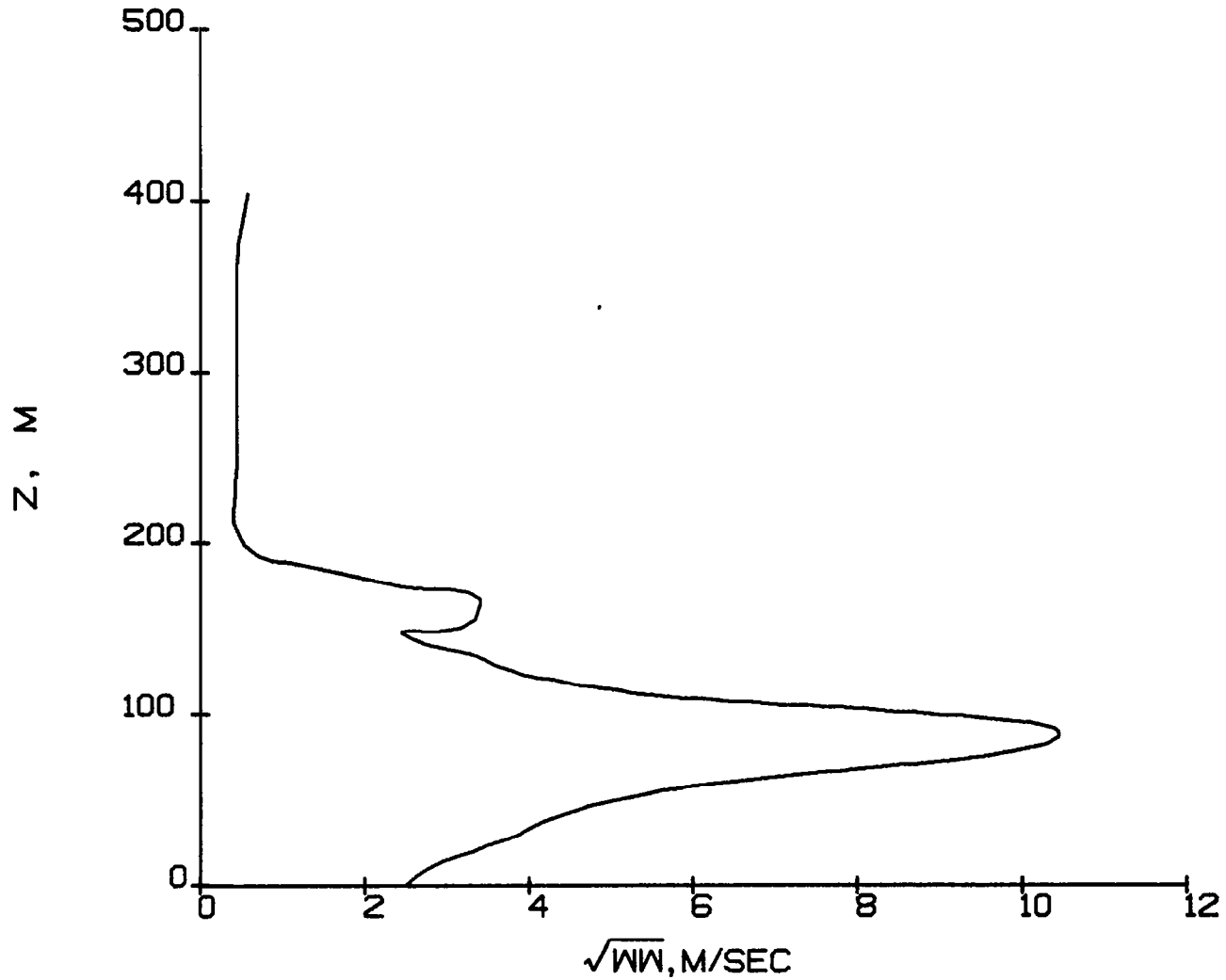

Figure 4.3.8. Altitude profile of variance of the vertical wind for Chattanooga, Tenn., November 27, 1973 accident.

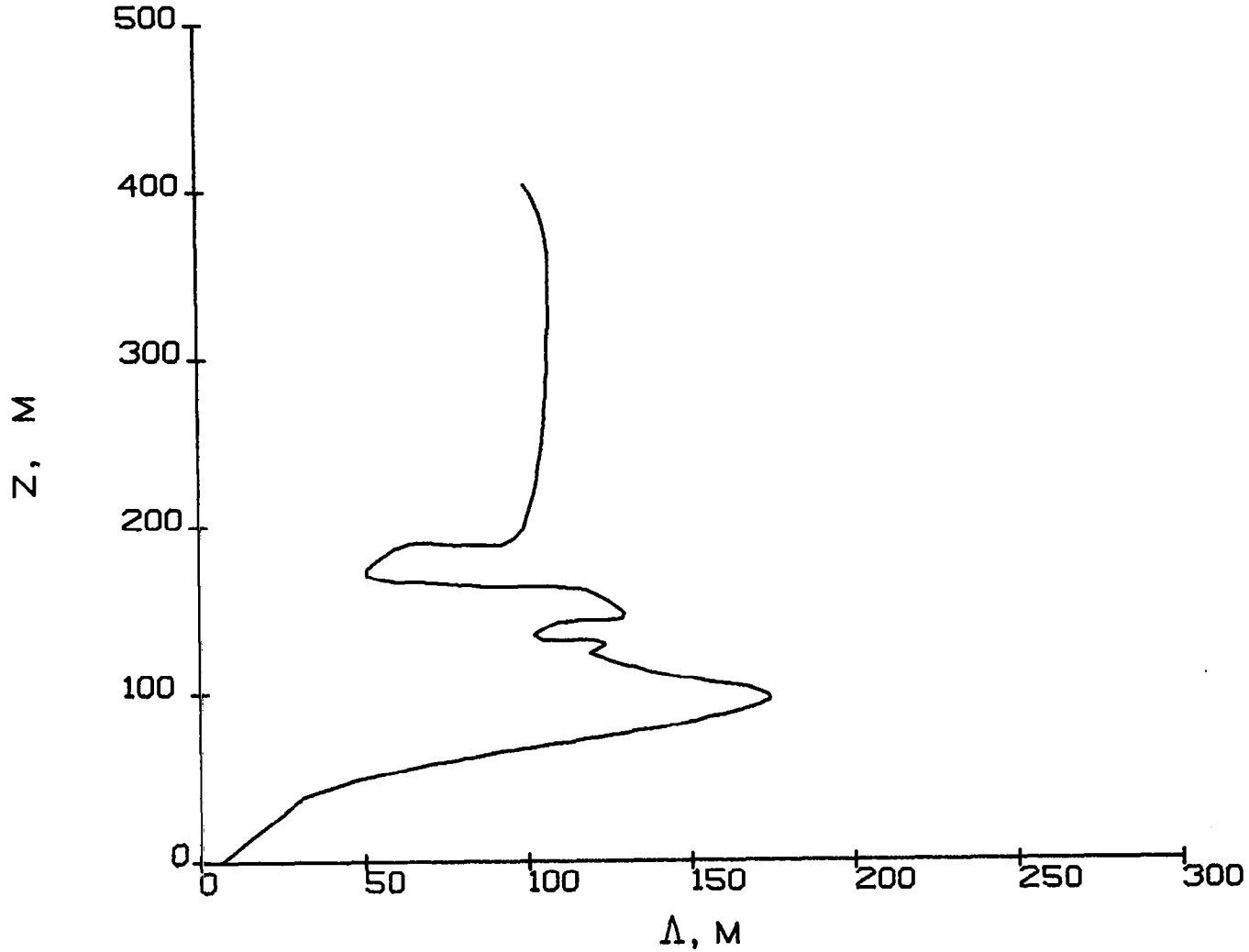

Figure 4.3.9. Altitude profile of scale of turbulence for Chattanooga, Tenn., November 27, 1973 accident.

4.4 ST. LOUIS, JULY 1973

At 1643 l.s.t. on July 23, 1973 Ozark Airlines FH-227B crashed while attempting to land on Runway 30L at St. Louis International Airport. A severe thunderstorm was moving from the southwest into the approach area. The pilot of TWA Flight 244 executed a missed approach 1.5 minutes prior to the accident, due to a strong updraft upsetting his approach speed. He also saw a "wall of water" paralleling the localizer course 0.5 to 1.0 km to his left. NWS studied the weather conditions at the time of the accident and concluded (Ref. 19) that there was a squall line south of the airport (ESE-WNW) moving northeasterly at 15 m/sec (figure 4.4.1).

The aircraft crashed 3.7 km short of the airport. A ground observer reported that the aircraft suddenly ascended 100 m to 150 m and then rapidly descended to 60 m above the ground (Page 3, Ref. 19). Unfortunately, the altimeter and airspeed indicator monitored by the flight recorder were inoperative, so a more quantitative description of the motion of the vehicle is not available.

Based on the description given above, A.R.A.P. has modeled the storm as a two-dimensional gust front nearly parallel to the runway. The gust simulation is done in the same manner as outlined in Section 2.3 except the 2-D version of the model is used rather than the axisymmetric version. All other conditions are identical to the 2 km spread simulation presented in Section 2.3. The flowfield at a simulated time of 1000 sec is presented in figures 4.4.2 - 4.4.7.

The trajectory of the aircraft relative to the squall line (two-dimensional gust front) and airport (figure 4.4.8) was determined as follows.

The approach velocity of the aircraft was 62 m/sec. The descent rate on a 3° glideslope is, therefore, 3.2 m/sec with no vertical winds or pilot correction. The horizontal velocity component of the aircraft relative to the gust front is a combination of the northeasterly velocity of the squall line, plus the angle between the squall line and the localizer, η .

$$V = V_{squall} + V_{approach} \sin \eta \qquad (5)$$

A horizontal velocity of 20 m/sec was chosen to accord with the pilot's updraft-downdraft experience. The vertical velocity is a combination of the nominal approach descent rate, updraft-downdraft from the storm, and pilot control inputs. For A.R.A.P.'s analysis it is assumed that the pilot did nothing until the updraft produced a notable glideslope error, at which time he arrested the climb rate, left the updraft, and developed an excessive sink rate. The

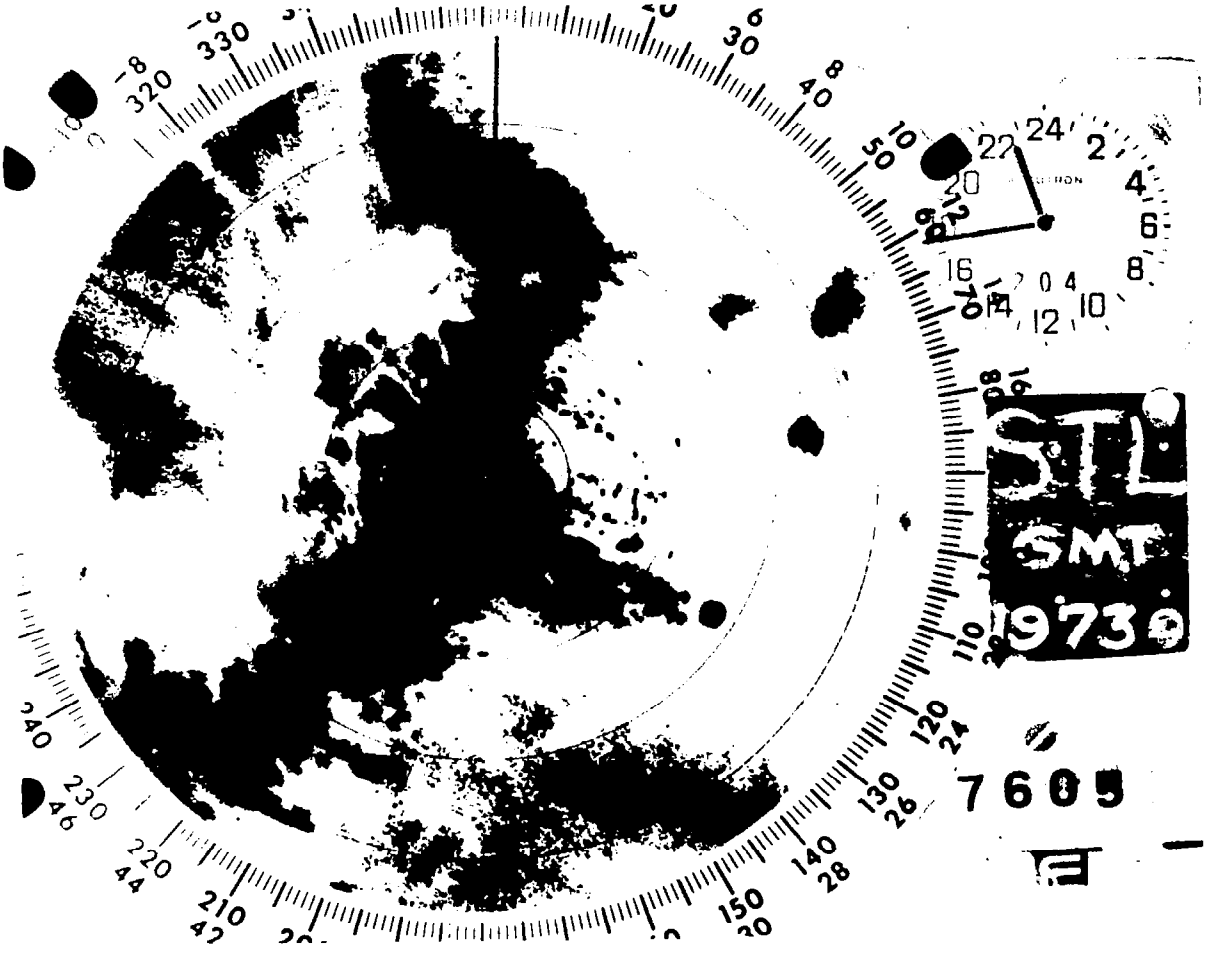

Figure 4.4.1. Radarscope picture near the time of the St. Louis, Mo., July 23, 1973 accident.

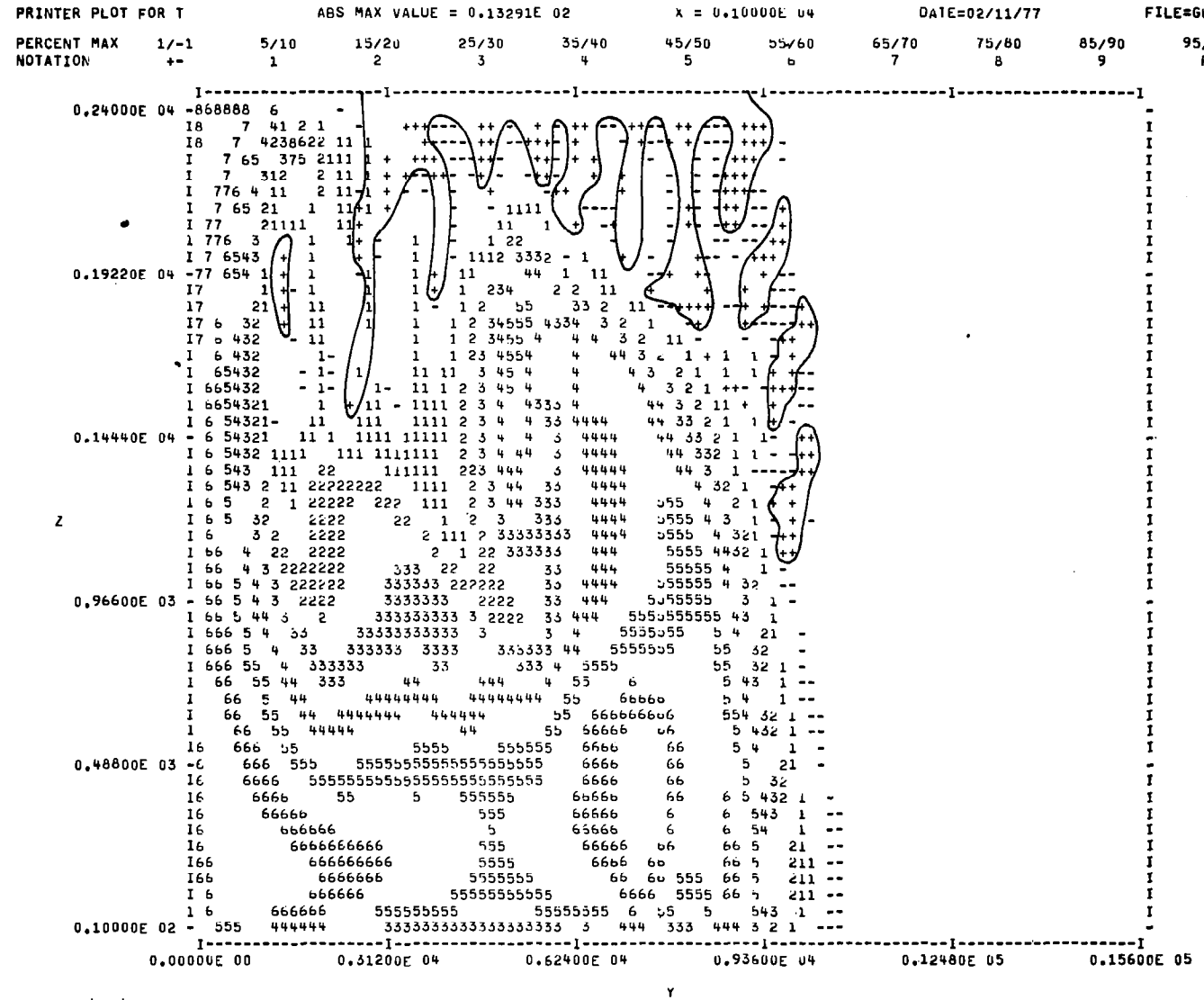

Figure 4.4.2. Normalized temperature contours as a function of z and y for a two-dimensional gust front with a 2000 m radius downdraft at t = 1000 sec. [See figure 2.3.2 for explanation of notation.]

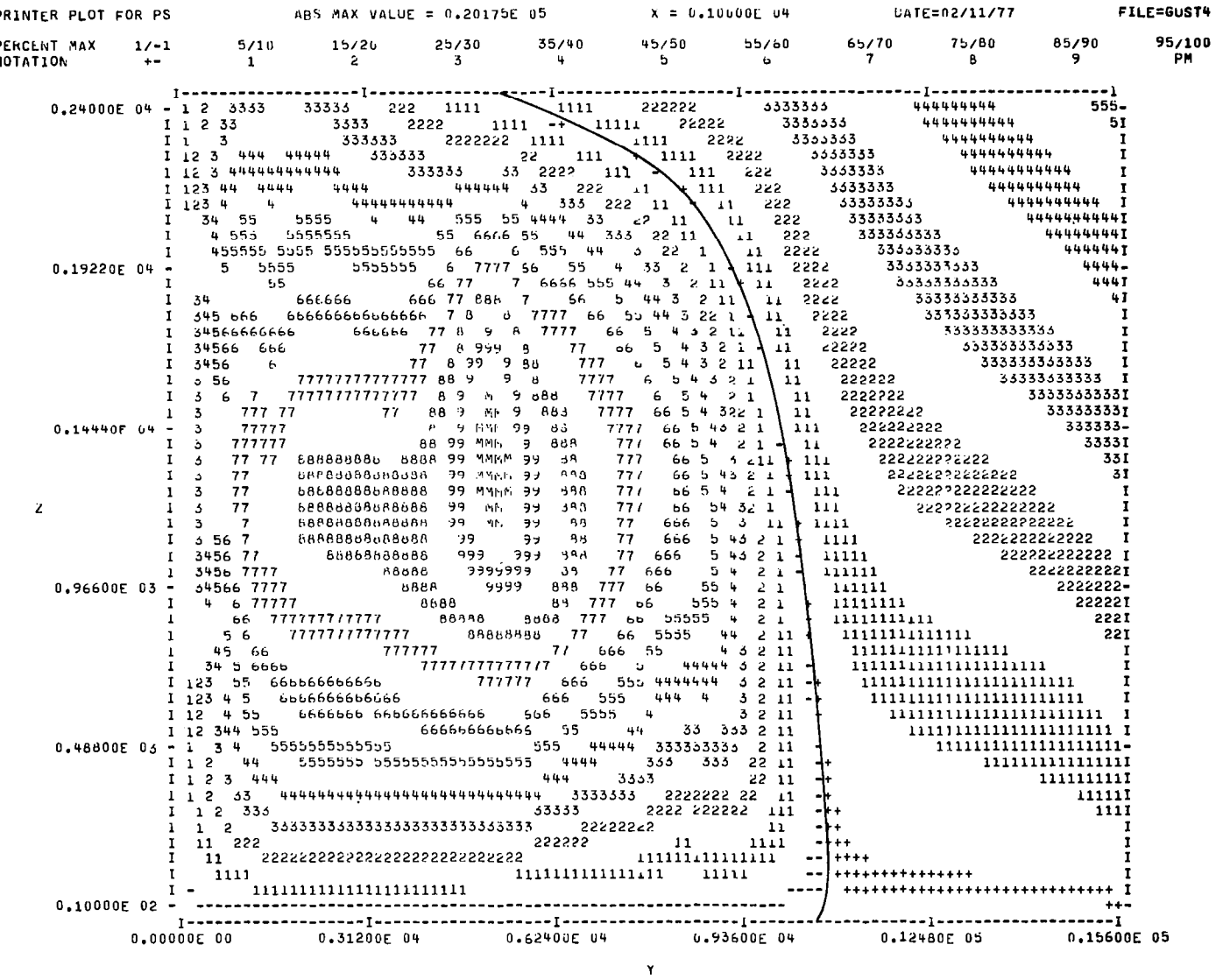

Figure 4.4.3. Normalized stream function contours as a function of z and y for a two-dimensional gust front with a 2000 m radius downdraft at t = 1000 sec. [See figure 2.3.2 for explanation of notation.]

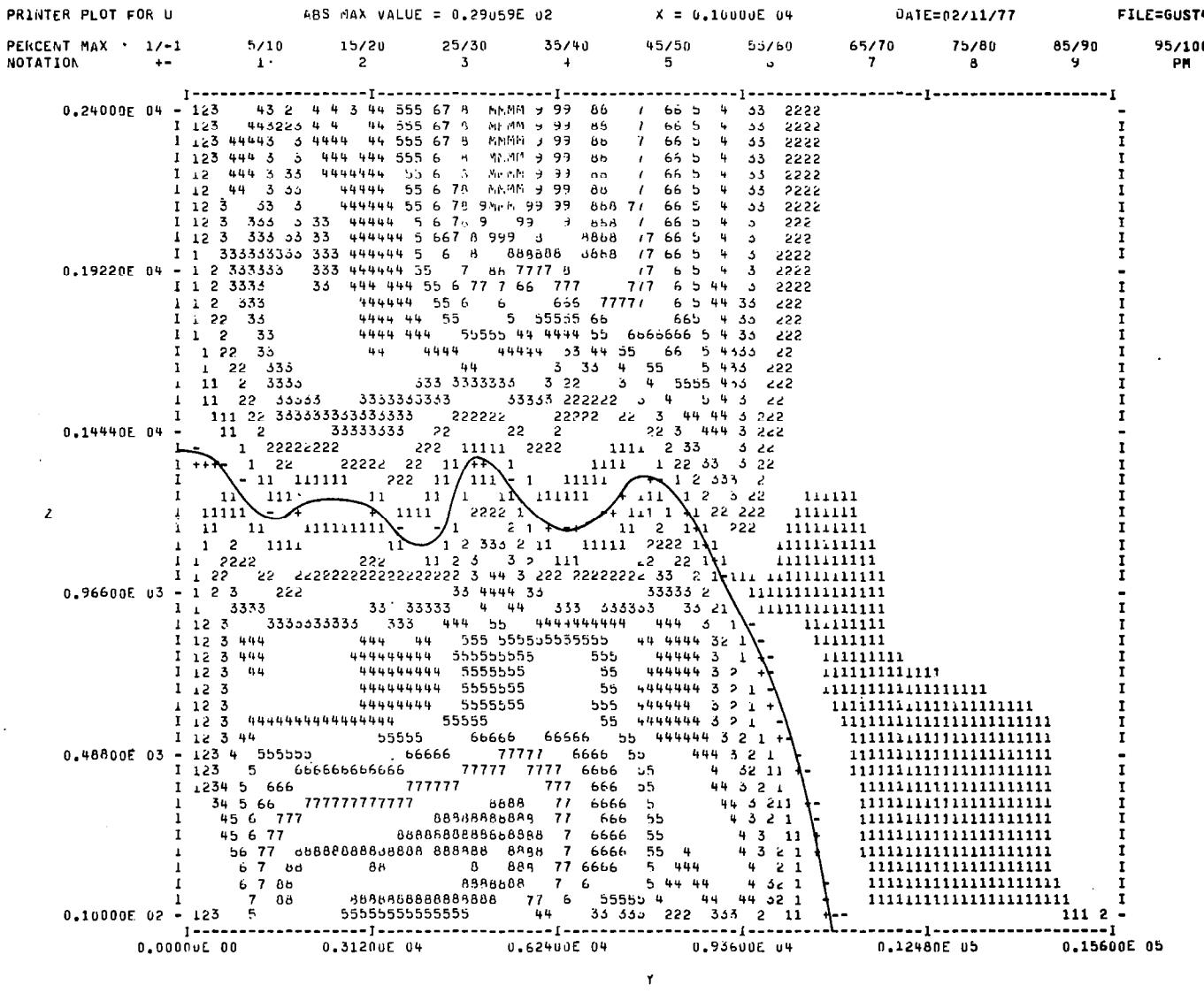

Figure 4.4.4. Normalized mean radial velocity contours as a function of z and y for a two-dimensional gust front with a 2000 m radius downdraft at t = 1000 sec. [See figure 2.3.2 for explanation of notation.]

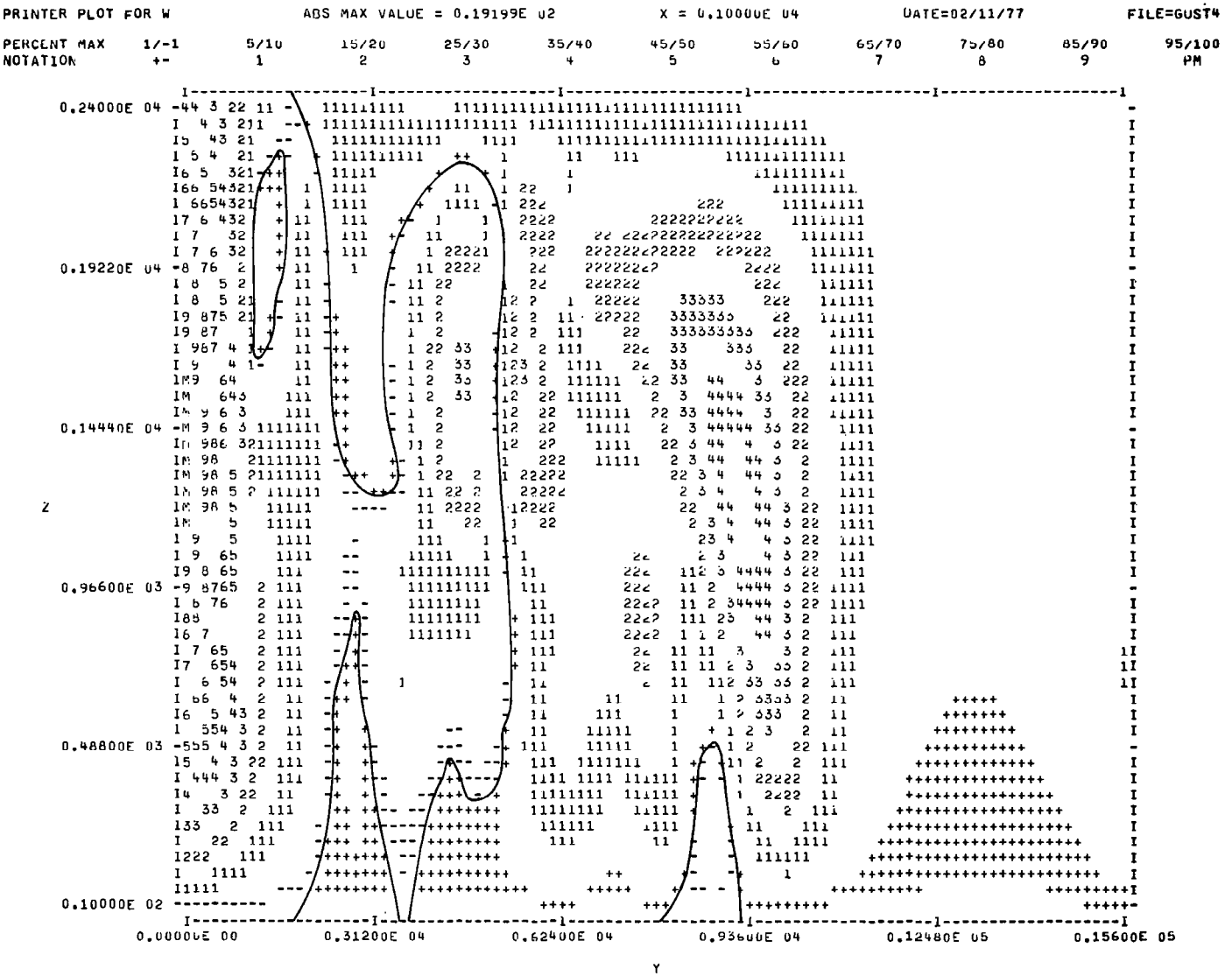

Figure 4.4.5. Normalized mean vertical velocity contours as a function of z and y for a two-dimensional gust front with a 2000 m radius downdraft at t = 1000 sec. [See figure 2.3.2 for explanation of notation.]

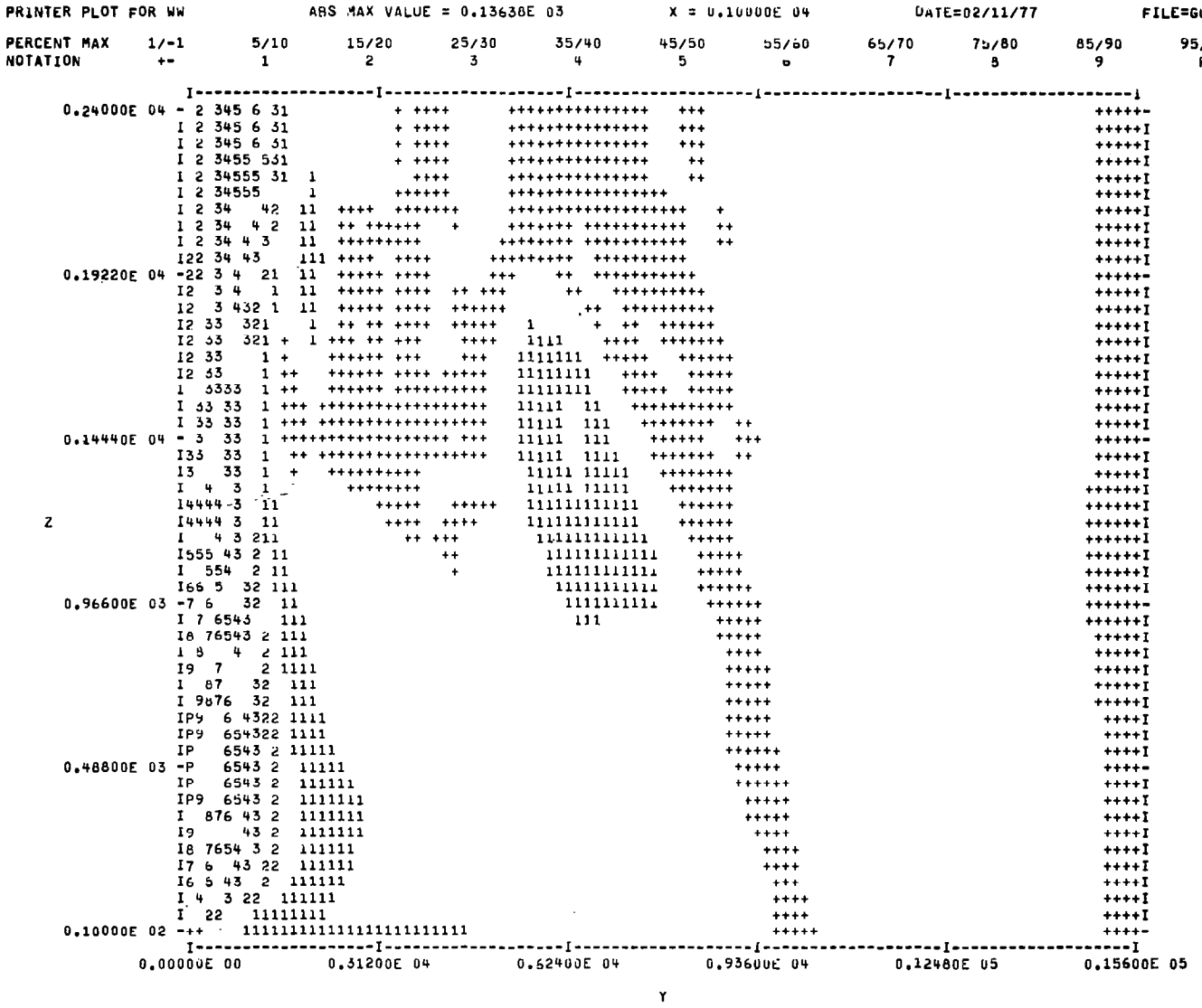

Figure 4.4.6. Normalized variance of vertical velocity contours as a function of z and y for a two-dimensional gust front with a 2000 m radius downdraft at t = 1000 sec. [See figure 2.3.2 for explanation of notation.]

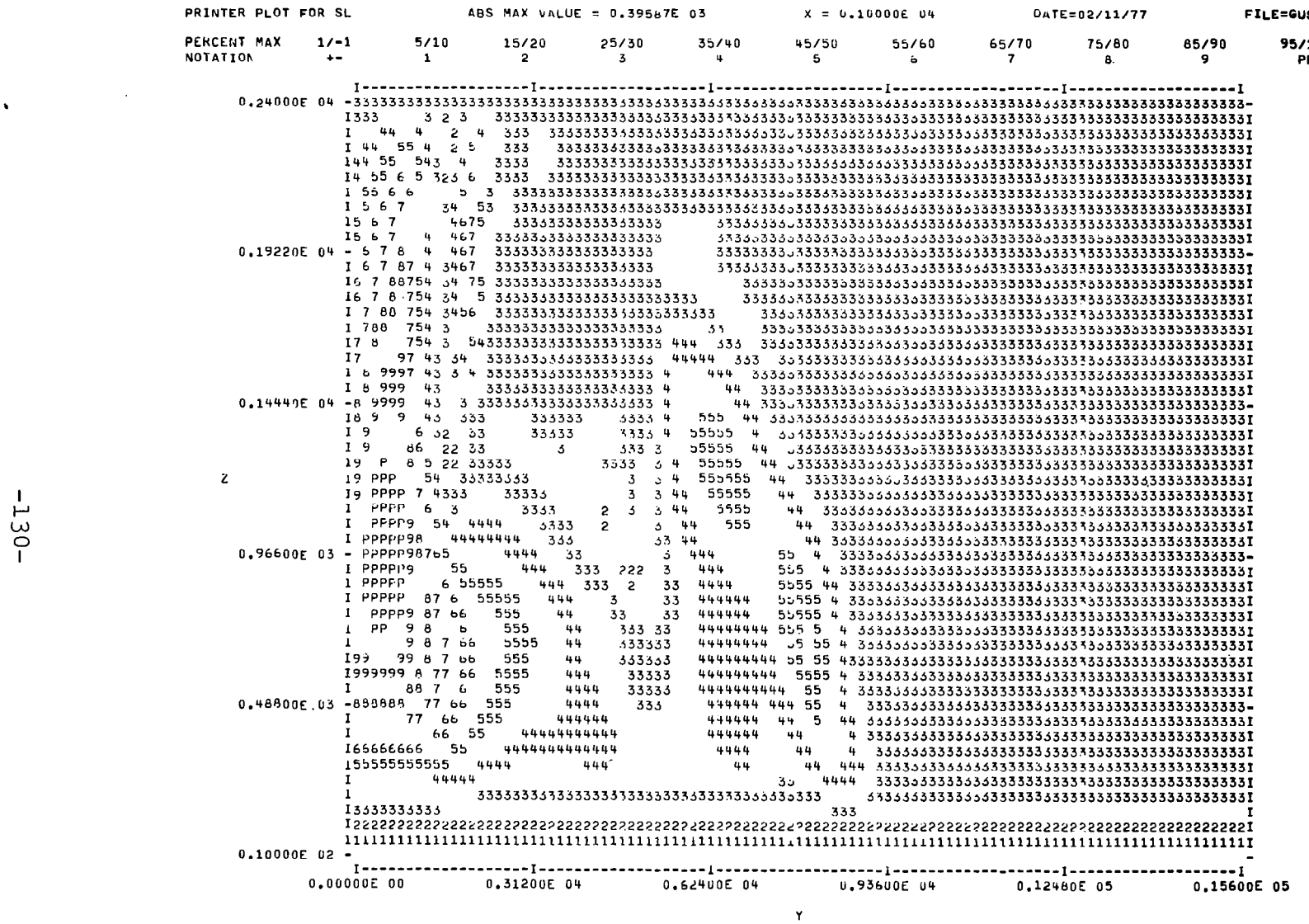

Figure 4.4.7. Normalized scale of turbulence contours as a function of z and y for a two-dimensional gust front with a 2000 m radius downdraft at t = 1000 sec. [See figure 2.3.2 for explanation of notation.]

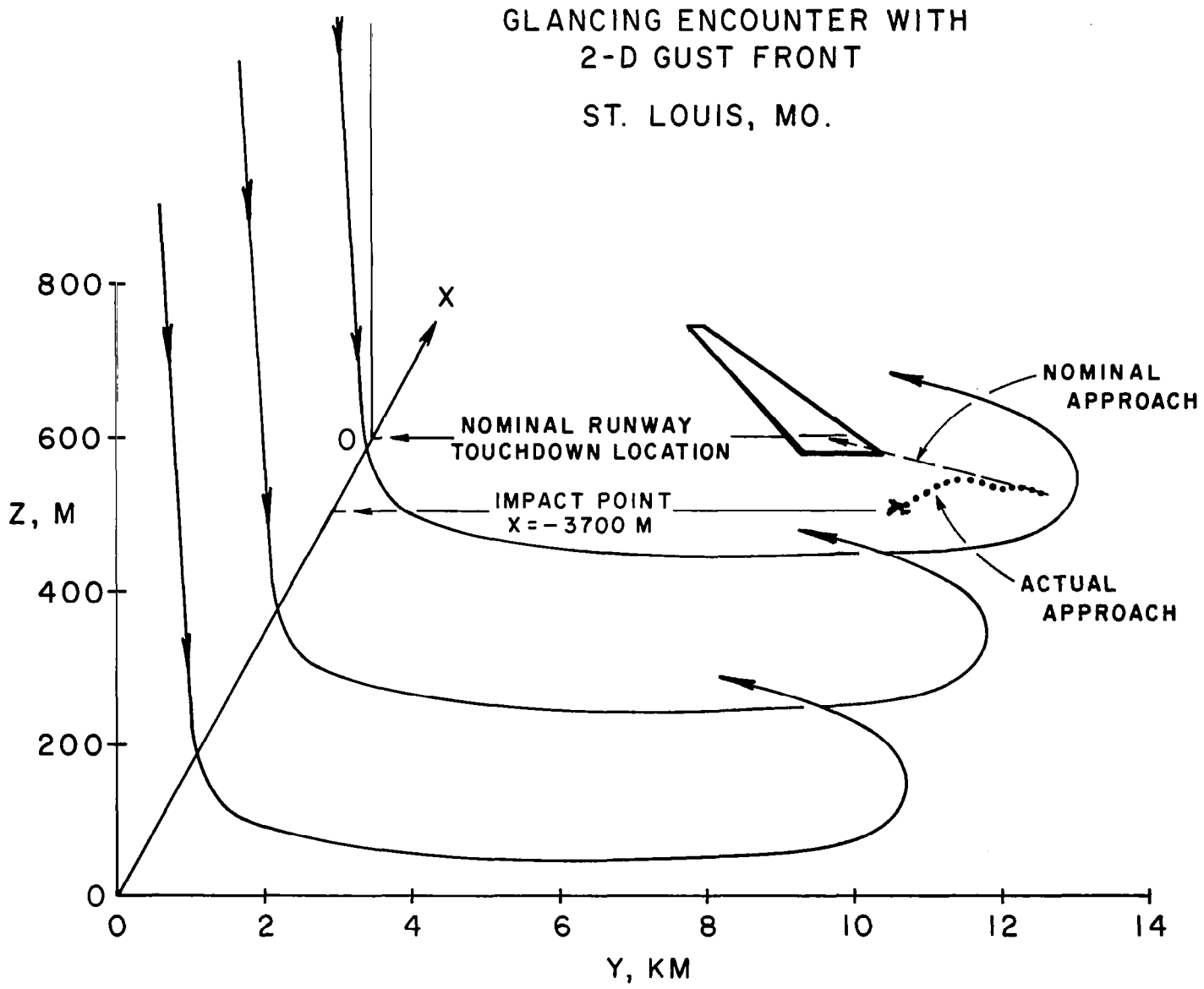

Figure 4.4.8. Aircraft-runway gust front orientation diagram for the St. Louis, Mo., July 23, 1973 accident.

resulting aircraft trajectory projected on the YZ plane of the gust front coordinate system is shown in figure 4.4.9.

The velocity, turbulence, and scale are shown as a function of altitude in figures 4.4.10 - 4.4.16. Note, that the aircraft ascends as well as descends and, therefore, these functions are multi-valued. Since the aircraft is travelling almost parallel to the 2-D gust front no significant changes occur in forward velocity. However, as shown in figure 4.4.11 there is a 9 m/sec updraft in the region of 400 m which causes the aircraft to ascend. The updraft suddenly decreases which feels like a downdraft to the pilot. At the same time, an increasing crosswind is encountered (figure 4.4.10) which further complicates the landing task. The rms turbulence level throughout most of this approach is approximately 4 m/sec.

The combination of these wind conditions encountered while shooting an approach nearly parallel to a 2-D gust front can produce hazardous flight conditions. This is particularly true if the updraft-downdraft sequence is encountered at even lower altitudes than examined here.

4.5 FORT LAUDERDALE-HOLLYWOOD, MAY 1972

At 1421 l.s.t. on May 18, 1972 an Eastern Airlines DC-9 crashed attempting to land on Runway 9L at Fort Lauderdale-Hollywood International Airport, Florida. Thunderstorm activity was observed on radar and heavy rainshowers were in progress at the airport at the time.

The approach was made with the glideslope system inoperative. Eye witnesses reported that the aircraft was high just over the end of the runway and that it was descending in a nose down attitude. The pilot indicated that he applied full flaps and closed the throttles in order to land within the touchdown zone. The aircraft then encountered heavy rain. The pilot pulled back on the elevators, noted very little response, and crashed approximately 128 m past the landing threshold (Ref. 20).

The aircraft was equipped with a flight data recorder which had been malfunctioning for some time prior to the accident. No useful flight data was obtained.

The accident appears to have been caused by sudden low visibility and wind shear associated with the storm cell located over the airport. A witness reported lines of showers (Page 228, aircraft accident file, Ft. Lauderdale, May 1972) parallel to the runway and moving northward across it at the time of the accident. This would agree with the Pilot's description, in that runway visibility went from satisfactory to non-existent, as a line of showers moved onto the runway from the south side. The type of storm cell described would best be modeled as a two-dimensional gust front almost parallel to the runway. This scenario

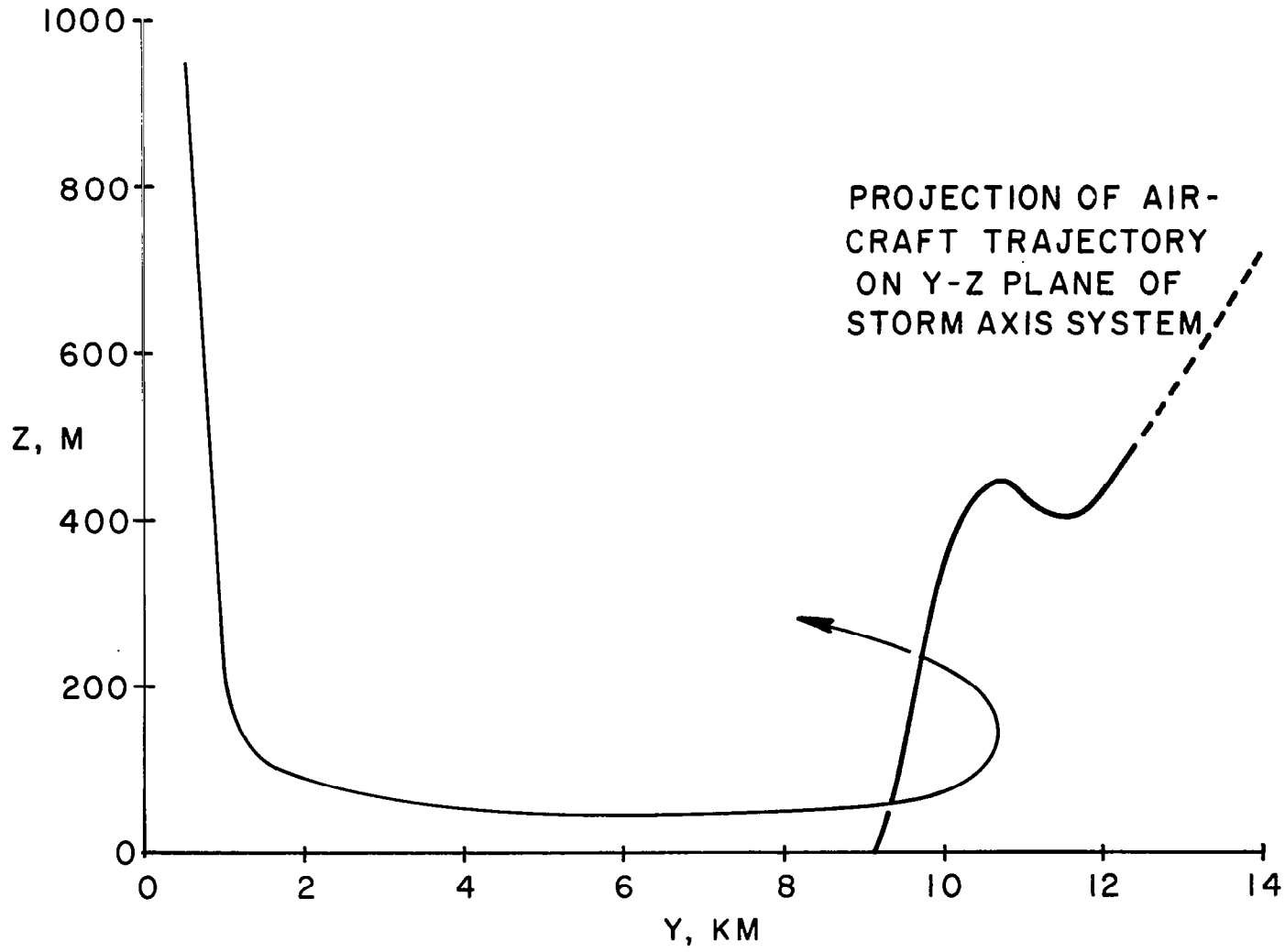

Figure 4.4.9. Projection of aircraft trajectory on the plane of the gust front for the St. Louis, Mo., July 23, 1973 accident.

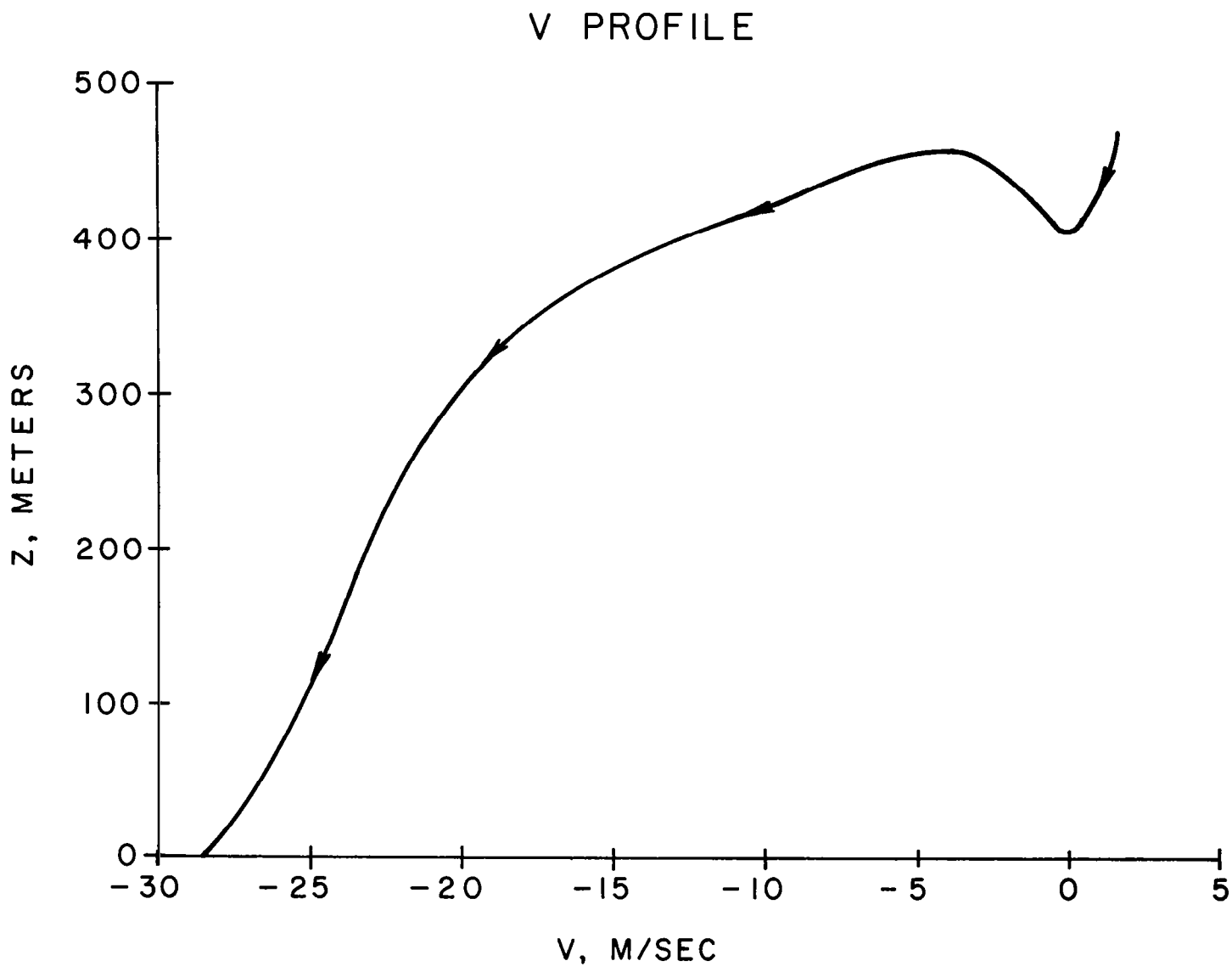

Figure 4.4.10. Altitude profile of horizontal mean wind velocity component along aircraft trajectory for the St. Louis, Mo., July 23, 1973 accident (+ V, crosswind from right).

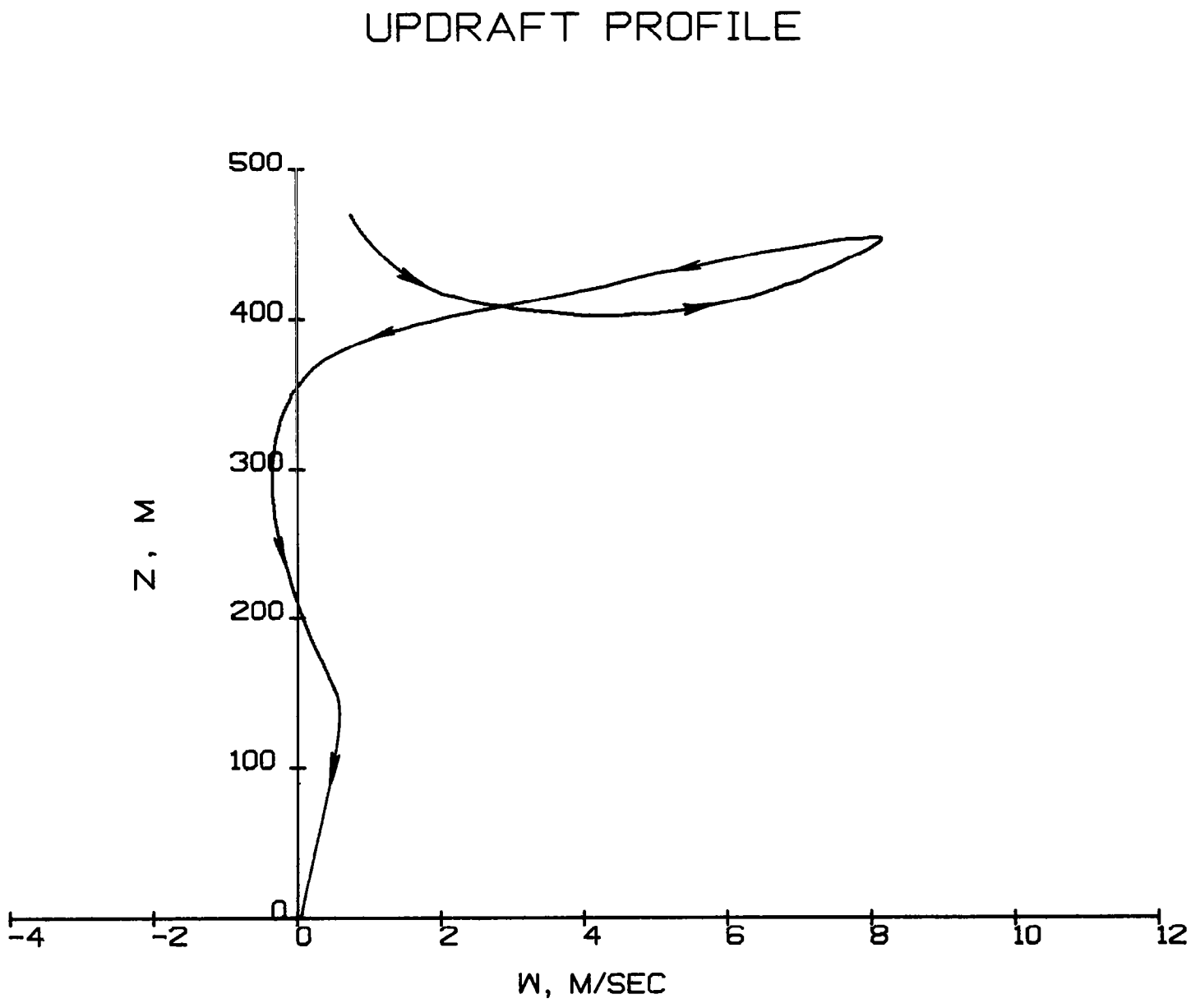

Figure 4.4.11. Altitude profile of vertical mean wind velocity component along aircraft trajectory for the St. Louis, Mo., July 23, 1973 accident, (+ W, updraft).

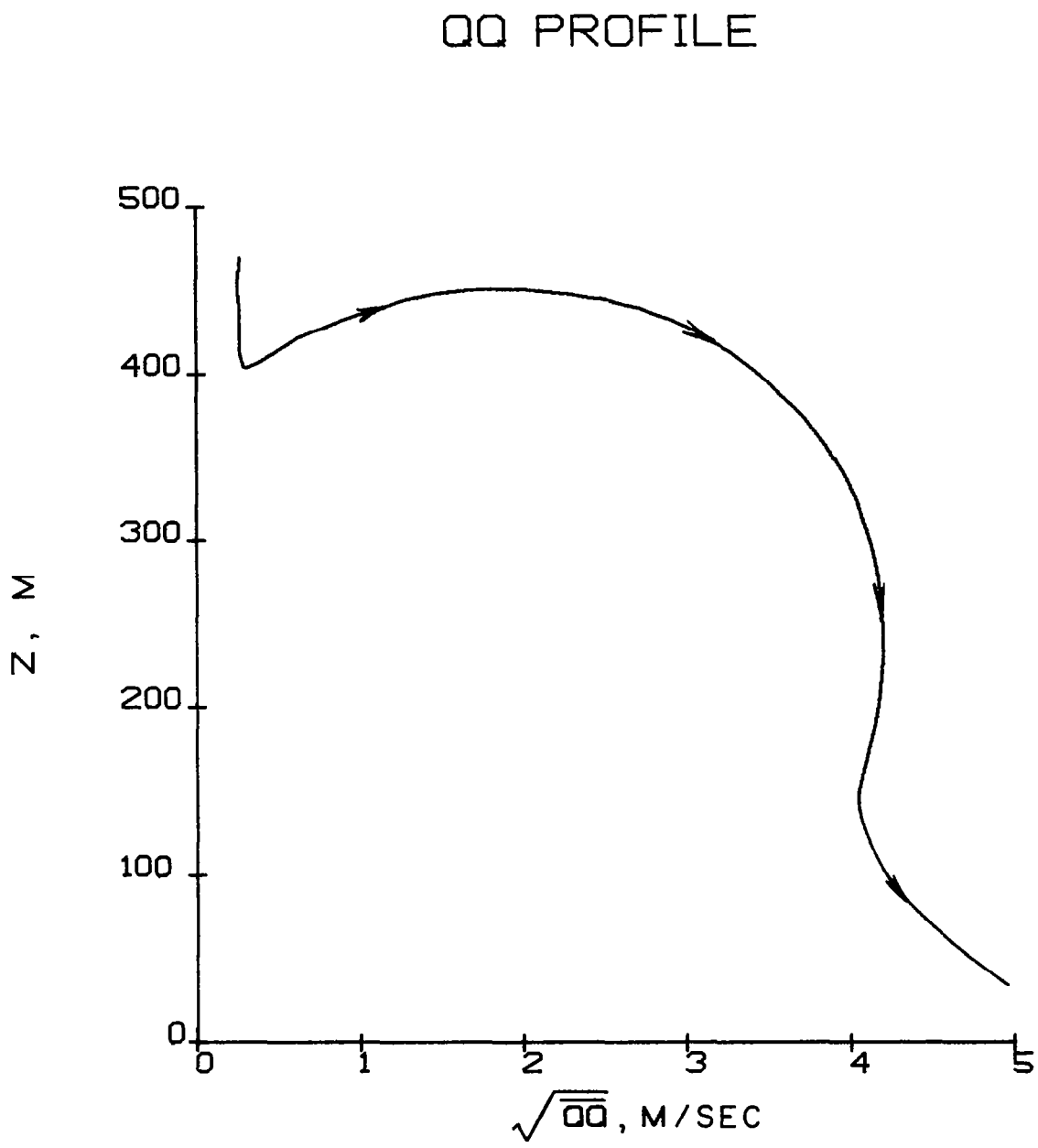

Figure 4.4.12. Altitude profile of variance of total velocity along aircraft trajectory for the St. Louis, Mo., July 23, 1973 accident.

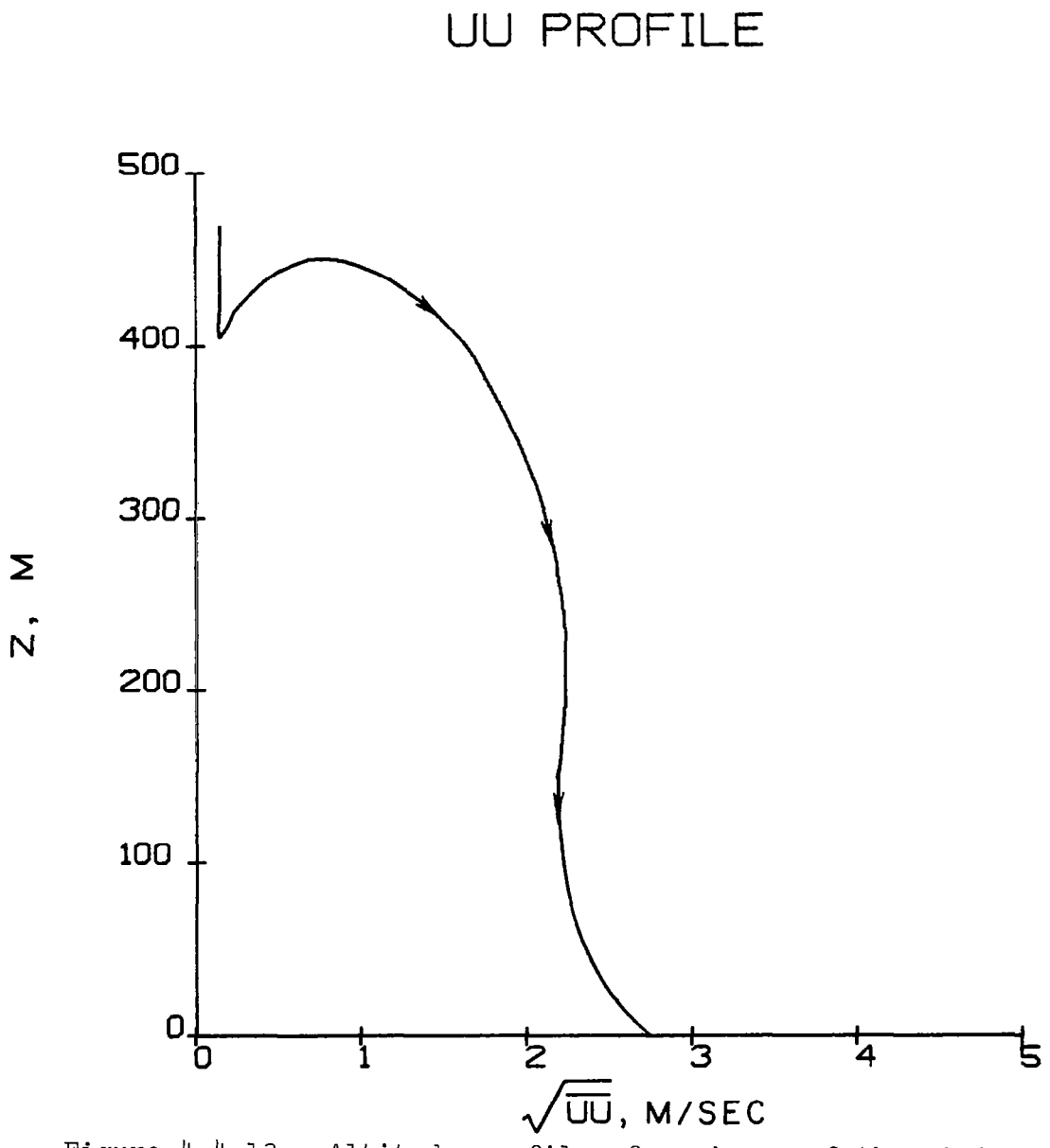

Figure 4.4.13. Altitude profile of variance of the wind parallel to aircraft trajectory for the St. Louis, Mo., July 23, 1973 accident.

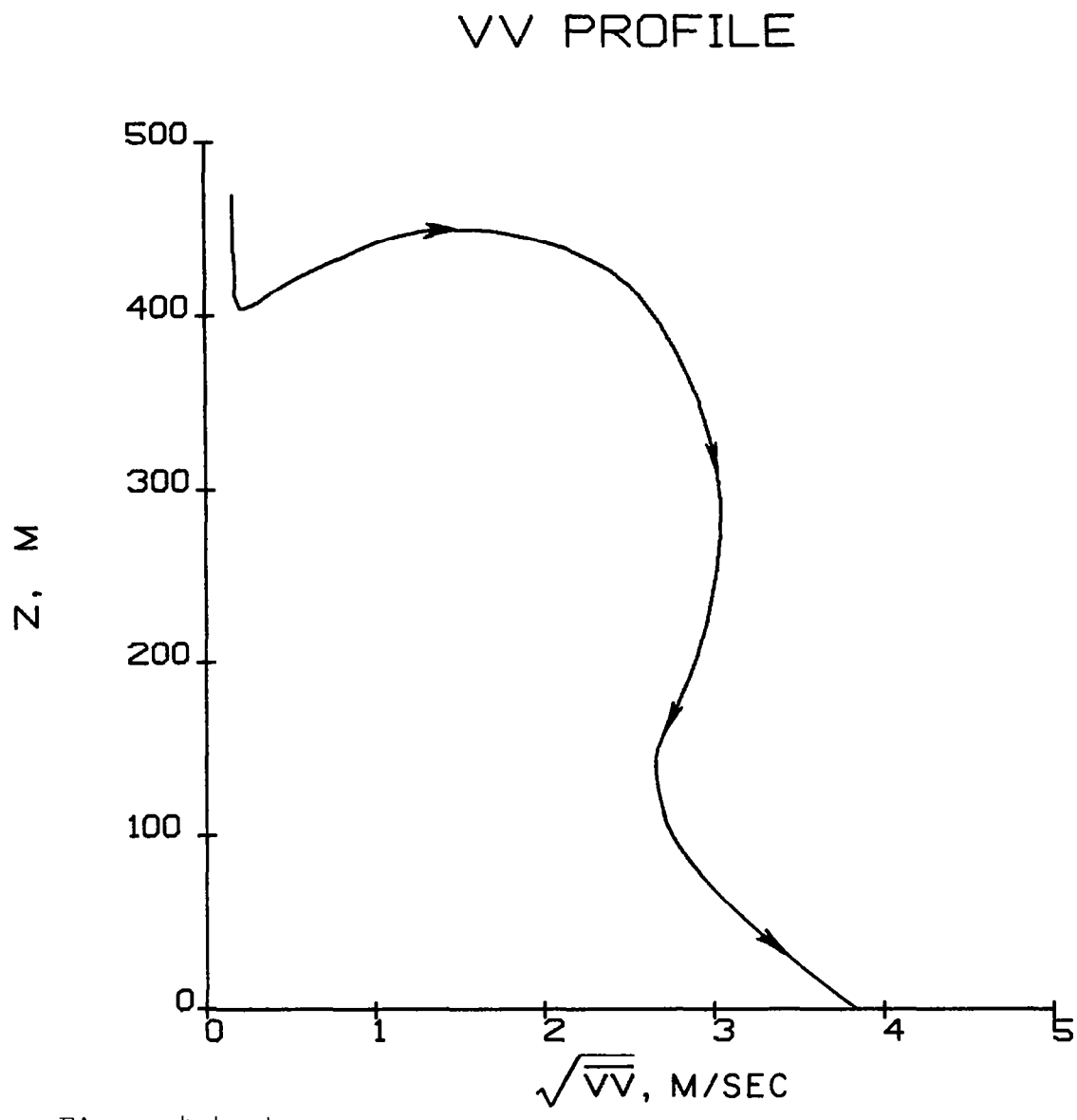

Figure 4.4.14. Altitude profile of variance of the wind perpendicular to aircraft trajectory for the St. Louis, Mo., July 23, 1973 accident.

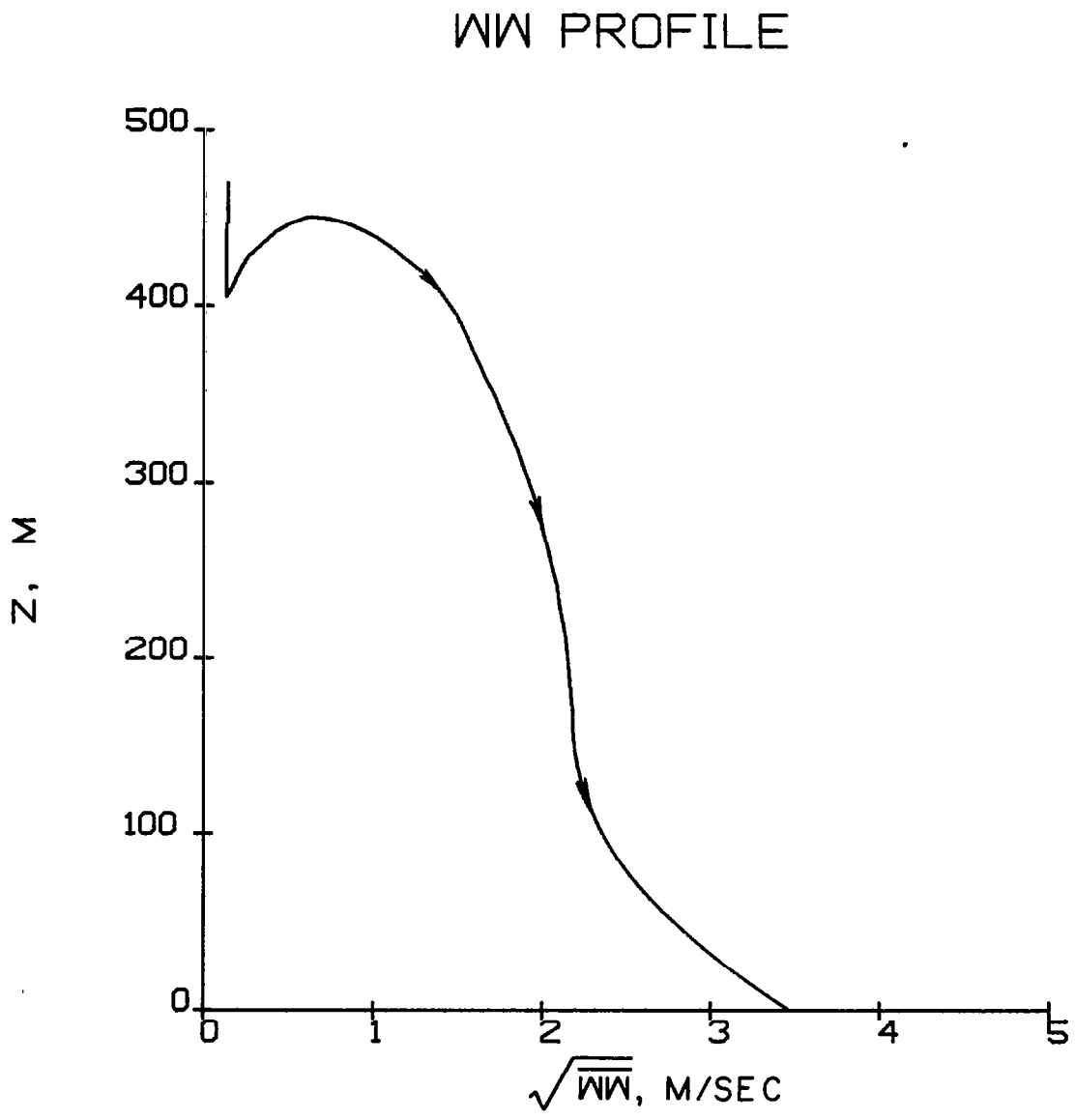

Figure 4.4.15. Altitude profile of variance of the vertical wind along aircraft trajectory for the St. Louis, Mo., July 23, 1973 accident.

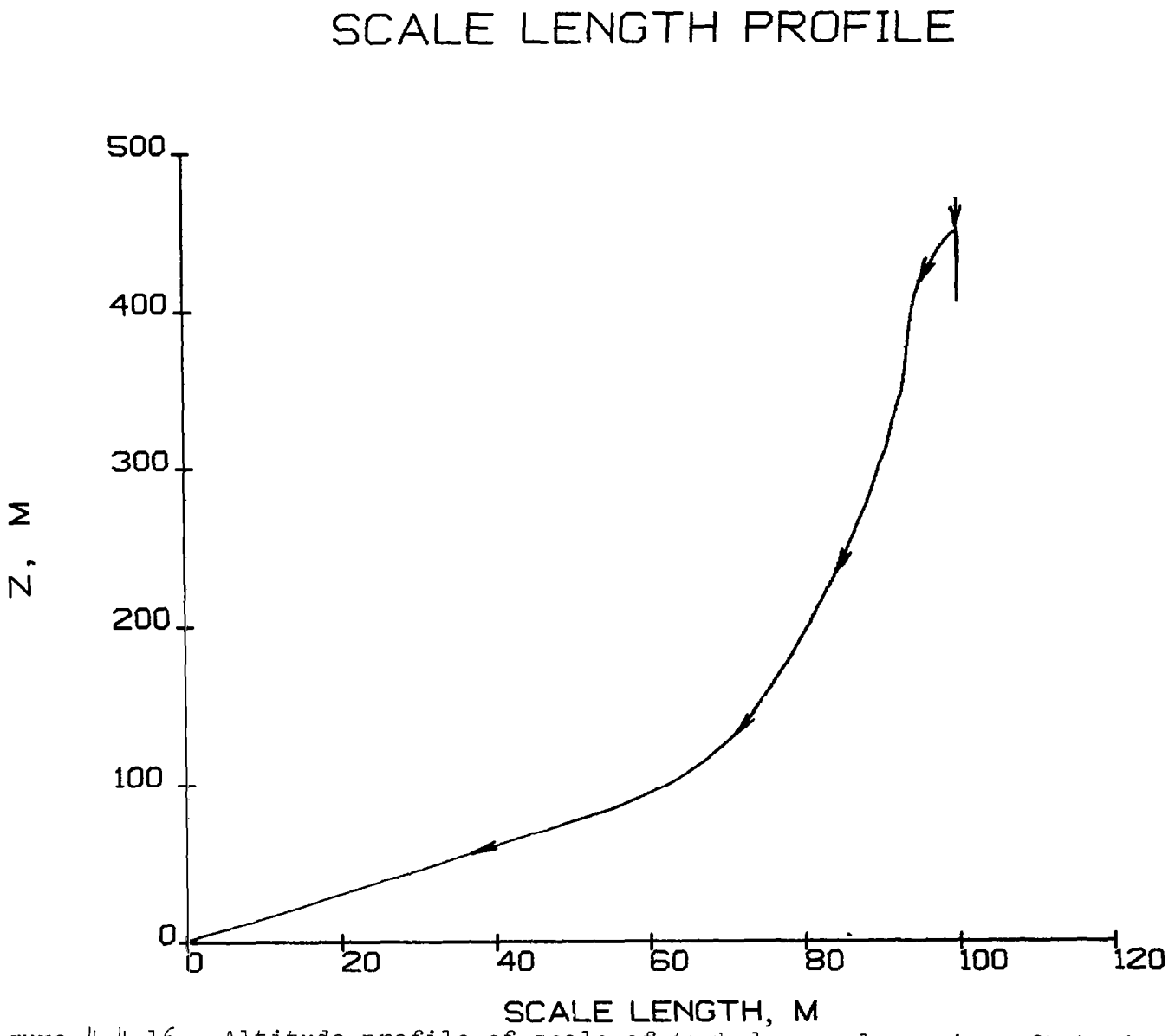

Figure 4.4.16. Altitude profile of scale of turbulence along aircraft trajectory for the St. Louis, Mo., July 23, 1973 accident.

is the same as that investigated in the St. Louis, Missouri, Ozark Airlines accident. Due to the similarity of the storm cells and the trajectory of the aircraft relative to them, no separate velocity and turbulence profile data are presented for this case.

5. ACCIDENTS NOT INVESTIGATED IN DETAIL

5.1 RALEIGH-DURHAM, APRIL 1970

At 1201 l.s.t. on April 2, 1970 a private Cessna 401A crashed on approach to Runway 5 at the Raleigh-Durham Airport, North Carolina. The aircraft collided with trees approximately 2.5 km short and 800 m to the right of the runway.

The weather at the time of the accident was in part light rain and fog, a shallow layer of absolutely unstable air at ground level with stable air on top, a surface wind of 6 m/sec from 160° and a geostrophic wind of 22 m/sec from 220° (figure 5.1.1).

These weather conditions are very similar to those at the time of the 1972 JFK Airport accident, discussed previously in this report. The major difference is that in this case, the wind shear is felt as a crosswind change whereas in the JFK case it was a headwind change. A pilot, that landed 20 minutes after the accident at the Raleigh-Durham Airport, stated that he had to crab right below 120 m because of just such a wind shift (Ref. 21).

Because of the strong similarity to the JFK accident it was decided not to calculate the velocity, variance, and scale distributions. For someone wishing to set up this case for flight simulation studies, the JFK results can be used with the crosswind and downwind velocities interchanged.

5.2 ST. THOMAS, DECEMBER 1970 AND APRIL 1976

It is well known that hazardous wind conditions can exist in the vicinity of large terrain variations (cliffs, mountain, etc.). These conditions include updrafts, downdrafts, and severe gusts as well as vertical wind shear.

Two accidents at an airport near significant terrain variations were considered for analysis. They were

1. St. Thomas, Virgin Islands, 1926 l.s.t. December 10, 1970 Caribair Convair 640.

2. St. Thomas, Virgin Islands, 1510 l.s.t. April 27, 1976 American Airlines Boeing 727

In both of these accidents the aircrafts landed and became airborne again either due to turbulence or low altitude wind shear. (Refs. 22, 23). In the first case the winds flow over a 300 m ridge In the second case the more easterly winds flow over a series of hills averaging 60 m in height.

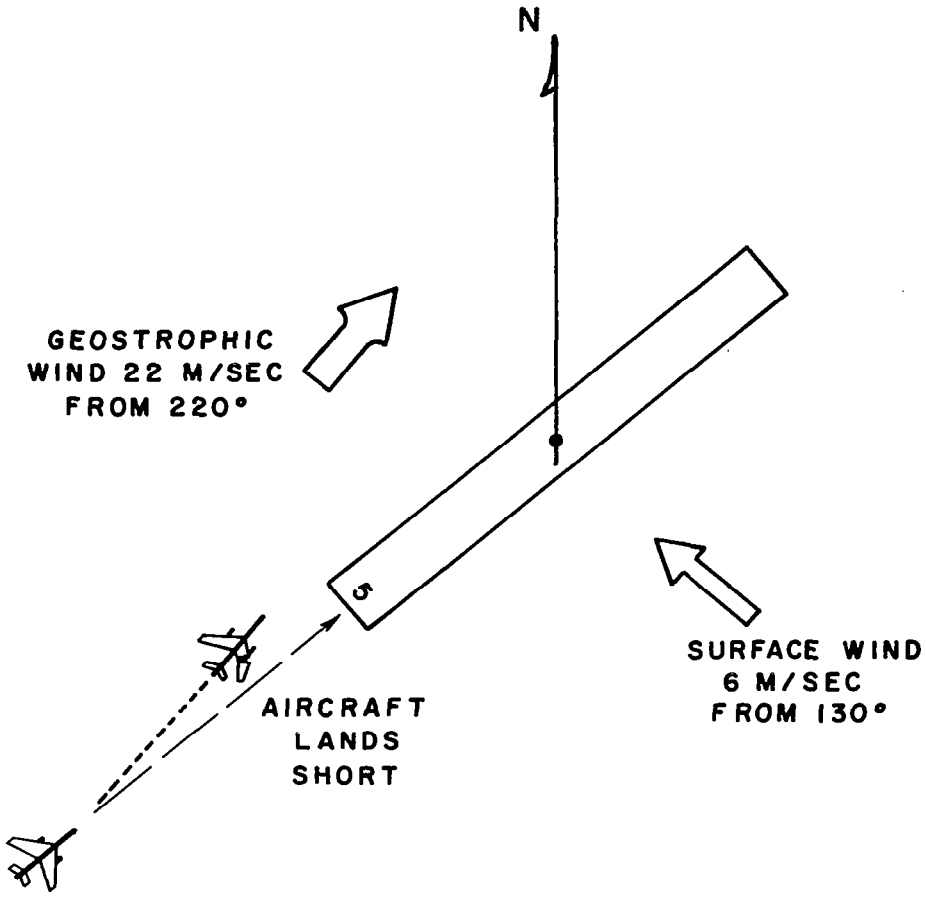

Figure 5.1.1. Aircraft-runway-winds orientation diagram for Raleigh-Durham, N.C., April 2, 1970 accident.

Airport orientation, island topography and wind conditions are shown in figure 5.2.1. In each case, the wind blows over a hilly region on its way to the airport. The resulting wind conditions near the airport (lee wave, separated flow, etc.) will depend on wind speed over the hills and hill height (see Section 1). Valid estimates of these wind conditions require the use of the two-dimensional boundary layer code modified to handle non-flat lower boundary conditions. This work is currently in progress under another contract. It is, therefore, recommended that further analyses of these accidents be accomplished after the computer code is updated.

5.3 PHILADELPHIA, JUNE 1976

About 1600 l.s.t. on June 24, 1976 an Allegheny Airlines DC-9 crashed while landing at Philadelphia International Airport, Pennsylvania. Analysis of the 850 mb pressure data and surface weather observations indicate that no large geostrophic wind shear existed at the time of the accident. If weather were a factor, it would most likely be in the form of a local storm cell. The NTSB accident file was not available for review in time for analysis under this present contract. However, passenger comments in newspaper accounts indicate that the aircraft did encounter local rain showers while landing (Ref. 24). Also, Atlantic City radar shows small scale rapidly changing precipitation echoes in the vicinity of the airport. Further analysis of this case requires more complete knowledge of the trajectory of the aircraft relative to the storm.

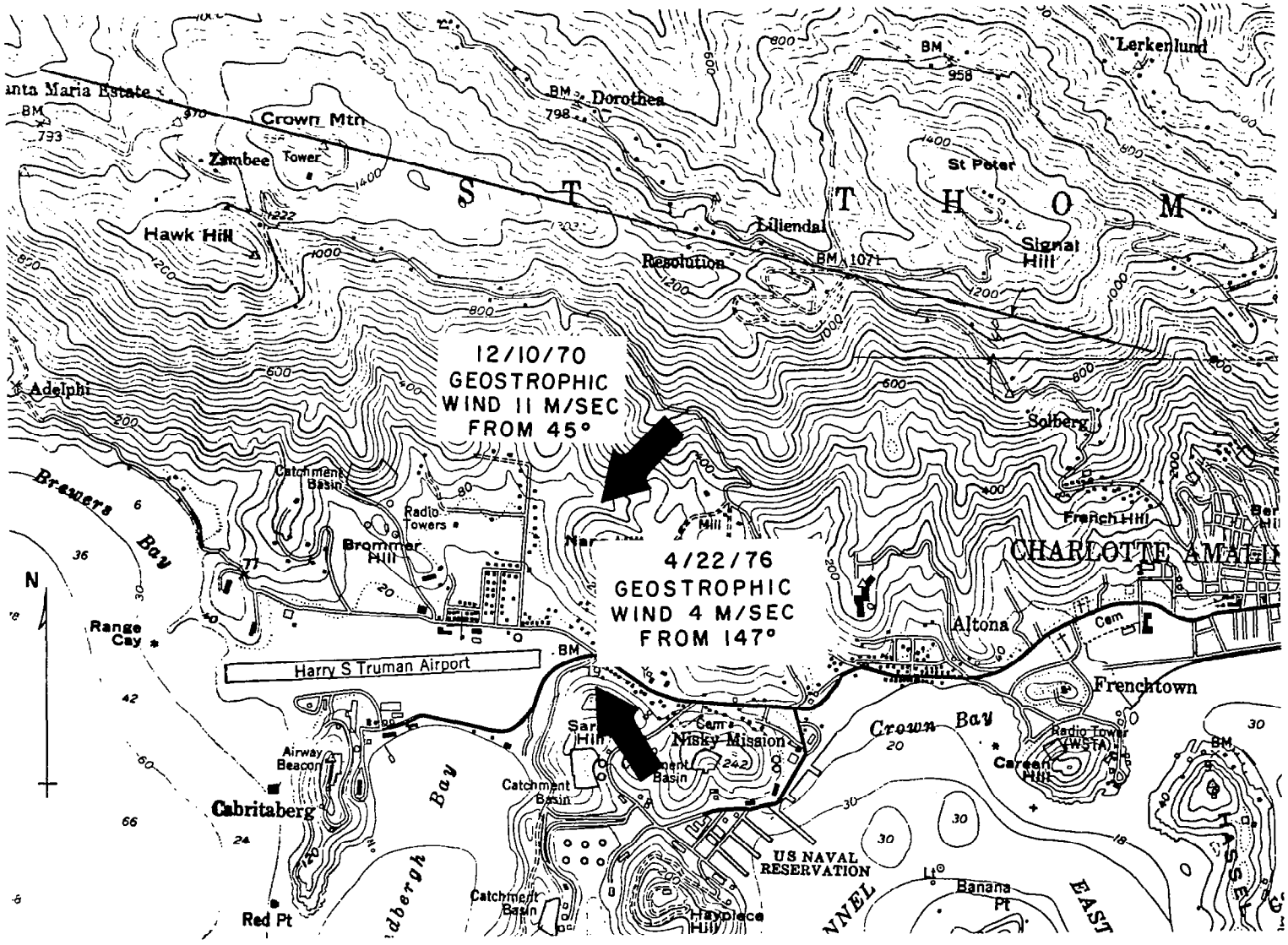

Figure 5.2.1. Airport-topography-wind orientation drawing for the two St. Thomas, V.I. accidents.

REFERENCES

1. Lewellen, W.S. and G.G. Williamson, "Wind Shear and Turbulence Around Airports," NASA Report No. NASA CR-2752, October, 1976.

2. Donaldson, Coleman duP., "Construction of a Dynamic Model of the Production of Atmospheric Turbulence and the Dispersal of Atmospheric Pollutants," Workshop on Micrometeorology, American Meteorological Society, Boston, 1973, pp. 313-392.

3. Donaldson, Coleman duP., "Calculation of Turbulent Shear Flows for Atmospheric and Vortex Motions," AIAA Journal 10, 1, 1972, pp. 4-12. DRYDEN RESEARCH LECTURE.

4. Lewellen, W.S. and M.E. Teske, "Turbulence Modeling and Its Application to Atmospheric Diffusion," Environmental Protection Agency Report EPA-600/4-75-016, 1975.

5. Lewellen, W.S., M.E. Teske and Coleman duP. Donaldson, "Turbulence Model of Diurnal Variations in the Planetary Boundary Layer," Proc. 1974 Heat Transfer and Fluid Mechanics Institute (L.R. Davis and R.E. Wilson, eds.), Stanford University Press, 1974, pp. 301-319.

6. Lewellen, W.S. and M.E. Teske, "Prediction of the Monin-Obukhov Similarity Functions from an Invariant Model of Turbulence," J. Atmos. Sciences 30, 7, 1973, pp. 1340-1345.

7. Lewellen, W.S., M.E. Teske and Coleman duP. Donaldson, "Examples of Variable Density Flows Computed by a Second-Order Closure Description of Turbulence," AIAA Journal 14, 3, 1976, pp. 382-387.

8. Lewellen, W.S. and M.E. Teske, "Atmospheric Pollutant Dispersion Using Second-Order Closure Modeling of the Turbulence," presented at the EPA Conference on Modeling and Simulation, Cincinnati, Ohio, April 20-22, 1976.

9. Lewellen, W.S., D.A. Oliver, M.E. Teske and G.G. Williamson, "Status Report on a Low Level Atmospheric Turbulence Model for Marine Development," A.R.A.P. Report No. 289, September, 1976.

10. Wurtele, M.G., "Meteorological Conditions Surrounding the Paradise Airline Crash of 1 March, 1964," J. Applied Meteorology, 9, October, 1970, pp. 787-795.

11. Lewellen, W.S., G.G. Williamson and M.E. Teske, "Estimates of the Low-Level Wind Shear and Turbulence in the Vicinity of Kennedy International Airport on June 24, 1975," NASA Report No. NASA CR-2751, October, 1976.

12. Aircraft Accident Report, National Transportation Safety Board, Washington, D.C., Report No. NTSB-AAR-74-14. December, 1973.

13. Aircraft Accident Report, National Transportation Safety Board, Washington, D.C., Report No. NTSB-AAR-71-11. January, 1971.

14. Aircraft Accident Report, National Transportation Safety Board, Washington, D.C., Report No. MKC73-A-K056. March, 1973.

15. Aircraft Accident Report, National Transportation Safety Board, Washington, D.C., Report No. NTSB-AAR-73-11. December, 1972.

16. Aircraft Accident Report, National Transportation Safety Board, Washington, D.C., Report No. NTSB-AAR-75-3. January, 1974.

17. Aircraft Accident Report, National Transportation Safety Board, Washington, D.C., Report No. NTSB-AAR-76-17. August, 1975.

18. Aircraft Accident Report, National Transportation Safety Board, Washington, D.C., Report No. NTSB-AAR-74-13. November, 1973.

19. Aircraft Accident Report, National Transportation Safety Board, Washington, D.C., Report No. NTSB-AAR-74-5. July, 1973.

20. Aircraft Accident Report, National Transportation Safety Board, Washington, D.C., Report No. NTSB-AAR-72-31. May, 1972.

21. Aircraft Accident Report, National Transportation Safety Board, Washington, D.C., Accident Identification No. NYC-70-A-N108. April, 1970.

22. Aircraft Accident Report, National Transportation Safety Board, Washington, D.C., Accident Identification No. MIA-71-A-M047. December, 1970.

23. Aircraft Accident Report, National Transportation Safety Board, Washington, D.C., Accident Identification No. DCA-76-A-Z025. April, 1976.

24. Philadelphia Inquirer, June 25, 26, 1976.